TOWARDS THE

DIRECTED EVOLUTION OF VIRUS-LIKE PARTICLES

DERIVED FROM POLYOMAVIRUSES

Erik Teunissen

Towards the directed evolution of virus-like particles derived from polyomaviruses
Erik A. Teunissen

Ph.D. Thesis

Department of Pharmaceutics, Utrecht Institute for Pharmaceutical Sciences,
Faculty of Science, Utrecht University, The Netherlands
June 2014

ISBN
978-90-393-6167-2

Cover
Erik A. Teunissen

Background
Dark matter distribution in the universe based on the Millennium Simulation (Springel, 2005)

Layout
Erik A. Teunissen

Print
CPI Wöhrmann Print Service, Zutphen

TOWARDS THE

DIRECTED EVOLUTION OF VIRUS-LIKE PARTICLES

DERIVED FROM POLYOMAVIRUSES

Op weg naar de gerichte evolutie van virusachtige partikels afgeleid van polyomavirussen

(met een samenvatting in het Nederlands)

Proefschrift

ter verkrijging van de graad van doctor
aan de Universiteit Utrecht
op gezag van de rector magnificus, prof.dr. G.J. van der Zwaan,
ingevolge het besluit van het college voor promoties
in het openbaar te verdedigen op donderdag 12 juni 2014
des middags te 4.15 uur

door

Erik Albert Teunissen

geboren op 9 juli 1986
te East Melbourne, Australië

Promotoren

Prof. dr. D.J.A. Crommelin
Prof. dr. P.J.M. Rottier

Copromotor

Dr. E. Mastrobattista

This research is supported by the Dutch Technology Foundation STW, which is part of the Netherlands Organisation for Scientific Research (NWO), and which is partly funded by the Ministry of Economic Affairs (project number 10243).

Take heed and bear witness to the truths that lie herein…
– Book of Cain

Table of contents

Chapter I

General introduction

Introduction

Gene therapy

Cancer, single gene hereditary diseases, cardiovascular diseases, infectious diseases, neurological diseases… These are just examples of diseases that could, in principle, be treated or even cured by gene therapy [1]. Defective genes could be corrected, missing genes could be added, and unwanted genes could be silenced [2]. However, due to their large size, hydrophilic nature, strong negative charge and susceptibility to nuclease attack, nucleic acids face impenetrable barriers and are rapidly degraded and cleared after injection [3]. This happens long before reaching their target, the interior – usually the nucleus – of diseased cells. Therefore, a lot of research has been undertaken in the development of delivery vehicles for nucleic acids. These vehicles should protect their cargo against degradation and specifically deliver the nucleic acids to their target. They are broadly divided into two categories, viral and non-viral vectors.

Viral vectors

Viral vectors are gene delivery vehicles derived from viruses, in which part of the viral genome has been replaced by the nucleic acid cargo [4]. Viruses have naturally evolved to be the perfect delivery vehicles of genetic material [5]. It is this delivery of their genomes that allows them to reproduce and that causes disease in infected hosts. Viral vectors exploit these intrinsic delivery characteristics for the delivery of therapeutic nucleic acids [6]. They can be either replication-competent [7] or replication-defective [8]. In general, they are very efficient at delivering their cargo to cells, but they are difficult and expensive to produce [9], often have a narrowly defined tropism [10], have only a limited delivery capacity [11], and carry the risk of serious adverse reactions caused by their immunogenicity [12] and insertional mutagenesis [13].

Non-viral vectors

Non-viral vectors comprise a broad class of synthetic delivery vehicles. They are usually based on complexes with cationic polymers or lipids [14], but can also be prepared using other materials, such as peptides [3], inorganic nanoparticles [15], and dendrimers [16]. These vectors benefit from relatively cheap and easy production, are usually not limited in their delivery capacity, and are relatively safe compared to viral vectors. However, these vectors are still generally plagued by very low delivery efficiencies [17,18].

Virus-like particles

An ideal delivery vehicle would combine the benefits of both systems, while eliminating the disadvantages [19]. As an intermediate between viral and non-viral vectors, virus-like particles (VLPs) might be able to fulfill this promise. VLPs are supramolecular assemblies of viral structural proteins. These particles form spontaneously after the recombinant expression of viral structural proteins and do not contain any viral nucleic acids. Some viruses even form such empty capsids as accidental by-products of infection [20,21]. They resemble their native viral capsids in structure, stability, tropism, and transduction efficiency, but do not contain any viral genetic material [22]. Because of this, they retain the efficient delivery characteristics of viral vectors, but the lack of viral DNA ensures that they no longer possess the dangers associated with insertion and reversion.

VLPs have been generated from different viruses of many distinct virus families [23]. Commercially, these particles are mainly used for vaccination. Several VLP-based vaccines are currently under clinical investigation [24,25], and some are already available on the market, such as the prophylactic human papillomavirus (HPV) vaccines Gardasil®

[26] and Cervarix® [27]. However, these particles also show potential for gene therapy.

VLPs derived from polyomaviruses

Of particular interest are the VLPs derived from polyomaviruses. These VLPs are able to encapsidate double-stranded DNA in a sequence-independent fashion [28,29], allowing them to be used for gene delivery. These VLPs are relatively easy to produce; they do not require any post-translational modifications and can form in prokaryotic expression systems after the expression of just one viral protein, the major capsid protein VP1 [30]. In **chapter 2**, we review the production and biomedical applications of these virus-like particles.
However, in their current format these VLPs cannot be used for gene therapy. For example, their limited natural tropism prevents them from transducing a wide variety of target cells, and pre-existing immunity will likely reduce efficacy. Therefore, we set out to modify these VLPs to improve their characteristics for gene therapy.

Directed evolution of virus-like particles derived from polyomaviruses

Despite the considerable progress in the field of rational protein design, enabling the complete *de novo* design of enzymes with novel catalytic activity [31–33], it is still seemingly impossible to predict the ramifications of mutations for gene delivery vectors. Directed evolution, on the other hand, permits the alteration of proteins without prior knowledge of structure-function relationships. Although this technique has mainly been used for the modification of enzymes (for recent reviews see references [34] and [35]), this technique is also suitable for the creation of novel viral vectors for gene therapy. Most of these studies have been performed with adeno-associated virus (AAV) [36–43], but other viruses, such as adenoviruses [44,45] and retroviruses [46–49] have also been subjected to directed evolution. Different properties, such as tropism [40–42], stability [47], and immunogenicity [36,50], have been altered, demonstrating the potential of directed evolution.

Principle of directed evolution

Directed evolution relies on iterative rounds of diversification and selection to improve proteins in a process that mimics natural selection. Large libraries of random mutants are created through high-throughput combinatorial techniques, followed by selection of those mutants that possess desired properties. The principle of this technique is shown in figure 1.
Directed evolution begins with the selection of a starting point. This is usually a gene from nature with characteristics similar to those desired, just to ensure that the evolutionary gap is not too large to bridge. If several homologues are available, as is the case for polyomavirus *VP1*, these genes can be recombined through a technique called DNA shuffling to create a library of hybrid *VP1* genes [51,52]. Diversification can also be achieved using other techniques, such as error-prone PCR [53] or random oligonucleotide insertion [54] (for an overview, see reference [55]). Before the libraries can be expressed, the genes have to be compartmentalized. Just like in cellular compartmentalization in life, the expressed proteins should be confined to the same space as their coding genes, thereby forming a link between the genotype and phenotype. This link ensures that the genetic origin of the selected proteins can later be uncovered, allowing the genes to be used for further rounds of directed evolution, or in the end for production. This compartmentalization can be achieved *in vivo*, by transforming the library into bacteria or by transfecting eukaryotic cells, or completely *in vitro*, using a technique called *in vitro* compartmentalization [56,57]. Next, the proteins are expressed. In the case of viral structural proteins, these proteins

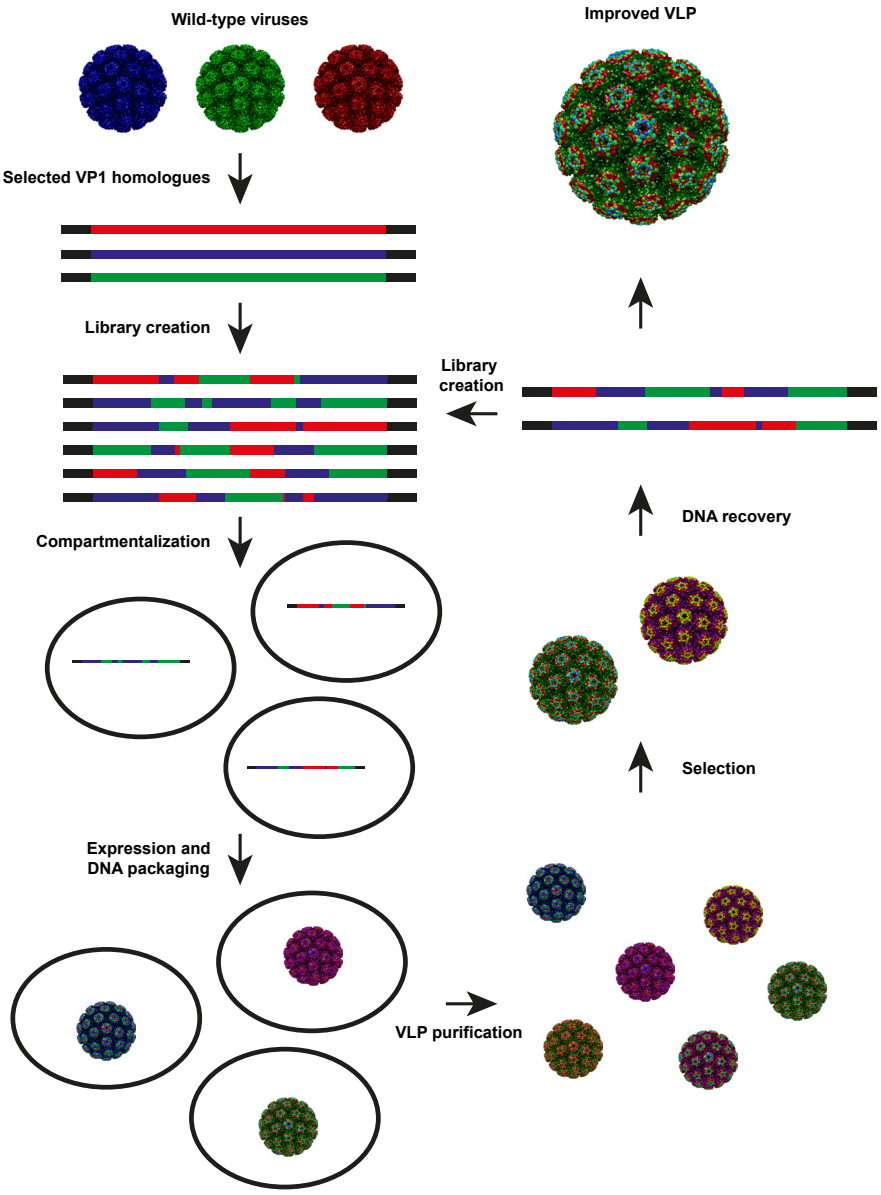

Figure 1. Principle of the directed evolution of virus-like particles. First, the *VP1* genes from several wild-type polyomaviruses are chosen as the starting point for directed evolution. These genes are then recombined through a technique called DNA shuffling to create a diverse library of hybrid *VP1* genes. These hybrid genes are then compartmentalized in a protein expression system, followed by protein expression. This way, the expressed VP1 proteins are confined to the same space as their coding genes, thereby forming a link between the genotype and phenotype. After expression, the VP1 proteins within a single compartment assemble to form VLPs, but can only encapsidate their own coding DNA, as they cannot leave their compartments. Once assembly is complete, the VLPs can be purified and subjected to selective pressure. VLPs with desired properties are isolated and DNA is extracted from them. This DNA can then be used for additional rounds of diversification and selection, further refining the properties of the VLPs. This process can then be repeated until sufficiently improved VLPs are obtained.

assemble to form VLPs, packaging their own coding DNA. We call these particles *artificial viruses* – VLPs that encapsidate their own synthetic genome. These VLPs can then be purified and, by applying selective pressure, mutants that possess desired properties can be selected. Several iterative rounds of diversification and selection are performed to obtain effective gene delivery vectors. By performing clever selection experiments, these vectors can be screened not only for transfection efficiency, but also other traits, such as immune evasion and tissue or organ specificity.

Aim of the thesis

In this project, we aimed to develop an evolution-based method for the improvement of polyomavirus-derived VLPs for gene delivery. The original plan was to use a technique called *in vitro* compartmentalization (IVC) for this [56,57]. This technique uses micrometer-scale droplets of a water-in-oil emulsion as compartments for directed evolution. The droplets each contain on average one gene from the library, and are formed by the emulsification of a cell-free expression (CFE) system, containing all components necessary for the transcription and translation of a gene. A commonly used CFE system is S30 extract, based on the soluble fraction of a lysate from the bacterium *Escherichia coli* (*E. coli*) after centrifugation at 30,000 g [58–61]. This system is supplemented with the T7 RNA polymerase [62]. This way, the droplets form artificial cells that can express proteins from genes under control of the T7 promoter. Every milliliter of emulsion contains approximately 10^{10} of these artificial cells, allowing the use of very large libraries [63]. This way, a very large part of the evolutionary landscape can be screened. Most published directed evolution experiments with viral vectors were performed with smaller libraries (up to 10^7 genes) [36,41,46,64]. Consequently, only single steps in the gene delivery process were changed, without taking into account the consequences these changes might have on other steps. By using such a large library, it might be possible to select for several steps at the same time.

We chose to use the VLPs derived from the hamster polyomavirus (HaPyV) as model vectors for most of our studies, because previous studies showed that these particles can be modified significantly without hampering VLP formation [65–68]. Moreover, these VLPs are not only promising vectors for gene therapy, but also for vaccine development. HaPyV VLPs can effectively display foreign epitopes on their capsid to induce strong immune responses [67,69,70].

Outline of the thesis

In **chapter 1**, the subject of this thesis is introduced and its outline is presented.

In **chapter 2**, we highlight the structural characteristics of VLPs derived from polyomaviruses and give an overview of their current applications in diagnostics, vaccine development and gene delivery.

In **chapter 3**, we investigated the high batch-to-batch variability of S30 extracts with the goal of reducing it. We established how S30 extracts can be normalized after their production. Furthermore, we examined the influence of extract protein concentration on the yield of expression.

In **chapter 4**, we further investigated the relationship between S30 extract protein concentration and the yield of expression. We tested this relationship for the expression of several different proteins and verified this relationship using a commercially available extract. We also tested different conditions, such as incubation time and temperature, and attempted to increase expression by adding excipients.

In **chapter 5**, we established that VLPs do not readily assemble after the cell-free expression of HaPyV VP1. In this chapter, we describe the many modifications to the CFE system we tested in an attempt to increase the assembly of VLPs to allow us to use this system for IVC.

In **chapter 6**, we give a proof of concept for the

directed evolution of polyomavirus VLPs after expression in eukaryotic cells. We demonstrate the existence of a genotype-phenotype linkage, and show that VLPs can be selected based on VLP formation. We also demonstrate the possibility to create diverse gene libraries from polyomavirus *VP1* homologues using DNA shuffling.

In **chapter 7**, we explored two approaches to study HaPyV VLPs in biological environments. First, we used a clonable tag based on murine metallothionein to provide additional contrast for transmission electron microscopy (TEM). We investigated how such a tag influences VLP formation. Second, we used a technique called nanoparticle tracking analysis (NTA) for the detection of VLPs. We examined the possibility of using fluorescently labeled VLPs for the study of the stability and behavior of VLPs in serum.

In **chapter 8**, we explored the possibility of combining DNA and epitope vaccination, based on the hypothesis that such co-delivery will lead to a synergistic effect. We prepared VLPs from HaPyV VP1 with model epitopes from ovalbumin inserted into surface-exposed loops, and investigated their immunogenicity using an *in vitro* antigen presentation assay. We also investigated different strategies for loading VLPs with plasmid DNA.

In **chapter 9**, the advancements presented in this thesis are summarized and their implications are discussed. Furthermore, several recommendations are presented that might benefit future research.

References

1 Ginn, S.L. *et al.* **Gene therapy clinical trials worldwide to 2012 – an update.** J Gene Med (2013) 15, 65–77.

2 Kay, M.A. **State-of-the-art gene-based therapies: the road ahead.** Nat Rev Genet (2011) 12, 316–328.

3 Mann, A. *et al.* **Peptides in DNA delivery: current insights and future directions.** Drug Discov Today (2008) 13, 152–160.

4 Thomas, C.E., Ehrhardt, A. and Kay, M.A. **Progress and problems with the use of viral vectors for gene therapy.** Nat Rev Genet (2003) 4, 346–358.

5 Kay, M.A., Glorioso, J.C. and Naldini, L. **Viral vectors for gene therapy: the art of turning infectious agents into vehicles of therapeutics.** Nat Med (2001) 7, 33–40.

6 Heilbronn, R. and Weger, S. **Viral vectors for gene transfer: current status of gene therapeutics.** Handb Exp Pharmacol (2010), 143–170.

7 Galanis, E., Vile, R. and Russell, S.J. **Delivery systems intended for *in vivo* gene therapy of cancer: targeting and replication competent viral vectors.** Crit Rev Oncol Hematol (2001) 38, 177–192.

8 Marconi, P. *et al.* **Replication-defective herpes simplex virus vectors for gene transfer *in vivo*.** Proc Natl Acad Sci U S A (1996) 93, 11319–11320.

9 Merten, O.W., Geny-Fiamma, C. and Douar, A.M. **Current issues in adeno-associated viral vector production.** Gene Ther (2005) 12 Suppl 1, S51–61.

10 Kootstra, N.A. and Verma, I.M. **Gene therapy with viral vectors.** Annu Rev Pharmacol Toxicol (2003) 43, 413–439.

11 Walther, W. and Stein, U. **Viral vectors for gene transfer: a review of their use in the treatment of human diseases.** Drugs (2000) 60, 249–271.

12 Nayak, S. and Herzog, R.W. **Progress and prospects: immune responses to viral vectors.** Gene Ther (2010) 17, 295–304.

13 Baum, C. *et al.* **Chance or necessity? Insertional mutagenesis in gene therapy and its consequences.** Mol Ther (2004) 9, 5–13.

14 Thomas, M. and Klibanov, A.M. **Non-viral gene therapy: polycation-mediated DNA delivery.** Appl Microbiol Biotechnol (2003) 62, 27–34.

15 Ghosh, P. *et al.* **Gold nanoparticles in delivery applications.** Adv Drug Deliv Rev (2008) 60, 1307–1315.

16 Dufes, C., Uchegbu, I.F. and Schatzlein, A.G. **Dendrimers in gene delivery.** Adv Drug Deliv Rev (2005) 57, 2177–2202.

17 Luo, D. and Saltzman, W.M. **Synthetic DNA delivery systems.** Nat Biotechnol (2000) 18, 33–37.

18 Lungwitz, U. *et al.* **Polyethylenimine-based non-viral gene delivery systems.** Eur J Pharm Biopharm (2005) 60, 247–266.

19 Mastrobattista, E. *et al.* **Artificial viruses: a nanotechnological approach to gene delivery.** Nat Rev Drug Discov (2006) 5, 115–121.

20 Mayr, G.A. *et al.* **Immune responses and protection against foot-and-mouth disease virus (FMDV) challenge in swine vaccinated with adenovirus-FMDV constructs.** Vaccine (2001) 19, 2152–2162.

21 Aposhian, H.V., Thayer, R.E. and Qasba, P.K. **Formation of nucleoprotein complexes between polyoma empty capsides and DNA.** J Virol (1975) 15, 645–653.

22 Teunissen, E.A., de Raad, M. and Mastrobattista, E. **Production and biomedical applications of virus-like particles derived from polyomaviruses.** J Control Release (2013) 172, 305–321.

23 Noad, R. and Roy, P. **Virus-like particles as immunogens.** Trends Microbiol (2003) 11, 438–444.

24 Roldao, A. *et al.* **Virus-like particles in vaccine development.** Expert Rev Vaccines (2010) 9, 1149–1176.

25 Kushnir, N., Streatfield, S.J. and Yusibov, V. **Virus-like particles as a highly efficient vaccine platform: diversity of targets and production systems and advances in clinical development.** Vaccine (2012) 31, 58–83.

26 Garland, S.M. *et al.* **Quadrivalent vaccine against human papillomavirus to prevent anogenital diseases.** N Engl J Med (2007) 356, 1928–1943.

27 Harper, D.M. *et al.* **Sustained efficacy up to 4.5 years of a bivalent L1 virus-like particle vaccine against human papillomavirus types 16 and 18: follow-up from a randomised control trial.** Lancet (2006) 367, 1247–1255.

28 Moreland, R.B., Montross, L. and Garcea, R.L. **Characterization of the DNA-binding properties of the polyomavirus capsid protein VP1.** J Virol (1991) 65, 1168–1176.

29 Voronkova, T. *et al.* **Hamster polyomavirus-derived virus-like particles are able to transfer *in vitro* encapsidated plasmid DNA to mammalian cells.** Virus Genes (2007) 34, 303–314.

30 Pattenden, L.K. *et al.* **Towards the preparative and large-scale precision manufacture of virus-like particles.** Trends Biotechnol (2005) 23, 523–529.

31 Jiang, L. *et al.* ***De novo* computational design of retro-aldol enzymes.** Science (2008) 319, 1387–1391.

32 Rothlisberger, D. *et al.* **Kemp elimination catalysts by computational enzyme design.** Nature (2008) 453, 190–195.

33 Siegel, J.B. *et al.* **Computational design of an enzyme catalyst for a stereoselective bimolecular Diels-Alder reaction.** Science (2010) 329, 309–313.

34 Goldsmith, M. and Tawfik, D.S. **Directed enzyme evolution: beyond the low-hanging fruit.** Curr Opin Struct Biol (2012) 22, 406–412.

35 Dalby, P.A. **Strategy and success for the directed evolution of enzymes.** Curr Opin Struct Biol (2011) 21, 473–480.

36 Perabo, L. *et al.* **Combinatorial engineering of a gene therapy vector: directed evolution of adeno-associated virus.** J Gene Med (2006) 8, 155–162.

37 Maheshri, N. *et al.* **Directed evolution of adeno-associated virus yields enhanced gene delivery vectors.** Nat Biotechnol (2006) 24, 198–204.

38 Grimm, D. *et al.* ***In vitro* and *in vivo* gene therapy vector evolution via multispecies interbreeding and retargeting of adeno-associated viruses.** J Virol (2008) 82, 5887–5911.

39 Li, W. *et al.* **Generation of novel AAV variants by directed evolution for improved CFTR delivery to human ciliated airway epithelium.** Mol Ther (2009) 17, 2067–2077.

40 Yang, L. *et al.* **A myocardium tropic adeno-associated virus (AAV) evolved by DNA shuffling and *in vivo* selection.** Proc Natl Acad Sci U S A (2009) 106, 3946–3951.

41 Maguire, C.A. *et al.* **Directed evolution of adeno-associated virus for glioma cell transduction.** J Neurooncol (2010) 96, 337–347.

42 Asuri, P. *et al.* **Directed evolution of adeno-associated virus for enhanced gene delivery and gene targeting in human pluripotent stem cells.** Mol Ther (2012) 20, 329–338.

43 Dalkara, D. *et al.* ***In vivo*-directed evolution of a new adeno-associated virus for therapeutic outer retinal gene delivery from the vitreous.** Sci Transl Med (2013) 5, 189ra176.

44 Kuhn, I. *et al.* **Directed evolution generates a novel oncolytic virus for the treatment of colon cancer.** PLoS One (2008) 3, e2409.

45 Uil, T.G. *et al.* **Directed adenovirus evolution using engineered mutator viral polymerases.** Nucleic Acids Res (2011) 39, e30.

46 Soong, N.W. *et al.* **Molecular breeding of viruses.** Nat Genet (2000) 25, 436–439.

47 Powell, S.K. *et al.* **Breeding of retroviruses by DNA shuffling for improved stability and processing yields.** Nat Biotechnol (2000) 18, 1279–1282.

48 Bupp, K. and Roth, M.J. **Altering retroviral tropism using a random-display envelope library.** Mol Ther (2002) 5, 329–335.

49 Bupp, K. and Roth, M.J. **Targeting a retroviral vector in the absence of a known cell-targeting ligand.** Hum Gene Ther (2003) 14, 1557–1564.

50 Lin, T.Y. *et al.* **A novel approach for the rapid mutagenesis and directed evolution of the structural genes of west nile virus.** J Virol (2012) 86, 3501–3512.

51 Stemmer, W.P. **Rapid evolution of a protein *in vitro* by DNA shuffling.** Nature (1994) 370, 389–391.

52 Crameri, A. *et al.* **DNA shuffling of a family of genes from diverse species accelerates directed evolution.** Nature (1998) 391, 288–291.

53 Cirino, P.C., Mayer, K.M. and Umeno, D. **Generating mutant libraries using error-prone PCR.** In: Directed Evolution Library Creation: Methods and Protocols (eds Frances H. Arnold and George Georgiou) 3–9 (Springer, 2003).

54 Muller, O.J. *et al.* **Random peptide libraries displayed on adeno-associated virus to select for targeted gene therapy vectors.** Nat Biotechnol (2003) 21, 1040–1046.

55 Arnold, F.H. and Georgiou, G. **Directed Evolution Library Creation: Methods and Protocols.** (2003).

56 Tawfik, D.S. and Griffiths, A.D. **Man-made cell-like compartments for molecular evolution.** Nat Biotechnol (1998) 16, 652–656.

57 Miller, O.J. *et al.* **Directed evolution by *in vitro* compartmentalization.** Nat Methods (2006) 3, 561–570.

58 Zubay, G. ***In vitro* synthesis of protein in microbial systems.** Annu Rev Genet (1973) 7, 267–287.

59 Kim, D.M. *et al.* **A highly efficient cell-free protein synthesis system from *Escherichia coli*.** Eur J Biochem (1996) 239, 881–886.

60 Kigawa, T. *et al.* **Preparation of *Escherichia coli* cell extract for highly productive cell-free protein expression.** J Struct Funct Genomics (2004) 5, 63–68.

61 Kim, T.W. *et al.* **Simple procedures for the construction of a robust and cost-effective cell-free protein synthesis system.** J Biotechnol (2006) 126, 554–561.

62 Kigawa, T., Muto, Y. and Yokoyama, S. **Cell-free synthesis and amino acid-selective stable isotope labeling of proteins for NMR analysis.** J Biomol NMR (1995) 6, 129–134.

63 Griffiths, A.D. and Tawfik, D.S. **Man-made enzymes – from design to *in vitro* compartmentalisation.** Curr Opin Biotechnol (2000) 11, 338–353.

64 Excoffon, K.J. *et al.* **Directed evolution of adeno-associated virus to an infectious respiratory virus.** Proc Natl Acad Sci U S A (2009) 106, 3865–3870.

65 Gedvilaite, A. *et al.* **Formation of immunogenic virus-like particles by inserting epitopes into surface-exposed regions of hamster polyomavirus major capsid protein.** Virology (2000) 273, 21–35.

66 Gedvilaite, A. *et al.* **Size and position of truncations in the carboxy-terminal region of major capsid protein VP1 of hamster polyomavirus expressed in yeast determine its assembly capacity.** Arch Virol (2006) 151, 1811–1825.

67 Gedvilaite, A. *et al.* **Segments of puumala hantavirus nucleocapsid protein inserted into chimeric polyomavirus-derived virus-like particles induce a strong immune response in mice.** Viral Immunol (2004) 17, 51–68.

68 Gedvilaite, A. *et al.* **Virus-like particles derived from major capsid protein VP1 of different polyomaviruses differ in their ability to induce maturation in human dendritic cells.** Virology (2006) 354, 252–260.

69 Zvirbliene, A. *et al.* **Generation of monoclonal antibodies of desired specificity using chimeric polyomavirus-derived virus-like particles.** J Immunol Methods (2006) 311, 57–70.

70 Dorn, D.C. *et al.* **Cellular and humoral immunogenicity of hamster polyomavirus-derived virus-like particles harboring a mucin 1 cytotoxic T-cell epitope.** Viral Immunol (2008) 21, 12–27.

Chapter II

Biomedical applications of virus-like particles derived from polyomaviruses

Erik A. Teunissen[1], Markus de Raad[1] and Enrico Mastrobattista[1]
[1]Department of Pharmaceutics, Utrecht Institute for Pharmaceutical Sciences, Faculty of Science, Utrecht University, Universiteitsweg 99, 3584 CG Utrecht, The Netherlands

J Control Release (2013) 172, 305–321

2

Abstract

Virus-like particles (VLPs), assemblies of capsid proteins devoid of viral genetic material, show great promise in the fields of vaccine development and gene therapy. These particles spontaneously self-assemble after heterologous expression of viral structural proteins. This review will focus on the use of virus-like particles derived from polyomavirus capsid proteins. Since their first recombinant production 27 years ago these particles have been investigated for a myriad of biomedical applications. These virus-like particles are safe, easy to produce, can be loaded with a broad range of diverse cargos and can be tailored for specific delivery or epitope presentation. We will highlight the structural characteristics of polyomavirus-derived VLPs and give an overview of their applications in diagnostics, vaccine development and gene delivery.

1. Introduction

Polyomaviruses (PyVs) are small, non-enveloped icosahedral viruses. Members include the type species simian virus 40 (SV40), the human JC (JCPyV) and BK polyomaviruses (BKPyV) and the murine polyomavirus (MPyV). Up to now, at least 32 different polyomaviruses have been identified, infecting both mammalian and avian species [1,2]. Originally identified for their ability to cause multiple types of tumors (hence the name), mammalian polyomavirus infections are usually asymptomatic. The human polyomaviruses are omniprevalent in the human population, but can cause serious illness in immunocompromised individuals [3,4]. The virus encodes three structural proteins, VP1, VP2 and VP3, which come together to form the viral capsid. However, capsid-like structures can also be formed upon overexpression of the major capsid protein VP1 alone [5]. This unique property of VP1 not only makes it an ideal protein to study mechanisms of protein self-assembly [6,7], but also enables the generation of virus-like particles (VLPs), particles resembling native virions, but devoid of genetic material. These VLPs are able to encapsidate DNA in a sequence-independent fashion [8,9], transfect mammalian cells, have a high insert capacity for peptide epitopes (*e.g.* for vaccination), and do not require post-translational modification to form [5,9]. Currently VLPs are mainly used for vaccination, but these particles also show potential for gene therapy, diagnostics and other biomedical purposes.

This review will focus on polyomavirus virus-like particles. We will first discuss their structure and origin, followed by the different production methods used to obtain these particles, the different methods to load these particles with therapeutics and the types of therapeutics loaded into the particles. Finally, their applications in the fields of diagnostics, vaccine development and gene therapy will be highlighted.

2. Structure

2.1. Polyomavirus structure

The crystal structure of several polyomavirus virions is known, including SV40 [10,11] and MPyV [12,13], while several other VP1 structures, some bound to receptor molecules, have been elucidated [13–20].

Polyomavirus virions are around 45 nm in diameter and consist of 72 capsomers, arranged as a $T=7$ icosahedral capsid (see figure 1). These capsomers each contain 5 major capsid proteins VP1 surrounding 1 minor capsid protein, either VP2 or VP3. The minor capsid proteins are encoded by the same coding DNA sequence, but translation of VP3 is initiated downstream of VP2, forming an N-terminally truncated form of VP2. The virion encapsidates a circular double-stranded DNA (dsDNA) genome averaging 5000 base pair (bp) in size. This

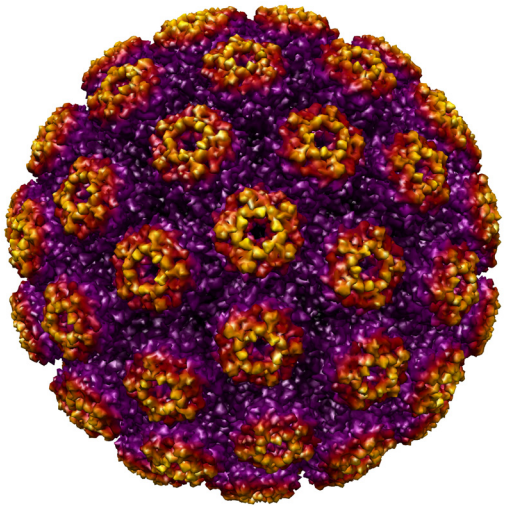

Figure 1. Structure of SV40. The 45 nm icosahedral capsid consists of 72 capsomers, each composed of 5 major capsid proteins VP1 and 1 minor capsid protein VP2 or VP3. The image was created from PDB: 1SVA [11] using Chimera [23].

genome is condensed by host-derived histones (H2A, H2B, H3, and H4) forming a minichromosome [2,21,22].

VP1 is composed of three different regions. The central part of VP1 forms an antiparallel β-sandwich with a jelly-roll topology. Four different loops protrude from the β-sheet core towards the exterior of the virion, designated BC, DE, HI, and EF (see figure 2) [10]. These surface exposed loops are highly variable [24] and confer receptor binding specificity [13,14,17,18].

The N-terminal region lies on the inside of the virion [25] and mediates DNA binding [8]. The positively charged residues among the first 12 amino acids (aas) are essential for this interaction [25]. VP2 and VP3 have no DNA binding properties in MPyV [26], while in SV40 VP2 and VP3 do bind DNA [27]. Overlapping the VP1 DNA binding domain lies a nuclear localization signal (NLS) [28–30]. The Hamster polyomavirus (HaPyV) has an additional N-terminally extended form. The N-terminally extended VP1 localizes to the nucleus, while the authentic VP1 does not, indicating the presence of a NLS in this N-terminal extension [31].

The C-terminus of VP1 forms arms which extend into neighboring capsomers, binding them together to form virions [10]. This is emphasized by truncations of the C-terminus. While C-terminally truncated VP1 does form capsomers, these capsomers cannot assemble to form normal VLPs [32–34]. However, complete removal of the C-terminus (69 aas) from HaPyV VP1 restores VLP formation [35].

2.2. Cell binding and tropism

Most polyomaviruses bind sialic acid attached to gangliosides or other membrane compounds [14,36], though at least SV40 [37,38] and murine pneumotropic virus (MPtV) [39] have different receptors.

Because sialic acid is present on (almost) all cells, the natural tropism of polyomaviruses is very broad. Most polyomaviruses can infect many different cell types and tissues [40]. Some polyoma-

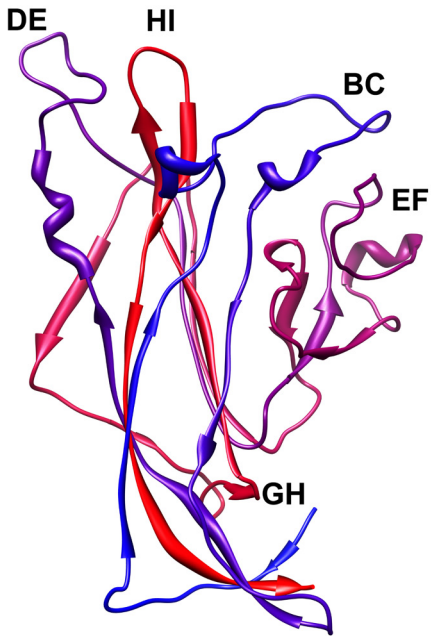

Figure 2. SV40 VP1 displaying its interior loop GH and its surface-exposed loops BC, DE, EF and HI. The image was created from PDB: 3BWQ [17] using Chimera [23].

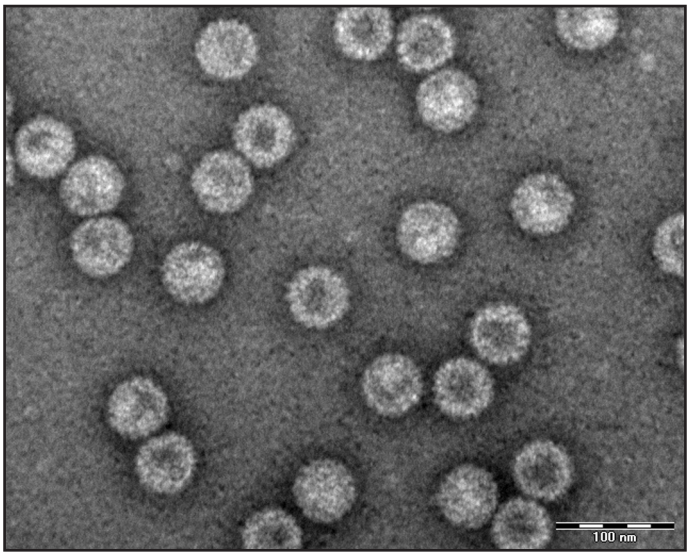

Figure 3. Transmission electron microscopy (TEM) picture of HaPyV VP1 VLPs produced in *E. coli*. After lysis the VLPs were purified by sequential (ultra)centrifugation. Bar = 100 nm.

viruses have a very limited tropism, such as the beta-lymphotropic polyomavirus (LPyV) [41].

2.3. Replication and assembly

After attachment most polyomaviruses are internalized in caveolae [36,42]. JC virus, on the other hand, uses clathrin-dependent endocytosis [43]. The viruses are subsequently transported along microtubules [42,44] to the endoplasmic reticulum (ER) [45], where the viruses are partially uncoated [46–48]. Nuclear targeting is mediated by the NLS of the capsid proteins [49], and nuclear entry is promoted by VP2/3 [50,51].

Replication and assembly of the virus occurs in the nucleus, and nuclear localization of VP1 after translation is achieved by its NLS [28,29]. The high calcium concentration in the nucleus is required for the formation of VLPs [52,53].

In eukaryotic systems, chaperones of the hsp70 family bind VP1 after translation and move with it to the nucleus [54]. Association of VP1 with hsp70 occurs at the C-terminal domain of VP1, preventing premature calcium-mediated assembly of virions [55]. When recombinantly producing VP1 in prokaryotic systems, the hsp70 homolog DnaK performs the same function [54]. However, by supplying additional members of the prokaryotic hsp70 family, or the J-domain of the SV40 large T antigen, capsid assembly can take place without calcium [55].

As far as is currently known [56], only the SV40 genome contains a packaging signal [57]. This signal, *ses*, can bind transcription factors Sp1 and AP-2 [58]. These transcription factors recruit viral proteins to *ses*, conferring packaging specificity [59]. However, *ses* is not required for naked DNA packaging into SV40 VLPs [60], nor is DNA packaging required for virion formation. After replication, both DNA-loaded virions and empty virions are observed [61]. One report claims that these empty particles are artifacts formed during purification as the result of CsCl centrifugation [62].

2.4. Virus-like particles

Salunke *et al.* were the first to demonstrate the formation of polyomavirus virus-like particles [5].

Table 1. Different systems used for the recombinant production of VP1.

Production system	Post-translational modifications	Nucleic acid contamination	Yield
Prokaryotic production systems	No	A lot [93]	4.38 g per liter (GST-VP1) [94]
Yeast	Yes	Negligible [24,31,74,95,96]	0.2 g per liter (VP1) [97]
Insect cells	Yes	A lot [41,98]	1 mg per liter (VLP) [41] 4 mg per liter (VP1) [99]
Mammalian cells	Yes	Yes [100,101]	1 mg per 225 cm^2 flask (VLP) [100,101]
Cell-free expression	Depends on the system used	Yes	40 mg per liter (VP1) [102]

This was achieved by exposing MPyV VP1 to high ionic strength after overexpression in *Escherichia coli* [63]. These particles resemble the native viral capsid in structure, tropism and transduction efficiency, but do not contain any viral genetic material (see figure 3). These VLPs are not post-translationally modified, in contrast to wild-type virions, which are extensively modified by acetylation and phosphorylation [64–66]. Many PyV VLPs are able to agglutinate erythrocytes [67–70], although at least SV40, HaPyV [71], MPtV [39] chimpanzee polyomavirus (ChPyV) [72] and finch polyomavirus (FPyV) [70] lack this ability.

PyV VLPs are stable for over a month at 4 °C in high salt (> 1 M), and can be further stabilized at lower ionic strength (0.15 M) by addition of calcium (0.5 mM) [5]. No morphological or immunological changes were observed after storage in phosphate buffered saline (PBS) at room temperature for at least 9 weeks [73]. PyV VLPs can be lyophilized and re-dissolved while remaining stable [74,75].

The VLPs are stabilized by disulfide bonds and calcium ions, and both need to be broken or removed to disassemble VLPs [76,77]. Under certain conditions, disulfide bonds do not seem to be necessary for VLP formation for MPyV [78]. However, mutation of all disulfide bonds in SV40 prevented the formation of VLPs [79], although no individual disulfide bond is required for SV40 virion formation [80]. Calcium ions stabilize VLPs by strengthening the bonds between capsomers [6,10,11]. Calcium plays a crucial role in the assembly and disassembly of PyV during infection [46]. Nuclear chaperones also aid the formation [55,60] and disassembly [81] of PyV. It has been shown that DNA inhibits VLP assembly [8]. However, studies with MPyV [82] and SV40 [83,84] indicated the opposite, showing that VLP assembly is in fact induced by DNA, even under dissociating conditions [82,84].

Next to being composed solely of VP1, VLPs can also be constructed using VP1 and the minor capsid proteins VP2 and VP3 [85]. VP2/3 can promote the assembly of VLPs under otherwise dissociating conditions [86]. Early reports using transmission electron microscopy (TEM) found these VLPs to be morphologically indistinguishable from VP1 VLPs [85]. Later reports using the more sensitive asymmetrical-flow field flow fractionation (AFFFF) with multiple-angle light scattering (MALS) showed that VLPs undergo morphological changes upon encapsulation of DNA and proteins [87–89].

Apart from the formation of $T=7$ icosahedral VLPs, it was also shown that VP1 can form other structures, depending on the solvent/buffer conditions, including smaller $T=1$ and octahedral capsids [90–92].

3. Production systems

Different production hosts can be used for the expression and formation of PyV VLPs. The application of these hosts for the production of PyV VLPs will be discussed below, along with their advantages and disadvantages. For a summary, see tables 1 and 2, and figure 4.

Table 2. List of polyomaviruses along with the different systems in which their VLPs have been successfully produced. Only polyomaviruses for which at least one report showed the formation of VLPs have been included in the list.

Abbreviation	Full name	Forms VLPs after production in			
		Prokaryotic production systems	Yeast	Insect cells	Mammalian cells
LPyV	Beta-lymphotropic polyomavirus			Yes [41]	
BKPyV	BK polyomavirus		Yes [95,96]	Yes [103]	Yes [101]
APyV	Avian polyomavirus (Budgerigar fledgling disease polyomavirus)	Yes [104]	Yes [96]	Yes [105]	Yes [106]
HaPyV	Hamster polyomavirus	Yes [9]	Yes [31]	Yes [9]	
JCPyV	JC polyomavirus	Yes [93]	Yes [76]	Yes [77]	Yes [107]
MPtV	Murine pneumotropic virus			Yes [39]	
MPyV	Murine polyomavirus	Yes [5]	Yes [96]	Yes [52,98]	Yes [100]
SV40	Simian virus 40	Yes [108]	Yes [96]	Yes [85]	
MCPyV[a]	Merkel cell polyomavirus			Yes [109]	Yes [100]
ChPyV[a]	Chimpanzee polyomavirus		Yes [72]		
CPyV[a]	Crow polyomavirus		Yes [70]		
FPyV[a]	Finch polyomavirus		Yes [70]		
HPyV6[a]	Human polyomavirus 6			Yes [110]	
HPyV7[a]	Human polyomavirus 7			Yes [110]	
HPyV9[a]	Human polyomavirus 9			Yes [111]	
TSPyV[a]	Trichodysplasia spinulosa-associated polyomavirus			Yes [112]	
GHPyV[a]	Goose hemorrhagic polyomavirus		Yes, with VP2 [113]	Yes [113]	

[a]Not officially classified as polyomavirus

3.1. Prokaryotic production systems

Bacteria were the first organisms to be used for the overexpression of VP1 [63] and production of PyV VLPs [5]. Since then, many other VLPs have been produced in prokaryotes (table 2). In all cases we could find, the production host was *Escherichia coli* (*E. coli*). VP1 produced in bacteria, in contrast to VP1 produced in eukaryotes, lacks post-translational modifications [5]. Assembly of VLPs usually does not occur within the bacteria, but rather as a result of the purification process [5,104], although JCPyV [93] and HaPyV [9] were shown to form VLPs inside bacteria.

VLPs purified from *E. coli* are frequently contaminated with nucleic acids. For example, JCPyV VLPs were associated with host DNA (~20 kb) and RNA (<2 kb) [93]. Such contaminations can be removed by reassembling the VLPs before use (see figure 4) [82,114]. However, this has a negative impact on the yield. After reassembly, the yield was only 1.5–1.8 mg MPyV VP1 per liter of bacterial culture [82]. Without optimization or reassembly the yields can be as high as 15 % total soluble cellular protein (10–15 mg per gram wet bacterial weight), as described for HaPyV [9]. More recently, Middelberg *et al.* have published several reports on an *E. coli* based platform for the large-scale production and purification of MPyV VLPs [94,115–118]. They investigated the effect of the host strain, expression

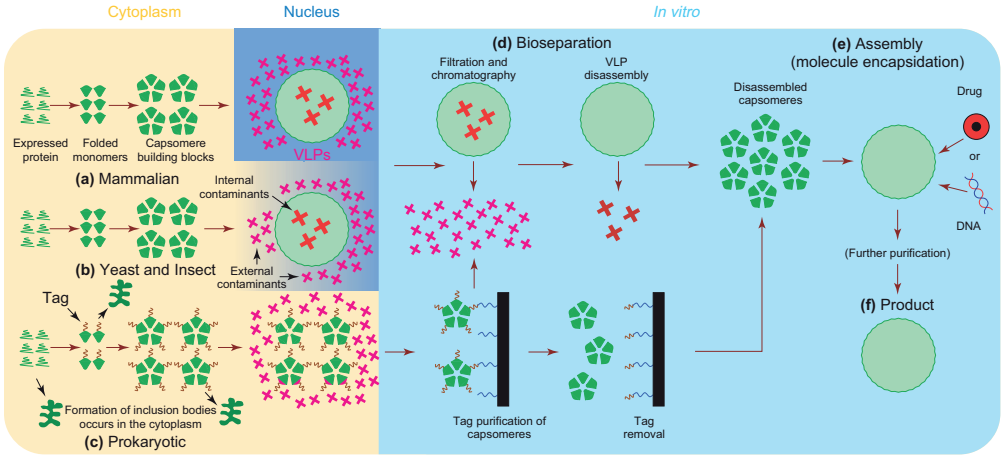

Figure 4. Production and purification of PyV VLPs. In eukaryotic expression systems VLPs form in the nucleus (and sometimes in the cytoplasm) (a, b), while in prokaryotic expression systems VLPs generally do not form (c). After lysis VLPs are purified, followed by their disassembly into capsomers to remove internal contaminants (d). In the case of VP1 fusion tag constructs, VP1 capsomers are purified by affinity chromatography followed by cleavage of the fusion tag. The capsomers are finally reassembled to form VLPs (e). Different cargos can be added during the reassembly, resulting in their encapsidation within the VLPs. These VLPs are then purified and formulated, leading to the final product (f). Reproduced with permission from reference [114].

plasmid, and culture conditions on the expression. After optimization a yield of up to 180 mg soluble MPyV VP1 per liter of medium, or 90 mg per liter of medium for an easy-to-purify glutathione S-transferase (GST) VP1 fusion, was achieved in low-density shake flask cultures [115]. In high-density fed-batch cultures, yields of up to 4.38 g GST VP1 fusion per liter of medium were reached [94]. Although GST VP1 exists as large soluble aggregates, pure VP1 pentamers are obtained after cleavage of the tag [119], which can be reassembled to form VLPs [117,118]. Because bacteria do not require expensive serum-containing media, this allows for the cheap production of large quantities of VLPs. However, complete removal of the fusion tag, a requirement for pharmaceutical formulations, can pose a problem during manufacture.

3.2. Eukaryotic production systems

3.2.1. Yeast

Another well-established system for the production of VLPs is yeast, where *Saccharomyces cerevisiae* (*S. cerevisiae*) is typically used for this production. Its GRAS (generally recognized as safe) status makes it perfectly suitable for the production of therapeutics [31], and thus the human papillomavirus (HPV) vaccine Gardasil® is produced in yeast [120].

The first PyV VLPs produced in yeast were HaPyV VLPs [31]. Authentic VP1 yielded VLPs mainly in the cytoplasm, while N-terminally extended VP1 VLPs were found both in the nucleus and in the cytoplasm [31]. This was in contrast to the same VP1 expressed in insect cells, where VLPs were found only in the nucleus [9]. The particles appeared to be devoid of DNA, and only traces of RNA were found [24,31,74], making them suitable for vaccination purposes. While this is generally the case for yeast-produced VLPs, one study showed host and plasmid DNA uptake during production, although this DNA was not associated with host histones [97]. The yield of recombinant VP1 was 5–10 % of the total soluble protein (0.1–0.2 g per liter of medium) [24]. Later, the same group showed the expression of JCPyV, BKPyV [95], SV40, MPyV and avian polyomavirus (APyV) VLPs [96]. In all cases, DNA contamina-

tion was minor, and could be removed completely by dialysis and nuclease treatment without reassembly. The yield of VLPs was around 40 mg per liter of medium, except for APyV, which was only 5 mg per liter of medium. In this case less VLPs were formed, while a regular amount of VP1 was expressed.

Not all yeast strains work equally well for the production of PyV VLPs [97]. Sasnauskas *et al.* tested several yeast strains, and found that induction of expression caused growth inhibition in several of the assayed strains. *S. cerevisiae* AH22 was found to be optimal with no noticeable growth inhibition [96].

3.2.2. Insect cells

Expression in insect cells allows the formation of VLPs closely similar to the wild-type. The system is well established and commercially used for the production of the HPV vaccine Cervarix® [121]. When PyV VLPs are produced in insect cells, this is typically done using the well-characterized baculovirus expression system with *Spodoptera frugiperda* (Sf) cells. Different cell lines can be used for VLP production. For example, JCPyV VP1 was expressed in Sf21 cells [77] and Sf158 cells [122]. VP1 is expressed in the cytoplasm, and then transported to the nucleus using its own NLS, where it self-assembles to form VLPs [77].

VLPs produced in insect cells are contaminated with both host and baculovirus derived DNA. One study showed that 65 % of LPyV VLPs were filled after assembly in Sf9 cells [41]. Based on their DNA content, at least 10 % of the particles contained a 4.5 kb DNA fragment. The DNA was linear dsDNA, and derived from both host and baculovirus. Furthermore, they showed that longer incubation times resulted in higher expression levels, but also higher DNA contamination. The same was found with MPyV produced in Sf9 cells [98]. The purified VLP fractions also contained histones, indicative of DNA packaging. It was shown that DNA uptake is preceded by fragmentation of the cellular genomic DNA by the baculovirus [98]. After dissociation of the VLPs during purification, these contaminations can be removed by strong anion exchange chromatography, followed by reassembly of the VLPs (see figure 4) [89].

Yields are rather low, with 1 mg LPyV VLPs per liter of culture in Sf9 cells [41], or 2–3 mg purified and reassembled JCPyV VLPs per liter of culture in Sf158 cells [89].

One of the advantages of the baculovirus expression system is that several different proteins can easily be expressed in the same cell, making it possible to produce VLPs composed of more than one viral protein. This has been done for several polyomaviruses, including SV40 in Sf6 [85] and Sf9 [60,123] cells and MPyV in Sf9 [124–127] cells, where VLPs based on VP1, VP2 and VP3 were produced. These VLPs comprised the three structural proteins in the same ratios as wild-type virions [126]. Next to the production of VP1–3 at the same time, insect cells have also been used to produce different chimeric VP1 molecules simultaneously, such as the production of MPyV VP1 with a fragment of urokinase plasminogen activator in the EF loop, and another VP1 with a FLAG epitope in the HI loop, forming hybrid VLPs [128]. Likewise, MPyV VP1 was co-expressed with the C-terminal part of VP2 linked to enhanced green fluorescent protein (EGFP), forming VLPs with EGFP inside [129]. Similar results have been obtained for other proteins [87,130–133].

Insect cells can also be used for the production of PyV VLPs without baculovirus by vector-based expression. HaPyV [9] and MPyV [99] VP1s were expressed in *Drosophila* S2 cells, leading to the production of their respective VLPs, which accumulated in the nucleus. This way, the yield of VP1 can be as high as 4 mg per liter of culture [99].

3.2.3. Mammalian cells

Mammalian cells are normally not used for the production of VLPs, primarily because of their low yields, expensive serum-containing media, and the

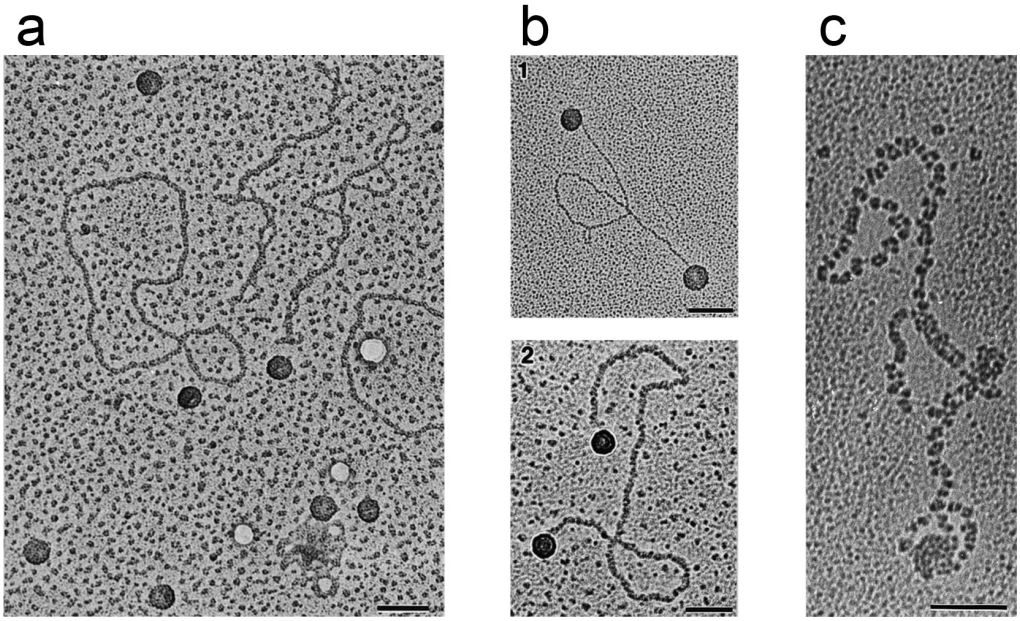

Figure 5. Association of MPyV VLPs and capsomers with DNA after osmotic shock; (a) VLPs with circular plasmid DNA; (b) VLPs with linearized plasmid DNA; (c) capsomers with DNA. A 6.2 kb plasmid (pCDNA3-CAT) was used. Reproduced with permission from reference [143]. Bars = 100 nm.

inherent risk of contaminating viruses, although several reports of their utilization exist. APyV VLPs were produced in chicken embryo cells [106], JC virus VLPs were produced in COS-7 cells after transfection with a construct coding for VP1–3 [107] and 293TT cells were used for the expression of BKPyV, MPyV and Merkel cell polyomavirus (MCPyV) VLPs consisting of VP1 + VP2 [100,101]. VLP yields were rather low, ranging from several micrograms to 1 mg per 225 cm^2 flask. Cellular and plasmid DNA was co-purified with the VLPs, but this was not further investigated.

3.3. Cell-free expression

Next to *in vivo* production of proteins, *in vitro* production is also possible using cell-free expression systems [134]. Cell-free production of VP1 from viral mRNA was already reported a long time ago in wheat germ cell-free expression system for MPyV [135,136], and SV40 in wheat germ [137,138], rabbit reticulocyte lysate [137] and Chinese hamster ovary cell extract [138]. Pentamers and aggregates of up to 700 kDa of SV40 VP1 have been produced in rabbit reticulocyte lysates [79,102]. However, the assembly of this cell-free produced VP1 into VLPs has not been shown so far. The yields are generally very low, with reported yields up to 40 µg/ml for SV40 VP1 [102]. Moreover, cell-free produced VP1 showed different disulfide bonding than insect produced VP1, possibly due to oxidation [139].

4. Preparation of DNA-loaded PyV VLPs

The interior of PyV VLPs is shielded from the environment, allowing VLPs to protect their cargo from degradation and specifically deliver their cargo to target cells, making them attractive carriers for the delivery of therapeutics. To benefit from these

properties, the therapeutics have to be loaded into the VLPs. Several methods have been developed to load therapeutics, particularly nucleic acids, into VLPs, which will be discussed below.

4.1. Osmotic shock

The osmotic shock method was first described by Barr *et al.* in 1979 for empty MPyV capsids (isolated from MPyV-infected cells) and is based on lowering of the ionic strength and thus increasing the electrostatic interaction between DNA and VLPs [140]. Nucleic acids, both single and double-stranded DNA molecules, and RNA molecules, can be taken up using osmotic shock [141,142]. The uptake was shown to be irrespective of the primary, secondary, or tertiary structure of the nucleic acids. The formed polyoma-like particles (PLPs) protect their nucleic acid content against nuclease activity up to approximately 2 kb. Most likely, the remainder of the nucleic acid chain remains outside the PLP and can be degraded by nucleases [141]. While empty virions can bind DNA without this osmotic shock [61], the DNA is not protected against DNases.
Similar results have been obtained for recombinant VP1 VLPs. After osmotic shock MPyV VLPs seem to attach strongly to ends of DNA strands and less strongly along DNA strands, clearly visualized by electron microscopy (see figure 5a and 5b) [143]. VP1 capsomers completely coat DNA molecules instead (see figure 5c). However, this did not result in DNaseI protection [143]. Filled VLPs cannot bind additional DNA during osmotic shock [143].
Osmotic shock results in partial protection against nucleases [82]. Based on the reduction in size as visualized by TEM of linear plasmids with VLPs attached, the encapsidated length was found to be around 1.2 kb per VLP. This resulted in DNaseI protection of about 2.5 kb DNA of the 6.2 kb plasmid used [143]. Another study with MPyV showed that DNaseI treatment of complexes with a 6.2 kb plasmid yielded protection of fragments up to only 2 kb, while 5–10 % of linear 1.6 kb DNA fragments could be fully protected against DNaseI after osmotic shock [144]. Similar results were obtained with JCPyV VLPs [145]. Another report describes no protection [146]. These complexes could, however, be used for transfections *in vitro* and *in vivo* [146]. Likewise, Ou *et al.* showed transfection with pEGFP-C1 despite treatment with DNaseI, although no transfection efficiency is stated [93]. It was shown for MPyV that larger VLP/DNA complexes result in higher transfection efficiency than smaller complexes, with an optimum of 5 VLPs per DNA molecule [44].
DNA uptake is pH-dependent with higher loading at pH 5 than pH 7.2 [82]. An encapsidation yield of up to 260 ng of a 3.9 kb plasmid / µg VP1 was obtained. It was found, however, that osmotic shock did not influence the protection of plasmid DNA. DNase digestion assays clearly showed that DNA digestion was delayed by VP1 binding, but still complete. It was even shown that the samples with DNA directly mixed without osmotic shock showed better DNase protection.
Oligonucleotides can also be loaded by osmotic shock, and this process too is pH-dependent, with a higher uptake at acidic pH [82,147]. Oligonucleotides were incorporated by osmotic shock up to 28 ng/µg VP1. This corresponds to approximately 1 oligonucleotide per VP1 capsomer. Up to 55 % was protected against DNase action, though this depended on the DNase concentration.

4.2. Reassembly

Unlike osmotic shock, which does not result in full disassembly of the VLPs, exposure of VLPs to specific conditions can allow the capsomers to be fully dissociated and reassembled to form VLPs again. If this happens in the presence of genetic material or other therapeutics, these compounds can be taken up in a (sequence) independent fashion. Reassembly was first reported in 1986 by Salunke *et al.* [5]. Purification of MPyV VP1 after expression in *E. coli* yielded capsomers, which could be assembled to form VLPs *in vitro* by exposure to high ionic strength.

Generally, to perform controlled reassembly, VLPs are first incubated in a buffer with a chelating agent (typically EGTA or EDTA) and a reducing agent (DTT) for a short period of time (30 min) and mixed with the target DNA. This mixture is then dialyzed against a buffer with calcium and usually a higher ionic strength, although this higher ionic strength might not be necessary [103]. Host-derived factors, such as chaperones, can be included to facilitate the assembly [60,148].

Using this method VLPs can package approximately 5 kb DNA, the same size as the normal polyomavirus genome, without the aid of VP2, VP3, or the T antigens [98,148]. Shorter DNA fragments result in the packaging of multiple copies in the same VLP. For example, on average 2.9 copies of 600 bp DNA could be encapsidated per SV40 VLP [84]. Not only nucleic acids, but also small molecules [149], DNA dendrimers [147], peptide nucleic acids [150], quantum dots [151] and gold nanoparticles [152] have been encapsidated within PyV VLPs by reassembly.

Not much is known about the encapsidation efficiency, although one report stated that 10 µg of VLPs yielded only 10 ng of DNA, even though an excess of DNA had been used during reassembly [9]. This very low efficiency might have been caused by losses during recovery, although it is later stated that the majority of the VLPs did not contain DNA after reassembly. If the reassembly reaction is carried out in the presence of host-derived factors, such as in Sf9 nuclear extract [148], this results in very efficient packaging. After CsCl purification, one plasmid per SV40 VP1 VLP was found. Moreover, full protection of this 5 kb pGL3 plasmid against DNaseI was observed. Another group showed that addition of hyper-acetylated histones and VP2/3 improved packaging and protection of up to 5.2 kb DNA in SV40 VLPs [153]. Kimchi-Sarfaty *et al.* even reported the delivery of up to 17.6 kb DNA to cells after *in vitro* assembly of SV40 VLPs [154], a modified version of reassembly using nuclear lysate.

Goldmann *et al.* compared reassembly with osmotic shock using JCPyV VLPs and the 4.5 kb pCMV-β-Gal. Reassembly was found to be far superior to osmotic shock. Using reassembly, they could reach a plateau encapsidation efficiency of around 30 % [122].

One of the main advantages of this method is that the resulting VLPs are basically free from host nucleic acids and other contaminants, as these can be removed prior to reassembly [9,89]. This is especially important for VLPs produced in insect cells, as these VLPs are shown to be heavily contaminated with host DNA (see section 3.2.2). The reassembly efficiency, however, is only around 50 % [149], resulting in a clear loss of product.

4.3. Direct interaction

VLPs can also be mixed with DNA without any further treatment. This method has been used for the encapsidation of DNA with mixed results.

Some studies show that DNase digestion is delayed [82], while others report no protection at all [9]. In the last case, however, loaded VLPs were used, which might have prevented the interaction with additional DNA. Capsids filled with host DNA cannot be used for direct interaction, as they do not interact with plasmid DNA [44]. Clark *et al.* tested direct interaction at different MPyV VLP:DNA ratios for transfection efficiency of COS-7 cells with 7.2 kb pCMVβ. However, none of the ratios tested yielded significantly higher transfection efficiency than naked DNA [155].

Just like osmotic shock, loading using direct interaction was shown to be pH-dependent, at least for an MPyV mutant with extra glutamic acids inserted into the coat. Loading occurred at pH 5, but no DNA binding took place at pH 7 [156].

Touze *et al.* compared different loading methods (osmotic shock, reassembly and direct interaction) using BKPyV, and found direct interaction between VLPs and linearized reporter plasmids to be the most efficient [103]. Not only did this result in the highest transfection efficiency, it also resulted in the highest DNase protection, although all three methods resulted in protection. Just as with osmotic shock, DNA is not taken up by the VLPs,

but the VLPs associate with the DNA as beads on a string [82,103]. It must be mentioned that the DNA used in their studies was larger (7.1 kb) than the uptake limit of the capsid, which might have reduced the reassembly efficiency. In contrast to the other methods, the size of the DNA is not that limiting with direct interaction.

4.4. Co-expression

By replacing SV40 viral genes with genes of interest, while maintaining the packaging signal, *ses*, a replication-incompetent viral genome is created which can be packaged into SV40 capsids. If this genome is transfected into cells which express the large T antigen, such as COS cells, and the capsid genes are provided *in trans*, this genome can be efficiently encapsidated within virions [157]. These particles are, however, not true VLPs, as they still contain viral genetic information.
Recently Chen *et al.* showed that it is possible to perform a similar method without encapsidating viral DNA sequences [158,159]. Here, both the expression plasmid encoding VP1 and the cargo plasmid are transformed into *E. coli*. VP1 is then produced, and the cargo plasmid is encapsidated. This was successfully done packaging 4.7 kb pEGFP-N3 and 5.1 kb pUMVC1-tk in JCPyV VLPs [158]. These VLPs could be used for transfection, with no loss in efficiency found after DNaseI treatment, showing full protection. In a later report, the same group showed the packaging of up to 9.4 kb in the form of two fused pEGFP-C1 plasmids [160]. However, they did not analyze whether whole plasmids had been encapsidated, or that truncations occurred prior to or after packaging. Furthermore, they also showed that the VP1 expression plasmid contaminated the produced VLPs. They did not test if VLPs were further contaminated with host nucleic acids, which might be expected based on previous results [93]. Contaminations form a major problem with this method, as there is no control over which plasmid is encapsidated.
Similar results had already been published by Pastrana *et al.* after expression of MCPyV VP1 and VP2 in eukaryotic 293TT cells along with pEGFP-N1 [101]. They showed that a fraction of the produced VLPs had encapsidated the reporter plasmid, enough for transfection of HeLa cells. MCPyV, MPyV and BKPyV VLPs were also produced in the same cells harboring phGluc, which could be used for serological neutralization tests with 293TT cells [101].

5. Cargo

5.1. Nucleic acids

Among the different classes of therapeutics, nucleic acids tend to benefit the most from being delivered by VLPs. This has spawned a great number of investigations into the encapsidation capabilities of VLPs for nucleic acids.
During production in several hosts both DNA and RNA are already loaded into VLPs as contaminants (see section 3). These contaminants have to be removed first, before the VLPs can be used.
However, loading nucleic acids into VLPs is not as easy as it may seem, and with most methods the nucleic acids are not fully encapsidated by the VLPs and therefore prone to degradation by nucleases (see section 4).

5.1.1. Plasmid DNA

Plasmid DNA can be taken up by polyomaviruses in a sequence-independent way. This can be done both during expression and later by osmotic shock, reassembly or simply mixing DNA with VLPs (see section 4).
Generally, sequences of up to 2.5 kb are protected against DNases after osmotic shock [143,144]. With direct interaction, the results are mixed, with some groups reporting encapsidation of plasmids as large as 7.1 kb [103], while others report no protection at all [9]. Plasmids up to the size of the polyomavirus genome, 5 kb, can be encapsidated by re-

assembly and protected against DNases [9,122,148,153], although *in vitro* packaged SV40 VLPs reported to package up to 17.6 kb [154]. Similar results were obtained with co-expression, where plasmids of up to 5 kb could be encapsidated and protected against DNases [101,158]. Recently, encapsidation of up to 9.4 kb was shown using this method [160].

5.1.2. Linear DNA

PyV VLPs can also take up linear DNA, including restriction fragments [144], linearized plasmids [103,143] and PCR products [145,161]. Packaging of linear DNA seems to be slightly more efficient than circular DNA [103], while protection is similar to plasmid DNA [145].

5.1.3. Oligonucleotides

Loading of oligonucleotides is generally easier than loading of plasmid DNA, as DNase digestion poses fewer challenges [82]. Braun *et al.* showed the successful incorporation of two different 18-mer antisense oligonucleotides into MPyV VLPs by osmotic shock, with a yield of up to 28 ng/µg VP1 [82]. The same group later showed the encapsidation and delivery of a 19-mer ssDNA fragment to NIH 3T3 mouse fibroblasts [147]. JCPyV VLPs were used in a similar approach to package 21-mer ssDNA [145].
In addition to normal oligonucleotides, short 15-mer peptide nucleic acids (PNA) can also packaged in SV40 by reassembly [150].

5.1.4. RNA

RNA is normally not encapsidated by polyomavirus VLPs *in vitro* or *in vivo*. Ou *et al.* speculate that eukaryotic chaperones may prevent the interaction between RNA and VP1 [93]. However, PLPs can encapsidate RNA, although not as efficiently as DNA [141], and host RNA frequently contaminates recombinant VLPs (see section 3).
One report describes the packaging of synthetic siRNA by reassembly and its delivery to cells [162], while another recent report describes the encapsidation of short 75-mer tRNAs, 500-mer and 800-mer RNA molecules in SV40 VLPs after reassembly [163]. The formed particles displayed the smaller T=1 conformation and each contained either one 500-mer RNA molecule, or two 75-mer tRNAs. However, the binding affinity of RNA to VP1 was found to be much lower than that of DNA.

5.1.5. DNA dendrimers

DNA dendrimers, prepared using the polycationic dendrimer SuperFect reagent and an 1.8 kb dsDNA fragment could be incorporated into MPyV VLPs during reassembly. Dendrimers produced with the 4.7 kb pEGFP-N1 were not encapsidated [147].

5.2. Proteins

Another class of biopharmaceuticals that would benefit from the delivery by VLPs is proteins. VLPs provide ample space for proteins. Theoretically, over 400 GFP molecules would fit into a single VLP [164].
Proteins are mainly loaded into PyV VLPs through fusion to (truncated) VP2/3, allowing the C-terminus of VP2 to interact with capsomers. For example, by fusion to the N-terminus of a 49 aa linker of C-terminal VP2, GFP could be loaded into MPyV VLPs at 64 GFP per VLP [164]. Inoue *et al.* compared linkage of EGFP to the N- and C-terminus of VP2 and several of its truncations [133]. Of the tested fusion constructs, only C-terminal fusions resulted in regularly shaped VLPs, and fusion to a 36 aa C-terminal portion of VP2 was sufficient for encapsidation. Another group, however, found that N-terminal linkage to a 225 aa linker worked better than the shorter ones [165]. Many different proteins have been loaded using VP2, including the 683 aa transmembrane domain of HER2 [130–132] and the whole prostate specific antigen (PSA) [166]. The loading efficiency varies quite a lot, ranging from 1–2 HER2-VP2 fusions per MPtV VLP [130] to 64 GFP per MPyV VLP [164].

The fusion proteins can be encapsidated *in vitro* by reassembly [164,165] or *in vivo* by co-expression in insect cells [87,88,129–131]. Co-expression prevented the encapsidation of host DNA, which the authors ascribed to a different localization in the nucleus due to the fusion protein [88].

Protein-loaded VLPs are stable for several months at −80 °C [164] and for at least 1 month at 4 °C [129]. Packaged enzymes retain their enzymatic activity, as was shown for yeast cytosine deaminase [133] and *Gaussia* luciferase [167]. Because small molecules can penetrate the VLP, the enzymes could successfully convert their substrates from within the VLPs [133,167].

Normally, the C- and N-terminal VP2/3 fusion proteins remain hidden within the VLP and are not accessible to large molecules such as antibodies [130–132,166,168–170]. However, recent reports show that fusion of different proteins to the N-terminus of truncated VP2 resulted in the formation of HaPyV VLPs displaying the antigens on the outside of the VLP [171,172].

Next to fusions to (truncated) VP2/3, proteins can also be linked to the N-terminus of VP1. This was done through a polyproline-binding WW domain, which was fused to the N-terminus of MPyV VP1. The produced VLPs were able to bind polyproline-tagged proteins. 230 PPLP-tagged peptides, or 260 PPLP-tagged GFP molecules could be encapsidated per VLP, significantly more than what has been achieved using VP2/3. These particles could be delivered to NIH 3T3 cells, showing uptake [173].

5.3. Small molecules

Low-molecular weight drugs can be loaded into VLPs by covalent linkage. Methotrexate was loaded into MPyV VLPs at 462 methotrexate molecules per VLP by covalently linking the drug to the same 49 aa VP2 linker mentioned above [164]. The drug could be delivered to methotrexate sensitive CCRF-CEM cells, showing clear concentration-dependent toxicity of methotrexate in these cells. Another method to link molecules to VLPs involved mutating MPyV VP1 removing all cysteines and introducing a new cysteine in the GH loop on the interior of the VLP (see figure 2) [174]. This way it was possible to link fluorescent dyes using a maleimide linker. The particles retained their receptor binding capacity and were taken up by C2C12 mouse cells.

Non-covalent linkage is possible using a His_6-tag fused to the N-terminus of a 225 aa VP2 linker. This way, molecules coupled to nitrilotriacetic acid (NTA), such as the fluorescent dye sulforhodamine 101 (SR101), could be taken up by JCPyV VLPs [165]. Because this link is pH-dependent, these particles can be used for pH-dependent release. A recent report also showed the non-covalent linkage of hydrophobic molecules such as paclitaxel (PTX) using β-cyclodextrin coupled to VP1 of JCPyV [175]. Up to 12.3 PTX could be loaded per VLP, and a clear cytotoxic effect could be observed after addition of PTX-VLPs to NIH 3T3 cells.

Small molecules can also be loaded into VLPs without the use of a linker. The fluorescent dye propidium iodide was packaged into JCPyV VLPs by reassembly [149]. No packaging capacity was reported.

5.4. Other

Larger structures, such as gold nanoparticles [152], magnetic nanoparticles [176] and quantum dots [151], have been encapsidated in SV40 VLPs. Packaging of quantum dots was achieved by reassembly, resulting in smaller T=1 VLPs with one quantum dot per VLP. These VLPs were taken up by cells following the same route as wild-type SV40.

6. Applications

VLPs can be used to study not only the intrinsic properties of viruses, such as their structure [76] and assembly [7], but also the interaction of viruses with their environment, such as their binding to cells [20], their uptake by cells [177] and intracellular trafficking [178]. This is especially helpful in cases where the wild-type virus cannot easily be cul-

tured in cells [113]. Apart from these basic research topics, VLPs can be used for biomedical applications such as vaccination, gene delivery and diagnostics. These three fields will be discussed in the following sections.

6.1. Diagnostics

Because VLPs resemble their native parent virion in their antigenic structure, they can be used for diagnostic purposes. Applications include ELISA [70,72,100,109–111,113,179–182], where VLPs act as antigens to detect antibodies against the native virus in serum, or more specific haemagglutination inhibition assays [70].

The VLPs are particularly valuable for the detection of viruses which cannot easily be cultured. One example is goose hemorrhagic polyomavirus (GHPyV). While GHPyV normally cannot be propagated in cell culture, VLPs could be generated in insect cells and yeast [113]. These VLPs could subsequently be used as antigens in serological tests.

Next to enzyme-linked immunoassays, a neutralization assay was developed for MCPyV, BKPyV, and MPyV, based on VLPs encapsidating a reporter gene construct [101]. Addition of neutralizing antibodies during transfection reduces transfection efficiency, and thus allows quantification of antibody titers.

Despite their usefulness in these cases, two problems might prevent the use of VLPs in a clinical setting. First, during infection, antibodies are produced not only against VP1, but also against the other viral proteins, such as the T antigens. Because these VLPs consist solely of VP1 or VP1+VP2/3, these antibodies would not be detected. Second, just as for gene therapy, cross-reactivity of sera with different VLPs forms a significant problem [96,181,183], resulting in a high rate of false positives.

6.2. Vaccines

VLPs provide a safe alternative to attenuated and inactivated virus vaccines, as they mimic their parent virus in antigenic structure, while lacking the viral genetic material and the associated risks of recombination and reversion. Due to their repetitive structure, VLPs can activate the immune system via pattern-recognition receptors on immune cells and cross-link B-cell receptors, leading to a potent immune response [184]. This allows VLPs to be used as vaccines without the need of an adjuvant. Several VLP-based vaccines are under clinical investigation [185,186], and some are already available on the market, such as the prophylactic HPV vaccines Gardasil® [187] and Cervarix® [121].

In a similar fashion polyomavirus VLPs can be designed to vaccinate against the native PyV capsid, but foreign epitopes can also be inserted into variable loops on the surface of the VLP (see figure 2) to induce both humoral and cellular responses against these epitopes [188]. Furthermore, large antigens can be fused to (truncated) VP2/3, resulting in strong T-cell mediated immune responses and even breaking of tolerance. Finally, VLPs can be loaded with plasmids encoding antigens [155,189] and are rapidly taken up by dendritic cells (DCs) [190], thus showing potential for DNA vaccination.

6.2.1. Vaccines against the native polyomavirus capsid

Most mammalian polyomaviruses are generally asymptomatic, rendering prophylactic vaccination cost-ineffective. Avian polyomaviruses, on the other hand, cause a much more acute disease, associated with high mortality. Using VLPs produced in insect cells, a vaccine was produced against GHPV, which protected 95 % of the animals after one single administration, and protected all animals after a boosted administration [191].

In vitro studies showed that some PyV VLPs are able to activate DCs. HaPyV VLPs were added to immature murine spleen-derived DCs in culture [190]. After uptake the VLPs were able to activate the DCs, as was evident from IL-12 production and the activation of naïve T-helper cells by the DCs. Similarly, HaPyV and MPyV VLPs were able to activate

human DCs, while VLPs derived from SV40, BKPyV and JCPyV were not [71].

The repetitive structure of VLPs is crucial for a good T-cell independent humoral response. This is clearly shown by comparing vaccination with VLPs and vaccination with VP1 capsomers. A single intraperitoneal injection of MPyV VLPs produced 10 times higher IgM titers in T-cell deficient mice than the injection of VP1 alone [192]. An anti-VP1 IgG response was possible in T-cell deficient mice by using a 30 times higher dose of VLPs and repeating the injection 4 times [193]. Cytokine secretion after immunization with MPyV VP1 pentamers was also 10–20 fold lower than that of after immunization with MPyV VLPs [67].

Random aggregation of capsomers cannot substitute this effect. Mice were immunized subcutaneously with or without adjuvant with MPyV VLPs or MPyV VP1 GST fusions [69]. These GST fusions are deficient in forming VLPs, although these tagged capsomers tend to form aggregates [119]. While both were able to protect all normal C57BL/6 mice against polyomavirus infection, only the VLPs were able to do so in T-cell deficient mice. Moreover, anti-VP1 antibody responses were higher after immunization with VLPs in T-cell deficient mice than after immunization with VP1 fusions. Again, another report showed that mice, immunized with MCPyV VLPs, produced high titers of antibodies, while a similar study with non-assembled VP1 failed to do so [109]. Taken together these reports clearly show the benefit of PyV VLPs for a good humoral immune response.

Immunization with MPyV VLPs protected mice against some MPyV-induced tumors, despite the fact that most MPyV-induced tumors do not overexpress VP1 [194]. However, antibodies alone are probably not enough to prevent Merkel cell carcinoma (MCC), as MCC patients have very high titers against MCPyV [101].

PyV VLP vaccines are very stable, and retain their immunological properties even after long-term storage. Intranasal administration of MPyV VLPs without adjuvant in BALB/c mice resulted in strong humoral and cellular response, even after storage for 9 weeks at room temperature in PBS [73]. A clear dose-dependent response was observed.

6.2.2. Vaccines against epitopes displayed on the capsid surface

Foreign epitopes can be displayed on the outside of PyV VLPs. This can be done by insertion of the epitope into the variable loops on the surface of VP1, forming chimeric VLPs. Based on the crystal structure of SV40, four distinct insertion sites have been predicted for HaPyV [24]. These insertion sites were called 1–4, and correspond to loops BC, EF, FG, and HI, respectively. All four sites were tested by inserting the 5 aa long pre-S1 epitope from hepatitis B virus [24]. All VP1-epitope fusions resulted in VLPs after production in yeast. *In vitro* all of the VLPs retained similar VP1 immunogenicity, while pre-S1 antigenicity depended on the insertion site, with insertion into the BC loop clearly being the most immunogenic. C57Bl6 mice immunized intraperitoneally with different fusion VP1s (along with Freund's complete adjuvant) all developed anti-VP1 antibodies, slightly less than against wild-type. Also all mice (except for controls) developed antibodies against the pre-S1 epitope, but the levels were again not the same for all insertion sites. The BC loop yielded the highest response among all 4 sites, and combinations of BC with another site yielded even higher responses. The immune response was mainly IgG.

A similar study was performed with 45 and 120 aa N-terminal fragments of the Puumala hantavirus (PUUV) nucleocapsid protein (NP) inserted into all four different HaPyV sites, and a 80 aa fragment inserted into the BC and HI loops [74]. VLPs could be formed after insertions into BC and HI, but sites EF and FG did not tolerate this. *In vitro* it was shown that anti-VP1 immunogenicity depended on the insert length, with longer inserts lowering VP1 immunogenicity. For anti-PUUV immunogenicity, the longer inserts provided more immunogenicity. Immunization of BALB/c mice with these chimeric

VLPs resulted in high immune responses against the PUUV NP, even without any adjuvant, where the 120 aa insertion yielded the highest responses. However, adjuvant treatment did increase the response ten-fold. Repeated injections resulted in increased immune responses, indicating memory. The response was a mixed Th1/Th2 response, which was similar to the response against VP1 itself. Both cellular and humoral immune responses were observed. Anti-VP1 response was the lowest with 120 aa insertions. This shows that, by inserting longer fragments, the immune response can be shifted from an anti-VP1 response to an anti-insert response.

However, recently it was shown that even after prior immunization with wild-type VLPs, resulting in high levels of anti-VP1 antibodies, the immune response against displayed epitopes is not completely abolished [195]. Actually, differences in antibody titers were not statistically significant anymore after three rounds of subcutaneous vaccination of BALB/c mice without adjuvant with MPyV VLPs harboring the Group A streptococcus minimal epitope J8i in the HI loop, although the mice that received prior vaccination with the wild-type VLPs still displayed lower antibody titers against the insert than the control mice.

Cytotoxic T lymphocyte (CTL) responses can also be induced by epitopes displayed on the surface of VP1, as was shown for HaPyV VLPs carrying MUC1 epitopes in the BC and HI loops [188], although antibodies against the insert and VP1 were also produced [196]. The presence of antibodies against VLPs does not hamper a specific CTL response induced by VLPs. HaPyV VLPs carrying the CTL epitope GP33 from the Lymphocytic choriomeningitis virus (LCMV) in the BC or HI loop were processed by DCs and able to induce T-cell proliferation *in vitro* and *in vivo*, despite the induction of anti-VP1 antibodies [197]. Intravenous immunization without adjuvant protected 70 % of the B6 mice against LCMV infection.

In most studies the vaccine is administered by injection. A recent study demonstrated the potential of PyV VLPs as intranasal vaccine [198]. MPyV VLPs harboring the Group A streptococcus minimal epitope J8i in the HI loop were delivered intranasally without adjuvant to outbred Swiss mice, resulting in not only IgG, but also antigen-specific mucosal IgA responses. When the mice were challenged with a lethal dose of group A streptococcus, the vaccinated mice showed improved survival, although protection was far from complete. No data was reported on anti-carrier responses.

Constructs containing two copies of the same antigen inserted in tandem were also tested, but these did not result in any benefit [195,198]. Next to the insertion of a single epitope, it is also possible to insert several different antigens into one VP1 molecule, either divided among different insertion sites, or as a fusion into one insertion site. One study showed the insertion of 3 hydrophobic tumor associated antigens into HaPyV VP1, either into 3 different loops, or fused together into the HI loop [199]. No immunological assays were performed, but expression in yeast showed higher production yields for the VP1 with the inserts spread out than for the VP1 with the inserts fused together in the HI loop. All yields were, however, lower than that for wild-type VP1.

Recently, a new way to display large proteins on the surface of VLPs was reported [171,172]. While fusion of proteins to (truncated) VP2 usually results in the protein being hidden within the VLP, HaPyV VLPs displayed the antigen p16INK4A on the surface after fusion to the N-terminus of truncated VP2 [171]. These VLPs were successfully used to generate antibodies against p16INK4A.

Moreover, techniques for the (non-)covalent linkage of proteins to the surface of VLPs [167,200–202], which have been explored mainly for their use in retargeting gene therapy vectors (see section 6.3.2), could also be used to couple antigens.

6.2.3. Vaccines against epitopes buried within the capsid

One problem with insertion into the capsid might

be the disruption of the natural tropism of the VLPs, preventing their uptake and thus efficient CTL response. However, for the induction of CTL responses, display on the surface is not necessary. Two subcutaneous injections of MPyV VLPs with the immunodominant CTL epitope from ovalbumin ($OVA_{252-270}$) fused to the C-terminus of VP1 were able to protect mice from lethal challenges of OVA-expressing tumors [203], even if the injections were given 4 and 11 days after tumor inoculation [204]. However, incomplete protection was observed when injections were given 10 and 17 days post inoculation, so it is doubtful that these vaccines are useful in a therapeutic setting.

Not only epitopes, but also whole antigens can be fused and packaged inside PyV VLPs. MPyV VLPs were produced with VP2 fused to the transmembrane domain of HER2 [131]. A single subcutaneous injection with these VLPs alone was enough to protect BALB/c mice from HER2 expressing (D2F2/E2) tumors, and a single intraperitoneal injection protected BALB-neuT mice from spontaneous HER2-positive tumors, although the immunization had to happen at an early stage to prevent the development of these spontaneous tumors. Prior loading on DCs could enhance the specificity of the immunization [132]. Because similar results were obtained with MPtV VLPs [130], which do not cross-react with MPyV VLPs, repeated vaccination is possible. Both CD4+ and CD8+ T cells were redundantly involved in the immune response, and memory of at least 10 weeks could be obtained after a single injection with CpG as adjuvant [169]. These results were not limited to HER2, as MPyV VLPs with PSA fused to VP2 together were able to protect most BALB/c mice against PSA-positive D2F2/PSA tumor cells after a similar immunization protocol [166].

Not all such approaches are successful. No CTL responses were observed after intranasal administration of MPyV VLPs with EGFP fused to the C-terminus of truncated VP2 [168] or after intranasal or intraperitoneal injections with similar fusions with a 171 aa Bcr-Abl epitope [170].

6.2.4. DNA vaccines

The introduction of DNA encoding an epitope in cells can result in an immune response if the epitope is properly expressed and presented to immune cells [205]. Naked plasmid DNA can be used towards this end. However, the efficiency of delivery is very low. If the DNA is combined with VLPs, which can effectively deliver DNA to cells, the transfection efficiency, and thus the immune response, is enhanced.

Such an immunization was shown by Clark *et al.* [155] using β-galactosidase as a model antigen. pCMVβ DNA was loaded into MPyV VLPs by direct interaction and delivered intranasally to BALB/c mice. This resulted in an immune response against both β-galactosidase and VP1. Against VP1 high antibody titers were observed both in serum and in mucosa, as well as cellular proliferation. However, against β-galactosidase only cellular proliferation was found, but no antibodies.

Another study did show a humoral immune response against the DNA-encoded antigen [189]. DNA encoding the HIV-1 p24 and p17 NPs was loaded into MPyV VLPs by direct interaction and delivered intramuscularly in C57BL/6 mice, resulting in an increased humoral response compared to a DNA only control, although the results were very weak.

An attractive application of these methods would be the combination of DNA and epitope vaccines. By including the coding DNA sequence for an epitope within the VLP, while inserting the epitope into surface-exposed loops, the immune reaction might be boosted.

6.3. Gene delivery

Viral gene therapy has been plagued by problems involving its safety due to the inclusion of viral genetic sequences, while synthetic non-viral vectors still provide very low transfection efficiencies [206]. Virus-like particles provide a perfect combination of these two systems, maintaining the high transfection efficiencies of viral gene carriers without the safety issues due to viral genetic sequences.

Table 3. A selection of different reports showing nucleic acid delivery using polyomavirus VLPs, along with their relevant parameters.

Polyomavirus	Plasmid	Cell line	Loading method	Transfection efficiency	Reference
MPyV	pEGFP	COS-7	Osmotic shock	0.5 %	[44]
HaPyV	pCMV-GFP	COS-7	Reassembly	"Rather low"	[9]
HaPyV	pCMV-GFP	CHO	Reassembly	"Rather low"	[9]
JCPyV	pEGFP-N3	COLO-320 HSR	Co-expression	80 %	[158]
BKPyV	pCMV-β-Gal	COS-7	Direct interaction	50 %	[103]
JCPyV	pCMV-β-Gal	COS-7	Reassembly	20 %	[122]
MPtV	pEGFP-C1	293	Direct interaction	0.03 %	[39]
MPtV	pEGFP-C1	COS-1	Direct interaction	0.03 %	[39]
SV40	pEGFP-C1	Several	Reassembly	100 %	[208]
MPyV	pEGFP-N1	NIH 3T3	Reassembly	10 %	[147]
JCPyV	Oligonucleotides	SVG	Osmotic shock	100 %	[145]

Already before the recombinant production of VLPs, gene transfer had been shown using empty PyV capsids complexed with DNA [142]. Rat F111 cells were successfully transformed by MPyV PLPs harboring the BclI-EcoRI transforming fragment of the MPyV genome. Osmotic shock treatment was necessary for delivery, as simply mixing the empty virions with DNA did not result in transformation. However, these PLPs cannot easily be produced in large quantities and can potentially be contaminated with live infectious PyVs. VLPs are produced recombinantly, without the need for viral DNA sequences (except for *VP1*), and therefore provide a much safer alternative.

The first report of gene therapy with recombinant VP1 VLPs was made by Forstova *et al.* in 1995, who report the transfection of several genes into cells using MPyV VLPs after osmotic shock [144]. First, Rat-2 cells were transfected with a 1.6 kb linear *dl*8 MT gene fragment. The transfection was more efficient than calcium phosphate mediated transfection, even though the transfection protocol was not optimized. After transfection, DNA was integrated into the genome, in contrast to calcium phosphate mediated transfection. Copy numbers of the gene were shown to be very low for VLP mediated transfer, while calcium phosphate mediated transfer resulted in high copy numbers in the transfected cells. However, expression of the target protein was comparable. Next, human liver CCL 13 cells were transfected with a 6.2 kb plasmid harboring a CAT gene under a CMV promoter, and HEL fibroblasts with a plasmid containing the p43 gene under control of CMV. Although delivery took place, it was not reported if the whole plasmid was delivered, or just the necessary fragment with the promoter and the gene. The VLPs did not induce toxicity in any test.

Since then, PyV VLPs have been used to deliver countless different plasmids to many different cell lines. For some examples, see table 3. The reported transfection efficiencies vary substantially, ranging from almost complete transfection [158,207,208] to nearly no transfection [39]. This can be partially explained by the differences in loading method, although even with the same loading method the variance in transfection efficiency is still very large. There are simply too many changing variables to compare the different experiments effectively [209].

Next to plasmid DNA, oligonucleotides could also be delivered to cells [145,147], resulting in clear intranuclear fluorescence after delivery of fluorescent oligonucleotides using MPyV VLPs [147]. DNA

dendrimer complexes with VP1 could also be delivered to cells, but the reporter protein was not expressed [147].

6.3.1. Uptake

Productive uptake, that is, uptake resulting in gene expression, is accomplished through the same pathways used by wild-type PyVs, which, for most PyVs, are dependent on sialic acid and microtubules. The bulk of the VLPs, as shown for MPyV, is taken up by the clathrin-dependent endosomal route, which most non-viral systems use. This, however, is non-productive for most PyV VLPs and does not result in gene expression [44,156]. Also, plasmids might become trapped in the ER [210]. The uptake might be improved by addition of VP2/3 and condensation of DNA with hyper-acetylated histones [153]. By combining these two in SV40 VLPs, uptake was similar to wild-type SV40 virus. Uptake of VLPs by cells can be quick, as was demonstrated with MPtV VLPs, where 50 % of all membrane-bound VLPs were internalized within 40 min [39]. After successful uptake by the cell, VLPs are imported into the nucleus by their own NLS, as shown for JCPyV [178]. The cells do not necessarily have to be dividing, as non-dividing rabbit cornea cells were also transfected *ex vivo* using MPyV [211].

6.3.2. Tropism and retargeting

Unmodified, PyV VLPs have the same broad tropism as PyVs. Even PyVs such as JCPyV, which has a rather restricted tropism, can enter many different cell types [145]. In order to limit the tropism and target the VLPs to specific cell types, the variable loops on the surface of the VLPS, which function in receptor binding, can be modified.
As a pilot, 18 kDa dihydrofolate reductase (DHFR) was inserted into the HI-loop of MPyV [212]. Insertion was achieved using flexible glycine-serine linkers, and resulted in a functional enzyme and VLPs. The thermal stability of the enzyme was reduced, but its K_M value was only slightly higher. The size of the VLP population, however, was not homogeneous (smaller particles). This might have been caused by steric hindrance, as the attachment of large molecules to the surface of VLPs can cause steric hindrance. Such constructs can then be stabilized by co-expression with another VP1 with a FLAG epitope, as was shown for MPyV VP1 with the amino-terminal fragment of urokinase plasminogen activator inserted into surface exposed loops, which by itself was not soluble, but in combination with the VP1-FLAG was soluble and formed VLPs that bound to U-937 cells [128].
To reduce problems associated with steric hindrance, targeting factors can also be coupled to VLPs after assembly. Human epidermal growth factor (hEGF) was chemically coupled to SV40 VLPs, to which a surface-exposed cysteine was introduced [167]. Up to 46 hEGF were coupled per VLP, which resulted in the selective uptake by hEGF receptor overexpressing A431 cells.
Using a similar approach a protein A derivative, the 6.8 kDa protein Z, was inserted into the HI loop of MPyV VP1 [202]. This way antibodies could be coupled to VP1, thereby altering the tropism of the VLP. Stable particles were formed, and up to 80 % of the binding sites could be loaded with antibodies, although only 36 antibodies per VLP were necessary to reach plateau values for transfection [213]. By coupling the monoclonal antibody Herceptin to the VLPs, specific targeting and transfection of HER2-positive MCF 7 and SK-BR3 cells was achieved. In contrast to wild-type VLPs, uptake was realized by receptor-mediated endocytosis. This resulted in a very low transfection rate of up to 0.45 % [213]. The advantage of this system is that antibodies can be coupled directly to the VLP, without further modification of the coat proteins or antibodies. This way, the tropism can easily be changed. However, only antibodies can be coupled and no other molecules.
Another way to couple proteins to VLPs is through insertion of a WW domain, which can bind polyproline-tagged proteins, into VP1 [200]. Next to the HI loop, insertion into the DE loop was also attempted. Only the DE loop insertion proved to be active.

It was possible to couple a polyproline-tagged GFP, but the dissociation reaction was very fast.

Specific targeting could also be achieved by coupling only antibody fragments to VLPs. This could be done by inserting an E8C linker into the HI-loop of MPyV VP1 [201]. This linker, which consists of eight glutamic acids and a cysteine, could bind the Fv fragment of an antibody fused to an Arg8Cys-peptide. Specific targeting to Lewis Y positive cancer cells (MCF 7 cells) was accomplished by linking approximately 30 dsFv-B3-R8C molecules to each VLP [201]. Cell lines without the antigen would not bind these VLPs [156]. Various plasmid DNA cargos were loaded into the VLPs by direct interaction. However, even in the presence of chloroquine, only 0.12 % of the MCF 7 cells were transfected. Internalization occurred again by a clathrin-dependent endosomal process [156], explaining the lack of efficacy. Nevertheless, this system shows the potential to couple not only antibody fragments, but also any molecule, to VLPs, as long as it is linked to an R8C peptide.

Direct mutation of VLPs is also possible, as was shown by introduction of RGD peptides into the BC, DE and HI loops of LPyV [214]. All three loops tolerated the replacement of three amino acids, and the mutant VLPs did not bind to the LPV receptor anymore. Moreover, the BC mutants specifically bound to αvβ3 integrin, which recognizes RGD peptides.

A more comprehensive study was performed with SV40, where the BC, DE and HI loops were scanned with a FLAG-tag flanked by linkers of different lengths [215]. While insertion was only tolerated in two of the tested locations and the FLAG epitope had to be flanked by at least 3 glycine residues, insertion of an RGD motif into those locations completely retargeted the VLPs.

6.3.3. *IN VIVO* GENE DELIVERY

Although various groups have attempted gene delivery *in vivo*, good data is generally lacking. For example, 9 kb *dl*1023-pBR322 DNA, after direct interaction with MPyV VLPs, could be delivered to various tissue-types in both normal and immune-deficient mice [216]. The delivery was sustained for up to 6 months and very efficient compared to naked DNA alone, although wild-type MPyV infection resulted in even higher transfection rates. Normal mice were more difficult to transfect than immune-deficient mice, but the study lacked the proper controls to quantify the differences.

In another study mice were injected with pEGFP-C1 bound to MPtV VLPs by direct interaction [39]. DNA was detected by PCR 3 weeks after inoculation, despite the low transfection efficiency of 0.03 % reported with cultured cells. DNA was found in mice inoculated with VLP/DNA complexes, but not with DNA alone.

Similarly, Wang *et al.* showed the uptake of JCPyV VLPs carrying fluorescent oligonucleotides by neuroblastoma cells in mice harboring a tumor nodule [145]. Delivery was again only compared to the naked DNA, and despite showing uptake of the complexes, no release of DNA or physiological effect was noted.

In vivo transfection was shown to be stable [217]. Nude mice were injected with MPyV VLPs loaded with pCMV-β by osmotic shock. Stable expression of β-galactosidase was observed for over 7 weeks in multiple organs including the heart, spleen, kidney and brain. However, β-galactosidase expression was only scored for its presence, and not quantified.

Based on these experiments performed with DNA loaded by direct interaction or osmotic shock, methods which generally show almost no *in vitro* transfection, it can be predicted that with more efficient loading methods much better results could be obtained. This was demonstrated by Chen *et al.*, who show the transfection of tumor cells with pEGFP-N3 in nude mice bearing a COLO-320 HSR tumor nodule [158]. In this case, JCPyV VLPs loaded with DNA through co-expression, which were previously shown to transfect cells in culture with an efficiency of over 90 %, were injected intravenously [158]. Green fluorescence was only found in the tumor, and not in other organs. The same experiment

was repeated with pUMVC1-tk. After treatment with ganciclovir (GCV) clear cell death was observed *in vitro* for the samples treated with pUMVC1-tk VLPs. After intravenous injection of VLPs harboring these plasmids and treatment with GCV, tumor growth was almost entirely inhibited, while controls did not have that effect.

Very efficient delivery was also reported after reassembly in the presence of nuclear extract [218]. SV40 VLPs containing the 5.3 kb luciferase expression plasmid pGL3-control were injected in BALB/c mice by hydrodynamic tail-vein injection. One day after the injection, very efficient transduction of the liver was observed, similar to recombinant SV40 vectors. Another study using the same loading technique showed a clear anti-tumor effect of SV40 VLPs carrying the suicide gene PE38 in athymic nude mice carrying a KB-3-1 tumor [219]. The mice were injected either intratumorally or intraperitoneally 4–5 times a week starting on the day of tumor inoculation. After 30 days, the tumors in the mice treated with PE38-VLPs had barely grown, while the control animals had developed significant tumors, and several of the VLP-treated mice were still tumor-free after more than a year. However, both this study and the study by Chen *et al.* use immunocompromised mice bearing a human tumor, raising the question of how realistic these results are.

One of the downsides of using VLPs for gene delivery is the possible immunogenicity of the VLPs. Neutralizing antibodies might already exist in the population (for example for JCPyV and BKPyV), or might be acquired after the first round of therapy. This could severely limit the applicability, and lead to loss of efficacy and potentially severe immune reactions. Also, because of the high similarity between the different polyomaviruses, a high cross-reactivity exists between the different VLPs [96]. However, this is not the case for all serotypes, and could therefore be circumvented by using different serotypes, for which no cross-reactivity exists [130]. Also, the VLPs could be made less immunogenic by modification, such as PEGylation; techniques which are already mainstream in non-viral gene delivery.

7. Summarizing conclusions

Virus-like particles resemble their parent virion in structure, immunogenicity, tropism and transduction efficiency, but do not contain any viral genetic material. They therefore represent a safe vector for vaccination and gene therapy. Although challenging in terms of large-scale production, the availability of two VLP-based vaccines demonstrates that this can be done in a cost-effective way. Moreover, the fact alone that PyV VLPs can be produced in prokaryotic hosts at high yields already significantly reduces the production costs.

7.1. Diagnostics

PyV VLPs have been used in epidemiological studies, and have shown that the human polyomaviruses are omniprevalent and already acquired at an early age. VLPs are particularly valuable for these studies, as many PyV cannot easily be cultured, and these particles thus represent the best method to detect seropositivity. Therefore, VLPs will continue to play an important role in the epidemiologic study of PyV.

7.2. Vaccines

The lack of viral genetic material makes VLPs a safe alternative to attenuated and inactivated virus vaccines. Their repetitive structure causes a potent immune response by binding to pattern-recognition receptors on immune cells and cross-linking B-cell receptors. While PyV VLPs alone can already induce strong immune responses, they can be loaded with activators of innate immunity, such as CpG, further enhancing their immunogenicity.

The increasing prevalence of disease caused by BKPyV and JCPyV in immunocompromised indi-

viduals, and the accumulating evidence of the role of MCPyV in Merkel cell carcinoma warrant the investigation into vaccines against these diseases. However, because the majority of the population is already seropositive for these diseases, and infection is mostly asymptomatic, it is questionable whether prophylactic vaccines would be cost-effective. On the other hand, prophylactic vaccines against avian polyomaviruses, which cause a much more acute disease, might be economically feasible for agricultural use. Because VP1 VLPs only give rise to anti-VP1 antibodies, while infection leads to antibody production against VP2/3 and the T antigens, VLP-based vaccines make it possible to differentiate infected from vaccinated animals (DIVA), which is very important for agricultural applications.

Different strategies have been developed to display foreign antigens on the surface of PyV VLPs. While direct insertion into surface-exposed loops is possible, and yields very high antibody titers, the development of such systems takes a lot of time. Moreover, large inserts can hamper VLP formation, and might not be folded correctly. However, PyV VLPs have been shown to tolerate the insertion of very large epitopes while still maintaining their antigenic structure, and this has already attracted attention from the industry [220].

Moreover, antigens loaded within PyV VLPs can induce strong antigen-specific CTL responses. Using these different strategies, antigens displayed by VLPs are able to break tolerance, a crucial step in the vaccination against autoimmune diseases and cancer, and a step towards the development of therapeutic vaccines.

7.3. Gene delivery

Virus-like particles provide a perfect combination of both viral and non-viral gene delivery systems, maintaining the high transfection efficiencies of viral gene carriers without the safety issues due to viral genetic sequences.

Several well-established protocols exist for the loading of cargo into PyV VLPs. Still, gene delivery using PyV VLPs is restricted to the packaging capacity of the VLP, which is close to the size of the PyV genome, although some groups reported delivery of larger DNA molecules. However, many applications stay below this size limit. For example, RNAi effectors can easily be accommodated within PyV VLPs. Moreover, the use of minicircle DNA could allow larger transgenes to be packaged.

Now that packaging can efficiently be achieved the new bottleneck in transfection will be the nuclear uptake of DNA. Several different variables have already been tested, including the addition of VP2/3 and hyper-acetylated histones. By further improving on these, it might be possible to achieve the same transfection efficiency as wild-type PyVs. However, the biggest challenge gene therapy is facing is still targeting. Using different protocols, targeting ligands have been coupled to PyV VLPs, resulting in the retargeting of these VLPs. Yet, this targeting was still not very specific. It can be envisioned that, by coupling different targeting ligands, or by using different chimeric VP1s in the same VLP, more specific targeting will be obtained. Another way to alter the tropism of VLPs is directed evolution. This technique has already proven its worth in the alteration of other viruses, such as adeno-associated virus [221]. In addition to random mutagenesis, the high homology between different PyV members would allow family DNA shuffling to be used for the creation of novel PyV VLPs.

Taken together, polyomavirus virus-like particles show great potential in diagnostics, vaccine development and gene delivery. Although PyV VLPs are already used in diagnostics, and vaccine development is very close, still many challenges have to be overcome before PyV VLPs can be applied to gene therapy.

Acknowledgements

We would like to thank Paulien van Bentum for her helpful support in the preparation of the manu-

script. Molecular graphics and analyses were performed with the UCSF Chimera package. Chimera is developed by the Resource for Biocomputing, Visualization, and Informatics at the University of California, San Francisco, with support from the National Institutes of Health (National Center for Research Resources grant 2P41RR001081, National Institute of General Medical Sciences grant 9P41GM103311).
This work was supported by Technologiestichting STW [budget number 10243].

References

1 Feltkamp, M.C. *et al.* **From Stockholm to Malawi: recent developments in studying human polyomaviruses.** J Gen Virol (2013) 94, 482–496.

2 King, A.M.Q. *et al.* **Virus Taxonomy – Ninth Report of the International Committee on Taxonomy of Viruses.** (2011).

3 DeCaprio, J.A. and Garcea, R.L. **A cornucopia of human polyomaviruses.** Nat Rev Microbiol (2013) 11, 264–276.

4 White, M.K., Gordon, J. and Khalili, K. **The rapidly expanding family of human polyomaviruses: recent developments in understanding their life cycle and role in human pathology.** PLoS Pathog (2013) 9, e1003206.

5 Salunke, D.M., Caspar, D.L. and Garcea, R.L. **Self-assembly of purified polyomavirus capsid protein VP1.** Cell (1986) 46, 895–904.

6 Chuan, Y.P. *et al.* **Virus assembly occurs following a pH- or Ca^{2+}-triggered switch in the thermodynamic attraction between structural protein capsomeres.** J R Soc Interface (2010) 7, 409–421.

7 Ding, Y. *et al.* **Modeling the competition between aggregation and self-assembly during virus-like particle processing.** Biotechnol Bioeng (2010) 107, 550–560.

8 Moreland, R.B., Montross, L. and Garcea, R.L. **Characterization of the DNA-binding properties of the polyomavirus capsid protein VP1.** J Virol (1991) 65, 1168–1176.

9 Voronkova, T. *et al.* **Hamster polyomavirus-derived virus-like particles are able to transfer *in vitro* encapsidated plasmid DNA to mammalian cells.** Virus Genes (2007) 34, 303–314.

10 Liddington, R.C. *et al.* **Structure of simian virus 40 at 3.8-A resolution.** Nature (1991) 354, 278–284.

11 Stehle, T. *et al.* **The structure of simian virus 40 refined at 3.1 A resolution.** Structure (1996) 4, 165–182.

12 Griffith, J.P. *et al.* **Inside polyomavirus at 25-A resolution.** Nature (1992) 355, 652–654.

13 Stehle, T. *et al.* **Structure of murine polyomavirus complexed with an oligosaccharide receptor fragment.** Nature (1994) 369, 160–163.

14 Stehle, T. and Harrison, S.C. **Crystal structures of murine polyomavirus in complex with straight-chain and branched-chain sialyloligosaccharide receptor fragments.** Structure (1996) 4, 183–194.

15 Stehle, T. and Harrison, S.C. **High-resolution structure of a polyomavirus VP1-oligosaccharide complex: implications for assembly and receptor binding.** Embo J (1997) 16, 5139–5148.

16 Chen, X.S., Stehle, T. and Harrison, S.C. **Interaction of polyomavirus internal protein VP2 with the major capsid protein VP1 and implications for participation of VP2 in viral entry.** EMBO J (1998) 17, 3233–3240.

17 Neu, U. *et al.* **Structural basis of GM1 ganglioside recognition by simian virus 40.** Proc Natl Acad Sci U S A (2008) 105, 5219–5224.

18 Neu, U. *et al.* **Structure-function analysis of the human JC polyomavirus establishes the LSTc pentasaccharide as a functional receptor motif.** Cell Host Microbe (2010) 8, 309–319.

19 Neu, U. *et al.* **Structures of the major capsid proteins of the human Karolinska Institutet and Washington University polyomaviruses.** J Virol (2011) 85, 7384–7392.

20 Neu, U. *et al.* **Structures of Merkel Cell Polyomavirus VP1 Complexes Define a Sialic Acid Binding Site Required for Infection.** PLoS Pathog (2012) 8, e1002738.

21 Knipe, D.M. and Howley, P.M. **Field's Virology.** 5th edn, (2007).

22 Saper, G. *et al.* **Effect of capsid confinement on the chromatin organization of the SV40 minichromosome.** Nucleic Acids Res (2013) 41, 1569–1580.

23 Pettersen, E.F. *et al.* **UCSF Chimera – a visualization system for exploratory research and analysis.** J Comput Chem (2004) 25, 1605–1612.

24 Gedvilaite, A. *et al.* **Formation of immunogenic virus-like particles by inserting epitopes into surface-exposed regions of hamster polyomavirus major capsid protein.** Virology (2000) 273, 21–35.

25 Ou, W.C. *et al.* **Identification of a DNA encapsidation sequence for human polyomavirus pseudovirion formation.** J Med Virol (2001) 64, 366–373.

26 Chang, D., Cai, X. and Consigli, R.A. **Characterization of the DNA binding properties of polyomavirus capsid protein.** J Virol (1993) 67, 6327–6331.

27 Clever, J., Dean, D.A. and Kasamatsu, H. **Identification of a DNA binding domain in simian virus 40 capsid proteins Vp2 and Vp3.** J Biol Chem (1993) 268, 20877–20883.

28 Chang, D. *et al.* **The use of additive and subtractive approaches to examine the nuclear localization sequence of the polyomavirus major capsid protein VP1.** Virology (1992) 189, 821–827.

29 Moreland, R.B. and Garcea, R.L. **Characterization of a nuclear localization sequence in the polyomavirus capsid protein VP1.** Virology (1991) 185, 513–518.

30 Li, P.P. *et al.* **Simian virus 40 Vp1 DNA-binding domain is functionally separable from the overlapping nuclear localization signal and is required for effective virion formation and full viability.** J Virol (2001) 75, 7321–7329.

31 Sasnauskas, K. *et al.* **Yeast cells allow high-level expression and formation of polyomavirus-like particles.** Biol Chem (1999) 380, 381–386.

32 Garcea, R.L., Salunke, D.M. and Caspar, D.L. **Site-directed mutation affecting polyomavirus capsid self-assembly *in vitro*.** Nature (1987) 329, 86–87.

33 Rodgers, R.E. and Consigli, R.A. **Characterization of a calcium binding domain in the VP1 protein of the avian polyomavirus, budgerigar fledgling disease virus.** Virus Res (1996) 44, 123–135.

34 Yokoyama, N. *et al.* **Mutational analysis of the carboxyl-terminal region of the SV40 major capsid protein VP1.** J Biochem (2007) 141, 279–286.

35 Gedvilaite, A. *et al.* **Size and position of truncations in the carboxy-terminal region of major capsid protein VP1 of hamster polyomavirus expressed in yeast determine its assembly capacity.** Arch Virol (2006) 151, 1811–1825.

36 Sapp, M. and Day, P.M. **Structure, attachment and entry of polyoma- and papillomaviruses.** Virology (2009) 384, 400–409.

37 Clayson, E.T. and Compans, R.W. **Characterization of simian virus 40 receptor moieties on the surfaces of Vero C1008 cells.** J Virol (1989) 63, 1095–1100.

38 Atwood, W.J. and Norkin, L.C. **Class I major histocompatibility proteins as cell surface receptors for simian virus 40.** J Virol (1989) 63, 4474–4477.

39 Tegerstedt, K. *et al.* **Murine pneumotropic virus VP1 virus-like particles (VLPs) bind to several cell types independent of sialic acid residues and do not serologically cross react with murine polyomavirus VP1 VLPs.** J Gen Virol (2003) 84, 3443–3452.

40 Ashok, A. and Atwood, W.J. **Virus receptors and tropism.** Adv Exp Med Biol (2006) 577, 60–72.

41 Pawlita, M. *et al.* **DNA encapsidation by viruslike particles assembled in insect cells from the major capsid protein VP1 of B-lymphotropic papovavirus.** J Virol (1996) 70, 7517–7526.

42 Richterova, Z. *et al.* **Caveolae are involved in the trafficking of mouse polyomavirus virions and artificial VP1 pseudocapsids toward cell nuclei.** J Virol (2001) 75, 10880–10891.

43 Pho, M.T., Ashok, A. and Atwood, W.J. **JC virus enters human glial cells by clathrin-dependent receptor-mediated endocytosis.** J Virol (2000) 74, 2288–2292.

44 Krauzewicz, N. *et al.* **Virus-like gene transfer into cells mediated by polyoma virus pseudocapsids.** Gene Ther (2000) 7, 2122–2131.

45 Norkin, L.C. *et al.* **Caveolar endocytosis of simian virus 40 is followed by brefeldin A-sensitive transport to the endoplasmic reticulum, where the virus disassembles.** J Virol (2002) 76, 5156–5166.

46 Kawano, M.A. *et al.* **Calcium bridge triggers capsid disassembly in the cell entry process of simian virus 40.** J Biol Chem (2009) 284, 34703–34712.

47 Schelhaas, M. *et al.* **Simian Virus 40 depends on ER protein folding and quality control factors for entry into host cells.** Cell (2007) 131, 516–529.

48 Kuksin, D. and Norkin, L.C. **Disassembly of simian virus 40 during passage through the endoplasmic reticulum and in the cytoplasm.** J Virol (2012) 86, 1555–1562.

49 Nakanishi, A. *et al.* **Association with capsid proteins promotes nuclear targeting of simian virus 40 DNA.** Proc Natl Acad Sci U S A (1996) 93, 96–100.

50 Nakanishi, A. *et al.* **Interaction of the Vp3 nuclear localization signal with the importin alpha 2/beta heterodimer directs nuclear entry of infecting simian virus 40.** J Virol (2002) 76, 9368–9377.

51 Nakanishi, A. *et al.* **Minor capsid proteins of simian virus 40 are dispensable for nucleocapsid assembly and cell entry but are required for nuclear entry of the viral genome.** J Virol (2007) 81, 3778–3785.

52 Montross, L. *et al.* **Nuclear assembly of polyomavirus capsids in insect cells expressing the major capsid protein VP1.** J Virol (1991) 65, 4991–4998.

53 Li, P.P. *et al.* **Importance of Vp1 calcium-binding residues in assembly, cell entry, and nuclear entry of simian virus 40.** J Virol (2003) 77, 7527–7538.

54 Cripe, T.P. *et al.* ***In vivo* and *in vitro* association of hsc70 with polyomavirus capsid proteins.** J Virol (1995) 69, 7807–7813.

55 Chromy, L.R., Pipas, J.M. and Garcea, R.L. **Chaperone-mediated *in vitro* assembly of Polyomavirus capsids.** Proc Natl Acad Sci U S A (2003) 100, 10477–10482.

56 Gillock, E.T., An, K. and Consigli, R.A. **Truncation of the nuclear localization signal of polyomavirus VP1 results in a loss of DNA packaging when expressed in the baculovirus system.** Virus Res (1998) 58, 149–160.

57 Oppenheim, A. *et al.* **A cis-acting DNA signal for encapsidation of simian virus 40.** J Virol (1992) 66, 5320–5328.

58 Dalyot-Herman, N. *et al.* **The simian virus 40 packaging signal ses is composed of redundant DNA elements which are partly interchangeable.** J Mol Biol (1996) 259, 69–80.

59 Gordon-Shaag, A. *et al.* **Cellular transcription factor Sp1 recruits simian virus 40 capsid proteins to the viral packaging signal, *ses*.** J Virol (2002) 76, 5915–5924.

60 Sandalon, Z. *et al.* ***In vitro* assembly of SV40 virions and pseudovirions: vector development for gene therapy.** Hum Gene Ther (1997) 8, 843–849.

61 Aposhian, H.V., Thayer, R.E. and Qasba, P.K. **Formation of nucleoprotein complexes between polyoma empty capsides and DNA.** J Virol (1975) 15, 645–653.

62 Yuen, L.K. and Consigli, R.A. **Generation of capsids from unstable polyoma virions.** J Virol (1983) 47, 620–625.

63 Leavitt, A.D., Roberts, T.M. and Garcea, R.L. **Polyoma virus major capsid protein, VP1. Purification after high level expression in *Escherichia coli*.** J Biol Chem (1985) 260, 12803–12809.

64 Ponder, B.A., Robbins, A.K. and Crawford, L.V. **Phosphorylation of polyoma and SV40 virus proteins.** J Gen Virol (1977) 37, 75–83.

65 Bolen, J.B. *et al.* **Differences in the subpopulations of the structural proteins of polyoma virions and capsids: biological functions of the multiple VP1 species.** J Virol (1981) 37, 80–91.

66 Garcea, R.L., Ballmer-Hofer, K. and Benjamin, T.L. **Virion assembly defect of polyomavirus hr-t mutants: underphosphorylation of major capsid protein VP1 before viral DNA encapsidation.** J Virol (1985) 54, 311–316.

67 Velupillai, P., Garcea, R.L. and Benjamin, T.L. **Polyoma virus-like particles elicit polarized cytokine responses in APCs from tumor-susceptible and -resistant mice.** J Immunol

(2006) 176, 1148–1153.

68 Li, T.C. *et al.* **Characterization of self-assembled virus-like particles of human polyomavirus BK generated by recombinant baculoviruses.** Virology (2003) 311, 115–124.

69 Vlastos, A. *et al.* **VP1 pseudocapsids, but not a glutathione-S-transferase VP1 fusion protein, prevent polyomavirus infection in a T-cell immune deficient experimental mouse model.** J Med Virol (2003) 70, 293–300.

70 Zielonka, A. *et al.* **Serological cross-reactions between four polyomaviruses of birds using virus-like particles expressed in yeast.** J Gen Virol (2012) 93, 2658–2667.

71 Gedvilaite, A. *et al.* **Virus-like particles derived from major capsid protein VP1 of different polyomaviruses differ in their ability to induce maturation in human dendritic cells.** Virology (2006) 354, 252–260.

72 Zielonka, A. *et al.* **Detection of chimpanzee polyomavirus-specific antibodies in captive and wild-caught chimpanzees using yeast-expressed virus-like particles.** Virus Res (2011) 155, 514–519.

73 Caparros-Wanderley, W., Clark, B. and Griffin, B.E. **Effect of dose and long-term storage on the immunogenicity of murine polyomavirus VP1 virus-like particles.** Vaccine (2004) 22, 352–361.

74 Gedvilaite, A. *et al.* **Segments of puumala hantavirus nucleocapsid protein inserted into chimeric polyomavirus-derived virus-like particles induce a strong immune response in mice.** Viral Immunol (2004) 17, 51–68.

75 Mohr, J. *et al.* **Virus-like particle formulation optimization by miniaturized high-throughput screening.** Methods (2013) 60, 248–256.

76 Chen, P.L. *et al.* **Disulfide bonds stabilize JC virus capsid-like structure by protecting calcium ions from chelation.** FEBS Lett (2001) 500, 109–113.

77 Chang, D. *et al.* **Self-assembly of the JC virus major capsid protein, VP1, expressed in insect cells.** J Gen Virol (1997) 78 (Pt 6), 1435–1439.

78 Schmidt, U., Rudolph, R. and Bohm, G. **Mechanism of assembly of recombinant murine polyomavirus-like particles.** J Virol (2000) 74, 1658–1662.

79 Jao, C.C. *et al.* **Cys9, Cys104 and Cys207 of simian virus 40 Vp1 are essential for inter-pentamer disulfide-linkage and stabilization in cell-free lysates.** J Gen Virol (1999) 80 (Pt 9), 2481–2489.

80 Li, P.P. *et al.* **Role of simian virus 40 Vp1 cysteines in virion infectivity.** J Virol (2000) 74, 11388–11393.

81 Chromy, L.R. *et al.* **Chaperone-mediated *in vitro* disassembly of polyoma- and papillomaviruses.** J Virol (2006) 80, 5086–5091.

82 Braun, H. *et al.* **Oligonucleotide and plasmid DNA packaging into polyoma VP1 virus-like particles expressed in *Escherichia coli*.** Biotechnol Appl Biochem (1999) 29 (Pt 1), 31–43.

83 Tsukamoto, H. *et al.* **Evidence that SV40 VP1-DNA interactions contribute to the assembly of 40-nm spherical viral particles.** Genes Cells (2007) 12, 1267–1279.

84 Mukherjee, S. *et al.* **Uncatalyzed assembly of spherical particles from SV40 VP1 pentamers and linear dsDNA incorporates both low and high cooperativity elements.** Virology (2010) 397, 199–204.

85 Kosukegawa, A. *et al.* **Purification and characterization of virus-like particles and pentamers produced by the expression of SV40 capsid proteins in insect cells.** Biochim Biophys Acta (1996) 1290, 37–45.

86 Kawano, M.A. *et al.* **The VP2/VP3 minor capsid protein of simian virus 40 promotes the *in vitro* assembly of the major capsid protein VP1 into particles.** J Biol Chem (2006) 281, 10164–10173.

87 Pease, L.F., 3rd *et al.* **Quantitative characterization of virus-like particles by asymmetrical flow field flow fractionation, electrospray differential mobility analysis, and transmission electron microscopy.** Biotechnol Bioeng (2009) 102, 845–855.

88 Lipin, D.I. *et al.* **Encapsulation of DNA and non-viral protein changes the structure of murine polyomavirus virus-like particles.** Arch Virol (2008) 153, 2027–2039.

89 Citkowicz, A. *et al.* **Characterization of virus-like particle assembly for DNA delivery using asymmetrical flow field-flow fractionation and light scattering.** Anal Biochem (2008) 376, 163–172.

90 Salunke, D.M., Caspar, D.L. and Garcea, R.L. **Polymorphism in the assembly of polyomavirus capsid protein VP1.** Biophys J (1989) 56, 887–900.

91 Kanesashi, S.N. *et al.* **Simian virus 40 VP1 capsid protein forms polymorphic assemblies *in vitro*.** J Gen Virol (2003) 84, 1899–1905.

92 Nilsson, J. *et al.* **Structure and assembly of a *T*=1 virus-like particle in BK polyomavirus.** J Virol (2005) 79, 5337–5345.

93 Ou, W.C. *et al.* **The major capsid protein, VP1, of human JC virus expressed in *Escherichia coli* is able to self-assemble into a capsid-like particle and deliver exogenous DNA into human kidney cells.** J Gen Virol (1999) 80 (Pt 1), 39–46.

94 Liew, M.W., Rajendran, A. and Middelberg, A.P. **Microbial production of virus-like particle vaccine protein at gram-per-litre levels.** J Biotechnol (2010) 150, 224–231.

95 Hale, A.D. *et al.* **Expression and antigenic characterization of the major capsid proteins of human polyomaviruses BK and JC in *Saccharomyces cerevisiae*.** J Virol Methods (2002) 104, 93–98.

96 Sasnauskas, K. *et al.* **Generation of recombinant virus-like particles of human and non-human polyomaviruses in yeast *Saccharomyces cerevisiae*.** Intervirology (2002) 45, 308–317.

97 Palkova, Z. *et al.* **Production of polyomavirus structural protein VP1 in yeast cells and its interaction with cell structures.** FEBS Lett (2000) 478, 281–289.

98 Gillock, E.T. *et al.* **Polyomavirus major capsid protein VP1 is capable of packaging cellular DNA when expressed in the baculovirus system.** J Virol (1997) 71, 2857–2865.

99 Ng, J. *et al.* **Extracellular self-assembly of virus-like particles from secreted recombinant polyoma virus major coat protein.** Protein Eng Des Sel (2007) 20, 591–598.

100 Tolstov, Y.L. *et al.* **Human Merkel cell polyomavirus infection II. MCV is a common human infection that can be detected by conformational capsid epitope immunoassays.** Int J Cancer (2009) 125, 1250–1256.

101 Pastrana, D.V. *et al.* **Quantitation of human seroresponsiveness to Merkel cell polyomavirus.** PLoS Pathog (2009) 5, e1000578.

102 Gharakhanian, E., Sajo, A.K. and Weidman, M.K. **SV40 VP1 assembles into disulfide-linked postpentameric com-**

plexes in cell-free lysates. Virology (1995) 207, 251–254.

103 Touze, A. *et al.* **Gene transfer using human polyomavirus BK virus-like particles expressed in insect cells.** J Gen Virol (2001) 82, 3005–3009.

104 Rodgers, R.E. *et al.* **Purification of recombinant budgerigar fledgling disease virus VP1 capsid protein and its ability for *in vitro* capsid assembly.** J Virol (1994) 68, 3386–3390.

105 An, K. *et al.* **Avian polyomavirus major capsid protein VP1 interacts with the minor capsid proteins and is transported into the cell nucleus but does not assemble into capsid-like particles when expressed in the baculovirus system.** Virus Res (1999) 64, 173–185.

106 Johne, R. and Muller, H. **Nuclear localization of avian polyomavirus structural protein VP1 is a prerequisite for the formation of virus-like particles.** J Virol (2004) 78, 930–937.

107 Shishido, Y. *et al.* **Assembly of JC virus-like particles in COS7 cells.** J Med Virol (1997) 51, 265–272.

108 Wrobel, B. *et al.* **Production and purification of SV40 major capsid protein (VP1) in *Escherichia coli* strains deficient for the GroELS chaperone machine.** J Biotechnol (2000) 84, 285–289.

109 Touze, A. *et al.* **Generation of Merkel cell polyomavirus (MCV)-like particles and their application to detection of MCV antibodies.** J Clin Microbiol (2010) 48, 1767–1770.

110 Nicol, J.T. *et al.* **Age-specific seroprevalences of merkel cell polyomavirus, human polyomaviruses 6, 7, and 9, and trichodysplasia spinulosa-associated polyomavirus.** Clin Vaccine Immunol (2013) 20, 363–368.

111 Nicol, J.T. *et al.* **Seroprevalence and cross-reactivity of human polyomavirus 9.** Emerg Infect Dis (2012) 18, 1329–1332.

112 Kumar, A. *et al.* **Trichodysplasia spinulosa-associated polyomavirus (TSV) and Merkel cell polyomavirus: correlation between humoral and cellular immunity stronger with TSV.** PLoS One (2012) 7, e45773.

113 Zielonka, A. *et al.* **Generation of virus-like particles consisting of the major capsid protein VP1 of goose hemorrhagic polyomavirus and their application in serological tests.** Virus Res (2006) 120, 128–137.

114 Pattenden, L.K. *et al.* **Towards the preparative and large-scale precision manufacture of virus-like particles.** Trends Biotechnol (2005) 23, 523–529.

115 Chuan, Y.P., Lua, L.H. and Middelberg, A.P. **High-level expression of soluble viral structural protein in *Escherichia coli.*** J Biotechnol (2008) 134, 64–71.

116 Middelberg, A.P. *et al.* **A microbial platform for rapid and low-cost virus-like particle and capsomere vaccines.** Vaccine (2011) 29, 7154–7162.

117 Liew, M.W.O., Chuan, Y.P. and Middelberg, A.P.J. **High-yield and scalable cell-free assembly of virus-like particles by dilution.** Biochemical Engineering Journal (2012) 67, 88–96.

118 Liew, M.W.O., Chuan, Y.P. and Middelberg, A.P.J. **Reactive diafiltration for assembly and formulation of virus-like particles.** Biochemical Engineering Journal (2012) 68, 120–128.

119 Lipin, D.I., Lua, L.H. and Middelberg, A.P. **Quaternary size distribution of soluble aggregates of glutathione-S-transferase-purified viral protein as determined by asymmetrical flow field flow fractionation and dynamic light scattering.** J Chromatogr A (2008) 1190, 204–214.

120 Villa, L.L. *et al.* **Prophylactic quadrivalent human papillomavirus (types 6, 11, 16, and 18) L1 virus-like particle vaccine in young women: a randomised double-blind placebo-controlled multicentre phase II efficacy trial.** Lancet Oncol (2005) 6, 271–278.

121 Harper, D.M. *et al.* **Sustained efficacy up to 4.5 years of a bivalent L1 virus-like particle vaccine against human papillomavirus types 16 and 18: follow-up from a randomised control trial.** Lancet (2006) 367, 1247–1255.

122 Goldmann, C. *et al.* **Molecular cloning and expression of major structural protein VP1 of the human polyomavirus JC virus: formation of virus-like particles useful for immunological and therapeutic studies.** J Virol (1999) 73, 4465–4469.

123 Sandalon, Z. and Oppenheim, A. **Self-assembly and protein-protein interactions between the SV40 capsid proteins produced in insect cells.** Virology (1997) 237, 414–421.

124 Delos, S.E. *et al.* **Expression of the polyomavirus VP2 and VP3 proteins in insect cells: coexpression with the major capsid protein VP1 alters VP2/VP3 subcellular localization.** Virology (1993) 194, 393–398.

125 Li, M. *et al.* **Polyomavirus VP1 phosphorylation: coexpression with the VP2 capsid protein modulates VP1 phosphorylation in Sf9 insect cells.** Proc Natl Acad Sci U S A (1995) 92, 5992–5996.

126 Forstova, J. *et al.* **Cooperation of structural proteins during late events in the life cycle of polyomavirus.** J Virol (1993) 67, 1405–1413.

127 An, K. *et al.* **Use of the baculovirus system to assemble polyomavirus capsid-like particles with different polyomavirus structural proteins: analysis of the recombinant assembled capsid-like particles.** J Gen Virol (1999) 80 (Pt 4), 1009–1016.

128 Shin, Y.C. and Folk, W.R. **Formation of polyomavirus-like particles with different VP1 molecules that bind the urokinase plasminogen activator receptor.** J Virol (2003) 77, 11491–11498.

129 Boura, E. *et al.* **Polyomavirus EGFP-pseudocapsids: analysis of model particles for introduction of proteins and peptides into mammalian cells.** FEBS Lett (2005) 579, 6549–6558.

130 Andreasson, K. *et al.* **Murine pneumotropic virus chimeric Her2/neu virus-like particles as prophylactic and therapeutic vaccines against Her2/neu expressing tumors.** Int J Cancer (2009) 124, 150–156.

131 Tegerstedt, K. *et al.* **A single vaccination with polyomavirus VP1/VP2Her2 virus-like particles prevents outgrowth of HER-2/neu-expressing tumors.** Cancer Res (2005) 65, 5953–5957.

132 Tegerstedt, K. *et al.* **Dendritic cells loaded with polyomavirus VP1/VP2Her2 virus-like particles efficiently prevent outgrowth of a Her2/neu expressing tumor.** Cancer Immunol Immunother (2007) 56, 1335–1344.

133 Inoue, T. *et al.* **Engineering of SV40-based nano-capsules for delivery of heterologous proteins as fusions with the minor capsid proteins VP2/3.** J Biotechnol (2008) 134, 181–192.

134 Spirin, A. and Swartz, J. **Cell-free Protein Synthesis – Methods and Protocols.** (2007).

135 Wheeler, T. *et al.* **Cell-free synthesis of polyoma virus capsid proteins VP1 and VP2.** J Virol (1977) 21, 215–224.

136 Mangel, W.F. *et al.* **Polyoma virus complementary RNA directs the *in vitro* synthesis of capsid proteins VP1 and VP2.** J Virol (1978) 25, 570–578.

137 Prives, C.L. and Shure, H. **Cell-free translation of simian virus 40 16S and 19S L-strand-specific mRNA classes to simian virus 40 major VP-1 and minor VP-2 and VP-3 capsid proteins.** J Virol (1979) 29, 1204–1212.

138 Lodish, H.F., Weinberg, R. and Ozer, H.L. **Translation of mRNA from simian virus 40-infected cells into simian virus 40 capsid protein by cell-free extracts.** J Virol (1974) 13, 590–595.

139 Ishizu, K.I. *et al.* **Roles of disulfide linkage and calcium ion-mediated interactions in assembly and disassembly of virus-like particles composed of simian virus 40 VP1 capsid protein.** J Virol (2001) 75, 61–72.

140 Barr, S.M., Keck, K. and Aposhian, H.V. **Cell-free assembly of a polyoma-like particle from empty capsids and DNA.** Virology (1979) 96, 656–659.

141 Slilaty, S.N., Berns, K.I. and Aposhian, H.V. **Polyoma-like particle: characterization of the DNA encapsidated *in vitro* by polyoma empty capsids.** J Biol Chem (1982) 257, 6571–6575.

142 Slilaty, S.N. and Aposhian, H.V. **Gene transfer by polyoma-like particles assembled in a cell-free system.** Science (1983) 220, 725–727.

143 Stokrova, J. *et al.* **Interactions of heterologous DNA with polyomavirus major structural protein, VP1.** FEBS Lett (1999) 445, 119–125.

144 Forstova, J. *et al.* **Polyoma virus pseudocapsids as efficient carriers of heterologous DNA into mammalian cells.** Hum Gene Ther (1995) 6, 297–306.

145 Wang, M. *et al.* **Inhibition of simian virus 40 large tumor antigen expression in human fetal glial cells by an antisense oligodeoxynucleotide delivered by the JC virus-like particle.** Hum Gene Ther (2004) 15, 1077–1090.

146 Yang, Y.W. and Chen, L.H. **Gene delivery via polyomavirus major capsid protein VP(1), isolated from recombinant *Escherichia coli*.** Biotechnol Appl Biochem (2000) 32 (Pt 1), 73–79.

147 Henke, S. *et al.* **Enhanced *in vitro* oligonucleotide and plasmid DNA transport by VP1 virus-like particles.** Pharm Res (2000) 17, 1062–1070.

148 Mukherjee, S. *et al.* **High cooperativity of the SV40 major capsid protein VP1 in virus assembly.** PLoS One (2007) 2, e765.

149 Goldmann, C. *et al.* **Packaging of small molecules into VP1-virus-like particles of the human polyomavirus JC virus.** J Virol Methods (2000) 90, 85–90.

150 Macadangdang, B. *et al.* **Inhibition of multidrug resistance by SV40 pseudovirion delivery of an antigene peptide nucleic acid (PNA) in cultured cells.** PLoS One (2011) 6, e17981.

151 Li, F. *et al.* **Imaging viral behavior in Mammalian cells with self-assembled capsid-quantum-dot hybrid particles.** Small (2009) 5, 718–726.

152 Wang, T. *et al.* **Encapsulation of gold nanoparticles by simian virus 40 capsids.** Nanoscale (2011) 3, 4275–4282.

153 Enomoto, T. *et al.* ***In vitro* reconstitution of SV40 particles that are composed of VP1/2/3 capsid proteins and nucleosomal DNA and direct efficient gene transfer.** Virology (2011) 420, 1–9.

154 Kimchi-Sarfaty, C. *et al.* **High cloning capacity of *in vitro* packaged SV40 vectors with no SV40 virus sequences.** Hum Gene Ther (2003) 14, 167–177.

155 Clark, B. *et al.* **Immunity against both polyomavirus VP1 and a transgene product induced following intranasal delivery of VP1 pseudocapsid-DNA complexes.** J Gen Virol (2001) 82, 2791–2797.

156 May, T., Gleiter, S. and Lilie, H. **Assessment of cell type specific gene transfer of polyoma virus like particles presenting a tumor specific antibody Fv fragment.** J Virol Methods (2002) 105, 147–157.

157 Oppenheim, A. *et al.* **Efficient introduction of plasmid DNA into human hemopoietic cells by encapsidation in simian virus 40 pseudovirions.** Proc Natl Acad Sci U S A (1986) 83, 6925–6929.

158 Chen, L.S. *et al.* **Efficient gene transfer using the human JC virus-like particle that inhibits human colon adenocarcinoma growth in a nude mouse model.** Gene Ther (2010) 17, 1033–1041.

159 Chang, C.F. *et al.* **Human JC virus-like particles as a gene delivery vector.** Expert Opin Biol Ther (2011) 11, 1169–1175.

160 Fang, C.Y. *et al.* **Analysis of the size of DNA packaged by the human JC virus-like particle.** J Virol Methods (2012) 182, 87–92.

161 Chou, M.I. *et al.* ***In vitro* and *in vivo* targeted delivery of IL-10 interfering RNA by JC virus-like particles.** J Biomed Sci (2010) 17, 51.

162 Kimchi-Sarfaty, C. *et al.* **Efficient delivery of RNA interference effectors via *in vitro*-packaged SV40 pseudovirions.** Hum Gene Ther (2005) 16, 1110–1115.

163 Kler, S. *et al.* **RNA encapsidation by SV40-derived nanoparticles follows a rapid two-state mechanism.** J Am Chem Soc (2012) 134, 8823–8830.

164 Abbing, A. *et al.* **Efficient intracellular delivery of a protein and a low molecular weight substance via recombinant polyomavirus-like particles.** J Biol Chem (2004) 279, 27410–27421.

165 Ohtake, N. *et al.* **Low pH-triggered model drug molecule release from virus-like particles.** Chembiochem (2010) 11, 959–962.

166 Eriksson, M. *et al.* **Murine polyomavirus virus-like particles carrying full-length human PSA protect BALB/c mice from outgrowth of a PSA expressing tumor.** PLoS One (2011) 6, e23828.

167 Kitai, Y. *et al.* **Cell selective targeting of a simian virus 40 virus-like particle conjugated to epidermal growth factor.** J Biotechnol (2011) 155, 251–256.

168 Fric, J. *et al.* **Cellular and humoral immune responses to chimeric EGFP-pseudocapsids derived from the mouse polyomavirus after their intranasal administration.** Vaccine (2008) 26, 3242–3251.

169 Andreasson, K. *et al.* **CD4+ and CD8+ T cells can act separately in tumour rejection after immunization with murine pneumotropic virus chimeric Her2/neu virus-like particles.** PLoS One (2010) 5, e11580.

170 Hruskova, V. *et al.* **Bcr-Abl fusion sequences do not induce immune responses in mice when administered in**

mouse polyomavirus based virus-like particles. Int J Oncol (2009) 35, 1247–1256.

171 Lasickiene, R. *et al.* **The use of recombinant pseudotype virus-like particles harbouring inserted target antigen to generate antibodies against cellular marker p16INK4A.** ScientificWorldJournal (2012) 2012, 263737.

172 Pleckaityte, M. *et al.* **Production in yeast of pseudotype virus-like particles harboring functionally active antibody fragments neutralizing the cytolytic activity of vaginolysin.** Microb Cell Fact (2011) 10, 109.

173 Schmidt, U. *et al.* **Protein and peptide delivery via engineered polyomavirus-like particles.** FASEB J (2001) 15, 1646–1648.

174 Schmidt, U. *et al.* **Site-specific fluorescence labelling of recombinant polyomavirus-like particles.** Biol Chem (1999) 380, 397–401.

175 Niikura, K. *et al.* **Virus-like particles with removable cyclodextrins enable glutathione-triggered drug release in cells.** Mol Biosyst (2013) 9, 501–507.

176 Enomoto, T. *et al.* **Viral protein-coating of magnetic nanoparticles using simian virus 40 VP1.** J Biotechnol (2013) 167, 8–15.

177 An, K. *et al.* **Use of the confocal microscope to determine polyomavirus recombinant capsid-like particle entry into mouse 3T6 cells.** J Virol Methods (2000) 84, 153–159.

178 Qu, Q. *et al.* **Nuclear entry mechanism of the human polyomavirus JC virus-like particle: role of importins and the nuclear pore complex.** J Biol Chem (2004) 279, 27735–27742.

179 Viscidi, R.P. *et al.* **Serological cross-reactivities between antibodies to simian virus 40, BK virus, and JC virus assessed by virus-like-particle-based enzyme immunoassays.** Clin Diagn Lab Immunol (2003) 10, 278–285.

180 Randhawa, P.S. *et al.* **Immunoglobulin G, A, and M responses to BK virus in renal transplantation.** Clin Vaccine Immunol (2006) 13, 1057–1063.

181 Viscidi, R.P. and Clayman, B. **Serological cross reactivity between polyomavirus capsids.** Adv Exp Med Biol (2006) 577, 73–84.

182 Stolt, A. *et al.* **Seroepidemiology of the human polyomaviruses.** J Gen Virol (2003) 84, 1499–1504.

183 Moens, U. *et al.* **Serological cross-reactivity between human polyomaviruses.** Rev Med Virol (2013) 23, 250–264.

184 Jennings, G.T. and Bachmann, M.F. **The coming of age of virus-like particle vaccines.** Biol Chem (2008) 389, 521–536.

185 Roldao, A. *et al.* **Virus-like particles in vaccine development.** Expert Rev Vaccines (2010) 9, 1149–1176.

186 Kushnir, N., Streatfield, S.J. and Yusibov, V. **Virus-like particles as a highly efficient vaccine platform: diversity of targets and production systems and advances in clinical development.** Vaccine (2012) 31, 58–83.

187 Garland, S.M. *et al.* **Quadrivalent vaccine against human papillomavirus to prevent anogenital diseases.** N Engl J Med (2007) 356, 1928–1943.

188 Dorn, D.C. *et al.* **Cellular and humoral immunogenicity of hamster polyomavirus-derived virus-like particles harboring a mucin 1 cytotoxic T-cell epitope.** Viral Immunol (2008) 21, 12–27.

189 Rollman, E. *et al.* **Genetic immunization is augmented by murine polyomavirus VP1 pseudocapsids.** Vaccine (2003) 21, 2263–2267.

190 Samonskyte, L. *et al.* **Immunogenic properties of polyomavirus-derived recombinant virus-like particles: activation of murine spleen cell-derived dendritic cells.** Biologija (2006), 80–84.

191 Mato, T. *et al.* **Recombinant subunit vaccine elicits protection against goose haemorrhagic nephritis and enteritis.** Avian Pathol (2009) 38, 233–237.

192 Szomolanyi-Tsuda, E. *et al.* **T-Cell-independent immunoglobulin G responses *in vivo* are elicited by live-virus infection but not by immunization with viral proteins or virus-like particles.** J Virol (1998) 72, 6665–6670.

193 Heidari, S. *et al.* **Immunization of T-cell deficient mice against polyomavirus infection using viral pseudocapsids or temperature sensitive mutants.** Vaccine (2002) 20, 1571–1578.

194 Franzen, A.V. *et al.* **Murine polyomavirus-VP1 virus-like particles immunize against some polyomavirus-induced tumours.** In Vivo (2005) 19, 323–326.

195 Chuan, Y.P. *et al.* **Effects of pre-existing anti-carrier immunity and antigenic element multiplicity on efficacy of a modular virus-like particle vaccine.** Biotechnol Bioeng (2013) 110, 2343–2351.

196 Zvirbliene, A. *et al.* **Generation of monoclonal antibodies of desired specificity using chimeric polyomavirus-derived virus-like particles.** J Immunol Methods (2006) 311, 57–70.

197 Mazeike, E., Gedvilaite, A. and Blohm, U. **Induction of insert-specific immune response in mice by hamster polyomavirus VP1 derived virus-like particles carrying LCMV GP33 CTL epitope.** Virus Res (2012) 163, 2–10.

198 Rivera-Hernandez, T. *et al.* **Self-adjuvanting modular virus-like particles for mucosal vaccination against group A streptococcus (GAS).** Vaccine (2013) 31, 1950–1955.

199 Aleksaite, E. and Gedvilaite, A. **Generation of chimeric hamster polyomavirus VP1 virus-like particles harboring three tumor-associated antigens.** Biologija (2006), 83–87.

200 Schmidt, U., Rudolph, R. and Bohm, G. **Binding of external ligands onto an engineered virus capsid.** Protein Eng (2001) 14, 769–774.

201 Stubenrauch, K. *et al.* **Conjugation of an antibody Fv fragment to a virus coat protein: cell-specific targeting of recombinant polyoma-virus-like particles.** Biochem J (2001) 356, 867–873.

202 Gleiter, S. and Lilie, H. **Coupling of antibodies via protein Z on modified polyoma virus-like particles.** Protein Sci (2001) 10, 434–444.

203 Brinkman, M. *et al.* **Recombinant Murine Polyoma Virus-like-particles Induce Protective Antitumour Immunity.** Letters in Drug Design & Discovery (2004) 1, 137–147(111).

204 Brinkman, M. *et al.* **Beneficial therapeutic effects with different particulate structures of murine polyomavirus VP1-coat protein carrying self or non-self CD8 T cell epitopes against murine melanoma.** Cancer Immunol Immunother (2005) 54, 611–622.

205 Liu, M.A. **DNA vaccines: a review.** J Intern Med (2003) 253, 402–410.

206 Mastrobattista, E. *et al.* **Artificial viruses: a nanotechno-**

logical approach to gene delivery. Nat Rev Drug Discov (2006) 5, 115–121.

207 Kimchi-Sarfaty, C. *et al.* ***In vitro*-packaged SV40 pseudovirions as highly efficient vectors for gene transfer.** Hum Gene Ther (2002) 13, 299–310.

208 Kimchi-Sarfaty, C. *et al.* **Transduction of multiple cell types using improved conditions for gene delivery and expression of SV40 pseudovirions packaged *in vitro*.** Biotechniques (2004) 37, 270–275.

209 van Gaal, E.V. *et al.* **How to screen non–viral gene delivery systems *in vitro*?** J Control Release (2011) 154, 218–232.

210 Kimchi-Sarfaty, C. *et al.* **The pathway of uptake of SV40 pseudovirions packaged *in vitro*: from MHC class I receptors to the nucleus.** Gene Ther Mol Biol (2004) 8, 439–450.

211 Krauzewicz, N. *et al.* **Sustained *ex vivo* and *in vivo* transfer of a reporter gene using polyoma virus pseudocapsids.** Gene Ther (2000) 7, 1094–1102.

212 Gleiter, S., Stubenrauch, K. and Lilie, H. **Changing the surface of a virus shell fusion of an enzyme to polyoma VP1.** Protein Sci (1999) 8, 2562–2569.

213 Gleiter, S. and Lilie, H. **Cell-type specific targeting and gene expression using a variant of polyoma VP1 virus–like particles.** Biol Chem (2003) 384, 247–255.

214 Langner, J. *et al.* **RGD-mutants of B-lymphotropic polyomavirus capsids specifically bind to alpha(v)beta3 integrin.** Arch Virol (2004) 149, 1877–1896.

215 Takahashi, R.U. *et al.* **Presentation of functional foreign peptides on the surface of SV40 virus-like particles.** J Biotechnol (2008) 135, 385–392.

216 Heidari, S. *et al.* **Persistence and tissue distribution of DNA in normal and immunodeficient mice inoculated with polyomavirus VP1 pseudocapsid complexes or polyomavirus.** J Virol (2000) 74, 11963–11965.

217 Soeda, E. *et al.* **Enhancement by polylysine of transient, but not stable, expression of genes carried into cells by polyoma VP1 pseudocapsids.** Gene Ther (1998) 5, 1410–1419.

218 Arad, U. *et al.* **Liver-targeted gene therapy by SV40-based vectors using the hydrodynamic injection method.** Hum Gene Ther (2005) 16, 361–371.

219 Kimchi-Sarfaty, C. *et al.* **SV40 Pseudovirion gene delivery of a toxin to treat human adenocarcinomas in mice.** Cancer Gene Ther (2006) 13, 648–657.

220 Neugebauer, M. *et al.* **Development of a vaccine marker technology: display of B cell epitopes on the surface of recombinant polyomavirus-like pentamers and capsoids induces peptide-specific antibodies in piglets after vaccination.** Biotechnol J (2006) 1, 1435–1446.

221 Grimm, D. *et al.* ***In vitro* and *in vivo* gene therapy vector evolution via multispecies interbreeding and retargeting of adeno-associated viruses.** J Virol (2008) 82, 5887–5911.

Chapter III

Batch-to-batch variability of *Escherichia coli* S30 extracts can be reduced by normalizing S30 total protein content

Erik A. Teunissen[1], Georgi Nadibaidze[1], Markus de Raad[1] and Enrico Mastrobattista[1]
[1]Department of Pharmaceutics, Utrecht Institute for Pharmaceutical Sciences, Faculty of Science, Utrecht University, Universiteitsweg 99, 3584 CG Utrecht, The Netherlands

Submitted for publication

Abstract

Most protocols for the preparation of *Escherichia coli* S30 extract define the S30 extract concentration based on the cell pellet wet weight. However, because of variability introduced during downstream processing, large differences between batches of S30 extract are observed. Here we show that by normalizing the S30 extract total protein concentration after production and before cell-free expression, we can significantly reduce the batch-to-batch variability of S30 extracts. This not only facilitates the comparison between studies performed with different S30 batches, but also between different production protocols for S30 extract. Finally, we find that, at least for β-galactosidase, the highest yield is obtained using 3.4–4.8 mg/ml S30 extract protein in the cell-free expression reaction.

1. Introduction

Cell-free expression (CFE) is an easy and rapid technique to obtain small quantities of desired proteins. CFE utilizes extracted cellular machinery for the *in vitro* transcription and translation of proteins from DNA.

CFE has several advantages over conventional *in vivo* overexpression of proteins. Because there are no membranes surrounding the reaction, the reaction can easily be modified allowing direct control over the reaction conditions. For example, components can be added to the reaction to optimize the expression conditions [1], to buffer the redox potential to allow proper formation of disulfide bonds [2,3], to label proteins with isotopes [4,5], or to enable the incorporation of unnatural amino acids [6–10]. Unnecessary or unwanted components can be removed prior to use, ultimately leading to a PURE system [11,12]. CFE is an excellent method for the production of otherwise difficult-to-express proteins, such as membrane proteins [13,14] or proteins that would normally be toxic to the host [15,16]. Furthermore, several different proteins can easily be expressed in the same reaction, allowing the formation of multiprotein complexes [15,17]. Because no lysis step is required, purification of proteins after CFE is much easier [18]. CFE is ideal for high-throughput screening. Genes can be screened directly from PCR products without the need for cloning [19] and proteins can be subjected to directed evolution using techniques such as *in vitro* compartmentalization [20].

The main drawback of CFE is its low expression yield [21]. Therefore, many studies have focused on increasing the yield by optimizing both the production protocol and CFE reaction.

One commonly used CFE system is the *Escherichia coli* (*E. coli*) S30 extract [22–25]. This system is based on the soluble fraction of a lysate from *E. coli* after centrifugation at 30,000 g, called S30 extract. During production, the concentration of the S30 extract is determined at the beginning of the protocol by the cell pellet wet weight [23,24,26–32]. However, many steps are performed before the final S30 extract is obtained, each resulting in slight variations in the concentration of the S30 extract. Of these steps, the lysis step seems to cause most variability between batches [24,33]. In the end, these slight variations results in high batch-to-batch variability. Most protocols for CFE with S30 extract use a fixed volume percentage of S30 extract in the CFE reaction (usually 24–35 %) [14,24,26–36], thus propagating the variability. This way, big differences between batches of S30 extract produced by the same protocol obscure conclusions based on expression levels and make comparisons between different expression protocols impossible.

In an effort to reduce the batch-to-batch variability of S30 extracts, we looked for ways to normalize the different S30 extracts. Based on our own results and the results obtained with condensed

extracts [4,23] we investigated the effect of the concentration of the S30 extract on the CFE activity. We investigated if we can reduce the variability between extracts arising from differences in protein content, or even increase the expression using an optimal protein concentration.

2. Materials and Methods

2.1. Chemicals

Adenosine-5'-triphosphate (ATP), ammonium acetate, β-galactosidase (G6008, 250–600 U/mg), bovine serum albumin (BSA), chloramphenicol, 3'-5'-cyclic adenosine monophosphate (cAMP), cytidine-5'-triphosphate (CTP), dimethyl sulfoxide (DMSO), dithiothreitol (DTT), folinic acid, guanosine-5'-triphosphate (GTP), LB broth culture medium, magnesium acetate, 2-mercaptoethanol, phosphoenolpyruvate (PEP), polyethylene glycol 8000 (PEG 8000), potassium hydroxide, pyruvate kinase, tris(hydroxymethyl)aminomethane (Tris), uridine-5'-triphosphate (UTP), and each of the 20 standard amino acids were purchased from Sigma-Aldrich (St. Louis, MO, USA). Acetic acid and potassium acetate were purchased from Merck KGaA (Darmstadt, Germany). Creatine kinase (CK), *E. coli* total tRNA, and cOmplete EDTA-free protease inhibitor cocktail tablets were purchased from Roche (Basel, Switzerland). HEPES was purchased from Acros Organics (Geel, Belgium). Creatine phosphate was purchased from Alfa Aesar (Ward Hill, MA, USA). T7 RNA polymerase was purchased from Thermo Scientific (Waltham, MA, USA). Fluorescein di-β-D-galactopyranoside (FDG) was purchased from Marker Gene Technologies (Eugene, OR, USA). RNase AWAY™ was purchased from Life Technologies (Carlsbad, CA, USA).

2.2. Plasmids

The plasmid pIVEX2.2EM-LacZ, which contains the wild-type *E. coli LacZ* gene under control of a T7 promoter, was prepared as described previously [20]. Suitable quantities of circular plasmid DNA were obtained using the NucleoBond® PC 10 000 kit (MACHEREY-NAGEL, Düren, Germany).

2.3. Bacteria

E. coli strains Rosetta-gami™ B(DE3), Rosetta-gami™ B, BL21(DE3), and Tuner™ were purchased from Merck KGaA.

2.4. Preparation of *E. coli* extracts

S30 extracts were prepared based on previously described protocols [24,25] with slight modifications and variations [37–39]. During preparation, all bottles, tubes, and glassware were washed with RNase AWAY™ prior to use. Overnight cultures of bacteria were diluted 50–100× in LB broth (usually 0.5–10 L). In the case of Rosetta-gami™ B or Rosetta-gami™ B(DE3), 34 µg/ml chloramphenicol was added. The bacteria were grown in 2 L Erlenmeyer flasks each with 500–800 ml LB broth at 37 °C shaking at 250 RPM until an OD600 of 0.8 was reached. The bacteria were then harvested by centrifuging at 5,000 g at 4 °C for 15 min, followed by resuspension in 20 ml precooled (4 °C) extract buffer (10 mM Tris-acetate buffer (pH 8.2) containing 14 mM magnesium acetate, 60 mM potassium acetate, and 1.0 mM DTT) with 0.050 % v/v 2-mercaptoethanol per gram of wet pellet. This step was repeated two more times. Afterwards, the pellet was frozen and stored overnight. The next day, the cells were resuspended in 1.14 ml precooled (4 °C) extract buffer with cOmplete EDTA-free protease inhibitor cocktail (1 tablet per 50 ml buffer) per gram of pellet. The bacteria were lysed by two passes through an EmulsiFlex-C5 high pressure homogenizer (AVESTIN, Ottawa, ON, Canada) at >15,000 psi or by 10–18 cycles of sonication (20 sec cycles, 80 % output, 0.5 sec active time interval) with a LABSONIC® P probe sonicator equipped with a 3-mm diameter probe (Sartorius AG, Göttingen,

Germany). The lysate was centrifuged twice at 4 °C at 30,000 g for 30 min (S30 extracts) or 18,000 g for 60 min (S18 extracts), discarding the pellet. The supernatant was incubated at 37 °C for 80 min with 0.30 volume of the preincubation buffer (293 mM Tris-acetate buffer (pH 8.2) containing 9.2 mM magnesium acetate, 13.2 mM ATP, 84 mM PEP, 4.4 mM DTT, 40 µM of each of the 20 standard amino acids, and 6.7 U/ml pyruvate kinase). This preincubation step was only performed for some of the extracts from figure 1. The supernatant was dialyzed 4 times for 30 min at 4 °C against 100 volumes of extract buffer using Slide-A-Lyzer membrane cassettes (Thermo Scientific) with a MWCO of 10 kDa. Debris was removed during a final centrifugation step at 4,000 g for 10 min at 4 °C. The supernatant, the S30 extract, was stored as 0.1–1.0 ml aliquots at –80 °C.

2.5. Protein quantification

Protein concentrations were determined using the Pierce™ BCA Protein Assay Kit and Pierce™ Micro BCA Protein Assay Kit (Thermo Scientific) according to the manufacturer's protocol. Results were corrected for DTT present in the S30 extracts.

2.6. Cell-free protein synthesis

Cell-free protein synthesis was performed with a total reaction volume of 25–100 µl. Each reaction contained 30–34 % (v/v) (diluted) S30 extract, 175 µg/ml *E. coli* total tRNA, 250 µg/ml creatine kinase, 5.8 mM magnesium acetate, 55 mM HEPES-KOH (pH 8.2), 1.7 mM DTT, 1.2 mM ATP, 0.8 mM CTP, 0.8 mM GTP, 0.8 mM UTP, 80 mM creatine phosphate, 0.64 mM cAMP, 68.9 µM folinic acid, 210 mM potassium acetate, 27.6 mM ammonium acetate, 1.0 mM of each of the 20 standard amino acids, 4.0 % w/v PEG 8000, and 2.5 U/µl T7 RNA polymerase. Plasmid DNA was added to a final concentration of 20 nM. The reactions were incubated for 4 hours at 30 °C.

2.7. Quantification of β-galactosidase activity

The activity of cell-free produced β-galactosidase was determined using FDG based on a previously described protocol [38]. From each CFE reaction, 10 µl was taken and added to 90 µl 33 mM Tris-acetate buffer (pH 7.9) with 10 mM magnesium acetate, 66 mM potassium acetate, and 5.0 mg/ml BSA in a black 96-well plate (Greiner Bio-One, Monroe, NC). To each well 100 µl substrate solution (0.2 mM FDG in 33 mM Tris-acetate buffer (pH 7.9) with 10 mM magnesium acetate, 66 mM potassium acetate, 0.2 % DMSO and 5.0 mg/ml BSA) was injected using a FLUOstar OPTIMA (BMG Labtech, Ortenberg, Germany) equilibrated at 37 °C, and the fluorescence (excitation, 485 nm; emission, 520 nm) was measured every 0.5 sec for 120 sec. A β-galactosidase standard curve was also measured (2-fold dilution series, 7.8–500 U/ml). The slope per minute was determined using the FLUOstar OPTIMA software, and based on the standard curve (4-parameter fit) the β-galactosidase activity was calculated.

3. Results

3.1. Batch-to-batch variability of S30 extracts

Over the past years we have noticed a very large variance in the protein synthesis activity of different batches of S30 extract. In an attempt to explain this variability, we investigated the effect of the concentration of the S30 extracts, measured in terms of total protein content, on the expression level of the extracts. We determined the total protein content of 20 extracts produced at our laboratory from different *E. coli* strains over the past 6 years and stored at –80 °C. Three of these extracts were S18 extracts, produced following the same protocol as for the S30 extracts, except that these extracts were centrifuged at 18,000 g for twice the

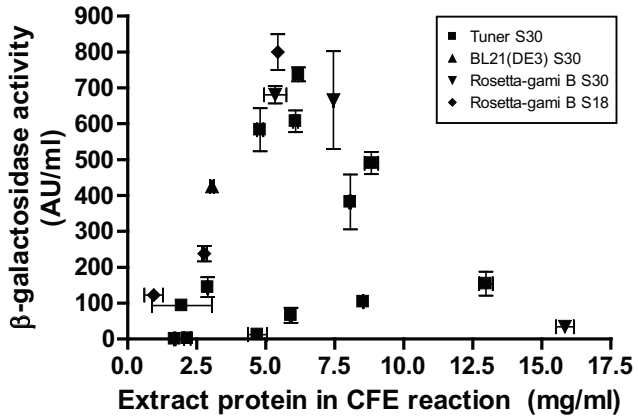

Figure 1. S30 extracts with different total protein contents result in different expression levels. The total protein content and protein expression activity of 20 extracts were determined. Different *E. coli* strains were used to produce the extracts as indicated by the symbols. The results were corrected for endogenous β-galactosidase activity. The error bars show the standard deviations of both measurements (n=2).

amount of time. We also quantified the protein expression activity of these extracts by measuring the β-galactosidase activity after cell-free expression with pIVEX2.2EM-LacZ under control of the T7 promoter (figure 1).

All highly active extracts were found to have total protein contents between 13 and 30 mg/ml, resulting in a final concentration of 4–9 mg/ml extract protein in the CFE reaction. At higher or lower extract protein concentrations, a concentration-dependent decrease in activity was observed. No difference in trend was found between extracts derived from different *E. coli* strains, nor was any difference found between S30 and S18 extracts. No relationship was found between storage time and activity (data not shown).

3.2. Variance of S30 extracts produced in parallel

The extracts in figure 1 were produced by different members of our laboratory using different bacterial

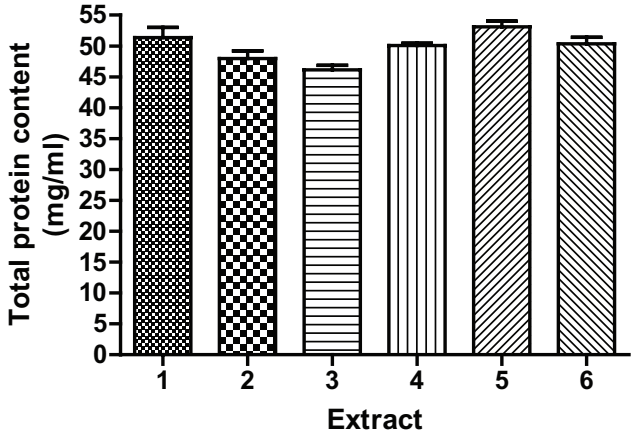

Figure 2. BCA protein quantification of six different extracts produced in parallel. Significantly different total protein concentrations were observed (one-way ANOVA, $p<0.05$; n=2).

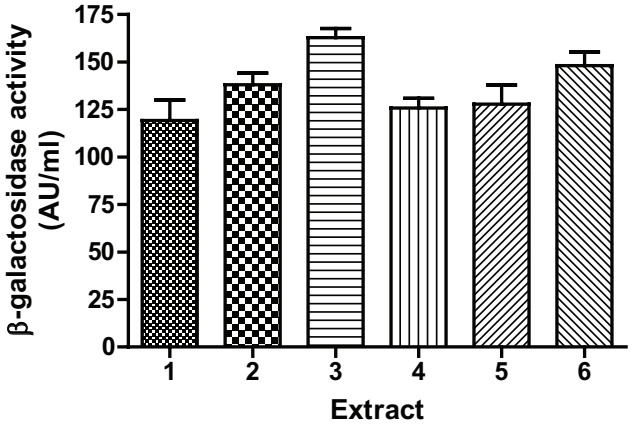

Figure 3. S30 extracts prepared using the same protocol in parallel have different CFE activities when using equal volumes of S30 extract. The activity of six different extracts produced in parallel was measured by quantifying β-galactosidase activity after CFE. Significantly different activities were observed (one-way ANOVA, $p<0.01$; $n=6$).

strains, and were stored for different durations. In order to eliminate any bias arising from these factors, we produced six S30 extracts in parallel from *E. coli* Rosetta-gami™ B, while trying to maintain as much homogeneity between the extracts as possible.

Figure 2 shows the result of the total protein quantification of these six extracts. Despite spending substantial effort in handling the extracts the same way in order to reduce variability, significant differences were found in total protein content, with the least concentrated extract containing 13 % less protein per volume than the most concentrated extract. Thus, even preparing S30 extracts in parallel still results in extracts with different total protein contents.

To see if these differences observed in total protein content also result in differences in CFE activities, CFE of β-galactosidase was performed with the six extracts produced in parallel (figure 3). CFE was performed with equal volumes of S30 extract (30 %) per CFE reaction, leading to different concentrations of S30 proteins in the final CFE reactions. Significant differences were observed between

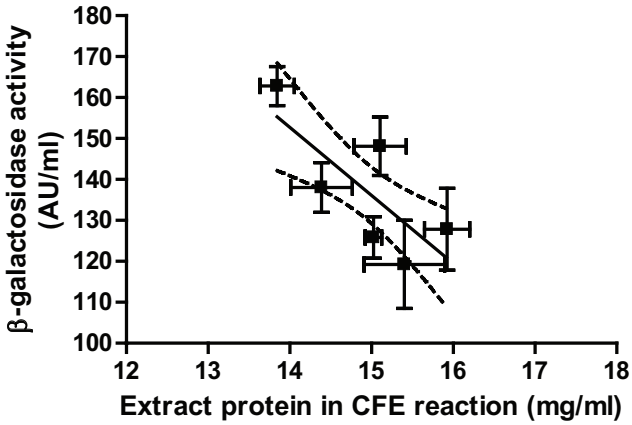

Figure 4. Correlation between extract protein concentration and β-galactosidase activity. The solid line shows the trend line, the dotted lines indicate the boundaries of the 95 % confidence interval. A clear negative trend is observed (linear regression, $p<0.01$).

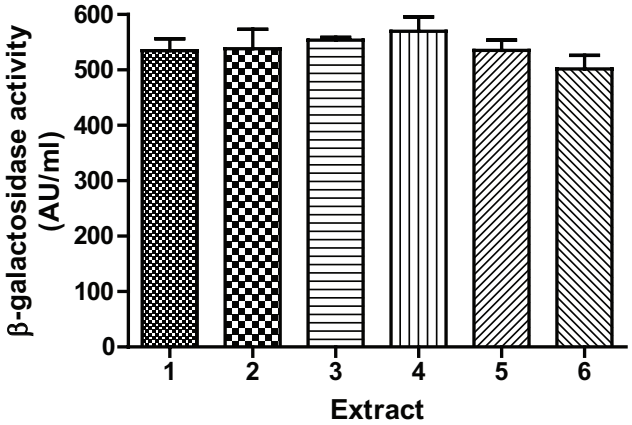

Figure 5. Normalizing the total protein content of different extracts decreases the variability in expression levels. CFE with pIVEX2.2EM-LacZ was performed with six different extracts normalized to an S30 protein concentration of 7.2 mg/ml in the CFE reactions. The expression was measured by quantifying β-galactosidase activity after CFE. No significant difference between the extracts was observed anymore (one-way ANOVA, p=0.50; n=5), while the average relative standard deviation decreased (0.09 here against 0.13 in figure 3).

the extracts, with the least active extract being 27 % less active than the most active one, indicating that the small differences between S30 concentrations can lead to much bigger differences in overall protein expression. A negative trend was found, with extracts with higher total protein contents being less active (figure 4). This correlates well with the data from figure 1, where a negative trend was observed above 9 mg/ml extract protein. The CFE reactions in figure 3 were performed with 13.8–15.9 mg/ml extract protein, which lies well within this region. We would thus expect that lowering the extract protein concentration would result in increased expression.

3.3. Normalization of S30 protein concentration

To investigate if normalizing the extract protein concentration results in less variance in CFE activ-

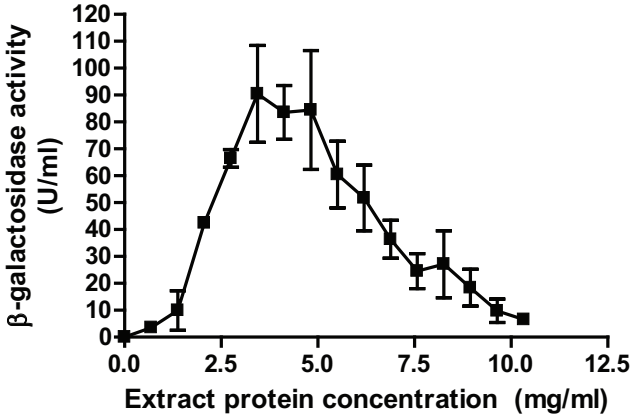

Figure 6. Relationship between extract protein concentration and CFE activity. CFE was performed with different concentrations of extract protein. The β-galactosidase activity after CFE was quantified and plotted relative to the activity using undiluted S30 extract. A clear trend is visible with a peak in activity at extract protein concentrations of 3.4–4.8 mg/ml. At concentrations below and above the peak a concentration-dependent decrease in activity is observed. n=3.

ity, the six S30 extracts were diluted in 10 mM Tris-acetate buffer (pH 8.2) containing 14 mM magnesium acetate, 60 mM potassium acetate, and 1.0 mM DTT – the same buffer against which the S30 extracts were dialyzed during preparation. This was done to keep the concentration of the buffer components constant, while reducing the extract protein concentration. The S30 extracts were diluted to achieve a final extract protein concentration of 7.2 mg/ml when using 30 % v/v diluted S30 extract. CFE with pIVEX2.2EM-LacZ was performed and the β-galactosidase activity was quantified (see figure 5). No significant differences between the extracts were observed anymore, while the average relative standard deviation in fact decreased, indicating that the difference can be explained by a reduced variance of the means. Interestingly, a 3.9-fold increase in average activity was observed compared to the undiluted extracts, clearly showing that the CFE reaction is concentration-dependent.

3.4. Relationship between extract protein concentration and CFE activity

The significant increase in average activity of the extracts upon dilution led us to investigate the influence of the S30 total protein content on the activity of the S30 extract. Not only might dilution increase the activity, but it would also save valuable S30 extract. S30 extract derived from Rosetta-gami™ B(DE3) was linearly diluted in the same buffer against which the extract was dialyzed during preparation, leading to final concentrations of 0.0–10.2 mg/ml extract protein in the CFE reactions. CFE was performed with pIVEX2.2EM-LacZ, and the β-galactosidase activity was quantified (see figure 6). A clear trend is visible with a peak in activity at 3.4–4.8 mg/ml extract protein. At concentrations below and above the peak a concentration-dependent decrease in activity is observed. Both this trend and the peak agree with the results in figure 1 from the different extracts prepared over the years.

4. Discussion and conclusion

In this study we show that normalization of the total protein content of batches of S30 extract can reduce the variability in CFE activity of these batches. Although this might seem logical, to our surprise this is not standard practice. Most protocols for the preparation of S30 extract define the S30 extract concentration based on the cell pellet wet weight. However, variability introduced during downstream processing often causes large differences between batches of S30 extract. According to these protocols, CFE is subsequently performed with a constant volume percentage of S30 extract. We show that this results in large differences in expression, even when the S30 extracts are produced in parallel and care is taken to treat the extracts the same way during downstream processing (figure 3). Relatively small fluctuations in S30 protein concentration were seen to cause significant differences in expression activity. These differences, observed when using equal volumes of different S30 extracts, can be decreased by normalizing the S30 protein concentration in CFE reactions (figure 5).

Many factors are responsible for the variation in extract protein concentration, such as incomplete resuspension of the bacteria, incomplete lysis, dilution or loss of the lysate during homogenization due to the dead volume of the equipment used to disrupt the bacterial cell walls, frothing during sonication, loss of proteins or bacteria due to adhesion, the inclusion of a preincubation step, dilution during dialysis, rounding of volumes, or pipetting errors. Of the different production steps, lysis was shown to have the most impact [24,33]. Because most of these factors do not qualitatively influence the S30 extract, normalization of the extract protein concentration would eliminate most differences. Some protocols suggest optimizing the S30 volume concentration for each new batch of extract [5]. Given the results presented in this

paper, we believe that this is time-consuming and unnecessary, and that normalization of the total protein concentration would be more appropriate.

Not all variation in activity is caused by differences in extract protein concentration. Even at the same protein concentration, different extracts still possess different activities (figure 1). These differences might result from other aspects such as different *E. coli* strains used for preparation, different extract preparation protocols, different lysis methods employed, loss of activity during storage, or accidental loss of activity due to faulty handling during preparation. Indeed, these variables are often the subject of studies. When these variables are expected to change the protein composition of the extract, it might be sensible to optimize the extract protein concentration first. However, when comparing these variables, it is paramount to normalize the extract protein concentrations to these optima after preparation, otherwise the random variation in protein concentration arising during downstream processing might obscure the conclusions. Thus, to make an unbiased comparison between extracts, normalized protein concentrations should be used.

We did not observe any significant difference between extracts derived from different *E. coli* strains, even though BL21(DE3) was expected to give slightly higher background FDG conversion activity due to endogenous β-galactosidase [38]. Nonetheless, all results were blank-corrected.

We did not find a relationship between storage time and activity of our S30 extracts, although we lacked the proper controls to draw any significant conclusions. We found that activity is retained, even after storage for up to 6 years at −80 °C.

The activity of S30 extracts is dependent on the proteins within the extracts. These proteins, including ribosomes, are the driving force behind CFE. Indeed, even if everything else is removed from the S30 extract and only the proteins and ribosomes remain, CFE can be achieved [11]. Among the many components of the S30 extract, elongation factors were previously shown to be restricting [21]. Another study tested the addition of purified translation factors, aminoacyl-tRNA synthetases, and ribosomes, but did not find any of these components to be limiting [40]. However, this study was performed with >17 mg/ml S30 extract protein in the CFE reaction. At such a high concentration, which lies far above the optimum (figure 1 and 6), proteins are already present in excess.

We believe that the results we describe here are caused by differences in extract protein concentration. However, we cannot exclude that other components of the S30 extracts add to the effects observed in this paper. We attempted to exclude some of these components by diluting the S30 extracts in extract buffer, thus keeping the concentration of the salts constant. Further studies would be required to determine the effect of the individual proteins, or ribosomes, on the CFE reaction. Here we sought to improve the basic production protocol for S30 extracts, and further standardization of the individual proteins would not be possible while keeping the production protocol the same.

We found that the CFE yield is dependent on the extract protein content of the final CFE reaction. At an S30 protein concentration of 3.4–4.8 mg/ml the highest activity is obtained, at least for the expression of active β-galactosidase (figure 6). We do not know if the same also applies to other enzymes or proteins, although a similar peak in expression was obtained before with condensed extracts after the expression of chloramphenicol acetyltransferase (CAT) [23] and superfolder green fluorescent protein (sfGFP) [41]. Further studies would have to point out if the drop in yield at higher extract concentrations is caused by loss of enzyme activity (*e.g.* aggregation), or by a decrease in production. Previous studies found that during incubation several key components (amino acids, energy compounds, mRNA) are degraded by enzymes present in the S30 extract [42–44]. Increasing the extract protein concentration would thus also increase degradation, possibly at a higher rate than protein synthesis. Since the most expensive component of the CFE reaction is the S30 extract, these results

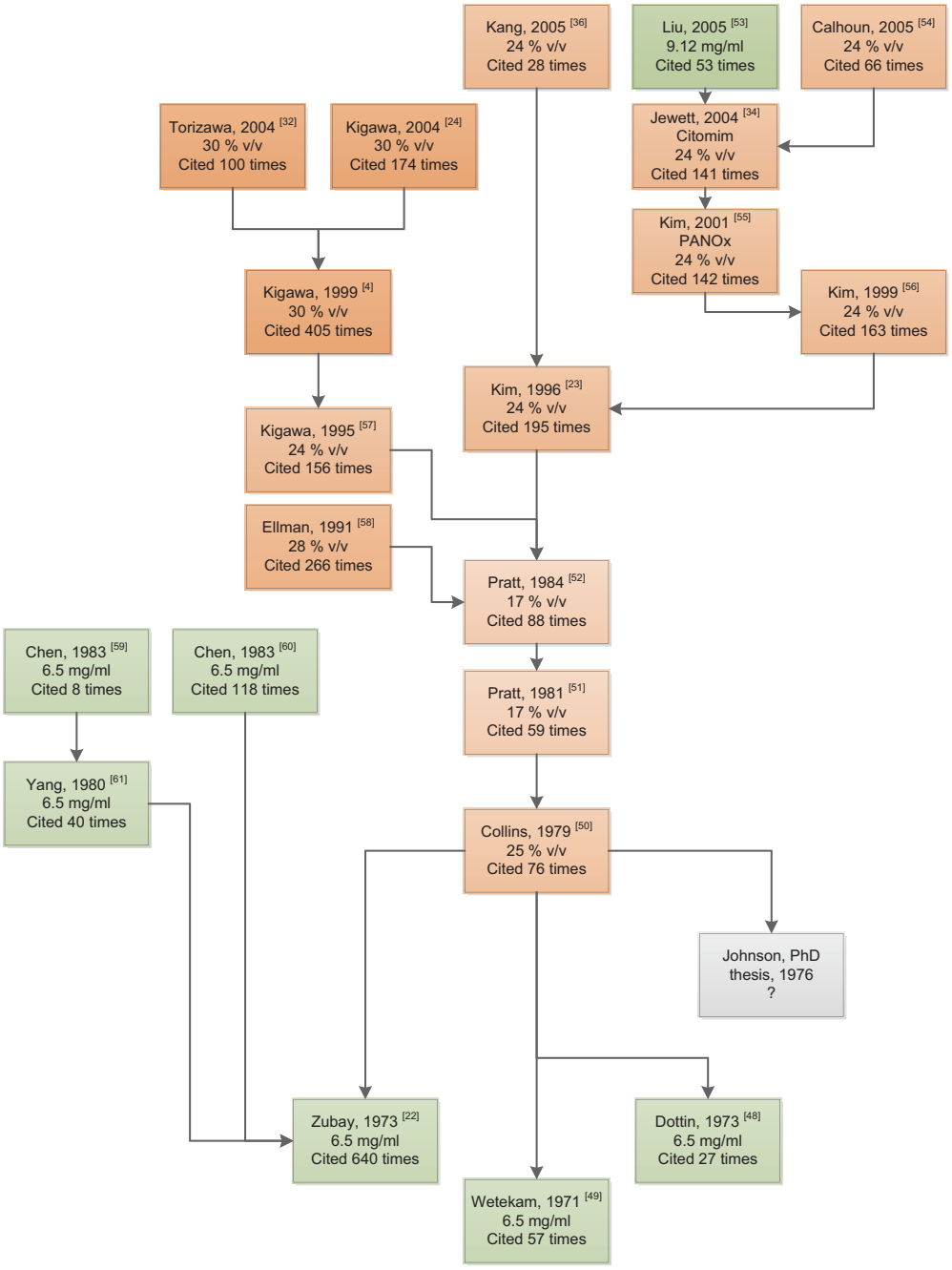

Figure 7. Tree structure showing select publications from the history of S30 extract. The arrows indicate the publications on which the CFE protocols were based. For each publication, the concentration of the S30 extract in CFE reactions is stated, along with the number of times the article has been cited according to Google Scholar [4,22–24,32,34,36,48–61]. After 2000, the structure becomes increasingly more complex due to the many variations of the CFE protocol.

show that by decreasing the extract concentration, one can gain in yield while reducing the cost.

Normalization of the total protein concentration of an S30 extract is not without precedent. In fact, early protocols for CFE used a fixed amount of S30 protein per reaction [22,45–49]. For example, in 1973, Zubay used 6.5 mg/ml S30 protein in the CFE reactions [22]. The first publication we could find to use a fixed volume concentration of S30 extract was by Collins in 1979 [50]. According to the paper, his method was based on the protocol from Zubay, with modifications from a PhD thesis. We believe this to be the source of this change (see figure 7). Later work from Pratt *et al.* [51,52] was based on this publication, and from that time on, most publications have used a fixed volume percentage of S30 extract. Pratt *et al.* also mention that they tested different extract protein concentrations, but that any S30 extract with a protein concentration between 30 and 200 mg/ml could be used with limited effect on the efficiency [51]. While this might have been the case for their old CFE system, in which the S30 extract was not the limiting factor, we show that this is definitely not true for currently used optimized CFE systems based on *E. coli* S30 extract.

In one recent publication, Liu *et al.* normalized their extracts to 9.12 mg/ml [53]. This was done by varying the volume of S30 extract added, thus also varying the amount of salts. Moreover, they did not investigate the effect of the normalization on the expression level or mention why the extract had been normalized to this concentration. We observed an 80 % drop in activity at 9 mg/ml compared to the optimal concentration of 3.4–4.8 mg/ml.

Despite all the different protocols we could not find any report investigating the effect of normalization on the expression activity of the extracts. Moreover, almost all recent publications still use extracts based on pellet wet weight instead of normalizing their extracts based on protein concentration. We now show that without normalization bias is introduced, obscuring the comparison of studies on the activity of S30 extracts. We propose that, in the future, the protein concentration of S30 extracts be determined and normalized before use.

Acknowledgements

We would like to thank Zahra Karjoo, Neda Rafiei Tabataei, Iris Ferretti, Valentino Coniglione, Maryam Amidi, Volkert de Bot, and Marijn Schouten for providing us with samples from the extracts they produced over the years.

This work was supported by Technologiestichting STW [budget number 10243].

References

1 Pedersen, A. *et al.* **Rational improvement of cell-free protein synthesis.** N Biotechnol (2011) 28, 218–224.

2 Bundy, B.C. and Swartz, J.R. **Efficient disulfide bond formation in virus-like particles.** J Biotechnol (2011) 154, 230–239.

3 Knapp, K.G., Goerke, A.R. and Swartz, J.R. **Cell-free synthesis of proteins that require disulfide bonds using glucose as an energy source.** Biotechnol Bioeng (2007) 97, 901–908.

4 Kigawa, T. *et al.* **Cell-free production and stable-isotope labeling of milligram quantities of proteins.** FEBS Lett (1999) 442, 15–19.

5 Apponyi, M.A. *et al.* **Cell-free protein synthesis for analysis by NMR spectroscopy.** Methods Mol Biol (2008) 426, 257–268.

6 Arthur, I.N. *et al.* ***In situ*** **deprotection and incorporation of unnatural amino acids during cell-free protein synthesis.** Chemistry (2013) 19, 6824–6830.

7 Kigawa, T. *et al.* **Selenomethionine incorporation into a protein by cell-free synthesis.** J Struct Funct Genomics (2002) 2, 29–35.

8 Bundy, B.C. and Swartz, J.R. **Site-specific incorporation of p-propargyloxyphenylalanine in a cell-free environment for direct protein-protein click conjugation.** Bioconjug Chem (2010) 21, 255–263.

9 Muranaka, N. *et al.* **Incorporation of unnatural non-alpha-amino acids into the N terminus of proteins in a cell-free translation system.** Chembiochem (2007) 8, 1650–1653.

10 Ozawa, K. *et al.* **High-yield cell-free protein synthesis for site-specific incorporation of unnatural amino acids at two sites.** Biochem Biophys Res Commun (2012) 418, 652–656.

11 Shimizu, Y. *et al.* **Cell-free translation reconstituted with purified components.** Nat Biotechnol (2001) 19, 751–755.

12 Swartz, J. **A PURE approach to constructive biology.** Nat Biotechnol (2001) 19, 732–733.

13 Isaksson, L. *et al.* **Expression screening of membrane proteins with cell-free protein synthesis.** Protein Expr Purif (2012) 82, 218–225.

14 Klammt, C. *et al.* **High level cell-free expression and specific labeling of integral membrane proteins.** Eur J Biochem (2004) 271, 568–580.

15 Smith, M.T. *et al.* **The incorporation of the A2 protein to produce novel Qbeta virus-like particles using cell-free protein synthesis.** Biotechnol Prog (2012) 28, 549–555.

16 Avenaud, P. *et al.* **Expression and activity of the cytolethal distending toxin of Helicobacter hepaticus.** Biochem Biophys Res Commun (2004) 318, 739–745.

17 Matthies, D. *et al.* **Cell-free expression and assembly of ATP synthase.** J Mol Biol (2011) 413, 593–603.

18 Kim, T.W. *et al.* **Cell-free synthesis and *in situ* isolation of recombinant proteins.** Protein Expr Purif (2006) 45, 249–254.

19 Woodrow, K.A. and Swartz, J.R. **A sequential expression system for high-throughput functional genomic analysis.** Proteomics (2007) 7, 3870–3879.

20 Mastrobattista, E. *et al.* **High-throughput screening of enzyme libraries: *in vitro* evolution of a beta-galactosidase by fluorescence-activated sorting of double emulsions.** Chem Biol (2005) 12, 1291–1300.

21 Underwood, K.A., Swartz, J.R. and Puglisi, J.D. **Quantitative polysome analysis identifies limitations in bacterial cell-free protein synthesis.** Biotechnol Bioeng (2005) 91, 425–435.

22 Zubay, G. ***In vitro* synthesis of protein in microbial systems.** Annu Rev Genet (1973) 7, 267–287.

23 Kim, D.M. *et al.* **A highly efficient cell-free protein synthesis system from *Escherichia coli*.** Eur J Biochem (1996) 239, 881–886.

24 Kigawa, T. *et al.* **Preparation of *Escherichia coli* cell extract for highly productive cell-free protein expression.** J Struct Funct Genomics (2004) 5, 63–68.

25 Kim, T.W. *et al.* **Simple procedures for the construction of a robust and cost-effective cell-free protein synthesis system.** J Biotechnol (2006) 126, 554–561.

26 Zawada, J.F. **Preparation and testing of *E. coli* S30 *in vitro* transcription translation extracts.** Methods Mol Biol (2012) 805, 31–41.

27 Klammt, C. *et al.* **Cell-free production of integral membrane proteins on a preparative scale.** Methods Mol Biol (2007) 375, 57–78.

28 Goerke, A.R. and Swartz, J.R. **Development of cell-free protein synthesis platforms for disulfide bonded proteins.** Biotechnol Bioeng (2008) 99, 351–367.

29 Dreier, B. and Pluckthun, A. **Rapid selection of high-affinity binders using ribosome display.** Methods Mol Biol (2012) 805, 261–286.

30 Miles, L.A. *et al.* **An *Escherichia coli* cell-free system for recombinant protein synthesis on a milligram scale.** Methods Mol Biol (2011) 752, 17–28.

31 Schwarz, D. *et al.* **Preparative scale expression of membrane proteins in *Escherichia coli*-based continuous exchange cell-free systems.** Nat Protoc (2007) 2, 2945–2957.

32 Torizawa, T. *et al.* **Efficient production of isotopically labeled proteins by cell-free synthesis: a practical protocol.** J Biomol NMR (2004) 30, 311–325.

33 Shrestha, P., Holland, T.M. and Bundy, B.C. **Streamlined extract preparation for *Escherichia coli*-based cell-free protein synthesis by sonication or bead vortex mixing.** Biotechniques (2012) 53, 163–174.

34 Jewett, M.C. and Swartz, J.R. **Mimicking the *Escherichia coli* cytoplasmic environment activates long-lived and efficient cell-free protein synthesis.** Biotechnol Bioeng (2004) 86, 19–26.

35 Kim, T.W. *et al.* **An economical and highly productive cell-free protein synthesis system utilizing fructose-1,6-bisphosphate as an energy source.** J Biotechnol (2007) 130, 389–393.

36 Kang, S.H. *et al.* **Cell-free production of aggregation-prone proteins in soluble and active forms.** Biotechnol Prog (2005) 21, 1412–1419.

37 Amidi, M. *et al.* **Antigen-expressing immunostimulatory liposomes as a genetically programmable synthetic vaccine.** Syst Synth Biol (2011) 5, 21–31.

38 Amidi, M. *et al.* **Optimization and quantification of protein synthesis inside liposomes.** J Liposome Res (2010) 20, 73–83.

39 Amidi, M. *et al.* **Induction of humoral and cellular immune responses by antigen-expressing immunostimulatory liposomes.** J Control Release (2012) 164, 323–330.

40 Freischmidt, A. *et al.* **Limiting factors of the translation machinery.** J Biotechnol (2010) 150, 44–50.

41 Fujiwara, K. and Nomura, S.M. **Condensation of an additive-free cell extract to mimic the conditions of live cells.** PLoS One (2013) 8, e54155.

42 Kim, R.G. and Choi, C.Y. **Expression-independent consumption of substrates in cell-free expression system from *Escherichia coli*.** J Biotechnol (2001) 84, 27–32.

43 Michel-Reydellet, N., Calhoun, K. and Swartz, J. **Amino acid stabilization for cell-free protein synthesis by modification of the *Escherichia coli* genome.** Metab Eng (2004) 6, 197–203.

44 Kitaoka, Y., Nishimura, N. and Niwano, M. **Cooperativity of stabilized mRNA and enhanced translation activity in the cell-free system.** J Biotechnol (1996) 48, 1–8.

45 Nirenberg, M.W. **Cell-free protein synthesis directed by messenger RNA.** Methods Enzymol (1963) 6, 17–23.

46 Lederman, M. and Zubay, G. **DNA-directed peptide synthesis. 1. A comparison of T2 and Escherichi coli DNA-directed peptide synthesis in two cell-free systems.** Biochim Biophys Acta (1967) 149, 253–258.

47 Lederman, M. and Zubay, G. **DNA directed peptide synthesis. V. The cell-free synthesis of a polypeptide with beta-galactosidase activity.** Biochem Biophys Res Commun (1968) 32, 710–714.

48 Dottin, R.P. and Pearson, M.L. **Regulation by N gene protein of phage lambda of anthranilate synthetase synthesis *in vitro*.** Proc Natl Acad Sci U S A (1973) 70, 1078–1082.

49 Wetekam, W., Staack, K. and Ehring, R. **DNA-dependent *in vitro* synthesis of enzymes of the galactose operon of *Escherichia coli*.** Mol Gen Genet (1971) 112, 14–27.

50 Collins, J. **Cell-free synthesis of proteins coding for mobilisation functions of ColE1 and transposition functions of Tn3.** Gene (1979) 6, 29–42.

51 Pratt, J.M. *et al.* **Identification of gene products programmed by restriction endonuclease DNA fragments using an *E. coli in vitro* system.** Nucleic Acids Res (1981) 9, 4459–4474.

52 Pratt, J.M. **Coupled transcription-translation in prokaryotic cell-free systems.** In: Transcription and translution: A practical approach (eds B. D. Hames and S. J. Higgins) Ch. 7, 179–209 (IRL Press, 1984).

53 Liu, D.V., Zawada, J.F. and Swartz, J.R. **Streamlining *Escherichia coli* S30 extract preparation for economical cell-free protein synthesis.** Biotechnol Prog (2005) 21, 460–465.

54 Calhoun, K.A. and Swartz, J.R. **An economical method for cell-free protein synthesis using glucose and nucleoside monophosphates.** Biotechnol Prog (2005) 21, 1146–1153.

55 Kim, D.M. and Swartz, J.R. **Regeneration of adenosine triphosphate from glycolytic intermediates for cell-free protein synthesis.** Biotechnol Bioeng (2001) 74, 309–316.

56 Kim, D.M. and Swartz, J.R. **Prolonging cell-free protein synthesis with a novel ATP regeneration system.** Biotechnol Bioeng (1999) 66, 180–188.

57 Kigawa, T., Muto, Y. and Yokoyama, S. **Cell-free synthesis and amino acid-selective stable isotope labeling of proteins for NMR analysis.** J Biomol NMR (1995) 6, 129–134.

58 Ellman, J. *et al.* **Biosynthetic method for introducing unnatural amino acids site-specifically into proteins.** Methods Enzymol (1991) 202, 301–336.

59 Chen, H.Z. and Zubay, G. **Analysis of ColE1 expression *in vitro* after chromosome fragmentation.** J Bacteriol (1983) 154, 650–655.

60 Chen, H.Z. and Zubay, G. **Prokaryotic coupled transcription-translation.** Methods Enzymol (1983) 101, 674–690.

61 Yang, H.L. *et al.* **Cell-free coupled transcription-translation system for investigation of linear DNA segments.** Proc Natl Acad Sci U S A (1980) 77, 7029–7033.

Chapter IV

Different proteins require different S30 extract protein concentrations for optimal expression

Erik A. Teunissen[1], Georgi Nadibaidze[1], Markus de Raad[1] and Enrico Mastrobattista[1]
[1]Department of Pharmaceutics, Utrecht Institute for Pharmaceutical Sciences, Faculty of Science, Utrecht University, Universiteitsweg 99, 3584 CG Utrecht, The Netherlands

Submitted for publication

Abstract

In this study we show that the yield of prokaryotic cell-free expression depends on the *Escherichia coli* S30 extract protein concentration in the reaction. We tested this relationship for the expression of several different proteins, and found that each protein requires its own unique extract protein concentration for optimal expression. Furthermore, this correlation changes under different incubation temperatures, although incubation time does not influence the correlation. We observed a similar dependency with a commercially available prokaryotic cell-free expression system as well. We tried adding stabilizing excipients to the reaction to allow higher extract protein concentrations to be used, but this did not result in higher levels of protein expression. We did observe some beneficial effects with DMSO at suboptimal extract protein concentrations. No single extract protein concentration was found at which all proteins were expressed optimally, although all proteins showed reasonable expression at 5–6 mg/ml extract protein. This study clearly shows that the extract protein concentration is an important variable that needs to be optimized when expressing a new protein.

1. Introduction

Cell-free expression (CFE) is an excellent technique for the small-scale production of recombinant proteins, utilizing an *in vitro* transcription and translation system such as an S30 bacterial extract [1–3]. The S30 extract prepared from *Escherichia coli* (*E. coli*) has been used successfully for many applications, including isotopic labeling [4,5], the incorporation of unnatural amino acids [6–10], high-throughput screening [11], directed evolution [12], vaccine development [13–15], and the production of toxic proteins [16,17], membrane proteins [18,19], proteins requiring specific disulfide bonds [20,21], and multiprotein complexes [16,22].

Despite the many advantages CFE expression has over conventional recombinant production, the technique remains plagued by low levels of protein synthesis. Many studies have focused on increasing the expression level of CFE. In most of these studies, either the reaction conditions were altered [23–25] or the energy supply was changed [26–29], but very few studies have focused on the S30 extract itself.

Most current protocols for CFE simply use a fixed volume percentage of S30 extract in the CFE reaction, without prior characterization or normalization of the S30 extract [2,19,25,29–38]. Given the many steps that are involved in the production of S30 extracts, and the countless variations of the preparation protocol that exist, using a fixed volume percentage often results in widely varying extract protein concentrations in the final CFE reaction [33,39,40].

We have previously shown that the yield of expression depends on the concentration of S30 extract protein in the CFE reaction [40]. Similar results have also been obtained with condensed extracts [1,4,41]. We found that, for the expression of active β-galactosidase, the highest yield is obtained using a final concentration of 3.4–4.8 mg/ml S30 extract protein. This concentration is significantly lower than the concentrations used in the few reports that do normalize S30 extracts based on protein concentration [42,43]. If this relationship holds true for all proteins expressed, and if the peak activity lies at the same extract concentration for each recombinant protein, this would mean that merely lowering the amount of extract used could result in a significant boost in CFE activity. On the other hand, if each protein requires a different extract protein concentration for optimal expression, this would have to be optimized to attain the highest expression, something that is not common practice.

In this study we zoomed in on this correlation be-

tween CFE yield and extract protein concentration. We tested if the relationship we previously observed for the expression of active β-galactosidase extends to the expression of other recombinant proteins. We also tested if a similar relationship is observed with commercially available systems. These systems, such as the Rapid Translation System (RTS) (5PRIME, previously Roche) and the S30 T7 High-Yield Protein Expression System (Promega), also use a fixed volume of S30 extract per reaction. According to the manufacturers, the supplied *E. coli* lysate is optimized to obtain the highest CFE activity. However, if the optimal concentration depends on the protein being expressed, a single best concentration would not be possible. Still, while Promega states that increasing the concentration might increase the yield, none of the manufacturers recommend optimizing the concentration of *E. coli* extract in the CFE reaction.

We found that the relationship between CFE yield and S30 extract protein concentration is not static. Different proteins required different extract protein concentrations for optimal expression, and this optimal concentration shifted under different incubation temperatures. Strikingly, the relative productivity at different S30 extract protein concentrations did not change during incubation. The addition of stabilizing excipients could not boost the expression at high extract protein concentrations, although addition of DMSO at suboptimal extract protein concentrations resulted in slightly increased protein expression.

2. Materials and Methods

2.1. Chemicals

Adenosine-5'-triphosphate (ATP), ammonium acetate, β-galactosidase (G6008, 250–600 U/mg), bovine serum albumin (BSA), bromophenol blue, chloramphenicol, 3'-5'-cyclic adenosine monophosphate (cAMP), cytidine-5'-triphosphate (CTP), dimethyl sulfoxide (DMSO), dithiothreitol (DTT), folinic acid, glycerol, guanosine-5'-triphosphate (GTP), LB broth culture medium, magnesium acetate, 2-mercaptoethanol, polyethylene glycol 8000 (PEG 8000), polysorbate 20 (TWEEN® 20), potassium hydroxide, sodium dodecyl sulfate (SDS), tris(hydroxymethyl)aminomethane (Tris), uridine-5'-triphosphate (UTP), and each of the 20 standard amino acids were purchased from Sigma-Aldrich (St. Louis, MO, USA). Acetic acid, hydrochloric acid, potassium acetate, and sucrose were purchased from Merck KGaA (Darmstadt, Germany). Creatine kinase (CK), *E. coli* total tRNA, and cOmplete EDTA-free protease inhibitor cocktail tablets were purchased from Roche (Basel, Switzerland). HEPES was purchased from Acros Organics (Geel, Belgium). Creatine phosphate was purchased from Alfa Aesar (Ward Hill, MA, USA). T7 RNA polymerase and DNA-modifying enzymes were purchased from Thermo Scientific (Waltham, MA, USA). Fluorescein di-β-D-galactopyranoside (FDG) was purchased from Marker Gene Technologies (Eugene, OR, USA). Phosphate buffered saline (PBS) was purchased from B. Braun Melsungen AG (Melsungen, Germany). RNase AWAY™ was purchased from Life Technologies (Carlsbad, CA, USA).

2.2. Plasmids

All genes were cloned into a pIVEX2.2EM or pDUAL GC backbone under control of a T7 promoter. The preparation of the pIVEX2.2EM backbone has been described elsewhere [12]. The plasmid pIVEX-LacZ, which contains the wild-type *E. coli LacZ* gene, was prepared as described previously [12]. The plasmid pIVEX-HaPyV-VP1/co, which contains the Hamster polyomavirus *VP1* gene codon-optimized for expression in *E. coli*, was prepared as follows. The VP1 protein sequence was obtained from Gedvilaite *et al.* [44]. The sequence was reverse translated and codon-optimized for expression in *E. coli* using GeneDesign [45]. Flanking sequences were added to create an NcoI restriction site overlapping the start codon and an XhoI restriction site directly

adjacent to the stop codon. The gene was synthesized by GenScript (Piscataway, NJ, USA) and delivered in a pUC57 vector. The *HaPyV-VP1/co* gene was excised from pUC57 using NcoI and XhoI, and cloned into pIVEX2.2EM digested with the same enzymes. The production of VP1 using this plasmid was validated previously [46]. pIVEX-EGFP, which contains the enhanced green fluorescent protein (*EGFP*) gene, was cloned as follows. The *EGFP* gene was amplified from pEGFP-C1 (Clontech) by PCR using primers EGFP-Fw CGGTCGCCACCATGGT and EGFP-Rv TGCAGAATTCGAAGCTTGAG. The PCR product was digested with NcoI and XhoI, and ligated into pIVEX2.2EM digested with the same enzymes. pIVEX-OVA, which contains the gene for soluble ovalbumin, was cloned as follows. The sOVA gene was amplified from pCI-neo-sOVA (obtained via Addgene from [47]) by PCR using primers OVA-Fw TCATGAAAATGGGCTCCATCGGCGC and OVA-Rv GGATCCTTAAGGGGAAACACATCTGCCAAAG. The PCR product was digested with BspHI and BamHI, and ligated into pIVEX2.2EM digested with NcoI and BamHI. The plasmid pDUAL-Luc-NP, which contains the firefly luciferase gene fused to the H3N2 influenza nucleoprotein epitope ($NP_{366-374}$, ASNENMDAM), was prepared and validated previously [15]. All genes were verified by sequencing (BaseClear; Leiden, The Netherlands). Suitable quantities of circular plasmid DNA were obtained using the NucleoBond® PC 10 000 kit (MACHEREY-NAGEL; Düren, Germany).

2.3. Preparation of *E. coli* S30 extracts

The preparation of S30 extracts was based on previous protocols [2,3] and has been detailed before [40]. Novagen® Rosetta-gami™ B(DE3) *E. coli* (Merck KGaA) were used for the preparation. The bacteria were lysed by two passes through an EmulsiFlex-C5 high pressure homogenizer (AVESTIN; Ottawa, ON, Canada) at >15,000 psi. No preincubation step was performed. The extracts were stored as 1.0 ml aliquots at −80 °C.

2.4. Protein quantification

Protein concentrations were determined using the Pierce™ BCA Protein Assay Kit (Thermo Scientific) according to the manufacturer's protocol. Results were corrected for reducing agents present in the S30 extract and reconstitution buffer (RTS 100 *E. coli* HY Kit).

2.5. Cell-free protein synthesis using S30 extract

Cell-free protein synthesis was performed with a total reaction volume of 25–100 µl. During preparation, the reactions and reaction components were kept on ice to prevent premature expression. Each reaction contained 34 % v/v (diluted) S30 extract, 175 µg/ml *E. coli* total tRNA, 250 µg/ml creatine kinase, 5.8 mM magnesium acetate, 55 mM HEPES-KOH (pH 8.2), 1.7 mM DTT, 1.2 mM ATP, 0.8 mM CTP, 0.8 mM GTP, 0.8 mM UTP, 80 mM creatine phosphate, 0.64 mM cAMP, 68.9 µM folinic acid, 210 mM potassium acetate, 27.6 mM ammonium acetate, 1.0 mM of each of the 20 standard amino acids, 4.0 % w/v PEG 8000, and 2.5 U/µl T7 RNA polymerase. Plasmid DNA was added to a final concentration of 20 nM. The reactions were incubated for 4 hours at 30 °C, unless specified otherwise.

2.6. Cell-free protein synthesis using RTS

The Rapid Translation System RTS 100 *E. coli* HY Kit (Roche; Basel, Switzerland) was used according to the manufacturer's protocol with pIVEX-LacZ as template. The reaction volume was 20 µl. Normally, reactions are performed with 24 % v/v *E. coli* lysate. We prepared different dilutions using the supplied reconstitution buffer, while keeping the total amount of reconstitution buffer per reaction the same.

2.7. Quantification of β-galactosidase activity

The activity of the cell-free produced β-galactosidase was determined using FDG based on a previously described protocol [14,40]. Briefly, from each CFE reaction 10 µl was taken and added to 90 µl 33 mM Tris-acetate buffer (pH 7.9) with 10 mM magnesium acetate, 66 mM potassium acetate, and 5.0 mg/ml BSA in a black 96-well plate (Greiner Bio-One; Monroe, NC). To each well 100 µl substrate solution (0.2 mM FDG in 33 mM Tris-acetate buffer (pH 7.9) with 10 mM magnesium acetate, 66 mM potassium acetate, 0.2 % DMSO and 5.0 mg/ml BSA) was injected using a FLUOstar OPTIMA (BMG Labtech; Ortenberg, Germany) equilibrated at 37 °C, and the fluorescence (excitation, 485 nm; emission, 520 nm) was measured every 0.5 sec for 120 sec. A β-galactosidase standard curve was also measured (2-fold dilution, 7.8–500 U/ml). The slope per minute was determined using the FLUOstar OPTIMA software, and based on the standard curve (4-parameter fit) the β-galactosidase activity was calculated.

2.8. Quantification of EGFP fluorescence

EGFP expression was quantified based on its fluorescence. From each CFE reaction 40 µl was taken and mixed with 160 µl PBS in a black 96-well plate (Greiner Bio-One; Monroe, NC). The plate was equilibrated to 30 °C in a FLUOstar OPTIMA, and the EGFP fluorescence was measured (excitation, 485 nm; emission, 520 nm; 200 flashes per well). All values were blank-corrected.

2.9. Quantification of firefly luciferase activity

Firefly luciferase activity was quantified by measuring luminescence after adding firefly luciferin. Reagents from the Dual-Luciferase® Reporter Assay System (Promega; Madison, WI, USA) were used. 5 µl of each CFE reaction was added to 45 µl 1× passive lysis buffer in a black 96-well plate (Greiner Bio-One; Monroe, NC). The firefly luciferase substrate was prepared according to the manufacturer's protocol, and to each well 50 µl was injected using a FLUOstar OPTIMA equilibrated at 22 °C. Luminescence was detected over a 10 sec period, 2 seconds after substrate injection.

2.10. Quantification of VP1

VP1 was detected by Western blotting and quantified based on band intensity. All incubations were performed with PBS containing 0.1 % v/v TWEEN® 20 (PBS-T). Each CFE sample was first diluted 10× in PBS, followed by the addition of 4× reducing loading dye (60 mM Tris-HCl buffer (pH 6.8) containing 25 % v/v glycerol, 2.0 % w/v SDS, 1.0 % w/v bromophenol blue, and 5.0 % v/v 2-mercaptoethanol) to a final concentration of 1×. The samples were incubated at 98 °C for at least 2 min. Next, 10 µl of each sample was loaded on NuPAGE 4–12% Bis-Tris gels (Life Technologies), which were run at 150 V for 70 min. An internal standard (HaPyV VP1) was included on each gel. Afterwards, the gels were blotted using an iBlot™ (Life Technologies) dry blotting machine (program P2) with Nitrocellulose iBlot® Gel Transfer Stacks (Life Technologies). The blots were blocked overnight at 4 °C with 5 ml PBS-T containing 5.0 % w/v BSA. Afterwards, the Western blots were rinsed 3 times with >5 ml PBS-T. The blots were incubated with 2.5 µl mouse-anti-HaPyV-VP1 (ab34755; Abcam; Cambridge, United Kingdom) in 5 ml PBS-T for 1 hour at 22 °C. The blots were rinsed 3 times with >5 ml PBS-T, and washed three times by incubation with >5 ml PBS-T for 5 min at 22 °C, followed by incubation with 4.0 µl Stabilized Goat Anti-Mouse IgG (H+L), Peroxidase Conjugated (#32430; Thermo Scientific) secondary antibody in 5 ml PBS-T for 1 hour at 22 °C. The blots were rinsed and washed again, and imaged with a ChemiDoc™ XRS (Bio-Rad; Hercules, CA, USA) using the SuperSignal West Femto substrate with an incubation time of 30 sec. The amount of VP1 was quantified using ImageJ [48],

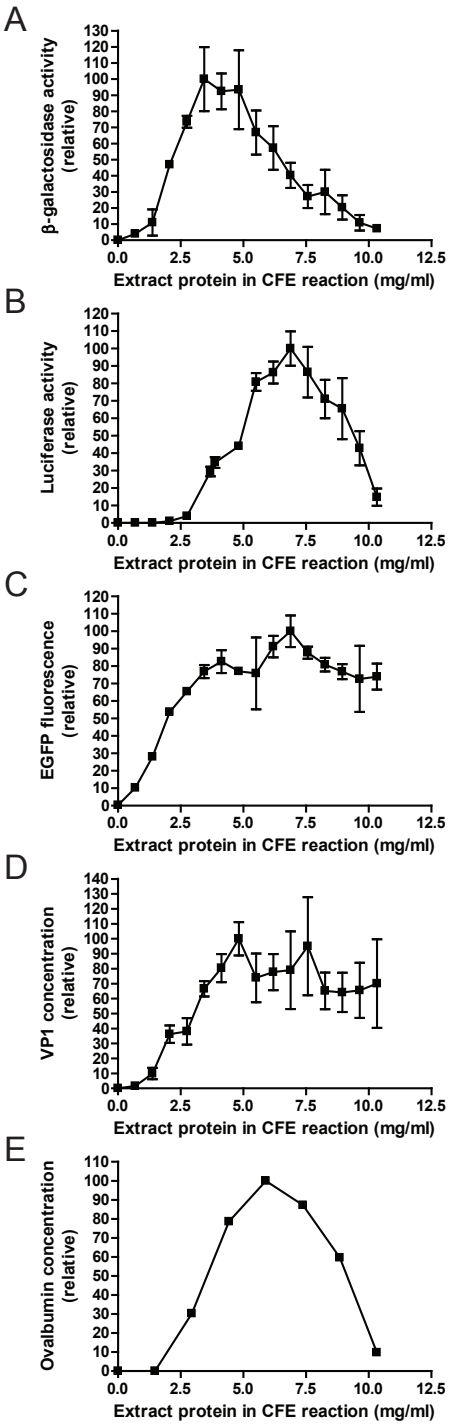

and the values were corrected using the internal standard on each blot.

2.11. Quantification of ovalbumin

Ovalbumin was detected by Western blotting and quantified based on band intensity. The protocol was identical to the quantification of VP1, except for the primary antibody, where 3.0 µl mouse-anti-ovalbumin (ab17293; Abcam) in 3 ml PBS-T was used.

2.12. Stabilizing excipients

Stock solutions of 80 % v/v glycerol, 66 % w/v sucrose, and 10 % v/v DMSO in demineralized water were prepared. The influence of the highest concentration of the three stabilizing excipients on β-galactosidase enzyme activity was tested by adding 10 µl of the stock solutions to 40 µl extract buffer (10 mM Tris-acetate (pH 8.2), 14 mM magnesium acetate, 60 mM potassium acetate, and 1 mM DTT) containing 0.045 U/µl β-galactosidase, and measuring the β-galactosidase activity as above.

The effect of the excipients on CFE was tested by adding up to 20 % v/v of the stock solutions to the CFE reactions. The final concentration of all CFE components remained constant as above.

2.13. EGFP expression over time

Cell-free expression was performed in a black 96-well plate (Greiner Bio-One; Monroe, NC) with a re-

Figure 1. Relationship between extract protein concentration and CFE yield. Five different proteins were produced by CFE. Expression was performed with different concentrations of extract protein. (a) β-galactosidase as previously quantified based on enzyme activity (conversion of FDG) (reproduced with permission from [40]). (b) Firefly luciferase activity was quantified based on luminescence. (c) EGFP was quantified based on fluorescence. (d) VP1 was quantified by Western blotting. (e) Ovalbumin was quantified by Western blotting. The results are shown relative to the peak activity, fluorescence, or concentration. (a–d, n=3; e, n=1).

action volume of 100 µl. The reaction components were kept on ice during preparation. Afterwards, the plate was incubated in a FLUOstar OPTIMA set to 30 °C. EGFP fluorescence was measured every 5 min for 500 min (excitation, 485 nm; emission, 520 nm; 200 flashes per well).

3. Results

3.1. Different proteins require different extract protein concentrations for optimal expression

We have previously shown that the expression of active β-galactosidase depends on the concentration of S30 extract protein used in the CFE reaction [40] (figure 1a). To investigate if the same also holds true for the expression of other proteins, CFE was performed using constructs bearing the genes encoding firefly luciferase, enhanced green fluorescence protein (EGFP), hamster polyomavirus VP1, and ovalbumin. Expression was performed at 16 linearly spaced extract protein concentrations (8 for ovalbumin) ranging from 0.0–10.3 mg/ml in the final CFE reaction. The same CFE reactions were also prepared without template DNA as a negative control. After CFE a precipitate had formed in the reactions, increasing in size with increasing extract concentration. Expression was quantified based on enzyme activity (β-galactosidase, figure 1a; and luciferase, figure 1b), fluorescence (EGFP, figure 1c), or by Western blotting (VP1, figure 1d; and ovalbumin, figure 1e). While all proteins show an extract protein concentration-dependent increase in yield at low extract protein concentrations, the yield peaks at different extract protein concentrations for the individual proteins. While β-galactosidase activity peaks at 3.4–4.8 mg/ml extract protein, luciferase activity increases up to 6.9 mg/ml extract protein. At this concentration, the β-galactosidase activity had already dropped 60 % from its peak activity. At extract protein concentrations above the peak a concentration-dependent decrease in yield is observed for all proteins. This decrease is most significant for β-galactosidase, firefly luciferase, and ovalbumin, while EGFP and VP1 reach more of a plateau. However, at least for VP1, the variability in expression yield above the

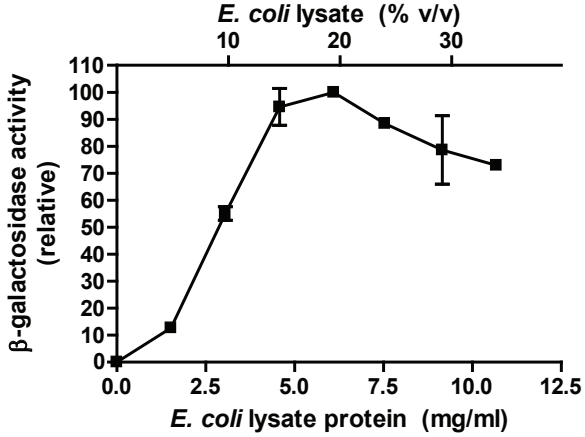

Figure 2. Relationship between *E. coli* lysate concentration and CFE yield using the RTS 100 *E. coli* HY kit. Expression of β-galactosidase was performed with the RTS 100 *E. coli* HY kit at different *E. coli* lysate concentrations. The concentration of the reconstitution buffer was kept constant. The β-galactosidase activity was quantified and plotted against the *E. coli* lysate concentration. The β-galactosidase activity increases in an *E. coli* lysate concentration-dependent manner until reaching a plateau at 4.6 mg/ml. At concentrations above 6.1 mg/ml, the activity decreases again. n=2.

peak extract protein concentration increases significantly.

3.2. Concentration optimization of commercial *E. coli* lysate

The previous data was obtained with S30 extract produced at our laboratory. To show that this relationship is a universal finding and not just an artifact of our own CFE system, we repeated the experiment with β-galactosidase with the commercially available RTS 100 *E. coli* HY CFE system. This *E. coli* lysate-based system uses a fixed 24 % v/v reconstituted *E. coli* lysate per CFE reaction. We found that for our lot this results in a final *E. coli* protein concentration of 7.5±0.2 (±SE) mg/ml in the CFE reaction. This concentration lies well above the peak for β-galactosidase as observed in figure 1a. We performed CFE with this system using 0.0–34 % v/v *E. coli* lysate, while keeping the concentration of the reconstitution buffer constant. Because the standard reaction contains 10 % v/v reconstitution buffer, the concentration did not deviate from the manual. The results are shown in figure 2.
A clear *E. coli* lysate concentration-dependent increase in activity is visible until reaching a plateau at 4.6 mg/ml. At concentrations above 6.1 mg/ml, the activity decreases again. At the concentration recommended by the supplier, a 12 % decrease in activity was observed compared to the peak. The location of the peak was slightly shifted to the right compared to the results from figure 1a, while the drop in activity at higher *E. coli* lysate concentrations was less significant.

3.3. Addition of stabilizing excipients to increase CFE yield

In an attempt to increase the expression at higher extract protein concentrations, three stabilizing excipients (sucrose, glycerol, and DMSO) were added to the CFE reaction at different concentrations. To exclude any influence of the excipients on the β-galactosidase assay the activity of the enzyme was tested in the presence of the highest concentration of the excipients used in the CFE reactions (figure 3). Sucrose and DMSO were not found to influence β-galactosidase activity, while glycerol mildly inhibited the activity.
Next, CFE of β-galactosidase was performed with different concentrations of sucrose (up to 13.2 % w/v), glycerol (up to 16.0 % v/v), and DMSO (up to 2.0 % v/v) in the reaction. An extract protein concentration of 6.1±0.1 (±SE) mg/ml was chosen.

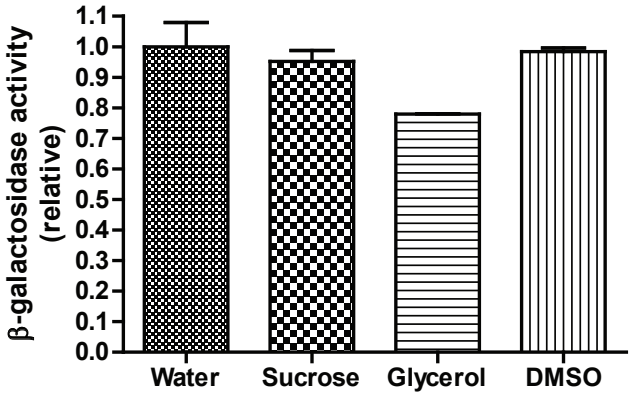

Figure 3. Influence of sucrose, glycerol, and DMSO on β-galactosidase activity. Sucrose (13.2 % w/v), glycerol (16.0 % v/v), and DMSO (2.0 % v/v) were added to an equal amount of β-galactosidase, followed by activity measurement. During the measurement the excipients were diluted 20×, just as is done with the CFE samples. Sucrose and DMSO did not influence the β-galactosidase activity. Glycerol caused a slight (22 %) decrease in activity, although our assay was not able to show statistical significance (p=0.11 for t-test, p=0.05 for one-way ANOVA, n=2).

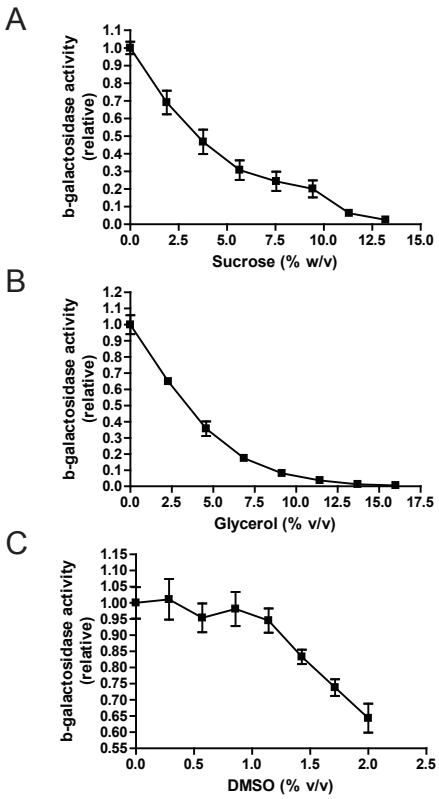

Figure 4. Effect of various excipients on the expression of β-galactosidase at high extract protein concentrations. Sucrose (a), glycerol (b), and DMSO (c) were added at different concentrations to CFE reactions producing β-galactosidase. The CFE reactions were prepared with an extract protein concentration of 6.1±0.1 (±SE) mg/ml. (a–b) Sucrose and glycerol caused a concentration-dependent decrease in CFE yield. (c) DMSO had no detectable effect at low concentrations, but caused a concentration-dependent decrease in CFE yield at concentrations above 1.0 % v/v. n=6.

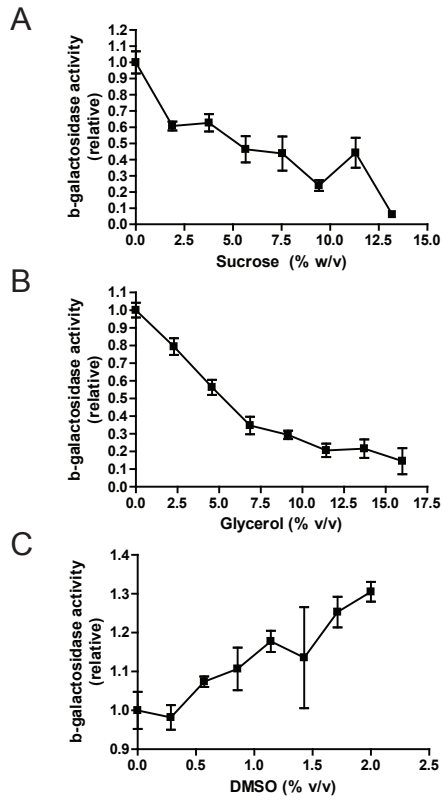

Figure 5. Effect of various excipients on the expression of β-galactosidase at suboptimal extract protein concentrations. Sucrose (a), glycerol (b), and DMSO (c) were added at different concentrations to CFE reactions producing β-galactosidase. The CFE reactions were prepared with an extract protein concentration of 2.0±0.0 (±SE) mg/ml. (a–b) Sucrose and glycerol caused a concentration-dependent decrease in CFE yield. (c) DMSO resulted in a concentration-dependent increase in CFE yield (linear regression, $p<0.0001$). n=3.

This lies well above the peak in figure 1a and contained a lot of precipitate after CFE. After CFE the β-galactosidase activity was measured. The results are shown in figure 4.

None of the excipients showed a beneficial effect on the CFE yield. Sucrose and glycerol led to a decrease in CFE yield, even at the lowest concentration added (figure 4a–b). DMSO, on the other hand, did not noticeably influence the CFE yield at lower concentrations, but caused a concentration-dependent decrease in CFE yield at higher concentrations (figure 4c). The excipients did not visually influence the amount of precipitate formed after CFE. To determine whether this decrease is caused by some form of molecular crowding or volume exclusion, leading to a higher local extract protein concentration and thereby a shift of optimal protein expression towards lower extract concentrations, the experiment was repeated using sub-optimal extract protein concentrations left of the peak. CFE

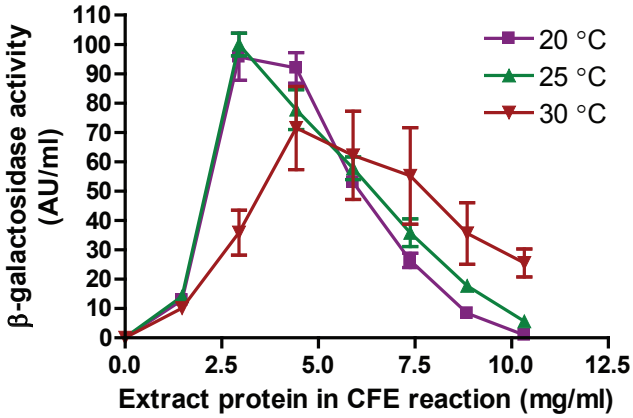

Figure 6. Effect of incubation temperature on the CFE yield at different extract protein concentrations. The relationship between β-galactosidase activity after CFE and the extract protein concentration was measured at different temperatures. At 30 °C, a peak in activity was found at 4.4 mg/ml. At 20 and 25 °C, CFE peaked at 3.0 mg/ml. At this protein concentration, the activity at 20 and 25 °C was significantly higher than at 30 °C ($p<0.05$). The height of the peak also differed, although this difference was not significant ($p=0.23$). n=2.

was performed with an extract protein concentration of 2.0±0.0 (±SE) mg/ml. At this concentration the reaction would significantly benefit from an increase in local protein concentration. The results are shown in figure 5.

Despite the lower extract protein concentration, the addition of sucrose and glycerol still caused a decrease in CFE yield. This indicates that the decrease in yield observed in figure 4a–b is attributed to direct inhibition of the CFE, rather than an increase in local protein concentration. Strikingly, DMSO caused a concentration-dependent increase in CFE yield. Although this increase might be caused by shifting the curve of figure 1a to the left, other explanations are more likely (see 4. Discussion).

3.4. Lower incubation temperatures increase CFE yield at lower extract protein concentrations

To determine the effect of the incubation temperature on the extract concentration curve, CFE of β-galactosidase at different extract protein concentrations was performed at different incubation temperatures. Figure 6 shows the result of the β-galactosidase activity quantification after CFE at 20, 25, and 30 °C.

In accordance with previous data (figure 1a) obtained at 30 °C, CFE yield at this temperature peaked at 4.4 mg/ml. Incubation at a lower temperature yielded a peak at a lower extract protein concentration, namely 3.0 mg/ml. The peak activity after incubation at 20 and 25 °C was on average 37 % higher than that after incubation at 30 °C, although this difference was not statistically significant. Importantly, the activity at a lower extract protein concentration was significantly higher at lower incubation temperatures than at 30 °C. Taken together, this shows that lower extract concentrations can be used to obtain higher yields by incubating at lower temperatures.

3.5. Incubation time does not influence CFE yield profile at different extract protein concentrations

Finally, we determined the effect of incubation time on the relationship between extract protein concentration and CFE yield. Increasing the extract protein concentration might not only lead to higher protein synthesis activity, but also to the faster

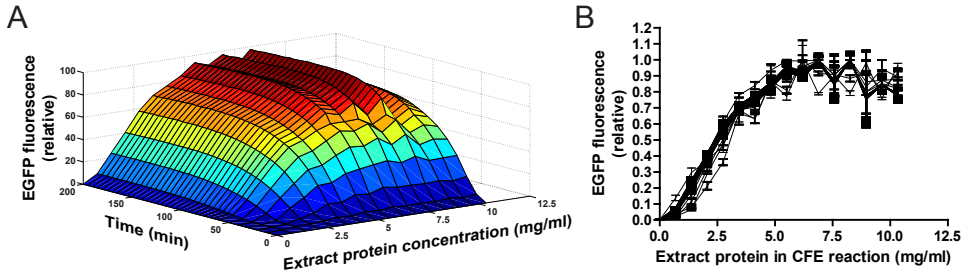

Figure 7. EGFP expression over time at different S30 protein concentrations. EGPF was produced by CFE using different extract protein concentrations, and its production was followed over time. (a) EGFP expression over time at different extract protein concentrations. EGFP fluorescence increases over time until it reaches a maximum at 140 minutes, regardless of the extract protein concentration. From that point on, the fluorescence slowly decreases. The points beyond 200 min were omitted for the sake of clarity. (b) Relative EGFP fluorescence at different extract protein concentrations over time. EGFP fluorescence is plotted at different time points relative to the maximum fluorescence at each time point. Each curve represents a single time point, and the points on that curve are shown relative to the maximum fluorescence at that time point, which has been normalized to one. Curves are drawn for all time points between 10 and 200 min. All curves overlap, indicating that the relative expression at different extract protein concentrations does not change over time. n=3.

degradation of key compounds (*e.g.* amino acids and energy compounds) by metabolic enzymes. Together this would result in a higher initial rate of protein synthesis, but also a faster termination of protein synthesis.

EGFP was produced by CFE using different extract protein concentrations, and the reaction was followed over time (see figure 7). EGFP fluorescence peaked at 140 min regardless of the extract protein concentration. From that point on, the fluorescence gradually decreased over time (figure 7a). The relationship between extract protein concentration and EGFP fluorescence did not change during the incubation (figure 7b). During the entire 500 minutes incubation, 20 % of the initial volume was lost due to evaporation.

4. Discussion

Many studies have focused on increasing the cell-free expression of recombinant proteins. Although significant advancements have been made, mainly with respect to the energy supply and the reaction conditions, few studies have actually focused on the S30 extract itself. While numerous protocols exist for the preparation of S30 extract, almost none of these protocols characterize the S30 extract after preparation. When the S30 extract is later used for CFE, it simply constitutes a fixed volume percentage of the reaction.

In our previous work we showed that the CFE yield depends on the protein concentration of the S30 extract [40]. An optimal concentration was found for the expression of β-galactosidase, and using higher concentrations led to a decrease in activity. Using uncharacterized S30 extracts might thus not always lead to the best concentration for CFE. We now show that this relationship is more complex. No single best S30 extract protein concentration exists. Each expressed protein requires its own unique extract protein concentration for optimal expression, and this concentration changes with different reaction conditions such as incubation temperature. We believe that by optimizing the extract protein concentration a lot could be gained in terms of productivity.

Although the peak in activity occurred at different extract concentrations for the different recombinant proteins expressed, the shape of the curves was generally the same. The productivity of the system rose as the concentration of extract protein increased, until the peak was reached. At protein concentrations above the peak, the productivity

of the system decreased again. This decrease was most significant for β-galactosidase, luciferase, and ovalbumin, while EGFP and VP1 reached more of a plateau. No single concentration was found at which all proteins were expressed optimally, although all proteins showed reasonable expression at 5–6 mg/ml extract protein.

One might argue that some bias is introduced by the way in which expression was quantified. The assays for β-galactosidase, luciferase, and EGFP all required the protein to be correctly folded; VP1 and ovalbumin expression was quantified by Western blotting, which does not require proper folding. However, we observed similar profiles for luciferase and ovalbumin, and for EGFP and VP1, despite the difference in measurement technique. Moreover, in the end the goal is to optimize the production of active and correctly folded protein, so quantifying expression based on enzymatic activity would be appropriate.

One reason for the shape of the curve might be solubility. Previous work on the expression of proinsulin showed a solubility cap. At higher extract percentages, more total proinsulin was produced, but the amount of soluble protein remained the same [49]. Unfortunately the authors did not mention the protein concentration of the S30 extract employed, so it is difficult to quantitatively compare the results. However, we did not find an increase in total VP1 production at higher extract protein concentrations, and even observed a substantial drop in total ovalbumin, suggesting that solubility alone is not the cause. It is unlikely that this decrease is caused by the total amount of protein in the reaction. In another study BSA was added to the CFE reaction at concentrations up to 150 mg/ml, but no difference in productivity was observed [50].

Another possibility might be the degradation of key compounds, such as amino acids, energy compounds, and mRNA, during incubation [51–53]. These compounds are degraded over time by metabolic enzymes present in the S30 extract. Increasing the extract protein concentration would thus expedite the loss of these compounds, causing a higher initial rate of protein synthesis, but also a faster termination of the reaction. However, we found that EGFP expression reaches a plateau after 140 minutes regardless of the extract protein concentration. Therefore, another mechanism must be behind the cessation of expression. Although denaturation or degradation of the protein synthesis machinery would explain these results, we find this very unlikely, because similar S30 extracts were shown to remain active for at least 20 hours in continuous CFE systems [4,54]. EGFP fluorescence steadily decreased after reaching its peak at 140 min. This shows that longer incubation times might have a negative impact on the yield, although the decrease could also be caused by photobleaching from the repeated measurements.

The results presented here are not limited to S30 extract produced at our laboratory. We observed a similar trend with the commercially available RTS 100 *E. coli* HY system, though the optimum was slightly shifted towards higher extract protein concentrations. Although not explicitly stated, the *E. coli* lysate also contains the T7 RNA polymerase and the enzyme(s) responsible for energy regeneration. These proteins would thus increase the total protein concentration of the lysate. Furthermore, since the *E. coli* lysate is delivered as a freeze-dried powder, the freeze-drying process might have caused some loss of specific activity. According to the manufacturer, the supplied *E. coli* lysate is optimized to obtain the highest CFE activity. Nevertheless, when we added the *E. coli* lysate at the recommended concentration, we obtained 12 % less β-galactosidase activity compared to the peak. In fact, using 39 % less *E. coli* lysate increased the expression. While the use of higher extract protein concentrations caused a rapid drop in CFE with the S30 extract produced at our laboratory, this drop was less significant for the RTS kit. This might indicate that the RTS kit is less contaminated with the inhibitory components mentioned earlier. A study using the Promega S30 T7 system determined the total protein concentration of the CFE reaction to be 3.6 mg/ml [50]. According to the

manufacturer, the expression level would increase if up to 25 % more extract is added. Given the peak concentrations we found, we believe that this system might indeed benefit from the addition of extra extract to the reaction.

The concentration of extract protein in the CFE reaction is much lower than inside bacteria, leading to slower synthesis rates and lower yields [55]. We envisioned that by increasing the extract concentration we might also be able to increase the protein synthesis rate, as long as we can keep the proteins stable in solution. In an attempt to prevent aggregation and precipitation, we tested the addition of excipients known to stabilize proteins in solution. Glycerol was previously shown to increase the productivity of a *Saccharomyces cerevisiae*-based CFE system [56], and sucrose is well-known to stabilize proteins [57]. However, when we added these excipients to CFE reactions containing high extract protein concentrations, all of them caused a concentration-dependent decrease in productivity. Sucrose and glycerol were not able to increase the expression at lower extract protein concentrations either, showing that the effect is not due to molecular crowding or volume exclusion. Transcription was not affected by the excipients (data not shown). We believe that sucrose and glycerol cause this drop in activity by directly inhibiting translation.

The increase in CFE yield witnessed after the addition of DMSO at lower extract protein concentrations might be caused by its beneficial effect on transcription. DMSO, a well-known cryoprotectant, destabilizes proteins at high concentrations [58], but promotes *in vitro* transcription at lower concentrations [59,60]. Furthermore, transcription and translation are not directly coupled in T7-based S30 extract systems [61], which allows mRNA to form secondary structures. These secondary structures can subsequently reduce transcription efficiency [62]. DMSO might also enhance translation by denaturing these mRNA secondary structures. Irrespective of its mode of action, DMSO could be a cheap and easy way to increase the expression with S30 extract at lower extract protein concentrations.

We observed that the optimum extract protein concentration shifts to the left, towards lower concentrations, upon incubation at lower temperatures. This did not decrease the productivity of the reaction; in fact, incubation at lower temperatures seemed to cause a slight increase in CFE yield. A similar temperature dependency has also been shown for the expression of active luciferase [61]. At a higher temperature, elongation might be too fast for the protein to fold correctly. Furthermore, protein folding, stability, and solubility might be better at a lower temperature.

Taken together, this study clearly shows that the extract protein concentration is an important variable that needs to be optimized when expressing a new protein.

Acknowledgements

We would like to thank Paulien van Bentum for her helpful support in the preparation of the manuscript. This work was supported by Technologiestichting STW [budget number 10243]. The authors declare that there are no conflicts of interest.

References

1 Kim, D.M. *et al.* **A highly efficient cell-free protein synthesis system from *Escherichia coli*.** Eur J Biochem (1996) 239, 881–886.

2 Kigawa, T. *et al.* **Preparation of *Escherichia coli* cell extract for highly productive cell-free protein expression.** J Struct Funct Genomics (2004) 5, 63–68.

3 Kim, T.W. *et al.* **Simple procedures for the construction of a robust and cost-effective cell-free protein synthesis system.** J Biotechnol (2006) 126, 554–561.

4 Kigawa, T. *et al.* **Cell-free production and stable-isotope labeling of milligram quantities of proteins.** FEBS Lett (1999) 442, 15–19.

5 Apponyi, M.A. *et al.* **Cell-free protein synthesis for analysis by NMR spectroscopy.** Methods Mol Biol (2008) 426, 257–268.

6 Arthur, I.N. *et al.* ***In situ*** **deprotection and incorporation of unnatural amino acids during cell-free protein synthesis.** Chemistry (2013) 19, 6824–6830.

7 Kigawa, T. *et al.* **Selenomethionine incorporation into a protein by cell-free synthesis.** J Struct Funct Genomics (2002) 2, 29–35.

8 Bundy, B.C. and Swartz, J.R. **Site-specific incorporation of p-propargyloxyphenylalanine in a cell-free environment for direct protein-protein click conjugation.** Bioconjug Chem (2010) 21, 255–263.

9 Muranaka, N. *et al.* **Incorporation of unnatural non-alpha-amino acids into the N terminus of proteins in a cell-free translation system.** Chembiochem (2007) 8, 1650–1653.

10 Ozawa, K. *et al.* **High-yield cell-free protein synthesis for site-specific incorporation of unnatural amino acids at two sites.** Biochem Biophys Res Commun (2012) 418, 652–656.

11 Woodrow, K.A. and Swartz, J.R. **A sequential expression system for high-throughput functional genomic analysis.** Proteomics (2007) 7, 3870–3879.

12 Mastrobattista, E. *et al.* **High-throughput screening of enzyme libraries: *in vitro* evolution of a beta-galactosidase by fluorescence-activated sorting of double emulsions.** Chem Biol (2005) 12, 1291–1300.

13 Amidi, M. *et al.* **Antigen-expressing immunostimulatory liposomes as a genetically programmable synthetic vaccine.** Syst Synth Biol (2011) 5, 21–31.

14 Amidi, M. *et al.* **Optimization and quantification of protein synthesis inside liposomes.** J Liposome Res (2010) 20, 73–83.

15 Amidi, M. *et al.* **Induction of humoral and cellular immune responses by antigen-expressing immunostimulatory liposomes.** J Control Release (2012) 164, 323–330.

16 Smith, M.T. *et al.* **The incorporation of the A2 protein to produce novel Qbeta virus-like particles using cell-free protein synthesis.** Biotechnol Prog (2012) 28, 549–555.

17 Avenaud, P. *et al.* **Expression and activity of the cytolethal distending toxin of Helicobacter hepaticus.** Biochem Biophys Res Commun (2004) 318, 739–745.

18 Isaksson, L. *et al.* **Expression screening of membrane proteins with cell-free protein synthesis.** Protein Expr Purif (2012) 82, 218–225.

19 Klammt, C. *et al.* **High level cell-free expression and specific labeling of integral membrane proteins.** Eur J Biochem (2004) 271, 568–580.

20 Bundy, B.C. and Swartz, J.R. **Efficient disulfide bond formation in virus-like particles.** J Biotechnol (2011) 154, 230–239.

21 Knapp, K.G., Goerke, A.R. and Swartz, J.R. **Cell-free synthesis of proteins that require disulfide bonds using glucose as an energy source.** Biotechnol Bioeng (2007) 97, 901–908.

22 Matthies, D. *et al.* **Cell-free expression and assembly of ATP synthase.** J Mol Biol (2011) 413, 593–603.

23 Kim, D.-M. and Swartz, J. **Oxalate improves protein synthesis by enhancing ATP supply in a cell-free system derived from *Escherichia coli*.** Biotechnology Letters (2000) 22, 1537–1542.

24 Pedersen, A. *et al.* **Rational improvement of cell-free protein synthesis.** N Biotechnol (2011) 28, 218–224.

25 Jewett, M.C. and Swartz, J.R. **Mimicking the *Escherichia coli* cytoplasmic environment activates long-lived and efficient cell-free protein synthesis.** Biotechnol Bioeng (2004) 86, 19–26.

26 Calhoun, K.A. and Swartz, J.R. **An economical method for cell-free protein synthesis using glucose and nucleoside monophosphates.** Biotechnol Prog (2005) 21, 1146–1153.

27 Kim, D.M. and Swartz, J.R. **Prolonging cell-free protein synthesis with a novel ATP regeneration system.** Biotechnol Bioeng (1999) 66, 180–188.

28 Kim, D.M. and Swartz, J.R. **Regeneration of adenosine triphosphate from glycolytic intermediates for cell-free protein synthesis.** Biotechnol Bioeng (2001) 74, 309–316.

29 Kim, T.W. *et al.* **An economical and highly productive cell-free protein synthesis system utilizing fructose-1,6-bisphosphate as an energy source.** J Biotechnol (2007) 130, 389–393.

30 Shrestha, P., Holland, T.M. and Bundy, B.C. **Streamlined extract preparation for *Escherichia coli*-based cell-free protein synthesis by sonication or bead vortex mixing.** Biotechniques (2012) 53, 163–174.

31 Klammt, C. *et al.* **Cell-free production of integral membrane proteins on a preparative scale.** Methods Mol Biol (2007) 375, 57–78.

32 Zawada, J.F. **Preparation and testing of *E. coli* S30 *in vitro* transcription translation extracts.** Methods Mol Biol (2012) 805, 31–41.

33 Goerke, A.R. and Swartz, J.R. **Development of cell-free protein synthesis platforms for disulfide bonded proteins.** Biotechnol Bioeng (2008) 99, 351–367.

34 Dreier, B. and Pluckthun, A. **Rapid selection of high-affinity binders using ribosome display.** Methods Mol Biol (2012) 805, 261–286.

35 Miles, L.A. *et al.* **An *Escherichia coli* cell-free system for recombinant protein synthesis on a milligram scale.** Methods Mol Biol (2011) 752, 17–28.

36 Schwarz, D. *et al.* **Preparative scale expression of membrane proteins in *Escherichia coli*-based continuous exchange cell-free systems.** Nat Protoc (2007) 2, 2945–2957.

37 Kang, S.H. *et al.* **Cell-free production of aggregation-prone proteins in soluble and active forms.** Biotechnol Prog (2005) 21, 1412–1419.

38 Torizawa, T. *et al.* **Efficient production of isotopically labeled proteins by cell-free synthesis: a practical protocol.** J Biomol NMR (2004) 30, 311–325.

39 Goerke, A.R. and Swartz, J.R. **High-level cell-free synthesis yields of proteins containing site-specific non-natural amino acids.** Biotechnol Bioeng (2009) 102, 400–416.

40 Teunissen, E.A. *et al.* **Batch-to-batch variability of *E. coli* S30 extracts can be reduced by normalizing S30 total protein content.** Manuscript in preparation (2014).

41 Fujiwara, K. and Nomura, S.M. **Condensation of an additive-free cell extract to mimic the conditions of live cells.** PLoS One (2013) 8, e54155.

42 Liu, D.V., Zawada, J.F. and Swartz, J.R. **Streamlining *Escherichia coli* S30 extract preparation for economical**

cell-free protein synthesis. Biotechnol Prog (2005) 21, 460–465.

43 Sun, Z.Z. *et al.* **Protocols for Implementing an *Escherichia coli* Based TX-TL Cell-Free Expression System for Synthetic Biology.** J Vis Exp (2013), e50762.

44 Gedvilaite, A. *et al.* **Formation of immunogenic virus-like particles by inserting epitopes into surface-exposed regions of hamster polyomavirus major capsid protein.** Virology (2000) 273, 21–35.

45 Richardson, S.M. *et al.* **GeneDesign: rapid, automated design of multikilobase synthetic genes.** Genome Res (2006) 16, 550–556.

46 Teunissen, E.A., de Raad, M. and Mastrobattista, E. **Production and biomedical applications of virus-like particles derived from polyomaviruses.** J Control Release (2013) 172, 305–321.

47 Yang, J. *et al.* **Kupfer-type immunological synapse characteristics do not predict anti-brain tumor cytolytic T-cell function *in vivo*.** Proc Natl Acad Sci U S A (2010) 107, 4716–4721.

48 Schneider, C.A., Rasband, W.S. and Eliceiri, K.W. **NIH Image to ImageJ: 25 years of image analysis.** Nat Methods (2012) 9, 671–675.

49 Kommer, A.A. *et al.* **Synthesis of functionally active human proinsulin in a cell-free translation system.** Dokl Biochem Biophys (2005) 401, 154–158.

50 Abulimiti, A. *et al.* ***Mycobacterium tuberculosis* Hsp16.3 nonamers are assembled and re-assembled via trimer and hexamer intermediates.** J Mol Biol (2003) 326, 1013–1023.

51 Kim, R.G. and Choi, C.Y. **Expression-independent consumption of substrates in cell-free expression system from *Escherichia coli*.** J Biotechnol (2001) 84, 27–32.

52 Michel-Reydellet, N., Calhoun, K. and Swartz, J. **Amino acid stabilization for cell-free protein synthesis by modification of the *Escherichia coli* genome.** Metab Eng (2004) 6, 197–203.

53 Kitaoka, Y., Nishimura, N. and Niwano, M. **Cooperativity of stabilized mRNA and enhanced translation activity in the cell-free system.** J Biotechnol (1996) 48, 1–8.

54 Spirin, A.S. *et al.* **A continuous cell-free translation system capable of producing polypeptides in high yield.** Science (1988) 242, 1162–1164.

55 Underwood, K.A., Swartz, J.R. and Puglisi, J.D. **Quantitative polysome analysis identifies limitations in bacterial cell-free protein synthesis**. Biotechnol Bioeng (2005) 91, 425–435.

56 Hodgman, C.E. and Jewett, M.C. **Optimized extract preparation methods and reaction conditions for improved yeast cell-free protein synthesis.** Biotechnol Bioeng (2013) 110, 2643–2654.

57 Lee, J.C. and Timasheff, S.N. **The stabilization of proteins by sucrose.** J Biol Chem (1981) 256, 7193–7201.

58 Arakawa, T., Kita, Y. and Timasheff, S.N. **Protein precipitation and denaturation by dimethyl sulfoxide.** Biophys Chem (2007) 131, 62–70.

59 Juang, J.K. and Liu, H.J. **The effect of DMSO on natural DNA conformation in enhancing transcription.** Biochem Biophys Res Commun (1987) 146, 1458–1464.

60 Chen, Z. and Zhang, Y. **Dimethyl sulfoxide targets phage RNA polymerases to promote transcription.** Biochem Biophys Res Commun (2005) 333, 664–670.

61 Spirin, A. and Swartz, J. **Cell-free Protein Synthesis Systems: Historical Landmarks, Classification, and General Methods.** In: Cell-Free Protein Synthesis: Methods and Protocols (eds A. Spirin and J. Swartz) Ch. 1, 1–34 (Wiley-VCH Verlag GmbH & Co. KGaA, 2008).

62 Freischmidt, A. *et al.* **RNA secondary structure and *in vitro* translation efficiency.** Protein Expr Purif (2012) 82, 26–31.

Chapter V

Assembly of hamster polyomavirus VP1 into virus-like particles takes place in *Escherichia coli* but not after cell-free synthesis

Erik A. Teunissen[1], Zahra Karjoo[1], Eelke P. Béguin[1], Emilie M.J. van Brummelen[1], Markus de Raad[1], Jan A. Post[2] and Enrico Mastrobattista[1]

[1]Department of Pharmaceutics, Utrecht Institute for Pharmaceutical Sciences, Faculty of Science, Utrecht University, Universiteitsweg 99, 3584 CG Utrecht, The Netherlands

[2]Biomolecular Imaging, Biology Department, Faculty of Science, Utrecht University, Padualaan 8, 3584 CH Utrecht, The Netherlands

Submitted for publication

Abstract

Cell-free expression is a viable alternative to conventional *in vivo* production of proteins. In this study we investigated the *Escherichia coli*-based cell-free expression and formation of hamster polyomavirus VP1 virus-like particles under different reaction conditions. These included conditions that were previously reported to cause the *in vitro* assembly of polyomavirus VP1 virus-like particles after VP1 purification from bacteria and conditions for the cell-free expression of other disulfide-bonded virus-like particles. While the capsid protein VP1 was produced at levels of 100 µg/ml or higher, none of these conditions led to significant virus-like particle assembly. This is a remarkable result, since VP1 readily forms virus-like particles inside bacteria. Even after purification the capsid proteins were still not able to form virus-like particles under otherwise favorable conditions, suggesting irreversible changes to the VP1 protein or improper synthesis of VP1 under the *in vitro* conditions. Further addition of chaperones did not increase the assembly efficiency. These results suggest that cell-free expression to our current understanding might not be adequate for the production of polyomavirus VP1 virus-like particles. Furthermore, these results clearly show that there are critical differences between bacterial and cell-free expression.

1. Introduction

Virus-like particles (VLPs) are promising agents for the delivery of genes and drugs to cells. Moreover, they show great promise in the field of vaccination, inducing potent B and T cell responses to displayed epitopes. VLPs are assemblies of viral proteins, resembling the native virus, but lacking viral nucleic acids. As such, they are non-replicating and safer to use than viral vectors. Such particles can be generated from many viruses, including polyomaviruses [1]. Polyomavirus VLPs spontaneously form after overexpression of the major coat protein VP1, with 360 VP1 proteins forming a 40–45 nm icosahedral capsid. The VLPs are stable under physiological conditions [2] and stabilized by calcium [3,4] and disulfide bonds [4,5]. In this study, we investigated VLPs derived from the hamster polyomavirus (HaPyV). HaPyV VLPs are able to encapsidate double-stranded DNA in a sequence-independent fashion and transfect mammalian cells [6], have a high insert capacity for signal peptides [7], and form after expression in a prokaryotic system [6].

One of the main challenges preventing the use of polyomavirus-derived VLPs in the clinic is their large-scale production [8]. Almost all current strategies are based on the production of VLPs in living cells, either bacteria [9], yeast [10], or insect cells [11]. Although recent advances have been made with respect to the large-scale production of polyomavirus VLPs in bacteria [9,12–14], all these methods suffer from the same inconveniencies, like contamination with cellular nucleic acids [15,16], or require the removal of fusion tags [13,17], increasing the production costs.

An interesting alternative would be the cell-free expression of VLPs. Cell-free expression (CFE) is an excellent technique for the synthesis of proteins using isolated transcription and translation machinery. Many different CFE systems exist, derived from different organisms, with one of the most common being the *Escherichia coli*-based S30 extract. CFE has several advantages over the conventional expression of proteins. The main advantage is the cell-free nature of the reaction, lacking membranes limiting accessibility. This allows the reaction conditions to be controlled directly, enabling the optimization of both the expression and assembly of VLPs using conditions that cannot be achieved in living cells [18,19]. DNA encapsidation can be tailored by removing endogenous DNA (*e.g.* the PURE system [20]) and adding target DNA for *in vitro* encapsidation. The technique is also much

faster than conventional expression, since CFE can be performed directly from PCR products without the need for cloning [21], and purification after CFE is also much easier because no membranes have to be disrupted [22]. Moreover, the ability to directly incorporate labels into the nascent proteins using CFE makes it an excellent technique to study the *in situ* assembly of VLPs. Finally, and of particular interest to us, CFE would allow directed evolution techniques, such as *in vitro* compartmentalization [23], to be applied to VLPs.

Bundy *et al.* have previously shown that VLPs can be synthesized using CFE [18,19,24]. First, they showed the synthesis of the MS2 bacteriophage coat protein VLP (MS2 VLP) and a C-terminally truncated Hepatitis B core protein VLP (HBc VLP) [18]. These VLPs did not form intramolecular disulfide bonds. HBc VLPs normally do form disulfide bonds, but these are not essential for assembly, making them rather easy to produce; this in contrast to polyomavirus-derived VLPs, which generally require intermolecular disulfide bridges for VLP assembly and stability. Later, they did manage to produce disulfide bonds in HBc VLPs during expression [19]. To prevent the reduction of the disulfide bonds, they used a *Δgor E. coli* strain, defective in glutathione reductase (Gor), to prepare the S30 extract. The extract was pretreated with iodoacetamide to inactivate remaining reductases. They also modified the reaction by buffering the redox potential with reduced and oxidized glutathione, and by adding purified DsbC, a disulfide bond isomerase. Surprisingly, this approach did not work for the production of Qβ bacteriophage VLPs. While Qβ VLPs lacking disulfide bonds were formed after expression under normal conditions, very few VLPs were formed in the modified system. In the end they managed to induce disulfide bonding in the VLPs by post-treatment with oxidizing agents such as hydrogen peroxide and diamide. However, this was done after purification of the preformed VLPs. In the case of polyomavirus VLPs this would not be possible, as disulfide bonding induced by oxidizing agents causes the capsomeres to form irregular aggregates [4]. Moreover, such a technique would not be compatible with our goal, *in vitro* compartmentalization (see **chapter 1**).

In this study we investigated the CFE and formation of polyomavirus-derived VLPs. We tested over 20 different reaction conditions, including conditions that were previously used for the *in vitro* assembly of polyomavirus VLPs [6] and for the CFE of other disulfide-bonded VLPs [19]. However, none of these conditions led to VLP synthesis at levels sufficient for *in vitro* compartmentalization, showing that CFE with our current understanding might not be adequate for the production of polyomavirus-derived VLPs.

2. Materials and methods

2.1. Chemicals

Adenosine-5'-triphosphate (ATP), ammonium acetate, ampicillin, bovine serum albumin (BSA), bromophenol blue, calcium chloride, CelLytic B, chloramphenicol, cesium chloride, 3'-5'-cyclic adenosine monophosphate (cAMP), cytidine-5'-triphosphate (CTP), dithiothreitol (DTT), ethidium bromide, folinic acid, glycerol, guanosine-5'-triphosphate (GTP), iodoacetamide, isopropyl β-D-1-thiogalactopyranoside (IPTG), kanamycin, LB agar, LB broth culture medium, magnesium acetate, 2-mercaptoethanol, polyethylene glycol 8000 (PEG 8000), polysorbate 20 (TWEEN® 20), potassium hydroxide, reduced L-glutathione (GSH), sodium acetate, sodium 5',5'-diethylbarbiturate, sodium dodecyl sulfate (SDS), sodium phosphate, tris(hydroxymethyl)aminomethane (Tris), uridine-5'-triphosphate (UTP), and each of the 20 standard amino acids were purchased from Sigma-Aldrich (St. Louis, MO, USA). Acetic acid, ethanol, hydrochloric acid, potassium acetate, propylene oxide, sodium chloride, and sucrose were purchased from Merck KGaA (Darmstadt, Germany). Creatine kinase (CK), Agarose MP, *E. coli*

total tRNA, and cOmplete EDTA-free protease inhibitor cocktail tablets were purchased from Roche (Basel, Switzerland). Ethylenediaminetetraacetic acid (EDTA) and HEPES were purchased from Acros Organics (Geel, Belgium). Creatine phosphate was purchased from Alfa Aesar (Ward Hill, MA, USA). GeneRuler 1 kb DNA Ladder, PageBlue Protein Staining Solution, PageRuler Prestained Protein Ladder, T7 RNA polymerase, and DNA-modifying enzymes were purchased from Thermo Scientific (Waltham, MA, USA). Phosphate buffered saline (PBS) was purchased from B. Braun Melsungen AG (Melsungen, Germany). RNase AWAY™ was purchased from Life Technologies (Carlsbad, CA, USA). Oxidized L-glutathione (GSSG) was purchased from SERVA (Heidelberg, Germany). Osmium tetroxide was purchased from Agar Scientific (Stansted, United Kingdom). Uranyl acetate was purchased from Electron Microscopy Sciences (Hatfield, PA, USA). Low melting point agarose (NuSieve™ GTG™ Agarose) was purchased from Lonza (Basel, Switzerland).

2.2. Plasmids

The cloning and preparation of plasmid pIVEX-HaPyV-VP1/co, which contains a codon-optimized version of the hamster polyomavirus *VP1* gene under control of a T7 promoter, was described before [25]. The plasmid pREP4, which contains a *lac* repressor, was obtained from *E. coli* M15[pREP4] (QIAGEN; Venlo, The Netherlands). All genes were verified by sequencing (BaseClear; Leiden, The Netherlands). Suitable quantities of circular plasmid DNA were obtained using the NucleoBond® PC 10 000 kit (MACHEREY-NAGEL; Düren, Germany).

2.3. Overexpression of HaPyV VP1 in *E. coli*

E. coli BL21(DE3)pREP4 were prepared by transforming BL21(DE3) competent cells (Novagen®, Merck KGaA) with pREP4. Bacteria were screened for the presence of pREP4, and chemically competent cells were produced according to standard protocols. BL21(DE3)pREP4 were transformed with pIVEX-HaPyV-VP1/co. Individual colonies were grown in LB medium at 37 °C. VP1 expression was induced at an OD600 of 0.8 by adding IPTG to a final concentration of 1.0 mM. Protein expression was allowed to continue overnight at 37 °C. Afterwards, the bacteria were harvested by centrifugation at 5,000 g for 15 min. The bacteria were either lysed by freeze-thawing, homogenization, or detergent lysis. For freeze-thawing, the bacteria were first washed twice in PBS, resuspended in 10 volumes of PBS, and lysed by three cycles of freezing in liquid nitrogen and thawing in a water bath at 37 °C. For homogenization, the bacteria were first washed once in reassembly buffer (10 mM Tris-HCl (pH 7.2), 1.0 M sodium chloride and 1.0 mM calcium chloride in demineralized water), followed by thorough resuspension in 20 volumes of reassembly buffer. The bacteria were lysed by two or three passes through an EmulsiFlex-C5 high pressure homogenizer (AVESTIN; Ottawa, ON, Canada) at >15,000 psi. For detergent lysis, the bacteria were first washed once in reassembly buffer, followed by resuspension in 10 volumes of CelLytic B. Once resuspended, the bacteria were incubated on a rotary shaker at room temperature for 15 min.

2.4. Purification of VLPs

VLPs were purified by sequential ultracentrifugation. Lysates of VP1-expressing *E. coli* were first cleared by centrifugation at 6,000–10,000 g for 10–30 min. VLPs in the supernatant were pelleted through a layer of 40 % w/v sucrose in reassembly buffer for 20 hours at 75,400 g at 4 °C. The pellets were resuspended in 1 ml reassembly buffer per 25 ml lysate. Cesium chloride was added to a final density of 1.30 g/cm^3, and the samples were centrifuged in an SW 41 Ti rotor (Beckman Coulter; Brea, CA, USA) at 40,000 RPM at 4 °C for 70 hours to allow a gradient to form. Afterwards, the tubes were carefully removed and 1 ml fractions were taken by puncturing the bottom of the

tubes with a needle and collecting the drops. The fractions were checked for VP1 by reducing SDS-PAGE, and fractions containing VP1 were dialyzed 4 times against 50 volumes of reassembly buffer using Slide-A-Lyzer membrane cassettes (Thermo Scientific) with a MWCO of 20 kDa. After purification, protein concentrations of pure samples were determined using the Pierce™ Micro BCA Protein Assay Kit (Thermo Scientific) according to the manufacturer's protocol.

2.5. Transmission electron microscopy of VLPs

Negative staining was performed as described before [26]. Briefly, samples were diluted 10–100 times in demineralized water, and 25 µl of each diluted sample was pipetted onto parafilm. Glow-discharged formvar/carbon-coated copper grids (Agar Scientific; Stansted, United Kingdom) were placed on top of the droplets for 2 min. After incubation, the grids were taken and excess liquid was removed by carefully touching filter paper. Next, the grids were placed on top of 20 µl 2 % uranyl acetate droplets for 2 min. After incubation, the grids were taken and excess liquid was again removed. The grids were dried at room temperature for 5 min before measurement. Transmission electron microscopy (TEM) imaging was performed using a Philips Tecnai 10 at 100 kV.

2.6. Transmission electron microscopy of bacteria

Ultrathin sections were prepared based on the protocol from Voronkova *et al.* [6]. VP1 was expressed in BL21(DE3)pREP4 (see above). Bacteria were harvested by centrifugation at 1,800 g for 20 min and fixed in 10 volumes of 1.0 % osmium tetroxide in Kellenberger buffer (pH 6.0) [27]. The samples were incubated on a rotary shaker for 1 hour, after which bacteria were washed 3 times with Kellenberger buffer, harvested, and resuspended in 1.3 volumes of warm 2.0 % low melting point agarose. The suspension was transferred onto parafilm and allowed to solidify on ice for 15 min, after which 2×2×2 mm cubes were excised. These cubes were briefly added to tubes with Kellenberger buffer. The cubes were dehydrated overnight in 70 % ethanol, followed by sequential dehydration with respectively 80, 90, 96, and 100 % ethanol, and 100 % propylene oxide. The samples were incubated for at least 15 min each step, and the medium was exchanged at least once during every step. The cubes were then incubated in sequentially 50, 67, 75, and 100 % Epon epoxy resin in propylene oxide, and embedded in Epon epoxy resin for 48 hours at 60 °C. Ultrathin 50 nm sections were cut using an Ultracut E ultramicrotome (Leica Microsystems; Wetzlar, Germany), using a diamond knife. The sections were transferred to formvar/carbon-coated copper grids and stained with 7 % uranyl acetate in 70 % methanol for 6 min. TEM was performed as above.

2.7. Preparation of *E. coli* S30 extracts

S30 extracts were prepared as described before [28]. Briefly, *E. coli* Rosetta-gami™ B (Novagen®, Merck KGaA) were grown until mid-log phase, harvested, lysed by two or three passes through an EmulsiFlex-C5 high pressure homogenizer at >15,000 psi, cleared by two rounds of centrifugation at 30,000 g, and dialyzed against extract buffer (10 mM Tris-acetate buffer (pH 8.2) containing 14 mM magnesium acetate, 60 mM potassium acetate, and 1.0 mM DTT) using Slide-A-Lyzer membrane cassettes with a MWCO of 10 kDa. No preincubation steps were performed. The extracts were stored as 1.0 ml aliquots at −80 °C. The standard protocol was modified in different ways as indicated in the results section. To prepare the heat-shock extracts, the bacteria were incubated at 42 °C for 30 before harvesting. Special extracts were prepared for the tests without DTT where no DTT and 2-mercaptoethanol were added during any of the steps from the production protocol. Some extracts were pretreated with iodoacetamide before

use. These extracts were incubated with a final concentration of 50 µM iodoacetamide at 30 °C for 30 min.

2.8. Nuclear extract preparation

Nuclear extract was prepared as a source of eukaryotic chaperones. To prepare nuclear extract, 1.6×10^6 human epidermoid carcinoma A431 cells were trypsinized, washed with PBS, and collected by centrifugation at 500 g for 5 min. Nuclei were collected using the Nuclei EZ Prep kit (Sigma-Aldrich; St. Louis, MO, USA) according to the manufacturer's protocol and stored at −80 °C until further use. Once thawed on ice, nuclei were collected by centrifugation, resuspended in 200 µl PBS, and lysed by 6 cycles of sonication (6 sec per cycle, 50 % output) with a LABSONIC® P probe sonicator equipped with a 3-mm diameter probe (Sartorius AG; Göttingen, Germany). The nuclear extract was stored at −80 °C.

2.9. Cell-free protein synthesis

Standard reactions contained pIVEX-HaPyV-VP1/co as template. Cell-free protein synthesis was performed with a total reaction volume of 25–100 µl. During preparation, the reactions and reaction components were kept on ice to prevent premature expression. Each S30 extract CFE reaction contained 30 % v/v S30 extract, 175 µg/ml *E. coli* total tRNA, 250 µg/ml creatine kinase, 5.8 mM magnesium acetate, 55 mM HEPES-KOH (pH 8.2), 1.7 mM DTT, 1.2 mM ATP, 0.8 mM CTP, 0.8 mM GTP, 0.8 mM UTP, 80 mM creatine phosphate, 0.64 mM cAMP, 68.9 µM folinic acid, 210 mM potassium acetate, 27.6 mM ammonium acetate, 1.0 mM of each of the 20 standard amino acids, 4.0 % w/v PEG 8000, and 2.5 U/µl T7 RNA polymerase, unless specified otherwise. Plasmid DNA was added to a final concentration of 20 nM, unless specified otherwise. The reactions were incubated for 3 hours at 30 °C, unless specified otherwise. The Rapid Translation System (RTS) 100 *E. coli* HY Kit, RTS DnaK Supplement, and RTS GroE Supplement (Roche; Basel, Switzerland) were used according to the manufacturer's protocols, unless specified otherwise. The PURExpress® *In Vitro* Protein Synthesis Kit and PURExpress® Disulfide Bond Enhancer (New England Biolabs; Ipswich, MA, USA) were used according to the manufacturer's protocols, unless specified otherwise. For the reactions with eukaryotic chaperones, the S30 extract concentration was reduced to 16.5 % v/v, and the reactions were supplemented with 16.5 % v/v nuclear extract (see above).

2.10. Nucleic acid degradation

To degrade nucleic acids, CFE reactions were spiked with Benzonase (Novagen®, Merck KGaA) to a final concentration of 2.5 U/µl and incubated at 37 °C for 3 h. The extent of the degradation was analyzed by agarose gel electrophoresis using standard protocols.

2.11. Quantification of VP1

SDS-PAGE was performed as before [25]. In addition to the samples, each gel was loaded with a standard (purified HaPyV VLPs of known concentration) and 5 µl PageRuler Prestained Protein Ladder. After running, the gels were either used for Western blotting as described before [25], or stained with PageBlue Protein Staining Solution according to the manufacturer's protocol using a microwave oven. After Western blotting, the band intensity of VP1 was quantified using ImageJ [29], and the values were corrected using the standard on each blot.

2.12. Mass spectrometry

Mass spectrometry analysis of individual bands on SDS-PAGE was performed by the Proteomics Center (Erasmus University Medical Center; Rotterdam, The Netherlands).

2.13. Reverse purification of VP1 after CFE

VP1 was purified from PURExpress® reactions by reverse his-tag purification using Dynabeads® His-Tag Isolation and Pulldown (Life Technologies) according to the manufacturer's protocol.

2.14. Disassembly and reassembly

VLPs were disassembled by adding DTT and EDTA at final concentrations of 10 mM and 50 mM, respectively. The samples were incubated on a roller mixer at 4°C overnight. VLPs were reassembled by dialyzing against reassembly buffer at 4 °C with Slide-A-Lyzer membrane cassettes with a MWCO of 20 kDa. The samples were first dialyzed for 2 hours, and after refreshing the buffer, the samples were dialyzed for another 18 hours at 4 °C.

3. Results and discussion

3.1. Expression of VLPs inside bacteria

When VP1 is expressed in *E. coli* and purified by gradient ultracentrifugation, a pure population of

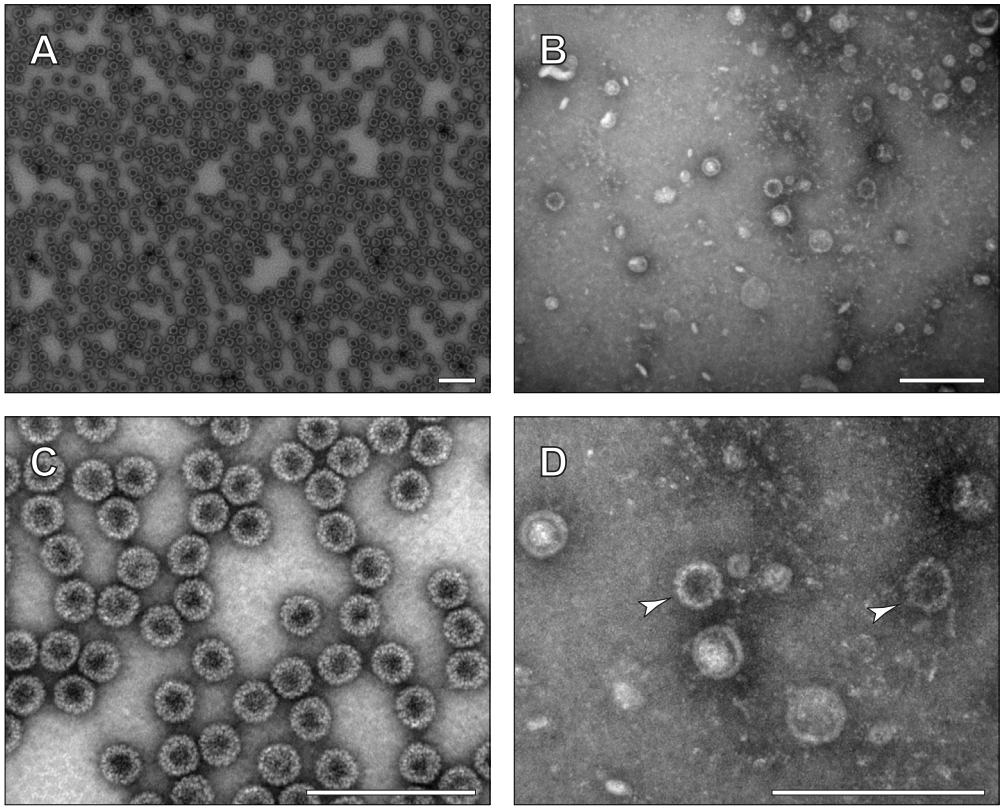

Figure 1. Purification of VLPs after expression of VP1 in bacteria. *E. coli* BL21(DE3)pREP4 were transformed with pIVEX-HaPyV-VP1/co and induced to express VP1. After expression, the bacteria were lysed and VLPs were purified by continuous CsCl gradient ultracentrifugation. Negative staining TEM was performed to visualize VLPs; (a) purified VLPs; (b) VLPs in the bacterial lysate directly after lysis by freeze-thawing; (c–d) close-ups of (a–b). Arrowheads indicate the VLPs in (d). Bars = 200 nm.

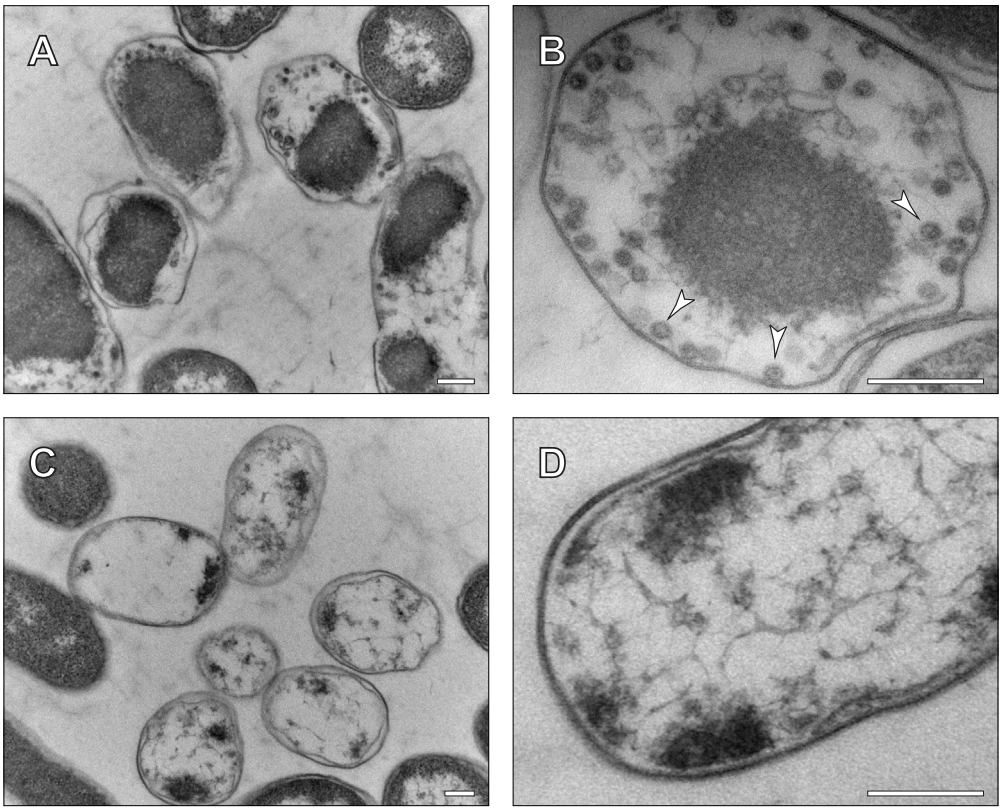

Figure 2. Expression of VP1 and formation of VLPs inside bacteria. Ultrathin sections were prepared from *E. coli* BL21(DE3)pREP4 expressing VP1 and normal *E. coli* BL21(DE3)pREP4. VLPs are clearly visible as dark spheres in the bacteria expressing VP1 (a–b). No VLPs are found in the negative control bacteria (c–d). Arrowheads indicate some of the VLPs in (b). Bars = 200 nm.

homogeneous VLPs is obtained (figures 1a and 1c). However, there is controversy whether these VLPs are formed directly after expression inside the bacteria, or rather as an artifact of the purification procedure. To investigate this, we looked at early steps of the purification process. We found that VLPs are already present in the bacterial lysate directly after lysis by freeze-thawing (figures 1b and 1d). We also observed VLPs after lysis using different methods such as homogenization or treatment with CelLytic B (supplementary figure S1). While this suggests that VLPs are already formed before lysis, it could still be a consequence of the lysis buffer or method. To exclude this possibility, ultrathin sections were prepared from *E. coli* expressing VP1 as well as normal *E. coli*. VLPs were clearly visible in the sections from BL21(DE3)pREP4 expressing VP1 (figures 2a–b), with at least 10 % of the bacteria showing multiple particles. No VLPs or anything similar to VLPs were found in the negative control BL21(DE3)pREP4 (figure 2c–d), despite extensive searching. These results are very similar to previous results obtained by Voronkova *et al.* [6], and unequivocally demonstrate that HaPyV VLPs are formed inside bacteria after expression in *E. coli*. This is a striking result, given the reducing environment in *E. coli* and the importance of disulfide bonds in the stability and assembly of polyomavirus VLPs [30]. However, previous studies with murine polyoma-

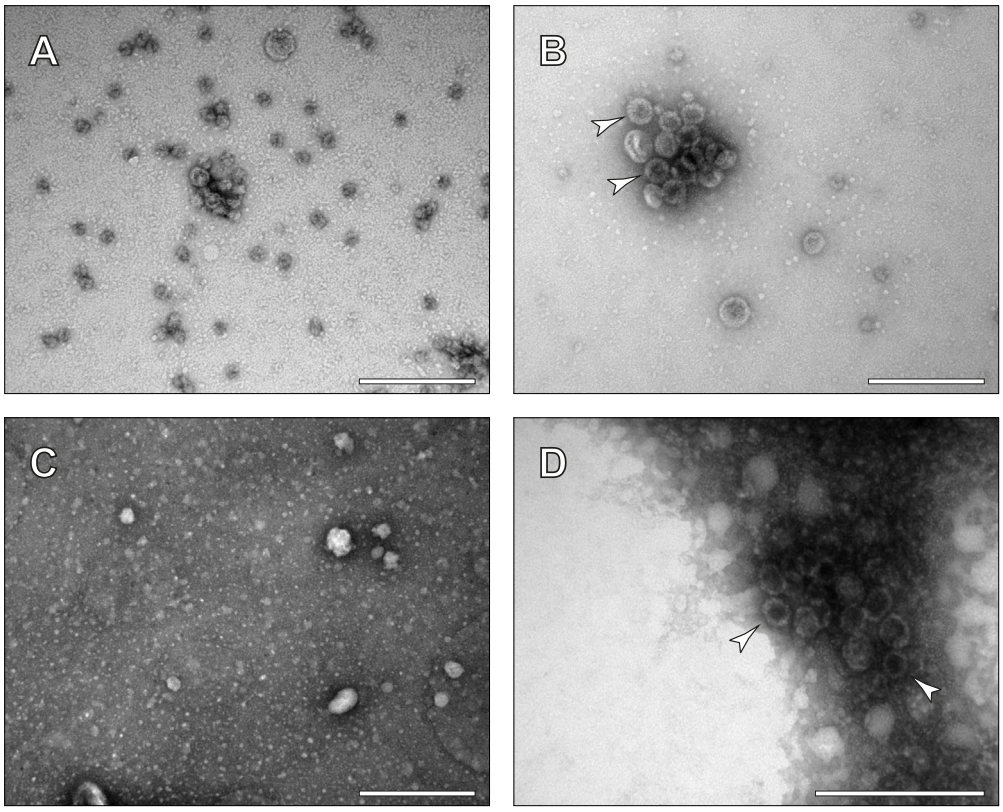

Figure 3. Expression of VP1 and formation of VLPs in S30 extract. CFE with pIVEX-HaPyV-VP1 was performed using an S30 extract prepared from *E. coli* Rosetta-gami™ B. After expression, the samples were imaged by negative staining TEM. Ribosomes were abundantly visible in all preparations. No VLPs were visible after CFE (a). VLPs were abundantly present in a negative control CFE reaction after spiking with purified VLPs (b), while no similar particles were found before spiking (c). VLPs could still be observed in the spiked sample after 24 hours of incubation at 30 °C (d). Arrowheads indicate some of the VLPs in (b) and (d). Bars = 200 nm.

virus have shown that VLPs can also form without disulfide bonding [31], and calcium alone was enough to reassemble JC VLPs treated with DTT and EGTA [4].

3.2. Cell-free expression of VLPs using S30 extract

These results gave good hope that VLPs would be formed after prokaryotic CFE. We expressed VP1 using *E. coli* S30 extract prepared at our laboratory, and quantified the expression using Western blotting (supplementary figure S2). Approximately 140 µg/ml VP1 was expressed using unmodified S30 extract. However, no VLPs were observed after expression (figure 3a). Because we were afraid that we might miss any formed VLPs due to the high amount of background particles, we spiked a negative control CFE reaction with purified VLPs to a final concentration of 140 µg/ml. VLPs were readily detectable in the spiked sample (figure 3b), while no similar structures were visible prior to spiking (figure 3c). VLPs were still detectable in the spiked sample after 24 h of incubation at 30 °C (figure 3d), showing that once formed, VLPs remain stable in the CFE reaction environment. Because we could not detect any VLPs in the CFE reaction expressing VP1, and given the amount of

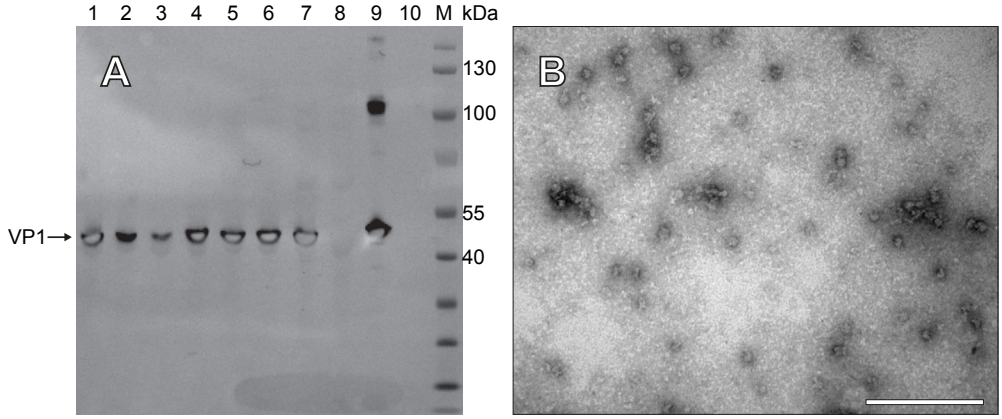

Figure 4. CFE of VP1 using bacterial lysates. (a) Western blot analysis after reducing SDS-PAGE of VP1 produced using different S30 extract intermediates. Lanes 1–2, crude *E. coli* lysate; lanes 3–4, supernatant after the first round of centrifugation; lanes 5–6, supernatant after the second round of centrifugation; lane 7; final dialyzed S30 extract; lane 8, negative control; lane 9, purified VLPs produced in *E. coli*; lane 10, empty; lane M, PageRuler Prestained Protein Ladder. (b) Typical example of a transmission electron micrograph of crude bacterial lysate expressing VP1 (the same sample from lane 1). Bars = 200 nm.

VLPs found in the spiked sample, we can safely assume that very few, if any, VLPs are formed upon CFE.

3.3. Cell-free expression of VLPs using bacterial lysates

Because VLPs do form inside bacteria, but not in the standard S30 extract, we hypothesized that some essential prokaryotic components are lost during extract production. For example, endogenous calcium might be lost during the dialysis of the S30 extract and is not replaced in the final CFE reaction. Also, prokaryotic chaperones, which were shown to cause the assembly of VLPs in otherwise dissociating conditions [32], might be lost during extract production, preventing the correct assembly of VLPs. Therefore, we used different intermediates of the S30 extract production process for CFE of VLPs. In accordance with previous results from Kim *et al.* [33], the intermediates were active and VP1 was expressed in all samples (figure 4a). However, no VLPs were found after expression in any sample (figure 4b). This might be caused by components from the lysis buffer or reaction mix, which are still added and might alter the physiological conditions preventing VLP formation. It could be that certain key components, such as calcium, are diluted too far.

An interesting observation is the high (~100 kDa) band visible on the Western blot in figure 4a. This band is only found in samples that contain VP1 produced in bacteria, and is not found in VP1 after CFE, correlating with VLP assembly. Mass spectrometry analysis confirmed that this band contains VP1. This band most likely represents multimeric VP1, despite the denaturing pretreatment for reducing SDS-PAGE. We did not further investigate this band, but this might be a good indicator for VLP formation.

3.4. Modification of the cell-free expression system

Because the previous data suggested that the reaction conditions in the CFE reaction might not allow VLPs to form, we attempted to modify the CFE reaction conditions in such a way to promote the formation of VLPs. The different modifications are listed in table 1. DTT was removed because reducing agents were previously shown to destabilize polyomavirus VLPs [4,5]. PEG was removed to im-

prove the detection of VLPs, as we found that this obscured the assays (data not shown). Calcium was added to a final concentration of up to 5.0 mM. Calcium is important for the assembly and stability of polyomavirus VLPs [3,4], and the standard S30 CFE reaction is expected to contain very little calcium, as the bacterial lysate is dialyzed and no calcium is added afterwards (see above). Other studies showed that both bacterial [32] and eukaryotic [34] chaperones can stimulate the formation of polyomavirus VLPs, so we also tested these. We also tested a heat-shock extract, previously shown to enhance protein folding [35]. Furthermore, based on the results from Bundy *et al.* [19], we added iodoacetamide to inactivate reductases and used glutathione to buffer the redox potential. We also tried the commercially available "PURExpress® Disulfide Bond Enhancer" from New England Biolabs, designed to increase the correct folding of proteins with multiple disulfide bonds. We tested different factors such as expression temperature (22–37 °C), incubation time (up to 24 hours), pH (6.0–8.2), and plasmid DNA template concentration (1.0–40 nM). To exclude any problems specific to our home-made S30 extract, we also tested two commercially available CFE systems. Most of these modifications did not alter the expression level of the system, although some modifications slightly reduced the expression of VP1 (primarily the removal of PEG). Individually, none of these modifications resulted in VLP formation observable by TEM (see supplementary figure S3). The only condition under which VLPs were observed combined the removal of DTT and PEG, and addition of calcium and a glutathione redox buffer (figure 5), and even under these conditions the amount of VLPs was very low and the results were difficult to reproduce. Based on the observed abundance of spiked VLPs (figure 3b) we estimate that even under these conditions less than 1 % of the total VP1 is assembled. This is not enough to make the system commercially competitive with conventional *in vivo* production, nor is this enough for our goal, *in vitro* compartmentalization. Given the molecular weight of VP1 (42 kDa) and assuming a droplet size of 2 µm [36], the concentration of assembled VP1 would need to be at least 6 µg/ml to generate at least 1 VLP per droplet. Indeed, early attempts to use this system for selections through *in vitro* compartmentalization failed (data not shown).

There are several possibilities for this low assembly efficiency. One problem might be the concentration of VP1. At low concentrations, VP1 tends to aggregate rather than form VLPs [37]. However, Ding *et al.* observed a critical assembly concentration of 20 µg/ml for murine polyomavirus [37]. The expression levels we attained here are an order of magnitute higher than this critical concentration,

Table 1. Overview of the different modifications of the CFE system used to produce VLPs. While all of these modifications allowed the expression of VP1, none of these modifications resulted in significant formation of VLPs (supplementary figures S3–5).

Modification of the CFE reaction conditions	**Removal of inhibitors**
• Expression temperature	• DTT-free systems
• Incubation time	• PEG-free systems
• pH	**Addition of stabilizers**
• DNA template concentration	• Addition of Ca^{2+}
Different cell-free expression systems	• Eukaryotic chaperones
• PURExpress® IVPS kit	• Bacterial chaperones
• Roche RTS *E. coli* HY kit	• Redox buffers
• Crude bacterial lysates	• Disulfide Bond Enhancer (NEB)
• Heat-shock extract	
• Iodoacetamide-treated extract	

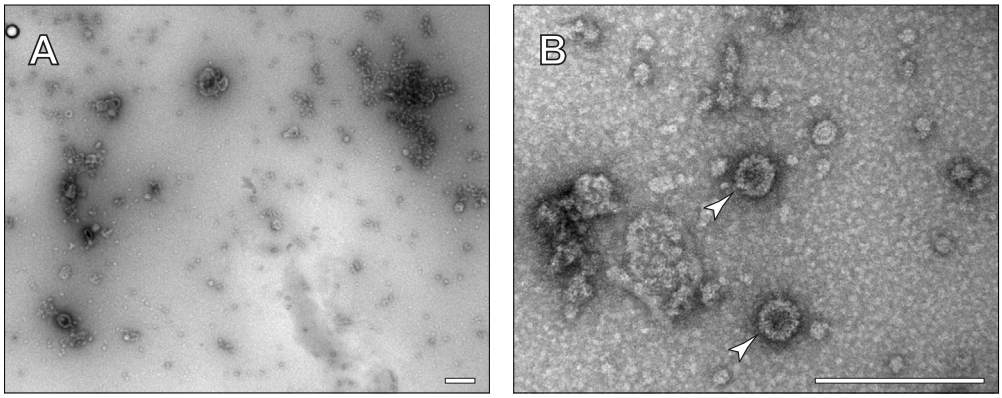

Figure 5. Lonely VLPs in a vast sea of extract. Cell-free expression was performed under ideal conditions in S30 extract, combining the removal of DTT and PEG with the addition of 5.0 mM calcium chloride and a glutathione redox buffer (1.0 mM GSH and 4.0 mM GSSG). (a) Representative image of the sample with no VLPs present. (b) VLPs (arrowheads) observed in the same sample after extensive searching. Bars = 200 nm.

so it is unlikely that the VP1 concentration alone causes these problems. Another possibility is that important components are still lacking in the CFE system. Even when the expression is performed directly in bacterial lysates, the bacterial components are diluted significantly compared to their cytoplasmic concentrations. The concentration of the bacterial components in the S30 CFE reaction is approximately 20 times lower than inside bacteria [38]. This dilution might cause certain components to fall below a critical concentration. Also, components from the reaction mixture might inhibit the assembly of VLPs. In this study, we excluded DTT and PEG from the reaction mix, and saw that this improved assembly. However, other components might still be responsible for the low assembly efficiency. We also tried the well-defined PURExpress® system, which contains only purified components necessary for transcription and translation. However, despite the supposed lack of inhibitors this system was not capable of assembly. Then again, PURExpress® might lack the necessary chaperones or other factors to assemble VLPs. We tried adding calcium chloride, a redox buffer, bacterial chaperones, and the PURExpress® Disulfide Bond Enhancer, but this did not lead to assembly (supporting figure S4). A potential solution would be the use of the Cytomim system, in which the reaction mixture more closely resembles the cytoplasmic conditions of *E. coli* [39]. Alternatively, one could try a mammalian extract with a sufficiently high expression yield, such as the recently published CHO extract [40], to more closely mimic the natural assembly conditions. Another problem preventing assembly might be the binding of VP1 to nucleic acids directly after translation. VP1 is known to bind to DNA, and, at high concentrations, DNA prevents the assembly of VLPs [41]. The binding of VP1 does not protect DNA from nucleases [42], and thus we added nucleases (DNase, RNase, and Benzonase) to the CFE reaction after expression to release VP1. Although these nucleases removed the nucleic acids as validated by agarose gel electrophoresis and reduced the background with TEM, no VLPs were observed (supplementary figures S5 and S6).

3.5. Purification of cell-free expressed VP1 and *in vitro* reassembly of VLPs

As we were unable to increase the assembly efficiency in the CFE reaction mixture, we investigated if VP1 was rendered in a state in which it was unable to assemble. To this end, we purified cell-free expressed VP1 and subjected it to controlled assembly conditions. VP1 was produced using PURExpress® and purified by reverse his-tag

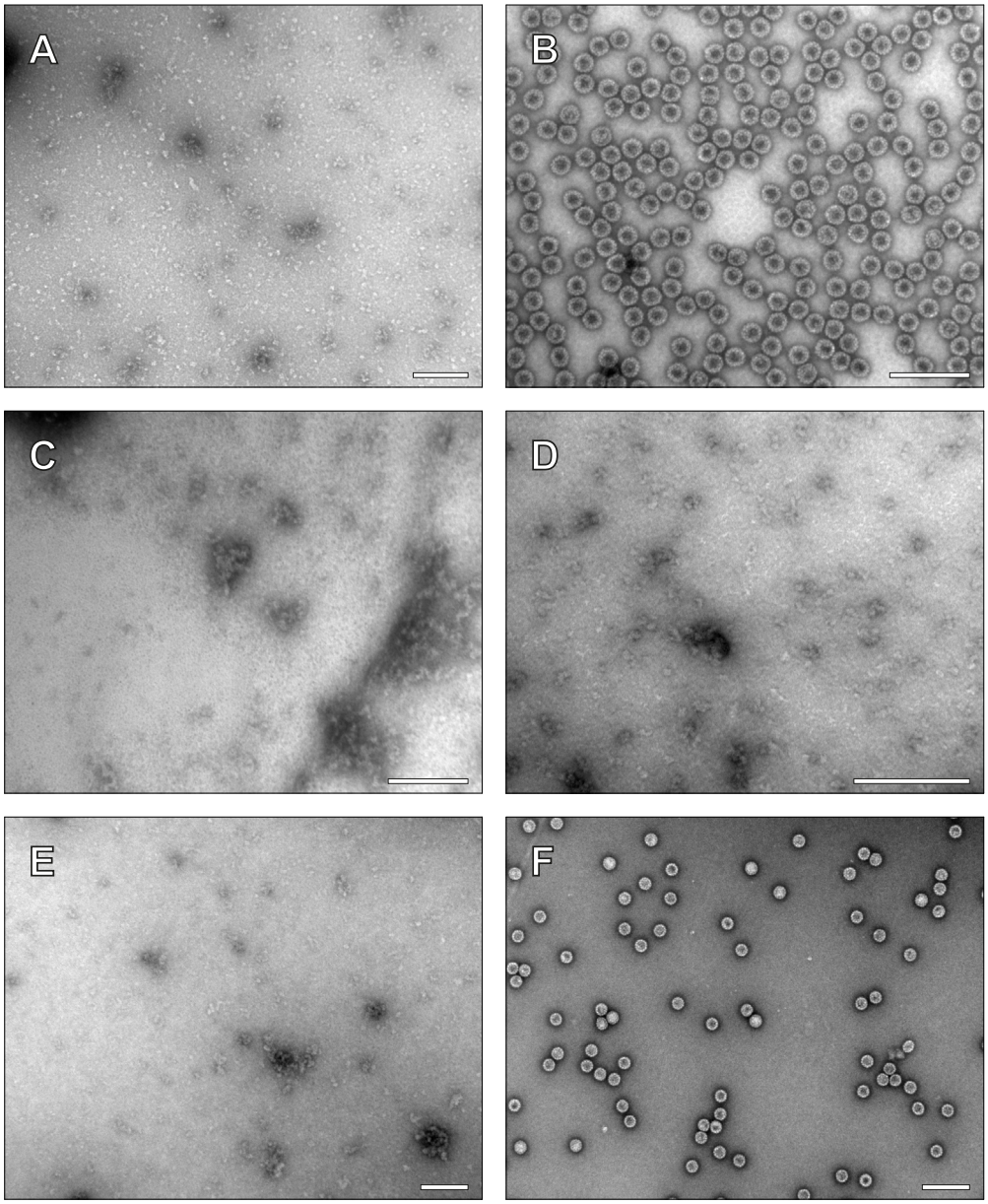

Figure 6. Reassembly of VLPs after purification from CFE (PURExpress®) and bacteria. (a) VP1 purified from CFE; (b) VP1 purified from bacteria; (c) VP1 purified from CFE after treatment with 10 mM DTT and 50 mM EDTA; (d) VP1 purified from bacteria after treatment with 10 mM DTT and 50 mM EDTA; (e) VP1 purified from CFE after reassembly; (f) VP1 purified from bacteria after reassembly. VLPs were only observed in (b) and (f). Bars = 200 nm.

purification. All proteins in the reaction, except the ribosomes and VP1, contain a his-tag. These proteins were removed by affinity purification, leaving pure VP1 with ribosomes. VP1 was also produced

in bacteria and purified as a positive control. VP1 was successfully purified from both sources (supplementary figure S7). After purification, VLPs were visible in the sample purified from bacteria (figure 6b), but not in the sample purified from CFE (figure 6a). Both samples were subjected to 10 mM EDTA and 10 mM DTT, causing the dissociation of VLPs (figures 6c–d). The samples were subsequently dialyzed against a high-salt buffer supplemented with calcium to reassemble the VLPs. This caused VLPs to reappear in the VP1 sample from bacteria (figure 6f), but no VLPs formed in the VP1 purified from the CFE reaction (figure 6e). The results did not change when the CFE reaction was treated with Benzonase before purification, nor when his-tagged VP1 was purified from homemade S30 extract (data not shown).

It thus appears that cell-free expressed VP1 not only fails to form VLPs after cell-free expression, it also did not acquire the ability to do so even under otherwise associative conditions. We do not know what causes this, but possible reasons include incorrect folding of the protein and aggregation due to random disulfide bonding. Perhaps the addition of disulfide bond isomerases might improve the reshuffling of the disulfide bonds, although such isomerases are likely to be present in the proprietary "Disulfide Bond Enhancer" supplement. Moreover, all disulfide bonds should have been broken upon treatment with DTT, allowing the bonds to reform upon dialysis. Therefore, it is more likely that incorrect folding causes unrecoverable aggregation of VP1. We cannot exclude the possibility that truncations of VP1 are responsible for this, given the importance of the C-terminus in the formation of polyomavirus VLPs [43,44]. However, hamster polyomavirus VP1 tolerates C-terminal truncations of at least 21 amino acids without hampering VLP formation [30], and most VP1 observed by Western blotting was full-length (supplementary figure S7). Furthermore, PURExpress® should not contain proteases, making proteolytic degradation unlikely. In conclusion we can infer that – probably subtle – qualitative differences between the *in vivo* and *in vitro* produced VP1 prevent the latter from assembling into *bona fide* particles.

Acknowledgements

The authors would like to thank Karin Vocking for preparing the ultrathin sections and Paulien van Bentum for her helpful support in the preparation of the manuscript. This work was supported by Technologiestichting STW [budget number 10243].

References

1 Teunissen, E.A., de Raad, M. and Mastrobattista, E. **Production and biomedical applications of virus-like particles derived from polyomaviruses.** J Control Release (2013) 172, 305–321.

2 Salunke, D.M., Caspar, D.L. and Garcea, R.L. **Self-assembly of purified polyomavirus capsid protein VP1.** Cell (1986) 46, 895–904.

3 Chuan, Y.P. *et al.* **Virus assembly occurs following a pH- or Ca2+-triggered switch in the thermodynamic attraction between structural protein capsomeres.** J R Soc Interface (2010) 7, 409–421.

4 Chen, P.L. *et al.* **Disulfide bonds stabilize JC virus capsid-like structure by protecting calcium ions from chelation.** FEBS Lett (2001) 500, 109–113.

5 Ishizu, K.I. *et al.* **Roles of disulfide linkage and calcium ion-mediated interactions in assembly and disassembly of virus-like particles composed of simian virus 40 VP1 capsid protein.** J Virol (2001) 75, 61–72.

6 Voronkova, T. *et al.* **Hamster polyomavirus-derived virus-like particles are able to transfer *in vitro* encapsidated plasmid DNA to mammalian cells.** Virus Genes (2007) 34, 303–314.

7 Gedvilaite, A. *et al.* **Segments of puumala hantavirus nucleocapsid protein inserted into chimeric polyomavirus-derived virus-like particles induce a strong immune response in mice.** Viral Immunol (2004) 17, 51–68.

8 Pattenden, L.K. *et al.* **Towards the preparative and large-scale precision manufacture of virus-like particles.** Trends Biotechnol (2005) 23, 523–529.

9 Middelberg, A.P. *et al.* **A microbial platform for rapid and low-cost virus-like particle and capsomere vaccines.** Vaccine (2011) 29, 7154–7162.

10 Palkova, Z. *et al.* **Production of polyomavirus structural protein VP1 in yeast cells and its interaction with cell structures.** FEBS Lett (2000) 478, 281–289.

11 Pawlita, M. *et al.* **DNA encapsidation by viruslike particles assembled in insect cells from the major capsid protein VP1 of B-lymphotropic papovavirus.** J Virol (1996) 70, 7517–7526.

12 Chuan, Y.P., Lua, L.H. and Middelberg, A.P. **High-level expression of soluble viral structural protein in *Escherichia coli*.** J Biotechnol (2008) 134, 64–71.

13 Liew, M.W., Rajendran, A. and Middelberg, A.P. **Microbial production of virus-like particle vaccine protein at gram-per-litre levels.** J Biotechnol (2010) 150, 224–231.

14 Liew, M.W.O., Chuan, Y.P. and Middelberg, A.P.J. **High-yield and scalable cell-free assembly of virus-like particles by dilution.** Biochemical Engineering Journal (2012) 67, 88–96.

15 Ou, W.C. *et al.* **The major capsid protein, VP1, of human JC virus expressed in *Escherichia coli* is able to self-assemble into a capsid-like particle and deliver exogenous DNA into human kidney cells.** J Gen Virol (1999) 80 (Pt 1), 39–46.

16 Gillock, E.T. *et al.* **Polyomavirus major capsid protein VP1 is capable of packaging cellular DNA when expressed in the baculovirus system.** J Virol (1997) 71, 2857–2865.

17 Lipin, D.I., Lua, L.H. and Middelberg, A.P. **Quaternary size distribution of soluble aggregates of glutathione-S-transferase-purified viral protein as determined by asymmetrical flow field flow fractionation and dynamic light scattering.** J Chromatogr A (2008) 1190, 204–214.

18 Bundy, B.C., Franciszkowicz, M.J. and Swartz, J.R. ***Escherichia coli*-based cell-free synthesis of virus-like particles.** Biotechnol Bioeng (2008) 100, 28–37.

19 Bundy, B.C. and Swartz, J.R. **Efficient disulfide bond formation in virus-like particles.** J Biotechnol (2011) 154, 230–239.

20 Shimizu, Y. *et al.* **Cell-free translation reconstituted with purified components.** Nat Biotechnol (2001) 19, 751–755.

21 Woodrow, K.A. and Swartz, J.R. **A sequential expression system for high-throughput functional genomic analysis.** Proteomics (2007) 7, 3870–3879.

22 Kim, T.W. *et al.* **Cell-free synthesis and *in situ* isolation of recombinant proteins.** Protein Expr Purif (2006) 45, 249–254.

23 Mastrobattista, E. *et al.* **High-throughput screening of enzyme libraries: *in vitro* evolution of a beta-galactosidase by fluorescence-activated sorting of double emulsions.** Chem Biol (2005) 12, 1291–1300.

24 Smith, M.T. *et al.* **The incorporation of the A2 protein to produce novel Qbeta virus-like particles using cell-free protein synthesis.** Biotechnol Prog (2012) 28, 549–555.

25 Teunissen, E.A. *et al.* **Different proteins require different S30 extract protein concentrations for optimal expression.** Manuscript in preparation (2014).

26 Samadi, N. *et al.* **The effect of lauryl capping group on protein release and degradation of poly(d,l-lactic-co-glycolic acid) particles.** J Control Release (2013) 172, 436–443.

27 Hayat, M.A. **Fixation for Electron Microscopy.** (Academic Press, 1981).

28 Teunissen, E.A. *et al.* **Batch-to-batch variability of *E. coli* S30 extracts can be reduced by normalizing S30 total protein content.** Manuscript in preparation (2014).

29 Schneider, C.A., Rasband, W.S. and Eliceiri, K.W. **NIH Image to ImageJ: 25 years of image analysis.** Nat Methods (2012) 9, 671–675.

30 Gedvilaite, A. *et al.* **Size and position of truncations in the carboxy-terminal region of major capsid protein VP1 of hamster polyomavirus expressed in yeast determine its assembly capacity.** Arch Virol (2006) 151, 1811–1825.

31 Schmidt, U., Rudolph, R. and Bohm, G. **Mechanism of assembly of recombinant murine polyomavirus-like particles.** J Virol (2000) 74, 1658–1662.

32 Chromy, L.R., Pipas, J.M. and Garcea, R.L. **Chaperone-mediated *in vitro* assembly of Polyomavirus capsids.** Proc Natl Acad Sci U S A (2003) 100, 10477–10482.

33 Kim, T.W. *et al.* **Simple procedures for the construction of a robust and cost-effective cell-free protein synthesis system.** J Biotechnol (2006) 126, 554–561.

34 Sandalon, Z. *et al.* ***In vitro* assembly of SV40 virions and pseudovirions: vector development for gene therapy.** Hum Gene Ther (1997) 8, 843–849.

35 Yamane, T. *et al.* **Enhanced cell-free protein synthesis using a S30 extract from *Escherichia coli* grown rapidly at 42 degrees C in an amino acid enriched medium.** Biotechnol Prog (2005) 21, 608–613.

36 Miller, O.J. *et al.* **Directed evolution by *in vitro* compartmentalization.** Nat Methods (2006) 3, 561–570.

37 Ding, Y. *et al.* **Modeling the competition between aggregation and self-assembly during virus-like particle processing.** Biotechnol Bioeng (2010) 107, 550–560.

38 Underwood, K.A., Swartz, J.R. and Puglisi, J.D. **Quantitative polysome analysis identifies limitations in bacterial cell-free protein synthesis.** Biotechnol Bioeng (2005) 91, 425–435.

39 Jewett, M.C. and Swartz, J.R. **Mimicking the *Escherichia coli* cytoplasmic environment activates long-lived and efficient cell-free protein synthesis.** Biotechnol Bioeng (2004) 86, 19–26.

40 Brodel, A.K., Sonnabend, A. and Kubick, S. **Cell-free protein expression based on extracts from CHO cells.** Biotechnol Bioeng (2014) 111, 25–36.

41 Moreland, R.B., Montross, L. and Garcea, R.L. **Characterization of the DNA-binding properties of the polyomavirus capsid protein VP1.** J Virol (1991) 65, 1168–1176.

42 Stokrova, J. *et al.* **Interactions of heterologous DNA with polyomavirus major structural protein, VP1.** FEBS Lett (1999) 445, 119–125.

43 Yokoyama, N. *et al.* **Mutational analysis of the carboxyl-terminal region of the SV40 major capsid protein VP1.** J Biochem (2007) 141, 279–286.

44 Garcea, R.L., Salunke, D.M. and Caspar, D.L. **Site-directed mutation affecting polyomavirus capsid self-assembly *in vitro*.** Nature (1987) 329, 86–87.

Supplementary data

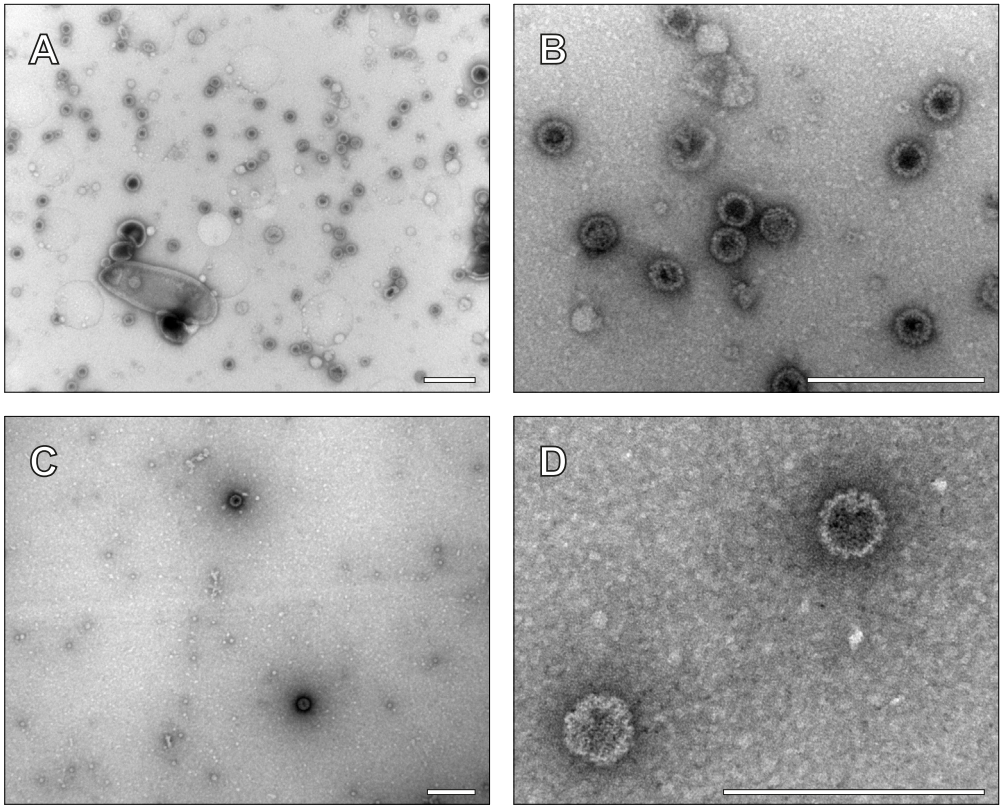

Figure S1. VLPs in the bacterial lysate directly after lysis. VLPs were detected in the lysate after 3 rounds of homogenization (a–b) or after treatment with CelLytic B (c–d). Bars = 200 nm.

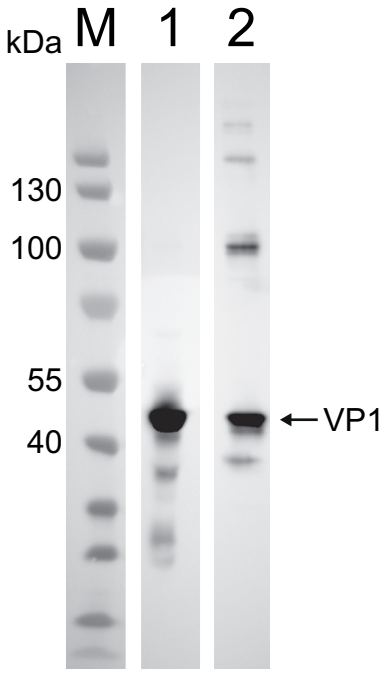

Figure S2. Quantification of VP1 expression using Western blotting. Lane M, PageRuler Prestained Protein Ladder; lane 1, VP1 produced by CFE; lane 2, 85 µg/ml purified VLPs (from bacteria).

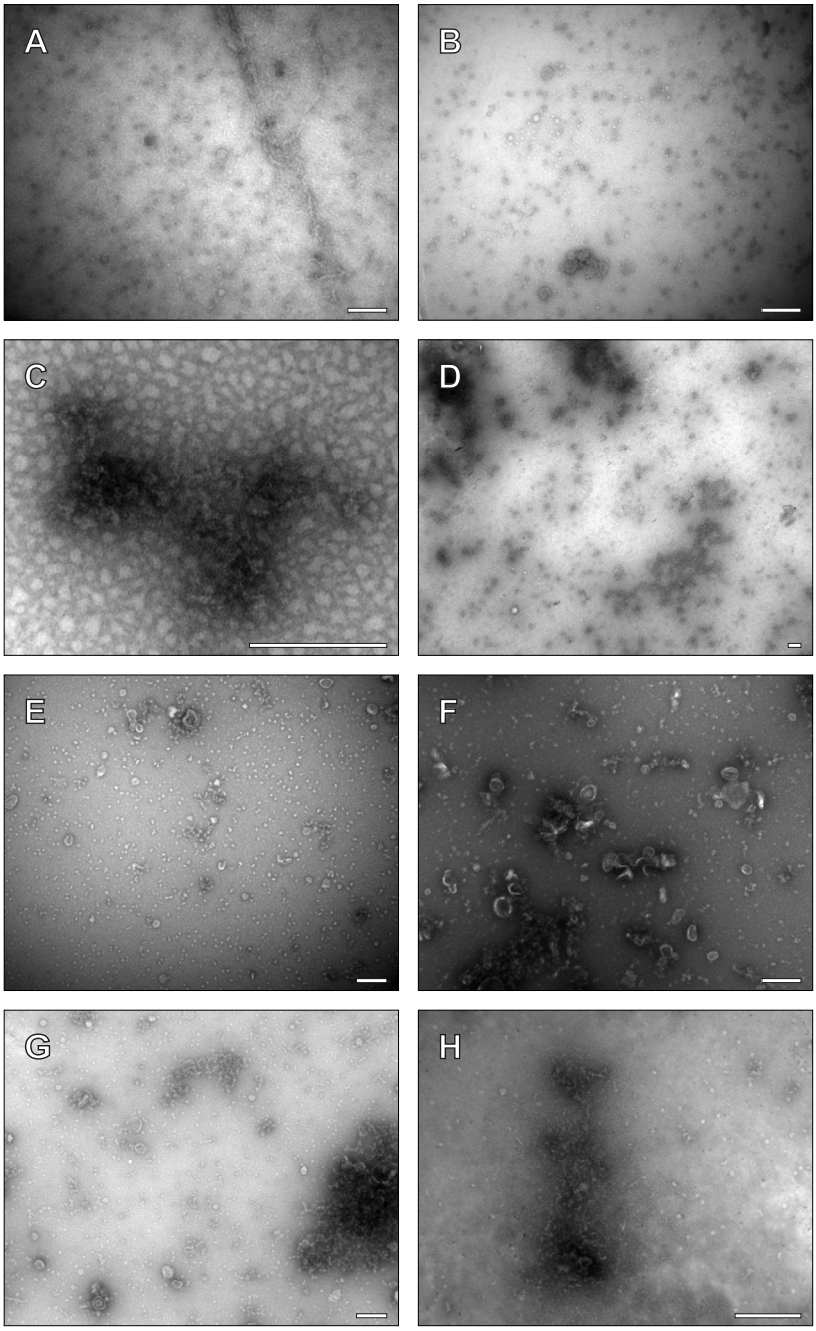

Figure S3. Different modifications of the reaction conditions using S30 extract. (a) Addition of 1.0 mM calcium chloride; (b) addition of 1.0 mM calcium chloride and removal of DTT; (c) incubation for 24 h; (d) incubation at 22 °C; (e) addition of eukaryotic chaperones; (f) pretreatment with iodoacetamide; (g) redox buffered with 1.0 mM GSH and 4.0 mM GSSG, and 5.0 mM calcium chloride; (h) heatshock S30 extract. No VLPs were visible in any of the samples. Bars = 200 nm.

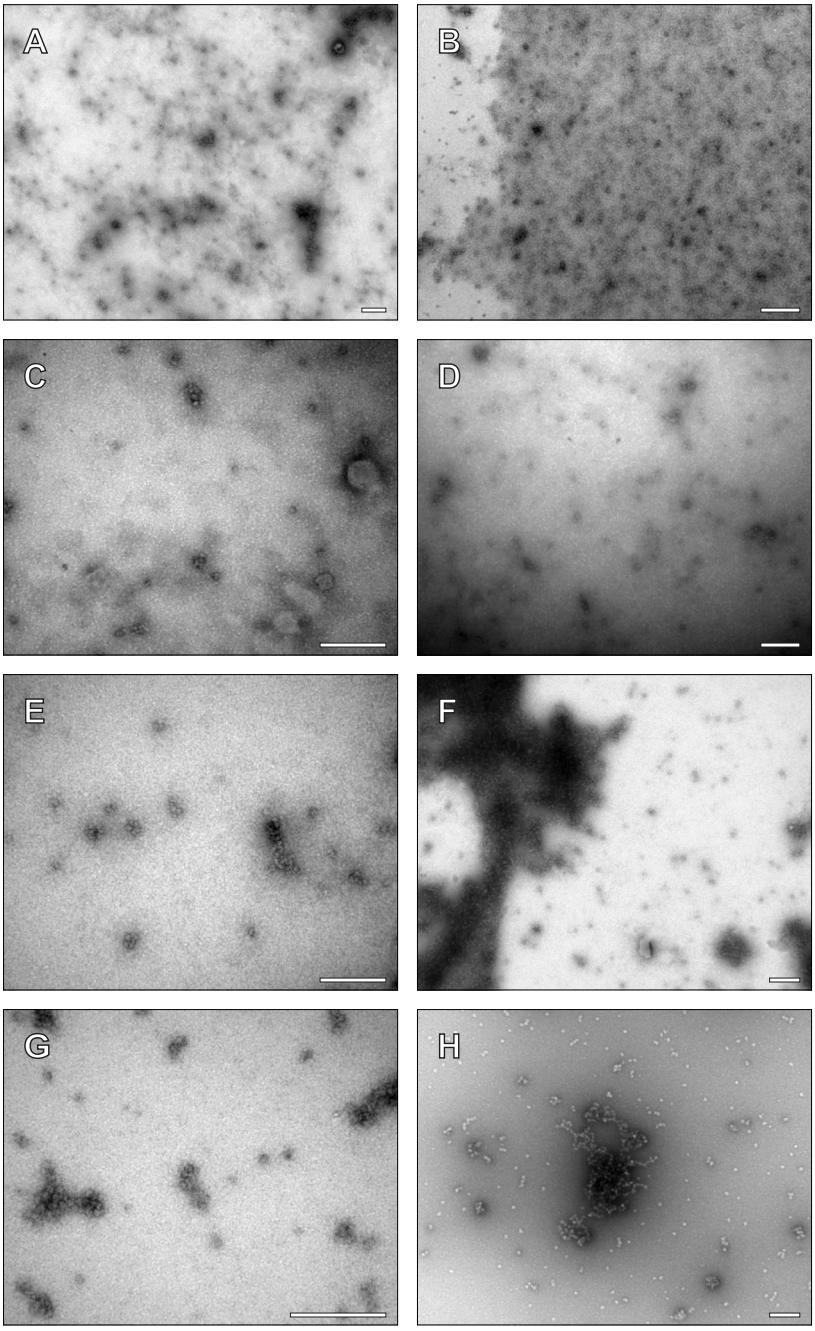

Figure S4. Different modifications of the reaction conditions using PURExpress®. (a) No template control (NTC); (b) normal reaction expressing VP1; (c) addition of 1.0 mM calcium chloride; (d) addition of PURExpress® Disulfide Bond Enhancer; (e) addition of RTS GroE Supplement; (f) addition of RTS DnaK Supplement; (g) addition of RTS GroE Supplement and RTS DnaK Supplement; (h) redox buffered with 1.0 mM GSH and 4.0 mM GSSG, and 5.0 mM calcium chloride. No VLPs were visible in any of the samples. Bars = 200 nm.

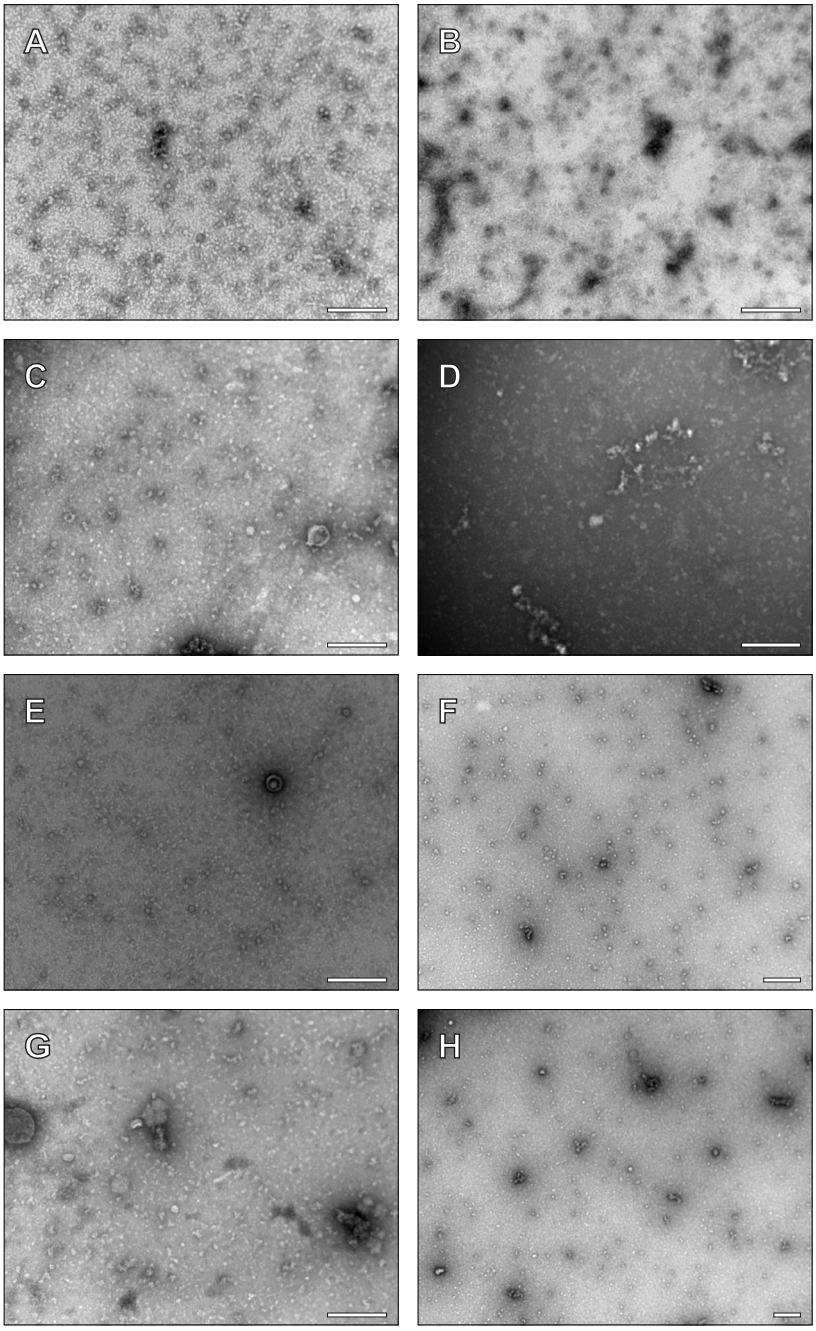

Figure S5. Different modifications of the reaction conditions using the Roche RTS *E. coli* HY kit. (a) NTC; (b) NTC with 1.0 mM calcium chloride; (c) normal reaction expressing VP1; (d) addition of 1.0 mM calcium chloride; (e) NTC post-treated with Benzonase®; (f) NTC with 1.0 mM calcium chloride post-treated with Benzonase®; (g) normal reaction expressing VP1 post-treated with Benzonase®; (h) addition of 1.0 mM calcium chloride post-treated with Benzonase®. No VLPs were visible in any of the samples. Bars = 200 nm.

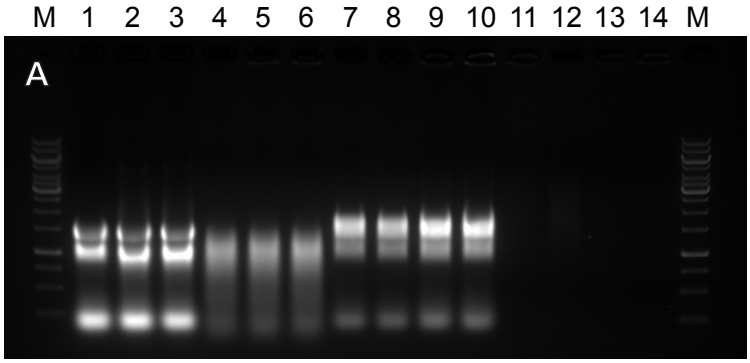

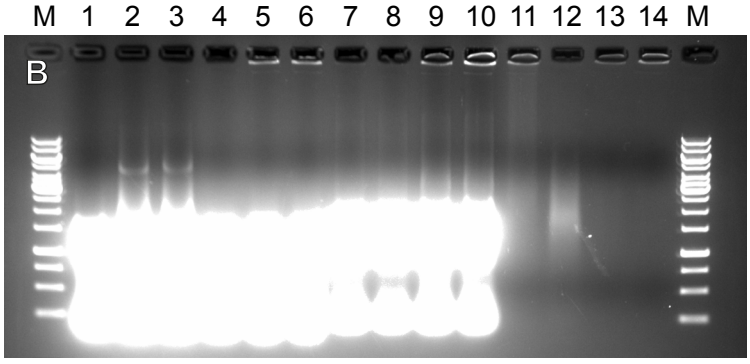

C

Lane	Sample
M	GeneRuler 1 kb DNA Ladder
1	PURExpress® NTC
2	PURExpress® VP1 expression
3	PURExpress® VP1 expression with 1.0 mM calcium chloride
4	Benzonase® treated – PURExpress® NTC
5	Benzonase® treated – PURExpress® VP1 expression
6	Benzonase® treated – PURExpress® VP1 expression with 1.0 mM calcium chloride
7	Roche RTS NTC
8	Roche RTS NTC with 1.0 mM calcium chloride
9	Roche RTS VP1 expression
10	Roche RTS VP1 expression with 1.0 mM calcium chloride
11	Benzonase® treated – Roche RTS NTC
12	Benzonase® treated – Roche RTS NTC with 1.0 mM calcium chloride
13	Benzonase® treated – Roche RTS VP1 expression
14	Benzonase® treated – Roche RTS VP1 expression with 1.0 mM calcium chloride
M	GeneRuler 1 kb DNA Ladder

Figure S6. Removal of nucleic acids by post-treatment with Benzonase®. Agarose gel electrophoresis of samples digested with Benzonase® after cell-free expression; (a) short exposure time; (b) long exposure time; (c) list of samples. The digestion of the Roche RTS samples was almost complete. Only a very faint band remained with the Roche RTS NTC (lane 11) and the Roche RTS NTC with calcium chloride (lane 12). The PURExpress® samples, on the other hand, were not fully digested, although all template plasmid was digested (the upper band from lanes 2 and 3 is no longer visible in lanes 5 and 6).

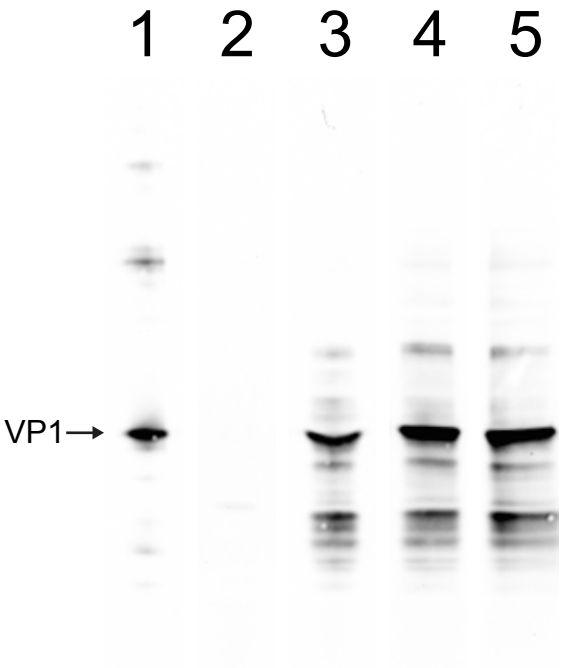

Figure S7. Western blot showing the purification of VP1 from PURExpress® by reverse his-tag purification. Lane 1, 64 µg/ml purified VLPs (from bacteria); lane 2, PURExpress® NTC; lane 3, VP1 expressed using PURExpress® before purification; lane 4, VP1 purified from PURExpress®; lane 5, VP1 reassembled after purification from PURExpress®.

Chapter VI

Proof of concept for the directed evolution of virus-like particles derived from polyomaviruses

Erik A. Teunissen[1], Jorrit J. Water[1], Kasper M. Kommeren[1], Joep B. van den Dikkenberg[1], Emilie M.J. van Brummelen[1], Markus de Raad[1] and Enrico Mastrobattista[1]

[1]Department of Pharmaceutics, Utrecht Institute for Pharmaceutical Sciences, Faculty of Science, Utrecht University, Universiteitsweg 99, 3584 CG Utrecht, The Netherlands

Manuscript in preparation

Abstract

Directed evolution provides an attractive alternative to rational design for the creation of novel viral vectors for gene therapy. Instead of rationally altering the viral coat protein to achieve changes in *e.g.* their tropism, high-throughput combinatorial techniques are used to create a very large library of random mutants. By applying selective pressure on this library, only those clones which possess desired properties remain. This way, the process resembles natural evolution, with the exception that we can define the selection criteria. So far directed evolution has been applied to change the activity of individual proteins or change the tropism of viruses. Here, we give a proof of concept that this method can also be applied for the functional selection of polyomavirus virus-like particles (VLPs) as a model delivery system. VLPs are assemblies of viral structural proteins. They resemble the native viral capsid in structure, tropism, and transduction efficiency, but do not contain any viral genetic material. To combine the beneficial properties of different polyomavirus species, vast libraries of hybrid *VP1* genes were created using DNA shuffling. Using this technique, up to 6 different polyomavirus *VP1* genes were successfully recombined. To demonstrate genotype-phenotype linkage, we transfected 293TT cells with two types of plasmids, one encoding wild-type VP1, the other one a mutant. After VLP purification, we analyzed the fractions for *VP1* DNA. As the VLPs form, they package available genetic material compartmentalized within the same cell. We observed a 10-fold enrichment of wild-type *VP1* DNA after one single selection step. This data shows that polyomavirus-derived VLPs are able to package their own coding DNA, and can thus be used for directed evolution.

1. Introduction

Despite the considerable progress in the field of rational protein design, predicting the effects of modifications remains very difficult. Even with a known structure, insufficient knowledge about structure-function relationships and a lack of computational power often make it impossible to calculate the result of mutations [1]. Changes to one part of a protein often cause unforeseen effects at other regions. Directed evolution has proven to be a valuable alternative to rational design for the modification of proteins. Instead of applying the changes one-by-one, large libraries of random mutants are prepared through high-throughput combinatorial techniques. Subsequently, mutants that possess desired properties are selected from the libraries by applying selective pressure, this way obtaining improved proteins without prior knowledge of structure-function relationships.

Directed evolution has mainly been used for the alteration of enzymes (for recent reviews see references [2] and [3]), but this technique can also be used to create novel viral vectors for gene therapy. Most studies have been performed with adeno-associated virus (AAV) [4–11], but also other viruses, such as adenoviruses [12,13] and retroviruses [14–17] have been subjected to directed evolution. Different properties, such as tropism [8–10], stability [15], and immunogenicity [4,18], have been changed.

In this chapter we investigate the application of directed evolution to adapt virus-like particles (VLPs). VLPs are assemblies of viral structural proteins. They resemble the native viral capsid in structure, tropism, and transduction efficiency, but do not contain any viral genetic material. This makes them a safer alternative to viral vectors for gene therapy. One class of promising VLPs is those derived from polyomavirus VP1 proteins [19]. The polyomavirus coat protein VP1 is one of the three structural proteins of the virus. After overexpression, VP1 proteins self-assemble to form VLPs [20–22]. These VLPs are able to encapsidate double-stranded DNA in a sequence-independent fashion

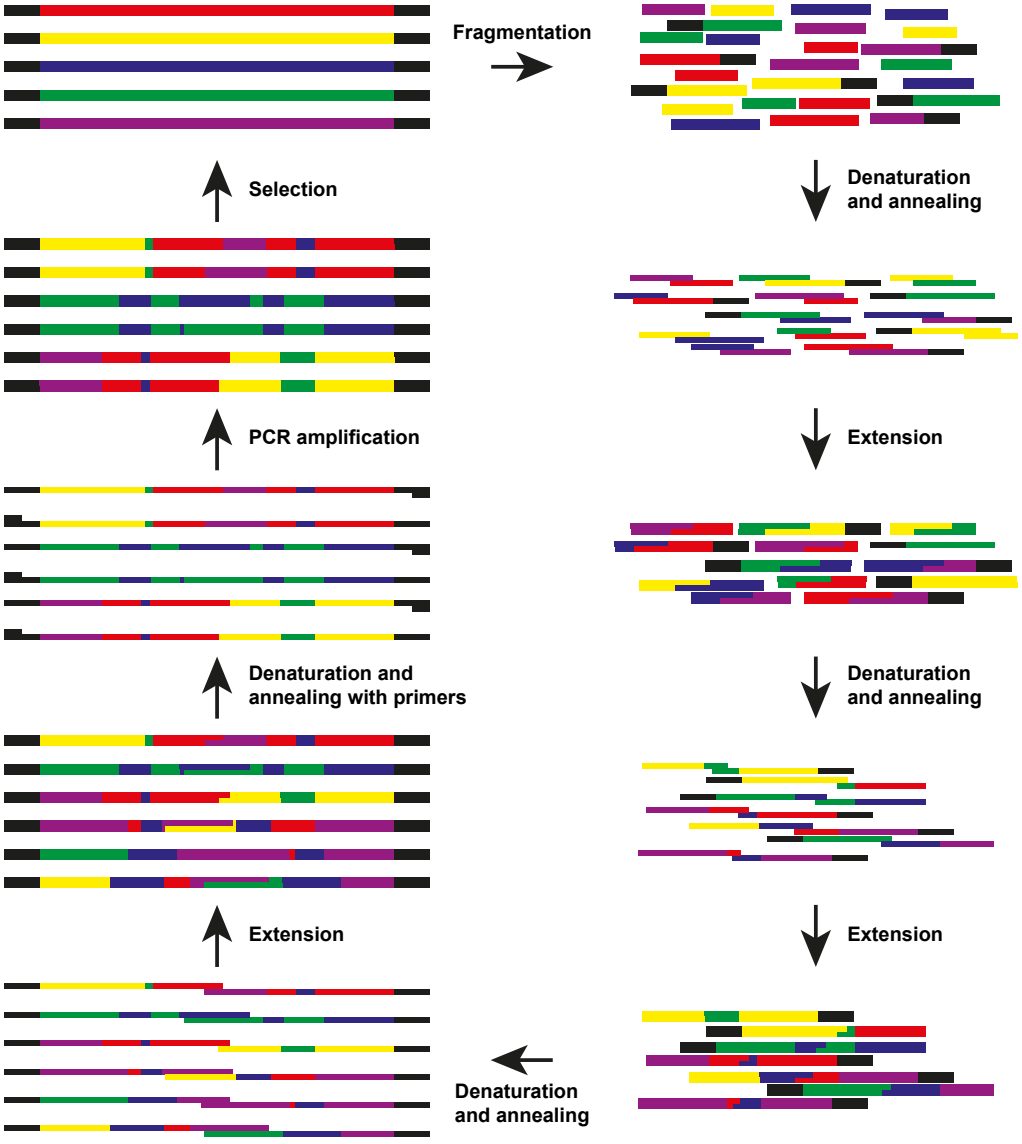

Figure 1. Principle of DNA shuffling. Homologous genes (indicated by the different colors) are digested with DNaseI to generate fragments of appropriate size. These fragments are denatured, allowed to anneal to one another based on homology, and extended through self-priming PCR. This process is repeated until full-length genes are reassembled. Primers complementary to the flanking regions are then added and the full-length genes are amplified by PCR, yielding a gene library which can be used for selection experiments. The selected genes can then be used as templates for further rounds of DNA shuffling, resulting in directed evolution.

[23,24], transfect mammalian cells [24,25], have a high insert capacity for peptides in their surface-exposed loops [26], and can be derived from many different polyomavirus species with widely diverse properties [19]. This makes them a good starting point for directed evolution.

We set out to prove that virus-like particles derived from polyomaviruses are suitable for directed evolution. We did this by proving that libraries of mutant polyomavirus *VP1* genes can be created, and proving that polyomavirus-derived VLPs demonstrate genotype-phenotype linkage, *i.e.* package their own coding DNA. Genotype-phenotype linkage is an important aspect in directed evolution. This linkage between coding DNA and encoded protein ensures that the selected proteins can be traced back to their genetic origin to identify, by sequencing, the mutations causing the beneficial properties. In a way this process mimics cellular compartmentalization in life.

To promote genotype-phenotype linkage, we made use of the SV40 signal for encapsidation, *ses*. This signal is responsible for the specific encapsidation of plasmid DNA *in cis* [27–29]. This sequence overlaps the SV40 origin of replication (*ori*), leading to its amplification in cells overexpressing the SV40 large T antigen [27]. This results in an increase in copy number, in turn resulting in enhanced production of VLPs. An excellent cell line for this purpose is 293TT [30]. This cell line stably overexpresses the SV40 large T antigen and has already been used for the production of reporter vectors based on several polyomaviruses [31,32]. To ensure the encapsidation of the VP1-encoding plasmid, the plasmid should be around 5 kb in size [27].

To combine the beneficial properties of different

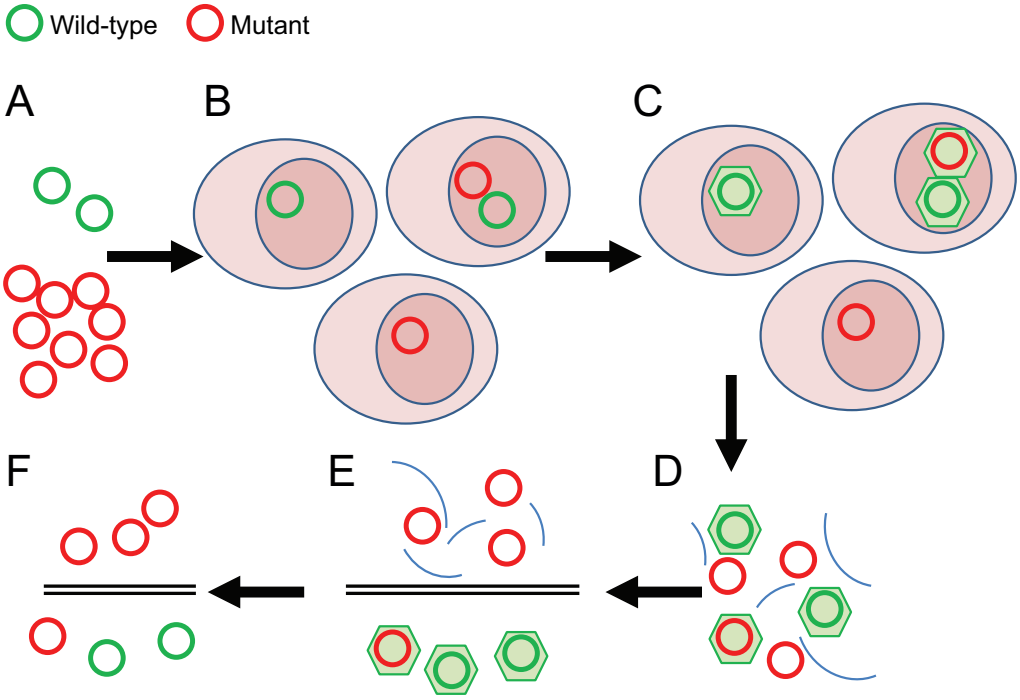

Figure 2. Design of the proof of concept study. Plasmid DNA encoding wild-type (green) and mutant (red) SV40 VP1 are mixed at a 1:100 ratio (a). The DNA is used to transfect 293TT cells (b), causing the cells to express VP1. Cells expressing wild-type VP1 will package available plasmid DNA, while cells expressing only the mutant VP1 will not be able to package DNA (c). This way, the genotype (plasmid DNA encoding wild-type VP1) becomes linked to the phenotype (VLP). After 48 hours the cells are lysed (d) and VLPs are purified by gradient ultracentrifugation (e). DNA is then extracted from the purified VLPs and analyzed for the ratio of wild-type to mutant *VP1* genes (f). Ideally this would lead to purification of only wild-type *VP1* genes. However, because individual cells can become transfected with more than one type of plasmid (b), the purified DNA will most likely be contaminated with some mutant *VP1* genes.

polyomavirus species, we recombined their *VP1* DNA sequences through a technique called DNA shuffling (see figure 1) [33,34], forming novel polyomavirus *VP1* hybrids. To demonstrate genotype-phenotype linkage, we transfected 293TT cells with two types of plasmids, one encoding wild-type VP1, the other one a mutant. After VLP purification, we analyzed the fractions for *VP1* DNA. The design of this study is shown schematically in figure 2.

2. Materials and methods

2.1. Chemicals

Ampicillin, bovine serum albumin (BSA), bromophenol blue, calcium chloride, dithiothreitol (DTT), ethidium bromide, glycerol, iodixanol (60 % w/v solution in water), isopropyl β-D-1-thiogalactopyranoside (IPTG), kanamycin, LB agar, LB broth culture medium, 2-mercaptoethanol, polysorbate 20 (TWEEN® 20), sodium dodecyl sulfate (SDS), and tris(hydroxymethyl)aminomethane (Tris) were purchased from Sigma-Aldrich (St. Louis, MO, USA). Agarose MP and cOmplete EDTA-free protease inhibitor cocktail tablets were purchased from Roche (Basel, Switzerland). Ethylenediaminetetraacetic acid (EDTA) was purchased from Acros Organics (Geel, Belgium). GeneRuler 1 kb DNA Ladder, GeneRuler 50 bp DNA Ladder, PageBlue Protein Staining Solution, PageRuler Prestained Protein Ladder, proteinase K, and DNA-modifying enzymes were purchased from Thermo Scientific (Waltham, MA, USA). Dulbecco's Modified Eagle's Medium (DMEM), fetal bovine serum (FBS), and Trypsin-EDTA (L11-004) were purchased from PAA Laboratories (Pasching, Austria). Phosphate buffered saline (PBS) was purchased from B. Braun Melsungen AG (Melsungen, Germany). Primers were purchased from Eurogentec (Seraing, Belgium). Acetic acid, hydrochloric acid, and sodium chloride were purchased from Merck KGaA (Darmstadt, Germany). iQ™ SYBR® Green Supermix was purchased from Bio-Rad (Hercules, CA, USA). Dulbecco's Phosphate Buffered Saline (DPBS) was purchased from GE Healthcare (Little Chalfont, United Kingdom).

2.2. Homology analysis

The list of polyomaviruses was taken from the NCBI Genome database using the search criteria '"Polyomaviridae"[Organism]' (retrieved 02/2011). VP1 protein sequences from the retrieved polyomaviruses were taken from the NCBI RefSeq database. Homology was calculated using ClustalW2 (pairwise alignment, standard settings) [35].

2.3. Plasmids

The *VP1* genes from six different polyomaviruses were cloned into pIVEX2.2EM under control of a T7 promoter. The preparation of the pIVEX2.2EM backbone has been described elsewhere [36]. The cloning and preparation of plasmid pIVEX-HaPyV-VP1, containing the *VP1* gene from the hamster polyomavirus, has been described elsewhere [37]. The plasmids pIVEX-BKPyV-VP1, pIVEX-JCPyV-VP1, pIVEX-MCPyV-VP1, pIVEX-MPyV-VP1, and pIVEX-SV40-VP1, which contain the *VP1* genes from BK polyomavirus (GenBank: AAA46882.1), JC polyomavirus (GenBank: AAA82101.1), Merkel Cell polyomavirus (GenBank: FM864207.1), murine polyomavirus (GenBank: CAA24468.1), and SV40 (GenBank: AAB59923.1), respectively, were prepared similar to pIVEX-HaPyV-VP1 [37]. Briefly, the VP1 protein sequences were reverse translated and codon-optimized for expression in *E. coli* using GeneDesign [38]. Flanking sequences were added to create an NcoI restriction site overlapping the start codon and an XhoI restriction site directly adjacent to the stop codon. The genes were synthesized by Mr. Gene (Regensburg, Germany) and delivered in a pMA-T or pMA vector. The genes were excised from the vectors using NcoI and XhoI, and cloned into pIVEX2.2EM digested with the same

enzymes. The expression of the VP1 proteins in *E. coli* was performed as described before [22]. Briefly, *E. coli* BL21(DE3)pREP4 were transformed with the different pIVEX-VP1 constructs, grown in LB medium, induced with 1.0 mM IPTG at an OD600 of 0.8, and analyzed for VP1 production by SDS-PAGE after overnight expression at 37 °C.

The plasmid pAU was created through a series of modifications of pEGFP-C1 (Clontech; Mountain View, CA, USA). First, the PciI site in pEGFP-C1 was removed; pEGFP-C1 was digested with PciI, blunted using T4 DNA polymerase, phosphorylated with T4 Polynucleotide Kinase, and re-ligated using T4 DNA Ligase. Next, the NcoI site at the start of the EGFP gene in pEGFP-C1ΔPciI was mutated into a PciI site using the QuikChange Lightning Site-Directed Mutagenesis Kit (Agilent Technologies; Santa Clara, CA, USA) according to the manufacturer's protocol with primers pEGFP-NcoI_to_Pci_fw (CGCTACCGGTCGCCAACATGTTGAGCAAGGGCGAGG) and pEGFP-NcoI_to_Pci_rv (CCTCGCCCTTGCTCAACATGTTGGCGACCGGTAGCG). Finally, the XbaI-site was mutated to prevent Dam methylation using the QuikChange Lightning Site-Directed Mutagenesis Kit according to the manufacturer's protocol with primers pEGFP-C1_XbaI_dam-_fw (GCGGGCCCGGGATCCACCGCCTCTAGATAACTGATCATAATC) pEGFP-C1_XbaI_dam-_rv (GATTATGATCAGTTATCTAGAGGCGGTGGATCCCGGGCCCGC). pAU-SV40-VP1, which contains the wild-type SV40 *VP1* gene under control of a CMV promoter, was cloned as follows. The SV40 *VP1* gene was amplified from pIVEX-SV40-VP1 by PCR using primers VP1_Shuffling_secondary_fw2 (CTTTAAGAAGGAGATATACCAT) and VP1_XbaI_C_term_rv (CTAGTCTAGAGCAGAGCTCGCTCGAG). The PCR product was digested with NcoI and XbaI, and ligated into pAU digested with PciI and XbaI. pGL3-SV40-VP1, which contains the wild-type SV40 *VP1* gene under control of a SV40 promoter, was cloned as follows. The SV40 *VP1* gene was amplified from pIVEX-SV40-VP1 by PCR using primers VP1_Shuffling_secondary_fw2 and VP1_XbaI_C_term_rv. The PCR product was digested with NcoI and XbaI, and ligated into pGL3-control (Promega; Madison, WI, USA) digested with NcoI and XbaI. The SV40 *VP1* mutant was created using the QuikChange Lightning Site-Directed Mutagenesis Kit according to the manufacturer's protocol with primers SV40_fs_mutant_fw (GCCGTGCTACTCTGTTGACTAGTATCCCGCTGCCGAACATC) and SV40_fs_mutant_rv (GATGTTCGGCAGCGGGATACTAGTCAACAGAGTAGCACGGC). All genes and mutations were verified by sequencing (BaseClear; Leiden, The Netherlands). Suitable quantities of circular plasmid DNA were obtained using the NucleoBond® PC 10 000 kit (MACHEREY-NAGEL; Düren, Germany).

2.4. SDS-PAGE and Western blotting

SDS-PAGE and Western blotting were performed as before [37] with the following modifications. In addition to the samples, 5 µl PageRuler Prestained Protein Ladder was included on each gel. No HaPyV VP1 internal standard was included. For Western blotting, the mouse-anti-JCPyV-VP1 (ab34756; Abcam; Cambridge, United Kingdom) monoclonal antibody, which cross-reacts with SV40 VP1, was used as primary antibody. For SDS-PAGE, the gels were stained with PageBlue Protein Staining Solution according to the manufacturer's protocol using a microwave oven.

2.5. Preparation of the gene libraries

For each polyomavirus, *VP1* DNA was excised from 100 µg pIVEX-VP1 by digestion with BlpI and BglII. The *VP1* DNA was gel purified using the NucleoSpin® Extract II kit (MACHEREY-NAGEL; Düren, Germany). Next, the *VP1* DNA was fragmented using DNaseI. Reaction mixtures were prepared in thin-walled polypropylene PCR tubes (Greiner Bio-One; Monroe, NC). Each reaction mixture contained 2.5 µg *VP1* DNA in 25 µl 2× DNaseI buffer. The samples were placed in a Primus 96 advanced thermocycler (PEQLAB; Erlangen, Germany) set to 25°C. The reactions were started by adding 25 µl 5.0 U/ml DNaseI (kept on ice). The samples were incubated at 25 °C for 30 seconds,

and then stopped by adding 5.0 µl 25 mM EDTA. The samples were immediately transferred to another Primus 96 advanced thermocycler preheated to 65 °C and incubated for 20 minutes to further inactivate the DNaseI. The fragments were separated on 2.0 % agarose gels. Fragments of the indicated sizes were gel purified as above.

To reassemble the *VP1* genes, a total of 200 ng of purified fragments of the different polyomaviruses were mixed together at equal weight ratios. Each reassembly reaction mixture (25 µl) contained 200 ng DNA fragments, 1.0× *Taq* buffer with ammonium sulfate, 2.5 mM magnesium chloride, 0.20 mM of each dNTP, and 0.10 U *Taq* DNA polymerase. PCR was performed in a Primus 96 advanced thermocycler with the lid temperature set to 110 °C. The PCR was started at 98 °C for 30 sec, followed by 40 cycles of 98 °C for 10 sec, 50 °C for 30 sec, and 72 °C for 45 sec. The PCR was completed at 72 °C for 10 min, followed by storage at 4 °C. After the PCR, the reassembled genes were run on a 1.0 % agarose gel, and all DNA between 1000 and 1500 bp was purified as above, eluting in 15 µl nuclease-free water.

Another PCR was performed to amplify the reassembled genes. Each amplification reaction mixture (25 µl) contained up to 3 µl purified reassembled genes, 1.0× *Taq* buffer with ammonium sulfate, 2.5 mM magnesium chloride, 0.20 mM of each dNTP, 0.20 µM VP1_Shuffling_primary_fw2 (CCACAACGGTTTCCCTCTA), 0.20 µM VP1_Shuffling_primary_rv (AGCAGCCAACTCAGCTTC), and 0.10 U *Taq* DNA polymerase. PCR was performed in a Primus 96 advanced thermocycler with the lid temperature set to 110 °C. The PCR was started at 98 °C for 5 min, followed by 30 cycles of 98 °C for 15 sec, 56 °C for 1 min, and 72 °C for 90 sec. The PCR was completed at 72 °C for 10 min, followed by storage at 4 °C. After the PCR, the amplified genes were purified using the GeneJET PCR Purification Kit (Thermo Scientific; Waltham, MA, USA). The flanking regions of the purified genes were removed by digesting with NcoI and XhoI. The digestions were run on a 1.0 % agarose gel, and all DNA between 1000 and 1500 bp was purified as above. The digested *VP1* genes were ligated into NcoI/XhoI-digested pIVEX2.2EM using a 3:1 insert:vector molar ratio. After ligation, the libraries were transformed into *E. coli* DH5α. To analyze the diversity of the libraries, the bacteria were plated out on LB agar plates. After overnight incubation at 37 °C, individual colonies were picked and grown in LB medium. DNA was extracted from the cultures using the GeneJET Plasmid Miniprep Kit (Thermo Scientific; Waltham, MA, USA). Sequencing was performed by BaseClear (Leiden, The Netherlands). Alignments were calculated using ClustalW2 (multiple sequence alignment, standard settings) [35]. For large scale production, the plating step was skipped and the libraries were grown directly in LB medium after transformation.

2.6. Cell culture

COS-7 cells were grown in DMEM supplemented with 10 % v/v FBS. 293TT cells were obtained from the NCI DCTD Tumor Repository (National Cancer Institute, Division of Cancer Treatment and Diagnosis; Frederick, MD, USA). The cells were grown in DMEM supplemented with 10 % v/v FBS without antibiotics. All cells were grown in a humidified incubator with 5 % CO_2 at 37 °C.

2.7. Maintenance of pEGFP-C1 in COS-7 cells

COS-7 cells were seeded onto six-well plates at 2.5 × 10^5 cells per well. After 24 hours, the cells were transfected in triplicate with pEGFP-C1 and pIVEX-(MCPyV/SV40)-VP1 mixed at different weight ratios (0:0; 1:0; 1:1; 1:8; 1:512; and 0:1) in DMEM using Lipofectamine® 2000 (Life Technologies; Carlsbad, CA, USA) according to the manufacturer's protocol (12.5 µg total DNA per well). The cells were monitored daily with light and fluorescence microscopy (Eclipse TE2000-U with GFP-B filter; Nikon; Tokyo, Japan). Starting after 24 hours, each day for five days, the cells were harvested

by adding 0.2 ml 1× Trypsin-EDTA for up to 5 minutes, followed by the addition of 1.3 ml DMEM + 5 % FBS. From each sample, 0.5 ml was taken for analysis and remaining the 1.0 ml was incubated for another 24 hours. Plasmid concentrations in the samples were determined using qPCR with primers Bla_qPCR_fw (AAGTTGGCCGCAGTGTTATC) and Bla_qPCR_rv (GCTATGTGGCGCGGTATTAT) for pIVEX, and eGFP_qPCR_fw (CGACGGCAACTACAAGAC) and eGFP_qPCR_rv (TAGTTGTACTCCAGCTTGTGC) for pEGFP-C1. Each reaction mixture (20 µl) contained 0.20 µM of a primer set, 10 µl 2× iQ™ SYBR® Green Supermix, and 1.0 µl sample. PCR was performed using a CFX96™ Real-Time System (Bio-Rad) with the lid temperature set to 105 °C. The PCR was started at 95 °C for 3 min, followed by 40 cycles of 95 °C for 10 sec, 58 °C for 30 sec, 72 °C for 30 sec, and plate reading. The PCR was completed with a melt curve from 65 °C to 95 °C. Next to the samples and controls, ten-fold dilution series of both pEGFP and pIVEX, ranging from 1.0×10^{-8} to 0.10 ng DNA, were also included.

2.8. Proof of concept for directed evolution of VLPs in 293TT cells

293TT cells were seeded onto 75 cm^2 flasks at 2×10^6 per flask. After 2 days the cells (90 % confluent) were transfected with pAU-SV40-VP1 wild-type and mutant mixed at different weight ratios (0:0; 1:0; 1:100; 0:1) in DMEM using Lipofectamine® 2000 according to the manufacturer's protocol (24 µg total DNA per flask). Small samples of the original transfection mixtures were kept for later use as negative control for enrichment. After 4 hours 2 ml FCS was added to each flask, making the final concentration 10 %. The medium was exchanged with fresh DMEM + 10 % FCS 18 hours after the transfection. Forty hours after the transfection the cells were harvested in 6 ml DPBS with 1.0 mM calcium chloride and cOmplete protease inhibitor cocktail (1 tablet per 50 ml). The cells were freeze-thawed 3 times, alternating between −20 °C and room temperature. Next, the cells were resuspended by vigorous vortexing and lysed by sonication (1 min, 80 % output, 0.5 sec active time interval) with a LABSONIC® P probe sonicator equipped with a 3-mm diameter probe (Sartorius AG; Göttingen, Germany) at 4 °C while keeping the samples on ice. The lysates were cleared at 10,000 g for 15 min. The supernatants were poured into ultracentrifuge tubes and equilibrated to 6.0 ml using DPBS with 1.0 mM calcium chloride. In each ultracentrifuge tube, 1.4 ml of 27 %, 33 %, and 39 % w/v iodixanol in reassembly buffer (10 mM Tris-HCl (pH 7.2), 1.0 M sodium chloride and 1.0 mM calcium chloride in demineralized water) was sequentially underlaid. The samples were ultracentrifuged at 40,000 RPM in a SW 41 Ti rotor (Beckman Coulter; Brea, CA, USA) at 4 °C for 11 hours. Afterwards, the tubes were carefully removed and 0.25 ml fractions were taken by puncturing the bottom of the tubes with a needle and collecting the drops. The fractions were checked for VP1 by reducing SDS-PAGE and Western blotting. Next, DNA was extracted from the fractions. First, 25 µl 5× VLP destruction solution (100 mM Tris-HCl (pH 8.0), 100 mM DTT, 100 mM EDTA, 1.0 % SDS, and 0.20 mg/ml proteinase K) was added to 100 µl of each fraction, followed by incubation at 50 °C for 15 min to release the DNA. Afterwards, the DNA was purified using the GeneJET PCR Purification Kit. During the drying step, the columns were spun for 5 min instead of 1 minute. DNA was eluted in 50 µl nuclease-free water. PCR was performed to amplify the part of the *VP1* gene covering the mutation. Each reaction mixture (20 µl) contained 0.20 µM SV40_qPCR_fw (CTGGGTGTTAAAACCGGTG), 0.20 µM SV40_qPCR_rv (GTTAGAACCCTGGATCGG), 10 µl 2× iQ™ SYBR® Green Supermix, and 1.0 µl sample. PCR was performed using a CFX96™ Real-Time System with the lid temperature set to 105 °C. The PCR was started at 95 °C for 3 min, followed by 40 cycles of 95 °C for 10 sec, 56 °C for 30 sec, 72 °C for 30 sec, and plate reading. The PCR was completed with a melt curve from 65 °C to 95 °C. Next to the extracted DNA, the original transfection mixtures were also included in the PCR. To differentiate between wild-type and

Table 1. Homology between the six selected polyomavirus *VP1* genes after codon optimization. The *VP1* DNA sequences were aligned using ClustalW2. The scores represent the total homology in percent over the full length of the *VP1* genes. Several conserved regions within the *VP1* genes are identical for all *VP1* genes, while other parts, such as the surface-exposed loops, are less homologous.

	BKPyV	HaPyV	JCPyV	MCPyV	MPyV	SV40
BKPyV		68	88	67	69	87
HaPyV	68		71	72	77	69
JCPyV	88	71		68	68	84
MCPyV	67	72	68		69	68
MPyV	69	77	68	69		69
SV40	87	69	84	68	69	

BKPyV	BK polyomavirus
HaPyV	Hamster polyomavirus
JCPyV	JC polyomavirus
MCPyV	Merkel cell polyomavirus
MPyV	Murine polyomavirus
SV40	Simian virus 40

mutant *VP1*, the PCR fragments were digested with SpeI directly in the PCR mixture. Glycerol was added to a final concentration of 10 %, and the samples were run on 2.0 % agarose gels without ethidium bromide. The gels were post stained using GelRed™ Nucleic Acid Gel Stain (Biotium; Hayward, CA, USA). The relative amount of wild-type and mutant DNA was quantified using Image Lab™ software (Bio-Rad).

3. Results and discussion

3.1. Creation of hybrid polyomavirus *VP1* gene libraries

Polyomavirus *VP1* genes were selected for DNA shuffling based on homology, tropism, and VLP formation. We reviewed the literature and created a

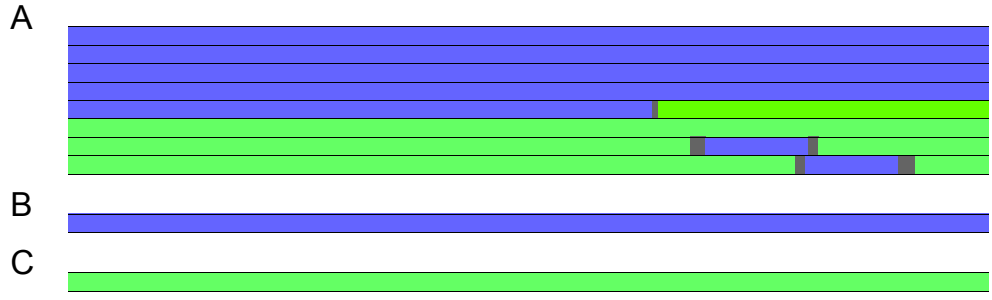

Figure 3. Sequence analysis of the pilot libraries. Every line in the image represents a single clone from a library, with the 5' end of the gene to the left and the 3' end to the right. Homology to the parental genes at each region is indicated by the different colors, with blue and green representing JCPyV and MPyV, respectively. The grey areas represent the regions where the crossovers took place; regions with homology to both parental genes. Only 3 out of 8 clones from the library with shuffled MPyV and JCPyV were hybrids, yielding a crossover frequency of 0.6 for the total library (a). All hybrids were unique. The control libraries with JCPyV (b) and MPyV (c) alone yielded their respective parental genes.

table with known properties of different polyomaviruses (supplementary table S1). We eliminated polyomaviruses without a genome sequence in the RefSeq database (as of 2011), and compared the homology of the VP1 proteins of the remaining polyomaviruses by pairwise alignment using ClustalW2 (supplementary table S2). The homology ranged from 22 to 87 %, with most polyomavirus VP1 proteins sharing 50–60 % homology. Polyomaviruses with an average homology of less than 40 % were discarded as such low homologies are unlikely to yield good recombinants through gene shuffling [39]. Based on this data we selected six polyomavirus *VP1* genes (see table 1). To increase the chance of success we selected polyomaviruses known to form VLPs after overexpression in mammalian cells [19], plus the well-studied SV40 and the HaPyV previously studied by our group [22]. All selected *VP1* genes were codon-optimized using the same codon usage table to maximize the homology (see table 1).

After validating the expression of the individual VP1 proteins (data not shown), we started out by preparing a library by shuffling two of the most unrelated polyomaviruses, JCPyV and MPyV (68 % homology). Relatively large fragments (100–400 bp) were used for this preliminary library to ensure reassembly. We also reassembled both parental genes as a control. Several clones from these libraries were sequenced, and the results were aligned with both parental genes (see figure 3). Hybrid *VP1* genes were found, proving that it is possible to shuffle the selected *VP1* genes, although a relatively large fraction of the clones contained reassembled parental genes. This could be prevented by using smaller fragments or lowering the annealing temperature [40], although there is always a tradeoff between higher diversity and viability of the mutants [41].

To investigate the influence of fragment size, libraries were created using different fragment sizes (50–200 bp, 200–400 bp and 400–1000 bp). This time three *VP1* genes were included: MPyV, JCPyV, and BKPyV. The latter two share a rather high homology (88 %), and we wondered if this might introduce bias into the reassembly

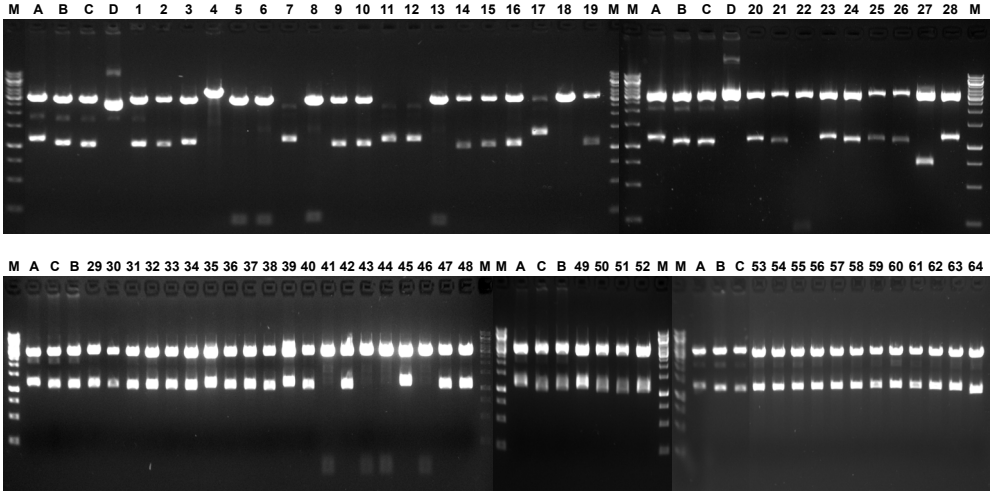

Figure 4. Restriction analysis of plasmid DNA obtained from colonies from the different libraries. The *VP1* gene was excised from plasmid DNA by digestion with NcoI and XhoI and loaded on a 1.5 % agarose gel. (M) GeneRuler 1 kb DNA Ladder; (A) pIVEX-MPyV-VP1 control; (B) pIVEX-BKPyV-VP1 control; (C) pIVEX-JCPyV-VP1 control; (D) pIVEX-HaPyV-VP1 undigested control; (1–28) clones from the library prepared using 50–200 bp fragments; (29–52) clones from the library prepared using 200–400 bp fragments; (53–64) clones from the library prepared using 400–1000 bp fragments. The higher bands (>3.0 kb) represent the pIVEX backbones, whereas the lower bands (1.0–1.5 kb) represent the hybrid *VP1* genes. Not all clones contained a *VP1* gene.

process. No noticeable difference was found in the absolute yield of the reassembly PCR among the different fragment sizes. However, the quality of the reassembled genes decreased with fragment size, with the lowest fragment size yielding the fewest correctly reassembled genes. This is not strange, as smaller fragments require more risky annealing steps to form full-length *VP1* genes. After cloning the libraries, 12–28 colonies from each library were picked and their plasmid DNA was analyzed (see figure 4). Most colonies contained a *VP1* gene with a length intermediate to that of the parental genes, indicative of a correctly reassembled hybrid *VP1* gene. However, 32 % of the colonies from the library prepared using 50–200 bp fragments did not contain a correct insert. This percentage dropped to 17 % for the library prepared using intermediate length fragments (200–400 bp), while no incorrect inserts were found in the library prepared from the largest fragments (400–1000 bp). These incorrect vectors will not qualitatively influence the selection experiments because these vectors will not demonstrate genotype-phenotype linkage. However, such a contamination of the library does have to be taken into account when dosing the library. Moreover, given the limited amount of transformation events, such incorrect vectors might significantly limit the total diversity of the library.

Several *VP1*-positive clones from each libraries were sequenced, and the results were aligned with the parental genes (see figure 5a–c). Hybrid *VP1*

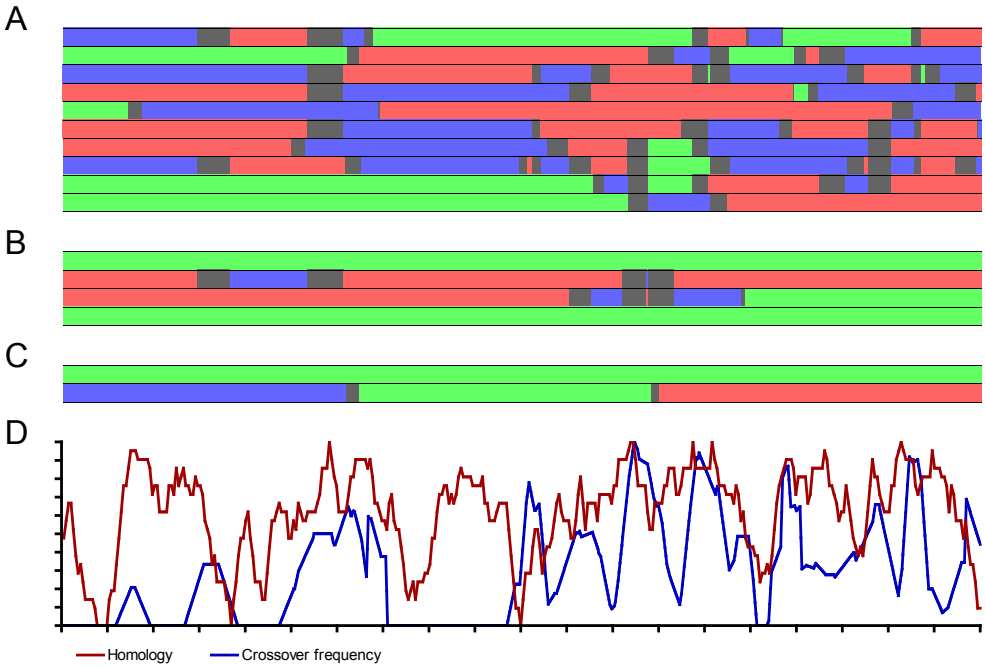

Figure 5. Sequence analysis of the libraries prepared using three parental *VP1* genes. The *VP1* genes of three different polyomaviruses were recombined by DNA shuffling. Different fragment sizes were used to prepare the libraries; (a) 50–200 bp; (b) 200–400 bp; (c) 400–1000 bp. Several clones from each library were sequenced. Every line in the image represents a single clone from a library, with the 5' end of the gene to the left and the 3' end to the right. Homology to the parental genes at each region is indicated by the different colors, with red, blue, and green representing BKPyV, JCPyV, and MPyV, respectively. The grey areas represent the regions where the crossovers took place; regions with homology to both parental genes. The different libraries yielded crossover frequencies of 5.7, 2.0 and 1.5, respectively. (d) Crossovers (blue line) took place in areas where the parental genes shared high homology (brown line). Both the crossover frequency and homology are shown as moving average over ±3 amino acids. No crossovers took place within the variable loops (BC, DE, and HI).

genes were found in all libraries, with the average number of crossovers per gene increasing from 1.5 for the library prepared using the large 400–1000 bp fragments to 5.7 for the library prepared using the smaller 50–200 bp fragments. No reassembled parental genes were found in the library prepared using the smallest fragments. All hybrid *VP1* genes were unique, and all libraries contained hybrids composed of all three parental genes. However, the crossovers were clearly biased towards the highly homologous BKPyV and JCPyV. With 43 events these crossovers were more abundant than those between BKPyV and MPyV (11 events) and JCPyV and MPyV (14 events) combined. Such bias could be reduced by lowering the annealing temperature during reassembly [40]. However, as stated above, this will probably decrease the viability of the library. Selection experiments would have to be performed to identify either the diversity or the viability of the library as the bottleneck, and this will probably depend on the individual selection experiment. As expected, the crossovers took place in regions of high homology between the parental genes (see figure 5d). No crossovers took place in the highly variable loops BC, DE, and HI. These surface-exposed loops are responsible for receptor binding and tropism [42–44]. Mutation of these loops leads to retargeting of the VLPs [45]. Our data show that these loops are efficiently exchanged during DNA shuffling, conceivably creating VLPs with a novel tropism. Multiple point mutations were also observed, further increasing the diversity of the library. These point mutations are most likely introduced by the error-prone *Taq* polymerase during amplification. Depending on the requirements for the library, the amount of point mutations can be regulated by changing the PCR conditions [46] or using different polymerases [41]. We do not expect that more crossovers will lead to better libraries. Previous studies with AAV showed that 2–6 crossovers already led to vectors with radically altered properties [7–9]. However, if more crossovers are required, other techniques, such as "random chimeragenesis on transient template" (RACHITT) [47], could be used as well.

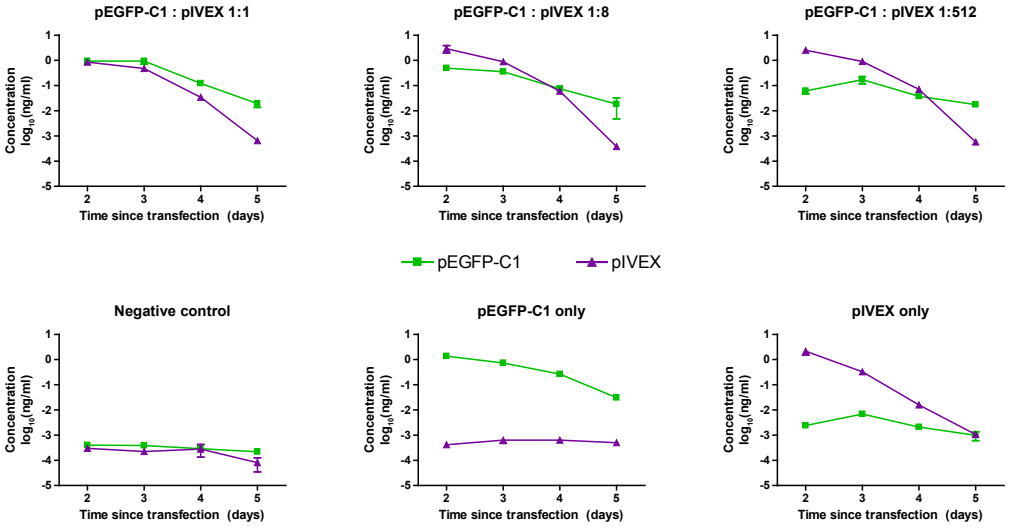

Figure 6. Maintenance of pEGFP-C1 and pIVEX in COS-7 cells over time. The plasmid concentrations were determined by qPCR with primers specific for β-lactamase (pIVEX) and EGFP (pEGFP-C1). The quantities were derived from a standard curve of both plasmids assuming an amplification efficiency of 100 %. The pEGFP content surpassed that of pIVEX within 5 days for all tested ratios, indicating maintenance of the plasmid in the cells and *ses* activity. n=2.

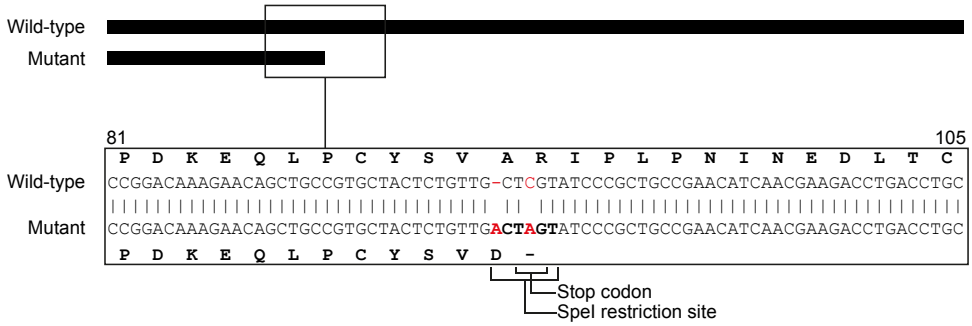

Figure 7. Schematic representation of the wild-type and mutant SV40 *VP1* used in the proof of concept experiment. Mutations are indicated in red. The frameshift and stopcodon are shown, as well as the new SpeI restriction site.

3.2. Selection of a suitable expression vector

Vector backbones were screened for use with the library based on the following criteria: the backbone should (1) measure between 4.5 and 5.5 kb in length after insertion of the library, (2) contain the SV40 signal for encapsidation, *ses*, (3) contain a strong eukaryotic promoter for the expression of the library, and (4) be commercially available. Searching through the NCBI nucleotide collection (nr/nt) database we found two different backbones satisfying these criteria, namely pEGFP-C1 and pGL3-control. We modified both of these vectors to enable easy insertion of the library. In pEGFP-C1, several restriction sites had to be altered before the EGFP gene could be excised to prepare the final vector, pAU; pGL3-control already contained the correct restriction sites, so the luciferase gene could directly be removed. The wild-type *VP1* gene from SV40 was inserted into both vectors. The vectors were tested for the expression of VP1 in 293TT cells. The CMV promoter on pAU caused a more than 10 fold higher expression of VP1 than the SV40 promoter on pGL3-control. Therefore, this vector was chosen for further studies.

3.3. Maintenance of pEGFP-C1 in COS-7 cells

To verify the activity of the *ses* sequence in pEGFP-C1, COS-7 cells were transfected with mixtures of pEGFP-C1 and pIVEX plasmids. The *ses* sequence on pEGFP-C1 should cause the large T antigen-mediated amplification of the plasmid [27], resulting in maintenance of the plasmid during propagation of the cells. After transfection, the cells were sampled daily and analyzed by fluorescence microscopy and qPCR. Steady EGFP fluorescence was observed during the entire assay in all pEGFP-C1 transfected samples. The plasmid content over time was quantified and plotted for each ratio (see figure 6). For all ratios, the pEGFP-C1 content had surpassed that of pIVEX by the fifth day, indicat-

Table 2. Different samples used in the proof of concept study. Vectors harboring wild-type and mutant *VP1* genes were mixed together at different molar ratios as indicated in the table. The total amount of vectors in each sample was kept constant.

Wild-type	Mutant	
1	0	Wild-type only, positive control
1	100	Diluted 100 times
0	1	Mutant only, negative control
0	0	No DNA control

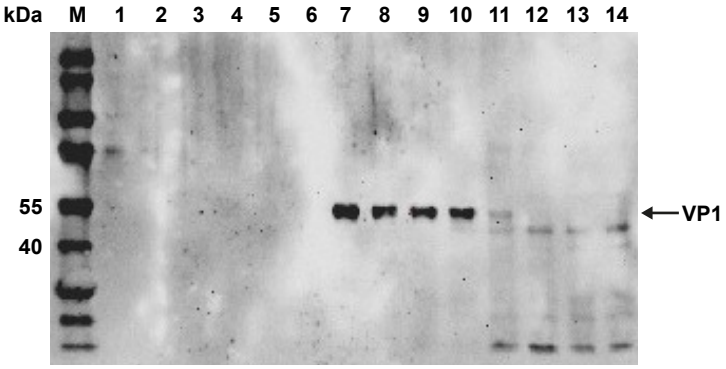

Figure 8. Western blot showing the distribution of SV40 VP1 in the iodixanol gradient. (1–14) Fractions 1–14 from the iodixanol gradient of cells transfected with wild-type *VP1* DNA only were analyzed by Western blotting using an antibody reactive against SV40 VP1. VP1 was found in fractions 7–10, matching the 33 % iodixanol portion of the gradient, indicating the formation of VLPs. (M) PageRuler Prestained Protein Ladder.

ing maintenance of the plasmid. However, the total quantity of pEGFP-C1 did drop over time. This drop is likely to be caused by the degradation of plasmids that did not achieve productive transfection. No drop in EGFP fluorescence was visible.

3.4. Proof of concept for directed evolution of VLPs in 293TT cells

To perform the proof of concept experiment shown in figure 2, a negative control for selection – a mutant *VP1* gene – was required. To prevent bias, the plasmid was kept mostly intact. We introduced a frameshift and a stop codon about a quarter into the gene, resulting in a truncated (9.9 kDa) form of VP1 (see figure 7). Moreover, the mutation also introduced a new restriction site (SpeI) into the gene, allowing us to distinguish the gene from wild-type *VP1* by gel electrophoresis after digestion. We confirmed that the mutant VP1 cannot form VLPs by demonstrating its inability to penetrate the iodixanol gradient during purification. We

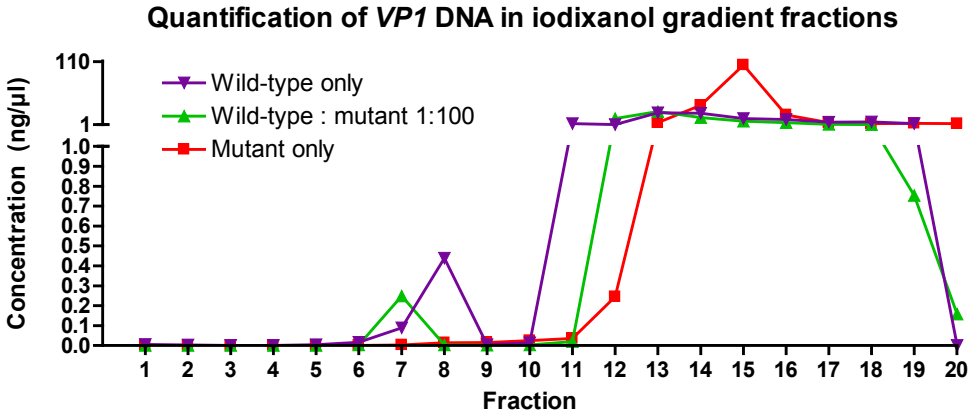

Figure 9. Quantification of *VP1* DNA in the iodixanol gradient fractions. *VP1* DNA was quantified by qPCR using primers specific for *VP1*. In the wild-type only samples, *VP1* DNA peaked in fractions 7–9, the same fractions that contained VLPs. A smaller *VP1* DNA peak was also observed in fraction 7 from the samples where wild-type *VP1* DNA had been mixed 1:100 with mutant *VP1* DNA. Fractions 11 and higher, which mainly represent the aqueous phase, contained non-encapsidated plasmid DNA.

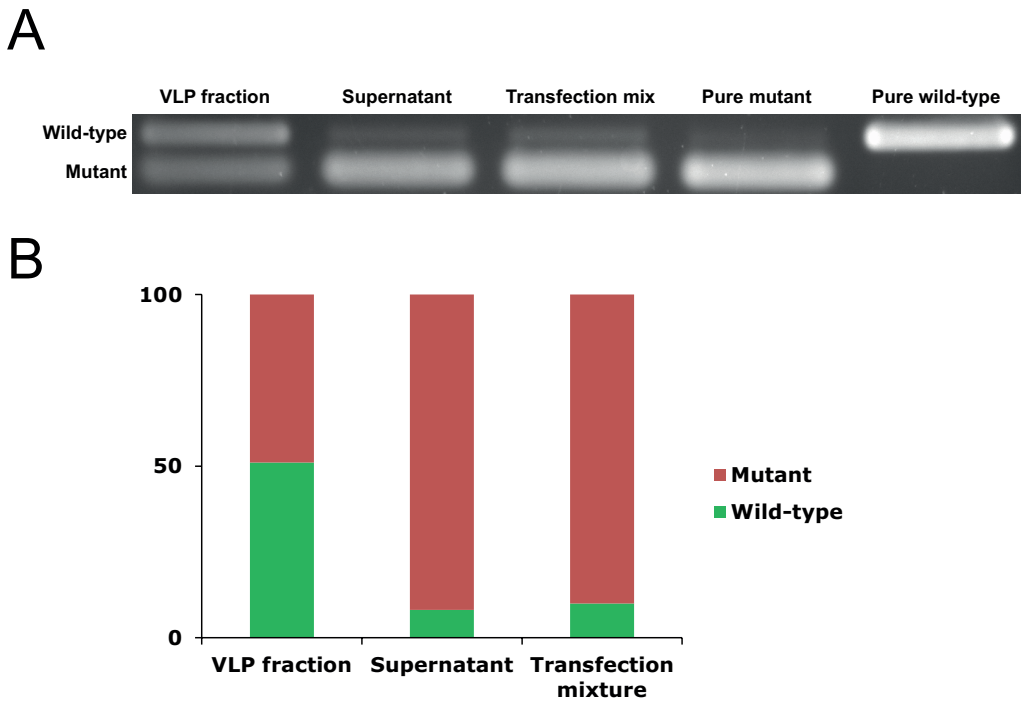

Figure 10. Enrichment of wild-type *VP1* genes from an excess of non-functional mutant *VP1* genes. 293TT cells were transfected with two types of plasmids, one encoding the wild-type SV40 VP1 protein, the other one a non-functional VP1 mutant. Both plasmids had the same size. Two days after transfection the cells were harvested and VLPs were purified by gradient ultracentrifugation. *VP1* DNA was extracted from the different fractions and amplified by PCR. Wild-type genes were distinguished from mutants by restriction analysis (A). The PCR primers were designed to yield two fragments of equal length for the mutant gene after digestion with SpeI, allowing direct comparison based on band intensity. The VLP fraction showed a 10-fold enrichment of wild-type *VP1* DNA compared to the original transfection mixture, while the residual supernatant did not show any enrichment (B). This proves that, by using this system, polyomavirus VLPs can selectively package their own coding DNA.

expect that the mutant can still bind DNA, as DNA binding is mediated by the N-terminus of SV40 VP1 [48].

The two vectors were mixed together at different ratios (see table 2) and used to transfect 293TT cells. Two days after transfection, VLPs were harvested from the cells by iodixanol gradient ultracentrifugation. Fractions were collected and analyzed for the presence of VP1 by Western blotting (see figure 8). VP1 was found in the 33 % iodixanol layer (fractions 7 through 10), consistent with previous results obtained with VLPs from other polyomaviruses [31]. VP1 was only observed in the gradient from cells that were transfected with the wild-type *VP1* gene only; the assay was not sensitive enough to demonstrate VP1 in the diluted samples. The mutant VP1 could not be detected with the used antibody.

Plasmid DNA was isolated from the fractions after protease digestion of the VLPs. The amount of *VP1* DNA in each fraction was quantified by qPCR (see figure 9). A peak in *VP1* DNA content was found in the same fractions that contained VLPs (see figure 8). This suggests that the plasmids were encapsidated by the VLPs. This peak was not only found in the wild-type only samples, but also in the samples where most of the wild-type DNA had been replaced with mutant DNA.

To confirm that these peaks contained wild-type *VP1* genes, and thus to demonstrate genotype-

phenotype linkage, the amplified DNA was digested with SpeI and analyzed by gel electrophoresis (see figure 10). The results clearly show the enrichment of the wild-type *VP1* gene from the excess of non-functional mutants. As the VLPs form, they package available genetic material compartmentalized within the same cell. This results in a 10-fold enrichment of the wild-type *VP1* gene after one single selection step, showing the potential of this system. This data shows that polyomavirus VLPs are able to package their own coding DNA after expression in 293TT cells, and can thus be used for directed evolution.

This system might benefit from the addition of the other structural proteins of the virus, VP2 and VP3. These proteins, derived from the same coding DNA sequence, are responsible for escape from the endoplasmic reticulum (ER) [49–51] and nuclear entry [52,53] after transfection. There is also some evidence of their involvement in DNA packaging [29,54]. Indeed, VLPs composed of all three structural proteins have been shown to possess improved transfection characteristics [55]. One possibility would be to add an expression vector encoding VP2 and VP3 during transfection. This vector should not be encapsidated by the VLPs, or lest it disturbs the genotype-phenotype linkage. This could be achieved by using a large (over 5.5 kb) vector without a functional *ses* sequence.

4. Conclusion

Virus-like particles derived from polyomaviruses are suitable candidates for gene delivery. We now show that these particles are also amenable to directed evolution to further improve their properties for gene therapy. We show that it is possible to recombine different polyomavirus *VP1* genes using DNA shuffling. This way, beneficial properties of the different polyomaviruses can be combined, and large evolutionary gaps can be bridged. We show that the binding domains are efficiently exchanged between the different viruses, allowing the creation of VLPs with novel tropism. For the expression of the library, we developed an efficient vector with a functional encapsidation signal. We also demonstrate that polyomavirus VP1 VLPs display genotype-phenotype linkage after expression in 293TT cells. The VLPs package their own coding DNA, making sure that the genetic origin of improved VLPs can be traced back after selection.

Together these results give the proof of concept for the directed evolution of VLPs derived from polyomaviruses. We are currently in the process of replicating these results. The next step would be to combine these two experiments, *i.e.* to perform selections with our library. The first selections might be based on VLP formation and DNA packaging. Once successful, more advanced selections, such as retargeting, could be performed. Ultimately, this technique could lead to novel viral vectors suitable for personalized medicine.

Acknowledgements

The authors would like to thank Paulien van Bentum for her helpful support in the preparation of the manuscript. This work was supported by Technologiestichting STW [budget number 10243]. This work has already been presented in part at the 16th Annual Meeting of the American Society of Gene & Cell Therapy [56] and the FIGON Dutch Medicines Days 2013.

References

1 Lanio, T., Jeltsch, A. and Pingoud, A. **On the possibilities and limitations of rational protein design to expand the specificity of restriction enzymes: a case study employing EcoRV as the target.** Protein Eng (2000) 13, 275–281.

2 Goldsmith, M. and Tawfik, D.S. **Directed enzyme evolution: beyond the low-hanging fruit.** Curr Opin Struct Biol (2012) 22, 406–412.

3 Dalby, P.A. **Strategy and success for the directed evolu-**

tion of enzymes. Curr Opin Struct Biol (2011) 21, 473–480.

4 Perabo, L. *et al.* **Combinatorial engineering of a gene therapy vector: directed evolution of adeno-associated virus.** J Gene Med (2006) 8, 155–162.

5 Maheshri, N. *et al.* **Directed evolution of adeno-associated virus yields enhanced gene delivery vectors.** Nat Biotechnol (2006) 24, 198–204.

6 Grimm, D. *et al.* ***In vitro* and *in vivo* gene therapy vector evolution via multispecies interbreeding and retargeting of adeno-associated viruses.** J Virol (2008) 82, 5887–5911.

7 Li, W. *et al.* **Generation of novel AAV variants by directed evolution for improved CFTR delivery to human ciliated airway epithelium.** Mol Ther (2009) 17, 2067–2077.

8 Yang, L. *et al.* **A myocardium tropic adeno-associated virus (AAV) evolved by DNA shuffling and *in vivo* selection.** Proc Natl Acad Sci U S A (2009) 106, 3946–3951.

9 Maguire, C.A. *et al.* **Directed evolution of adeno-associated virus for glioma cell transduction.** J Neurooncol (2010) 96, 337–347.

10 Asuri, P. *et al.* **Directed evolution of adeno-associated virus for enhanced gene delivery and gene targeting in human pluripotent stem cells.** Mol Ther (2012) 20, 329–338.

11 Dalkara, D. *et al.* ***In vivo*-directed evolution of a new adeno-associated virus for therapeutic outer retinal gene delivery from the vitreous.** Sci Transl Med (2013) 5, 189ra176.

12 Kuhn, I. *et al.* **Directed evolution generates a novel oncolytic virus for the treatment of colon cancer.** PLoS One (2008) 3, e2409.

13 Uil, T.G. *et al.* **Directed adenovirus evolution using engineered mutator viral polymerases.** Nucleic Acids Res (2011) 39, e30.

14 Soong, N.W. *et al.* **Molecular breeding of viruses.** Nat Genet (2000) 25, 436–439.

15 Powell, S.K. *et al.* **Breeding of retroviruses by DNA shuffling for improved stability and processing yields.** Nat Biotechnol (2000) 18, 1279–1282.

16 Bupp, K. and Roth, M.J. **Altering retroviral tropism using a random-display envelope library.** Mol Ther (2002) 5, 329–335.

17 Bupp, K. and Roth, M.J. **Targeting a retroviral vector in the absence of a known cell-targeting ligand.** Hum Gene Ther (2003) 14, 1557–1564.

18 Lin, T.Y. *et al.* **A novel approach for the rapid mutagenesis and directed evolution of the structural genes of west nile virus.** J Virol (2012) 86, 3501–3512.

19 Teunissen, E.A., de Raad, M. and Mastrobattista, E. **Production and biomedical applications of virus-like particles derived from polyomaviruses.** J Control Release (2013) 172, 305–321.

20 Salunke, D.M., Caspar, D.L. and Garcea, R.L. **Self-assembly of purified polyomavirus capsid protein VP1.** Cell (1986) 46, 895–904.

21 Pawlita, M. *et al.* **DNA encapsidation by viruslike particles assembled in insect cells from the major capsid protein VP1 of B-lymphotropic papovavirus.** J Virol (1996) 70, 7517–7526.

22 Teunissen, E.A. *et al.* **Assembly of hamster polyomavirus VP1 into virus-like particles takes place in *Escherichia coli* but not after cell-free synthesis.** Manuscript in preparation (2014).

23 Moreland, R.B., Montross, L. and Garcea, R.L. **Characterization of the DNA-binding properties of the polyomavirus capsid protein VP1.** J Virol (1991) 65, 1168–1176.

24 Voronkova, T. *et al.* **Hamster polyomavirus-derived virus-like particles are able to transfer *in vitro* encapsidated plasmid DNA to mammalian cells.** Virus Genes (2007) 34, 303–314.

25 Kimchi-Sarfaty, C. *et al.* **Transduction of multiple cell types using improved conditions for gene delivery and expression of SV40 pseudovirions packaged *in vitro*.** Biotechniques (2004) 37, 270–275.

26 Gedvilaite, A. *et al.* **Segments of puumala hantavirus nucleocapsid protein inserted into chimeric polyomavirus-derived virus-like particles induce a strong immune response in mice.** Viral Immunol (2004) 17, 51–68.

27 Oppenheim, A. *et al.* **A cis-acting DNA signal for encapsidation of simian virus 40.** J Virol (1992) 66, 5320–5328.

28 Dalyot-Herman, N. *et al.* **The simian virus 40 packaging signal ses is composed of redundant DNA elements which are partly interchangeable.** J Mol Biol (1996) 259, 69–80.

29 Gordon-Shaag, A. *et al.* **Cellular transcription factor Sp1 recruits simian virus 40 capsid proteins to the viral packaging signal, *ses*.** J Virol (2002) 76, 5915–5924.

30 Buck, C.B. *et al.* **Efficient intracellular assembly of papillomaviral vectors.** J Virol (2004) 78, 751–757.

31 Tolstov, Y.L. *et al.* **Human Merkel cell polyomavirus infection II. MCV is a common human infection that can be detected by conformational capsid epitope immunoassays.** Int J Cancer (2009) 125, 1250–1256.

32 Pastrana, D.V. *et al.* **Quantitation of human seroresponsiveness to Merkel cell polyomavirus.** PLoS Pathog (2009) 5, e1000578.

33 Stemmer, W.P. **Rapid evolution of a protein *in vitro* by DNA shuffling.** Nature (1994) 370, 389–391.

34 Crameri, A. *et al.* **DNA shuffling of a family of genes from diverse species accelerates directed evolution.** Nature (1998) 391, 288–291.

35 Larkin, M.A. *et al.* **Clustal W and Clustal X version 2.0.** Bioinformatics (2007) 23, 2947–2948.

36 Mastrobattista, E. *et al.* **High-throughput screening of enzyme libraries: *in vitro* evolution of a beta-galactosidase by fluorescence-activated sorting of double emulsions.** Chem Biol (2005) 12, 1291–1300.

37 Teunissen, E.A. *et al.* **Different proteins require different S30 extract protein concentrations for optimal expression.** Manuscript in preparation (2014).

38 Richardson, S.M. *et al.* **GeneDesign: rapid, automated design of multikilobase synthetic genes.** Genome Res (2006) 16, 550–556.

39 Stemmer, W.P. **DNA shuffling by random fragmentation and reassembly: *in vitro* recombination for molecular evolution.** Proc Natl Acad Sci U S A (1994) 91, 10747–10751.

40 Moore, G.L. *et al.* **Predicting crossover generation in DNA shuffling.** Proc Natl Acad Sci U S A (2001) 98, 3226–3231.

41 Zhao, H. and Arnold, F.H. **Optimization of DNA shuffling for high fidelity recombination.** Nucleic Acids Res (1997) 25, 1307–1308.

42 Stehle, T. *et al.* **Structure of murine polyomavirus complexed with an oligosaccharide receptor fragment.** Nature (1994) 369, 160–163.

43 Stehle, T. and Harrison, S.C. **Crystal structures of murine polyomavirus in complex with straight-chain and branched-chain sialyloligosaccharide receptor fragments.** Structure (1996) 4, 183–194.

44 Neu, U. *et al.* **Structure-function analysis of the human JC polyomavirus establishes the LSTc pentasaccharide as a functional receptor motif.** Cell Host Microbe (2010) 8, 309–319.

45 Langner, J. *et al.* **RGD-mutants of B-lymphotropic polyomavirus capsids specifically bind to alpha(v)beta3 integrin.** Arch Virol (2004) 149, 1877–1896.

46 Cirino, P.C., Mayer, K.M. and Umeno, D. **Generating mutant libraries using error-prone PCR.** In: Directed Evolution Library Creation: Methods and Protocols (eds Frances H. Arnold and George Georgiou) 3–9 (Springer, 2003).

47 Coco, W.M. *et al.* **DNA shuffling method for generating highly recombined genes and evolved enzymes.** Nat Biotechnol (2001) 19, 354–359.

48 Li, P.P. *et al.* **Simian virus 40 Vp1 DNA-binding domain is functionally separable from the overlapping nuclear localization signal and is required for effective virion formation and full viability.** J Virol (2001) 75, 7321–7329.

49 Daniels, R. *et al.* **SV40 VP2 and VP3 insertion into ER membranes is controlled by the capsid protein VP1: implications for DNA translocation out of the ER.** Mol Cell (2006) 24, 955–966.

50 Kuksin, D. and Norkin, L.C. **Disassembly of simian virus 40 during passage through the endoplasmic reticulum and in the cytoplasm.** J Virol (2012) 86, 1555–1562.

51 Rainey-Barger, E.K., Magnuson, B. and Tsai, B. **A chaperone-activated nonenveloped virus perforates the physiologically relevant endoplasmic reticulum membrane.** J Virol (2007) 81, 12996–13004.

52 Nakanishi, A. *et al.* **Minor capsid proteins of simian virus 40 are dispensable for nucleocapsid assembly and cell entry but are required for nuclear entry of the viral genome.** J Virol (2007) 81, 3778–3785.

53 Nakanishi, A. *et al.* **Interaction of the Vp3 nuclear localization signal with the importin alpha 2/beta heterodimer directs nuclear entry of infecting simian virus 40.** J Virol (2002) 76, 9368–9377.

54 Melucci-Vigo, G., Magnusson, G. and Risuleo, G. **Mouse polyomavirus late region mutants expressing a defective VP2 capsid protein exhibit an enhanced viral DNA replication.** Virus Genes (1994) 8, 137–141.

55 Enomoto, T. *et al.* ***In vitro* reconstitution of SV40 particles that are composed of VP1/2/3 capsid proteins and nucleosomal DNA and direct efficient gene transfer.** Virology (2011) 420, 1–9.

56 Teunissen, E.A. *et al.* **Directed evolution of artificial viruses.** In: 16th Annual Meeting of the American Society of Gene & Cell Therapy Vol. 21 e18–e19 (Molecular Therapy, Salt Lake City, Utah, 2013).

Table S1. Properties of the different polyomaviruses listed in the RefSeq database (as of 2011). VLP formation is taken from **chapter 2.**

Abbreviation	Name	Genome length (bp)	Genome accession number	VP1 length (aa)	VP1 accession number	Forms VLPs after expression in			
						Bacteria	Yeast	Insect cells	Mammalian cells
APyV	Avian polyomavirus (Budgerigar fledgling disease polyomavirus)	4981	NC_004764.2	343	YP_004061428.1	Yes [1]	Yes [2]	Yes [3]	Yes [4]
BKPyV	BK polyomavirus	5153	NC_001538.1	362	YP_717939.1		Yes [2,5]	Yes [6]	Yes [7]
BPyV	Bovine polyomavirus	4697	NC_001442.1	365	NP_040787.1				
ChPyV	Chimpanzee polyomavirus	5086	NC_014743.1	497	YP_004046682.1		Yes [8]		
CPyV	Crow polyomavirus	5079	NC_007922.1	353	YP_529827.1		Yes [9]		
CSLPyV	California sea lion polyomavirus 1	5112	NC_013796.1	495	YP_003429322.1				
FPyV	Finch polyomavirus	5278	NC_007923.1	358	YP_529833.1		Yes [9]		
GHPyV	Goose hemorrhagic polyomavirus	5256	NC_004800.1	353	NP_849169.1		Yes [10]	Yes [10]	
HaPyV	Hamster polyomavirus	5366	NC_001663.1	372	NP_056733.1	Yes [11]	Yes [12]	Yes [11]	
HPyV6	Polyomavirus HPyV6	4926	NC_014406.1	387	YP_003848918.1			Yes [13]	
HPyV7	Polyomavirus HPyV7	4952	NC_014407.1	380	YP_003848923.1			Yes [13]	
HPyV9	Human polyomavirus 9	5026	NC_015150.1	371	YP_004243705.1			Yes [14]	
JCPyV	JC polyomavirus	5130	NC_001699.1	354	NP_043511.1	Yes [15]	Yes [16]	Yes [17]	Yes [18]
KIPyV	KI polyomavirus	5040	NC_009238.1	378	YP_001111258.1				
LPyV	African green monkey polyomavirus	5270	NC_004763.2	368	NP_848007.2			Yes [19]	
MCPyV	Merkel cell polyomavirus	5387	NC_010277.1	423	YP_001651048.1			Yes [20]	Yes [21]
MPtV	Murine pneumotropic virus	4754	NC_001505.2	373	NP_041234.1			Yes [22]	
MPyV	Murine polyomavirus	5297	NC_001515.1	383	NP_041267.1	Yes [23]	Yes [2]	Yes [24,25]	Yes [21]
MyPyV	Myotis polyomavirus VM-2008	5081	NC_011310.1	357	YP_002261488.1				
OraPyV	Orangutan polyomavirus	5168	NC_013439.1	366	YP_003264533.1				
SA12	Simian virus 12	5230	NC_007611.1	364	YP_406554.1				
SqPyV	Squirrel monkey polyomavirus	5075	NC_009951.1	357	YP_001531348.1				
SV40	Simian virus 40	5243	NC_001669.1	364	YP_003708381.1	Yes [26]	Yes [2]	Yes [27]	
TSPyV	Trichodysplasia spinulosa-associated polyomavirus	5232	NC_014361.1	375	YP_003800006.1			Yes [28]	
WUPyV	WU Polyomavirus	5229	NC_009539.1	369	YP_001285487.1				

1 Rodgers, R.E. *et al.* **Purification of recombinant budgerigar fledgling disease virus VP1 capsid protein and its ability for *in vitro* capsid assembly.** J Virol (1994) 68, 3386–3390.

2 Sasnauskas, K. *et al.* **Generation of recombinant virus-like particles of human and non-human polyomaviruses in yeast *Saccharomyces cerevisiae*.** Intervirology (2002) 45, 308–317.

3 An, K. *et al.* **Avian polyomavirus major capsid protein VP1 interacts with the minor capsid proteins and is transported into the cell nucleus but does not assemble into capsid-like particles when expressed in the baculovirus system.** Virus Res (1999) 64, 173–185.

4 Johne, R. and Muller, H. **Nuclear localization of avian polyomavirus structural protein VP1 is a prerequisite for the formation of virus-like particles.** J Virol (2004) 78, 930–937.

5 Hale, A.D. *et al.* **Expression and antigenic characterization of the major capsid proteins of human polyomaviruses BK and JC in *Saccharomyces cerevisiae*.** J Virol Methods (2002) 104, 93–98.

6 Touze, A. *et al.* **Gene transfer using human polyomavirus BK virus-like particles expressed in insect cells.** J Gen Virol (2001) 82, 3005–3009.

7 Pastrana, D.V. *et al.* **Quantitation of human seroresponsiveness to Merkel cell polyomavirus.** PLoS Pathog (2009) 5, e1000578.

8 Zielonka, A. *et al.* **Detection of chimpanzee polyomavirus-specific antibodies in captive and wild-caught chimpanzees using yeast-expressed virus-like particles.** Virus Res (2011) 155, 514–519.

9 Zielonka, A. *et al.* **Serological cross-reactions between four polyomaviruses of birds using virus-like particles expressed in yeast.** J Gen Virol (2012) 93, 2658–2667.

10 Zielonka, A. *et al.* **Generation of virus-like particles consisting of the major capsid protein VP1 of goose hemorrhagic polyomavirus and their application in serological tests.** Virus Res (2006) 120, 128–137.

11 Voronkova, T. *et al.* **Hamster polyomavirus-derived virus-like particles are able to transfer *in vitro* encapsidated plasmid DNA to mammalian cells.** Virus Genes (2007) 34, 303–314.

12 Sasnauskas, K. *et al.* **Yeast cells allow high-level expression and formation of polyomavirus-like particles.** Biol Chem (1999) 380, 381–386.

13 Nicol, J.T. *et al.* **Age-specific seroprevalences of merkel cell polyomavirus, human polyomaviruses 6, 7, and 9, and trichodysplasia spinulosa-associated polyomavirus.** Clin Vaccine Immunol (2013) 20, 363–368.

14 Nicol, J.T. *et al.* **Seroprevalence and cross-reactivity of human polyomavirus 9.** Emerg Infect Dis (2012) 18, 1329–1332.

15 Ou, W.C. *et al.* **The major capsid protein, VP1, of human JC virus expressed in *Escherichia coli* is able to self-assemble into a capsid-like particle and deliver exogenous DNA into human kidney cells.** J Gen Virol (1999) 80 (Pt 1), 39–46.

16 Chen, P.L. *et al.* **Disulfide bonds stabilize JC virus capsid-like structure by protecting calcium ions from chelation.** FEBS Lett (2001) 500, 109–113.

17 Chang, D. *et al.* **Self-assembly of the JC virus major capsid protein, VP1, expressed in insect cells.** J Gen Virol (1997) 78 (Pt 6), 1435–1439.

18 Shishido, Y. *et al.* **Assembly of JC virus-like particles in COS7 cells.** J Med Virol (1997) 51, 265–272.

19 Pawlita, M. *et al.* **DNA encapsidation by viruslike particles assembled in insect cells from the major capsid protein VP1 of B-lymphotropic papovavirus.** J Virol (1996) 70, 7517–7526.

20 Touze, A. *et al.* **Generation of Merkel cell polyomavirus (MCV)-like particles and their application to detection of MCV antibodies.** J Clin Microbiol (2010) 48, 1767–1770.

21 Tolstov, Y.L. *et al.* **Human Merkel cell polyomavirus infection II. MCV is a common human infection that can be detected by conformational capsid epitope immunoassays.** Int J Cancer (2009) 125, 1250–1256.

22 Tegerstedt, K. *et al.* **Murine pneumotropic virus VP1 virus-like particles (VLPs) bind to several cell types independent of sialic acid residues and do not serologically cross react with murine polyomavirus VP1 VLPs.** J Gen Virol (2003) 84, 3443–3452.

23 Salunke, D.M., Caspar, D.L. and Garcea, R.L. **Self-assembly of purified polyomavirus capsid protein VP1.** Cell (1986) 46, 895–904.

24 Montross, L. *et al.* **Nuclear assembly of polyomavirus capsids in insect cells expressing the major capsid protein VP1.** J Virol (1991) 65, 4991–4998.

25 Gillock, E.T. *et al.* **Polyomavirus major capsid protein VP1 is capable of packaging cellular DNA when expressed in the baculovirus system.** J Virol (1997) 71, 2857–2865.

26 Wrobel, B. *et al.* **Production and purification of SV40 major capsid protein (VP1) in *Escherichia coli* strains deficient for the GroELS chaperone machine.** J Biotechnol (2000) 84, 285–289.

27 Kosukegawa, A. *et al.* **Purification and characterization of virus-like particles and pentamers produced by the expression of SV40 capsid proteins in insect cells.** Biochim Biophys Acta (1996) 1290, 37–45.

28 Kumar, A. *et al.* **Trichodysplasia spinulosa-associated polyomavirus (TSV) and Merkel cell polyomavirus: correlation between humoral and cellular immunity stronger with TSV.** PLoS One (2012) 7, e45773.

Table S2. Homology between the polyomavirus VP1 proteins. The VP1 protein sequences were obtained from the RefSeq database. The VP1 protein sequences were aligned using ClustalW2 (pairwise alignment). The scores represent the total homology in percent over the full length of the VP1 proteins.

	MyPyV	MCPyV	SqPyV	WUPyV	KIPyV	FPyV	CPyV	SA12	MPyV	JCPyV	LPyV	HaPyV	GHPyV	APyV	BKPyV	MPtV	SV40	BPyV	HPyV9	ChPyV	HPyV6	HPyV7	TSPyV	CSLPyV	OraPyV
MyPyV		59	60	24	24	60	59	55	55	55	61	54	62	58	52	67	54	57	59	53	27	26	63	60	58
MCPyV	59		53	27	23	55	55	48	52	48	59	55	55	52	48	46	49	51	59	51	27	27	57	44	53
SqPyV	60	53		27	24	52	56	51	50	49	55	49	58	49	50	56	52	55	54	53	26	25	56	54	56
WUPyV	24	27	27		67	29	27	26	26	29	28	25	27	29	26	24	27	25	28	26	35	37	23	27	24
KIPyV	24	23	24	67		27	26	26	26	28	25	22	25	27	27	23	26	25	25	26	35	34	22	28	24
FPyV	60	55	52	29	27		60	55	55	55	57	55	63	73	55	52	56	53	58	56	28	27	59	56	59
CPyV	59	55	56	27	26	60		57	55	55	62	53	71	57	54	54	56	58	62	56	26	27	56	59	56
SA12	55	48	51	26	26	55	57		51	81	54	47	58	53	83	49	79	47	55	50	24	26	55	51	55
MPyV	55	52	50	26	26	55	55	51		52	55	58	56	50	51	47	52	53	55	50	25	24	56	51	55
JCPyV	55	48	49	29	28	55	55	81	52		55	51	56	53	80	49	77	50	55	49	26	25	52	54	52
LPyV	61	59	55	28	25	57	62	54	55	55		56	60	55	54	51	53	53	87	56	27	27	59	54	57
HaPyV	54	55	49	25	22	55	53	47	58	51	56		54	50	46	45	47	49	56	51	25	23	52	51	53
GHPyV	62	55	58	27	25	63	71	58	56	56	60	54		60	54	54	56	59	59	56	26	27	61	60	59
APyV	58	52	49	29	27	73	57	53	50	53	55	50	60		51	53	52	50	55	53	27	27	56	54	55
BKPyV	52	48	50	26	27	55	54	83	51	80	54	46	54	51		47	82	48	54	51	25	25	54	51	54
MPtV	67	46	56	24	23	52	54	49	47	49	51	45	54	53	47		47	49	49	44	24	24	53	51	52
SV40	54	49	52	27	26	56	56	79	52	77	53	47	56	52	82	47		50	54	49	23	26	55	52	55
BPyV	57	51	55	25	25	53	58	47	53	50	53	49	59	50	48	49	50		52	53	27	25	56	59	55
HPyV9	59	59	54	28	25	58	62	55	55	55	87	56	59	55	54	49	54	52		60	25	25	61	55	60
ChPyV	53	51	53	26	26	56	56	50	50	49	56	51	56	53	51	44	49	53	60		24	28	58	41	59
HPyV6	27	27	26	35	35	28	26	24	25	26	27	25	26	27	25	24	23	27	25	24		69	25	22	25
HPyV7	26	27	25	37	34	27	27	26	24	25	27	23	27	27	25	24	26	25	25	28	69		26	23	25
TSPyV	63	57	56	23	22	59	56	55	56	52	59	52	61	56	54	53	55	56	61	58	25	26		55	80
CSLPyV	60	44	54	27	28	56	59	51	51	54	54	51	60	54	51	51	52	59	55	41	22	23	55		55
OraPyV	58	53	56	24	24	59	56	55	55	52	57	53	59	55	54	52	55	55	60	59	25	25	80	55	

Chapter VII

Detection of virus-like particles in serum by transmission electron microscopy and nanoparticle tracking analysis

Erik A. Teunissen[1], Markus de Raad[1] and Enrico Mastrobattista[1]
[1]Department of Pharmaceutics, Utrecht Institute for Pharmaceutical Sciences, Faculty of Science, Utrecht University, Universiteitsweg 99, 3584 CG Utrecht, The Netherlands

Abstract

The small size and low intrinsic contrast of virus-like particles make it difficult to study their behavior in cells and their stability in biological fluids using conventional methods. In this chapter we explored two alternative approaches to study model virus-like particles derived from hamster polyomavirus VP1. First, we used a clonable tag based on murine metallothionein, which is capable of binding heavy metal ions and providing additional contrast for transmission electron microscopy. We inserted this tag into surface-exposed loops of VP1. Although the insertion of the tag did not reduce the yield of prokaryotic expression of VP1, it completely abolished VLP formation. Second, we used a technique called nanoparticle tracking analysis for the detection of virus-like particles. Using a NanoSight instrument, we were able to measure the particle size distribution of virus-like particles. By using fluorescently labeled virus-like particles, we could detect these particles in a background of serum, which, under normal conditions, completely obscured detection.

1. Introduction

Virus-like particles (VLPs) are assemblies of viral structural proteins, resembling the native virus, but lacking viral nucleic acids. These particles are promising agents for gene delivery. They are non-replicating and thus safer to use than viral vectors. Moreover, their regular structure allows them to induce potent B and T cell responses towards epitopes displayed on their surface. One class of promising VLPs is those derived from polyomavirus VP1 proteins [1]. Polyomavirus VLPs spontaneously form after overexpression of the major coat protein VP1, with 360 VP1 proteins forming a 40–45 nm icosahedral capsid. This size is appropriate for applications such as gene delivery [2], tumor targeting [3], or for the uptake of antigens by dendritic cells [4]. However, this small size also makes it difficult to investigate their stability in biological environments and their behavior inside cells. The stability of gene delivery vectors in biological fluids is important, as the rapid clearance of vectors by the mononuclear phagocyte system, aided by the binding of the vectors to blood components, is one of the major challenges of gene delivery [2]. Also, the entry of the VLPs into cells, and their intracellular fate, are still not completely understood [5]. The low intrinsic contrast of VLPs makes them difficult to track inside cells by transmission electron microscopy (TEM), which generally still relies on negative staining or immunogold labeling for contrast [6,7].

In this chapter we investigated two alternative approaches to study VLPs in biological environments. In the first approach, we used a clonable contrasting tag for visualization with TEM based on the murine metallothionein-I (MT) protein. This protein is capable of binding heavy metal ions through the thiol groups of its 20 cysteine residues. The resulting metal clusters are easily detectable by TEM [8]. By fusing the tag to a target protein, it can be visualized and tracked by TEM [9–13], even in intact cells [14], analogous to the fusion with green fluorescent protein (GFP) for light microscopy.

The second approach employed a technique called nanoparticle tracking analysis (NTA). This technique is based on the correlation between the average velocity at which particles travel due to Brownian motion and the sphere-equivalent hydrodynamic diameter, given by the Stokes-Einstein equation, and yields the particle size distribution [15]. A laser is used to illuminate particles in suspension, and scattered light is captured using a camera coupled to a conventional light microscope. Video is recorded and analyzed by NTA software, tracking the motion of individual particles. In contrast to dynamic light scattering (DLS), individual particles are measured using NTA, reducing the bias introduced by large particles and making it possible to analyze heterogeneous and

polydisperse samples [16]. NTA has been used for the detection and quantification of many kinds of nanoparticles, including viruses [17–20] and VLPs [21,22]. It can be operated in two modes, normal and fluorescence. In the normal mode, all scattering is detected. While this is practical for quantification of purified samples, this is unusable for the study of VLPs in biological fluids due to the high amount of background scattering. The fluorescence mode, on the other hand, can be used to specifically detect labeled particles [23]. By labeling the VLPs with a fluorescent dye, these particles can be distinguished from other nano-sized particles in a complex biological environment.

2. Materials and methods

2.1. Chemicals

Ammonium chloride, ampicillin, bovine serum albumin (BSA), bromophenol blue, calcium chloride, cesium chloride, dimethyl sulfoxide (DMSO), glycerol, isopropyl β-D-1-thiogalactopyranoside (IPTG), kanamycin, LB agar, LB broth culture medium, 2-mercaptoethanol, polysorbate 20 (TWEEN® 20), sodium dodecyl sulfate (SDS), and tris(hydroxymethyl)aminomethane (Tris) were purchased from Sigma-Aldrich (St. Louis, MO, USA). Ethylenediaminetetraacetic acid (EDTA) and sodium bicarbonate were purchased from Acros Organics (Geel, Belgium). PageBlue Protein Staining Solution, PageRuler Prestained Protein Ladder, and DNA-modifying enzymes were purchased from Thermo Scientific (Waltham, MA, USA). Fetal bovine serum (FBS) was purchased from PAA Laboratories (Pasching, Austria). Phosphate buffered saline (PBS) was purchased from B. Braun Melsungen AG (Melsungen, Germany). Hydrochloric acid, sodium chloride, sodium hydroxide, and sucrose were purchased from Merck KGaA (Darmstadt, Germany). Uranyl acetate was purchased from Electron Microscopy Sciences (Hatfield, PA, USA). Tetramethylrhodamine-5-isothiocyanate (TRITC) was purchased from Life Technologies (Carlsbad, CA, USA).

2.2. Plasmids

The cloning and preparation of plasmid pIVEX-HaPyV-VP1/co, containing the wild-type *VP1* gene from the hamster polyomavirus (HaPyV) codon-optimized for expression in *E. coli*, has been described before [24]. The plasmids pIVEX-HaPyV-VP1/MT1 and pIVEX-HaPyV-VP1/MT4, which contain the HaPyV *VP1* gene with the amino acids at site 1 (81–88) and site 4 (289–294), respectively, replaced with a metallothionein-tag, were prepared similar to pIVEX-HaPyV-VP1/co [24]. Briefly, the VP1 protein sequence and location of the variable loops were obtained from Gedvilaite *et al.* [25]. The MT-tag sequence was derived from pMAL-c2x-MT1 [10], and consists of the full-length murine metallothionein-1 gene (RefSeq: NP_038630). The variable loops were completely replaced with the MT-tag sequence. The resulting sequences were reverse translated and codon-optimized for expression in *E. coli* using GeneDesign [26]. Flanking sequences were added to create an NcoI restriction site overlapping the start codon and an XhoI restriction site directly adjacent to the stop codon. The genes were synthesized by GenScript (Piscataway, NJ, USA) and delivered in a pUC57 vector. The genes were excised from pUC57 using NcoI and XhoI, and cloned into pIVEX2.2EM [27] digested with the same enzymes.

2.3. Production of virus-like particles

HaPyV VLPs were produced and purified as described before [28]. Briefly, *E. coli* BL21(DE3)pREP4 were transformed with pIVEX-HaPyV-VP1/co, pIVEX-HaPyV-VP1/MT1, or pIVEX-HaPyV-VP1/MT4 for the production of wild-type, MT1- or MT4-VLPs, respectively. Individual colonies were grown in LB medium at 37 °C. VP1 expression was induced at an OD600 of 0.8 by adding IPTG to a final concen-

tration of 1.0 mM. Protein expression was allowed to continue overnight at 37 °C. Afterwards, the bacteria were harvested by centrifugation at 5,000 g at 4 °C for 15 min. The bacteria were washed once in reassembly buffer (10 mM Tris-HCl (pH 7.2), 1.0 M sodium chloride and 1.0 mM calcium chloride in demineralized water), followed by thorough resuspension in 20 volumes of reassembly buffer. The bacteria were lysed by two passes through an EmulsiFlex-C5 high pressure homogenizer (AVESTIN; Ottawa, ON, Canada) at >15,000 psi. VLPs were purified by sequential ultracentrifugation. The lysates were first cleared by centrifugation at 6,000 g at 4 °C for 30 min. VLPs in the supernatant were pelleted through a layer of 60 % w/v sucrose in reassembly buffer for 20 hours at 75,400 g at 4 °C. The pellets were resuspended in 1 ml reassembly buffer per 25 ml lysate. Cesium chloride was added to a final density of 1.30 g/cm^3, and the samples were centrifuged in an SW 41 Ti rotor (Beckman Coulter; Brea, CA, USA) at 40,000 RPM at 4 °C for 70 hours to allow a gradient to form. Afterwards, the tubes were carefully removed and 1 ml fractions were taken by puncturing the bottom of the tubes with a needle and collecting the drops. The fractions were checked for VP1 by reducing SDS-PAGE, and fractions containing VP1 were dialyzed 4 times against 50 volumes of reassembly buffer using Slide-A-Lyzer membrane cassettes (Thermo Scientific) with a MWCO of 20 kDa. After purification, protein concentrations of pure samples were determined using the Pierce™ Micro BCA Protein Assay Kit (Thermo Scientific) according to the manufacturer's protocol.

2.4. SDS-PAGE and Western blotting

SDS-PAGE and Western blotting were performed as before [24] with the following modifications. In addition to the samples, 5 µl PageRuler Prestained Protein Ladder was included on each gel. For SDS-PAGE, the gels were stained with PageBlue Protein Staining Solution according to the manufacturer's protocol using a microwave oven.

2.5. Transmission electron microscopy

Negative staining was performed as described before [29]. Briefly, samples were diluted 10–100 times in demineralized water, and 25 µl of each diluted sample was pipetted onto parafilm. Glow-discharged formvar/carbon-coated copper grids (Agar Scientific; Stansted, United Kingdom) were placed on top of the droplets for 2 min. After incubation, the grids were taken and excess liquid was removed by carefully touching filter paper. Next, the grids were placed on top of 20 µl 2 % uranyl acetate droplets for 2 min. After incubation, the grids were taken and excess liquid was again removed. The grids were dried at room temperature for 5 min before measurement. Transmission electron microscopy (TEM) imaging was performed using a Philips Tecnai 10 at 100 kV.

2.6. Hemagglutination assay

Red blood cells (RBCs) were collected by centrifugation at 100 g for 5 min from mouse blood pretreated with potassium EDTA (SARSTEDT; Nümbrecht, Germany) to prevent clotting. The pellet was washed three times by resuspending in 20 volumes of PBS and centrifuging at 100 g for 5 min. The final pellet was resuspended in 100 volumes of PBS to create a 1.0 % RBC suspension. Samples were serially diluted in PBS and 50 µl of each diluted sample was added to a round-bottom 96-well plate. To each well, 50 µl of a 0.5 % or 1.0 % RBC suspension in PBS was added. The plate was incubated at room temperature for 60 min, after which pictures were taken.

2.7. Labeling of virus-like particles for NTA

Wild-type HaPyV VLPs were diluted in 0.10 M sodium bicarbonate (pH 9.0) to a final concentration of 2.0 mg/ml. The VLPs were dialyzed against 1000 volumes of 0.10 M sodium bicarbonate (pH 9.0) at 4 °C using Slide-A-Lyzer membrane cassettes

with a MWCO of 10 kDa. The samples were first dialyzed for 3 hours, and after refreshing the buffer, the samples were dialyzed for another 60 hours at 4 °C. TRITC (1.0 mg/ml), freshly dissolved in dry DMSO, was added to the dialyzed VLPs to a final concentration of 50 µg/ml. The reaction was incubated in the dark at 4 °C for 40 hours. The labeled VLPs were checked by TEM and NTA.

2.8. Labeling of antibodies for NTA

Fifty microliters of 1.5 mg/ml mouse-anti-HaPyV-VP1 (ab34755; Abcam; Cambridge, United Kingdom) was dialyzed against 200 ml 0.10 M sodium bicarbonate (pH 9.0) at 4 °C using a Slide-A-Lyzer MINI Dialysis Device (Thermo Scientific) with a MWCO of 10 kDa. The antibodies were first dialyzed for 3 hours, and after refreshing the buffer, the antibodies were dialyzed for another 60 hours at 4 °C. TRITC (1.0 mg/ml), freshly dissolved in dry DMSO, was added to the dialyzed antibodies to a final concentration of 50 µg/ml. The reaction was incubated in the dark at 4 °C for 40 hours. The reaction was stopped by adding ammonium chloride to a final concentration of 50 mM.

2.9. Nanoparticle tracking analysis

NTA measurements were performed using a NanoSight LM10 (NanoSight; Amesbury, UK), equipped with a 532 nm green laser, 565 nm cut-off emission filter, Andor electron-multiplying charged coupled device (EMCCD) camera, and LM14 sample viewing unit. Samples were diluted 500 to 50,000 times in PBS filtered using 0.02 µm syringe filters (Whatman; GE Healthcare, Little Chalfont, United Kingdom) before measurement. To some samples, FBS was added to a final concentration of 10 % v/v. Videos of 60 to 300 seconds were recorded and analyzed using the NTA 2.3 Analytical software, build 0011 RC1.

2.10. Protein modeling

All 3D models were predicted using the SWISS-MODEL server at ExPASy in Automated Mode [30].

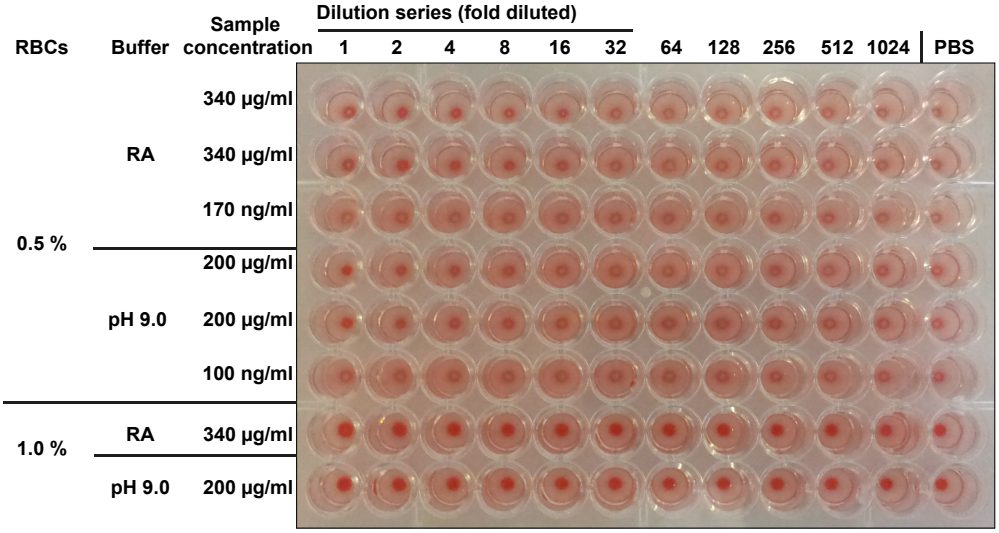

Figure 1. Hemagglutination assay. Wild-type HaPyV VLPs stored in different buffers were serially diluted in PBS from stock solutions of indicated concentrations. Next, an equal volume of 0.5 % or 1.0 % RBCs was added. Hemagglutination was assessed 60 minutes after the addition of murine RBCs. No hemagglutination was observed. RA, reassembly buffer; pH 9.0, 0.10 M sodium bicarbonate (pH 9.0).

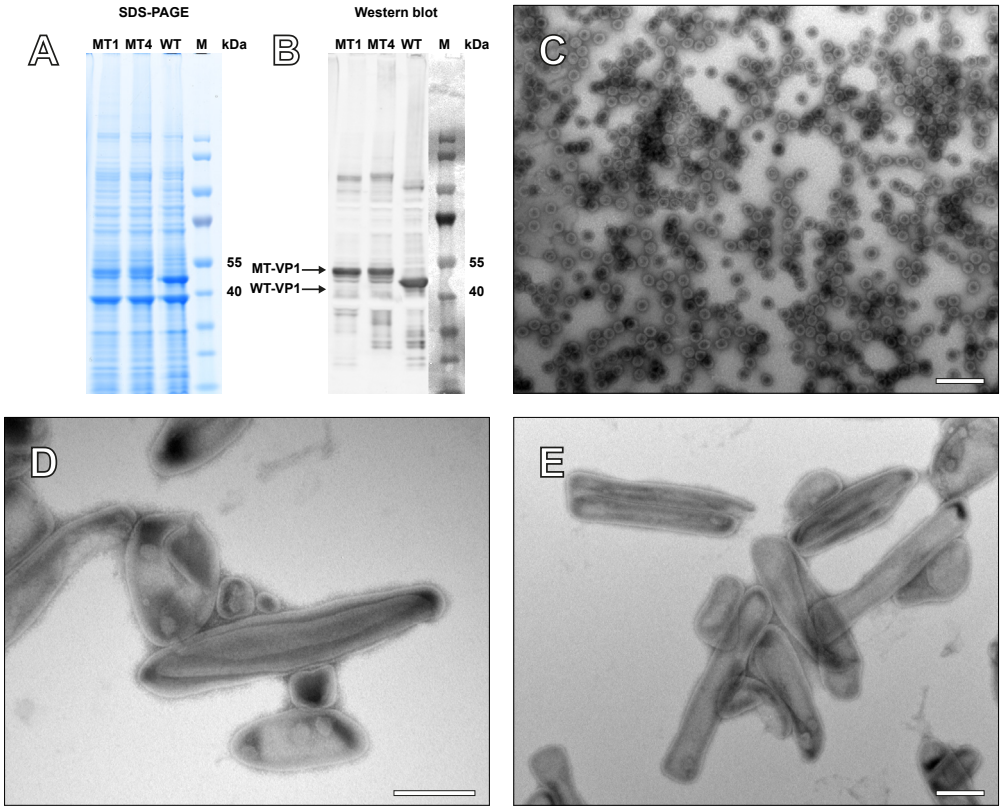

Figure 2. Production of VP1 in bacteria and purification of VLPs by sequential ultracentrifugation. VP1 was overexpressed in *E. coli* BL21(DE3)pREP4 and partially purified by pelleting through a sucrose layer. (a) SDS-PAGE after partial purification of VP1, showing the expression of MT1-VP1 (MT1), MT4-VP1 (MT4), and wild-type VP1 (WT). Lane M, PageRuler Prestained Protein Ladder. (b) Western blot of the same samples. VP1 was detected using an anti-HaPyV-VP1 antibody. VP1 was further purified using cesium chloride density gradient ultracentrifugation. Negative staining TEM was performed to visualize VLPs in the fractions containing wild-type HaPyV VP1 (c), MT1-VP1 (d), and MT4-VP1 (e). Regularly-shaped VLPs were only observed with wild-type HaPyV VP1. Bars = 200 nm.

The structures were analyzed using Swiss PDB Viewer (SPDBV) version 4.0.1 [31]. All structural images were created using Chimera version 1.6.2 [32].

3. Results

3.1. Hemagglutination assay

To be able to study the integrity of VLPs in blood using single particle tracking, the VLPs should be free in solution and not bound to cells. Since cell binding of various polyomaviruses via surface-exposed sialic acid residues has been described, we studied the binding of wild-type hamster polyomavirus (HaPyV) VLPs to murine erythrocytes. For this, a hemagglutination assay was performed. No hemagglutination was observed, regardless of the storage buffer, at any VLP concentration (see figure 1).

3.2. Production of MT-VLPs

Two *VP1* constructs with an MT-tag inserted into either site 1 (MT1-VP1) or site 4 (MT4-VP1), were prepared. The two MT-VP1 proteins, as well

as wild-type VP1, were overexpressed in *E. coli* BL21(DE3)pREP4. VP1 production was verified by SDS-PAGE (see figure 2a). All three VP1 proteins were expressed, and as expected based on their calculated molecular weights (wild-type VP1, 41.9 kDa; MT1-VP1, 47.1 kDa; MT4, 47.2 kDa), both MT-VP1 proteins were found to be larger than wild-type VP1. The insertion of the epitopes did not have a significant effect on the yield of expression, nor did it prevent the detection of the proteins using an anti-VP1 antibody (figure 2b). This antibody recognizes an epitope localized near amino acids 223/224 in the EF loop [33], which is indeed predicted to fold correctly in the MT-VP1s according to calculated models (see figure 3). VLPs were purified by density gradient ultracentrifugation and visualized by TEM (see figure 2c–e). For all three samples, the VP1 proteins were found in fractions with a density of approximately 1.30 g/cm^3. While regularly-shaped VLPs were found in fractions with wild-type VP1, no VLPs were observed for either MT-VP1 protein. Both samples contained large (up to 1 µm) rectangular and oval structures reminiscent of membranes. Similar structures were also

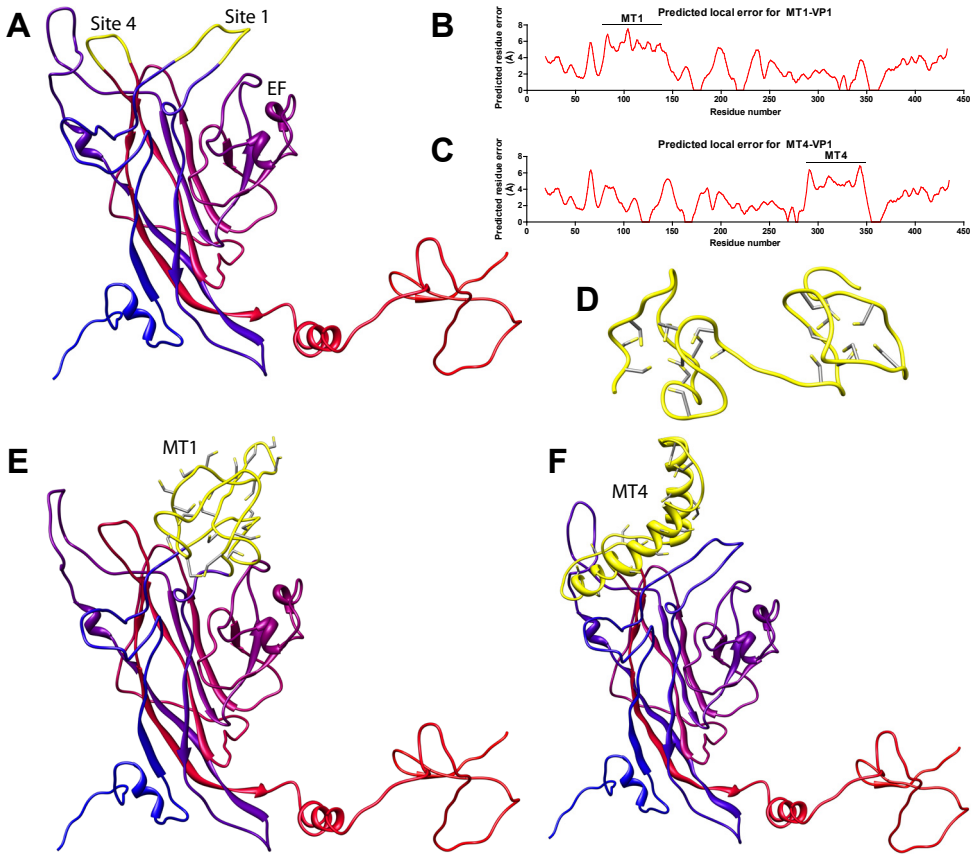

Figure 3. Predicted models of VP1, MT-VP1, and free MT. The 3D models were predicted using the SWISS-MODEL server at ExPASy [30]. (a) Structure of hamster polyomavirus VP1 based on the crystal structure of murine polyomavirus VP1 (PDB: 1VPN). Insertion sites 1 and 4 (yellow), corresponding to the surface-exposed loops BC and HI [1], as well as the antibody-binding region EF, are indicated. (e–f) Structure of MT1-VP1 and MT4-VP1 based on the crystal structure of murine polyomavirus VP1 (PDB: 1SID chain B). The MT-tags are shown in yellow. (b–c) Predicted local error of the MT-VP1 models based on the QMEANlocal score [34]. The quality of the models at the region of the MT-tag is relatively poor. (d) Structure of the free MT-tag based on the crystal structure of rat metallothionein-2 (PDB: 4MT2 chain A). The two metal-binding domains are clearly visible. All structural images were created using Chimera [32].

observed in off-peak (lower density) fractions containing wild-type VP1 (data not shown), and are likely to be bacterial contaminants. We also checked the bacterial lysates and pellets after sucrose cushion ultracentrifugation, but the results were the same (data not shown).

3.3. Modeling of MT-VP1

To investigate why MT-VP1 did not form VLPs, we predicted the structure of VP1 with and without an MT-tag inserted into loops 1 and 4 (see figure 3). The VP1 structures were predicted based on the crystal structure of murine polyomavirus VP1. The structure of the free MT-tag was also predicted based on the crystal structure of rat metallothionein-2. This model shows that the MT-tag normally contains two domains; each with inward-facing thiol groups which complex heavy metal ions forming metal clusters. In the models of MT-VP1, the MT-tag is squeezed tightly and unable to form similar domains. The distance between the attachment-points of the loops 1 and 4 in the wild-type VP1 model is 7.6 Å and 4.6 Å, respectively. In the MT-tag, the distance between the N- and C-terminus is 34.5 Å. Regardless of the predicted errors in modeling, such a large difference is likely to cause significant strain on the tag, disrupting not only the structure of the tag, but possibly also that of VP1 itself. In MT4-VP1, the MT-tag is even predicted to form helices, although the reliability of the model in this region is very low (figure 3c).

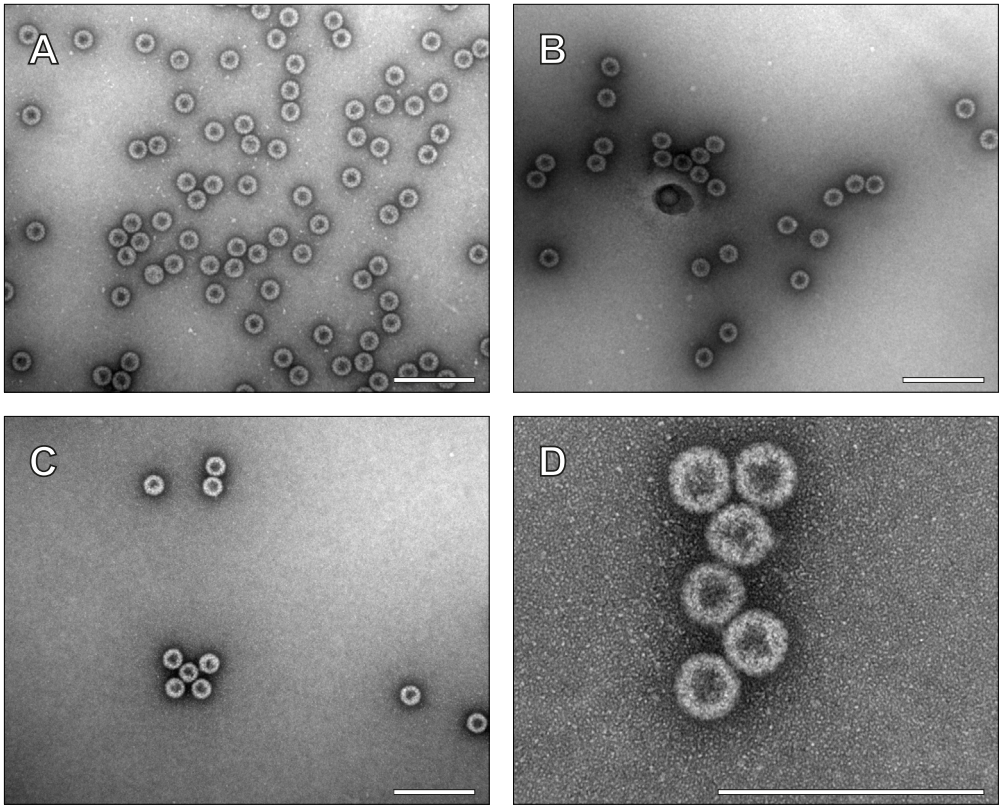

Figure 4. TEM of VLPs before, during, and after labeling with TRITC. (a) Untreated VLPs purified from bacteria; (b) VLPs after dialysis against 0.10 M sodium bicarbonate (pH 9.0), before labeling with TRITC; (c) VLPs after labeling with TRITC; (d) same sample as (c) at a higher magnification. No difference is observed between VLPs before and after labeling with TRITC. Bars = 200 nm.

3.4. Labeling of wild-type HaPyV VLPs for NTA

Wild-type VLPs were labeled with the amine-reactive fluorescent dye TRITC. Each VP1 molecule contains several surface-exposed lysine residues, allowing a large number of dye molecules to be conjugated to each VLPs. TEM was performed to check the VLPs during the labeling process (see figure 4). Dialysis against a low-salt pH 9.0 buffer and labeling with TRITC did not cause the dissociation of the VLPs; in fact, no noticeable differences in gross structure were observed before and after labeling.

3.5. Characterization of labeled VLPs by NTA

Unlabeled and TRITC-labeled VLPs were measured using a NanoSight LM10 instrument. VLPs were visible as bright randomly moving dots in both samples when viewed directly through the binoculars in normal mode. In fluorescence mode, unlabeled particles were not visible anymore, but TRITC-labeled VLPs could still be seen by eye. Nanoparticle tracking analysis was performed and the particle size distribution was determined (see figure 5a). Using the normal mode, both unlabeled and TRITC-labeled VLPs gave a clear peak at 40–45

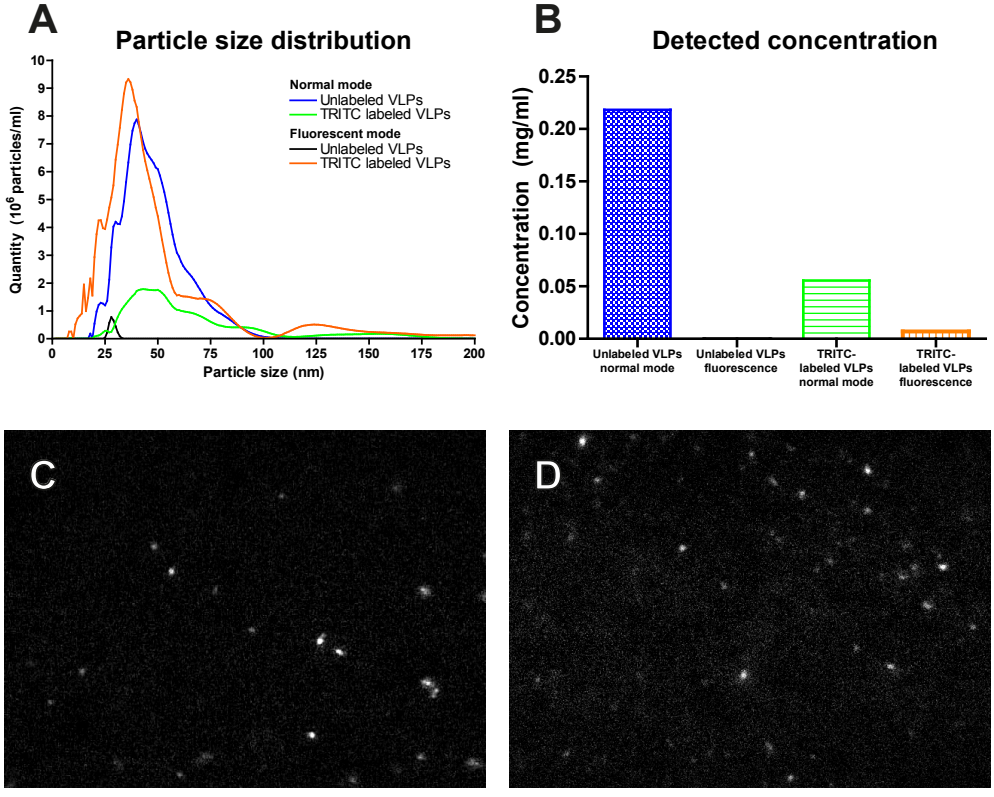

Figure 5. Nanoparticle tracking analysis of labeled and unlabeled VLPs. TRITC-labeled and unlabeled VLPs were measured using a NanoSight instrument. The VLPs (2.0 mg/ml) were diluted in filtered PBS before measurement (50,000 and 500 times for measurements in normal and fluorescence mode, respectively). (a) Particle size distribution obtained after NTA. (b) Detected concentration of particles between 30 and 60 nm in diameter, assuming each particle has the molecular weight of an empty wild-type VLP (15.1 MDa). The results were corrected for the employed dilution factor. (c) Background-subtracted screen capture of 50,000 times diluted unlabeled VLPs imaged using the normal mode. (d) Background-subtracted screen capture of 500 times diluted TRITC-labeled VLPs imaged using the fluorescence mode.

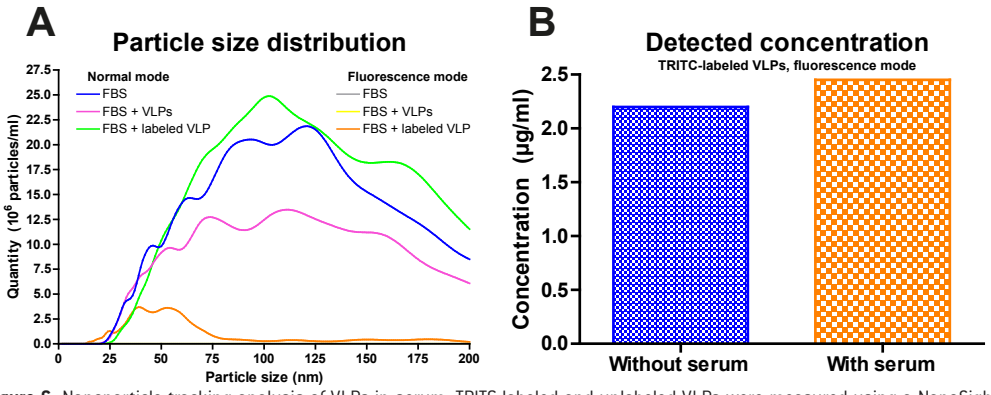

Figure 6. Nanoparticle tracking analysis of VLPs in serum. TRITC-labeled and unlabeled VLPs were measured using a NanoSight instrument. Before measurement, the VLPs were diluted 1,000 times in filtered PBS supplemented with 10 % v/v FBS. (a) Particle size distribution obtained after NTA. (b) Comparison of the detected concentrations of particles between 30 and 60 nm in diameter with and without serum, assuming each particle has the molecular weight of an empty wild-type VLP (15.1 MDa). The results were corrected for the employed dilution factor.

nm, corresponding to the size of wild-type HaPyV VLPs (see figure 4). No unlabeled VLPs were observed in fluorescence mode, while the labeled particles yielded a peak very similar to that of unlabeled VLPs measured in normal mode. However, for measurements in fluorescence mode, 100 times higher concentrations were used. The concentration of particles calculated after correcting for the different dilution factors was significantly lower than with normal detection (see figure 5b). Labeling itself already resulted in a 75 % drop in the number of particles between 30 and 60 nm in diameter, possibly caused by losses during labeling. Of the labeled particles, only 13 % was detected by fluorescence. The total concentration of unlabeled VLPs measured in normal mode was a factor 10 lower than the concentration as determined using the Pierce™ Micro BCA Protein Assay Kit (2.0 mg/ml).

3.6. Detection of labeled VLPs in serum

To determine the influence of serum on the detection of VLPs by NTA, the measurements were re-

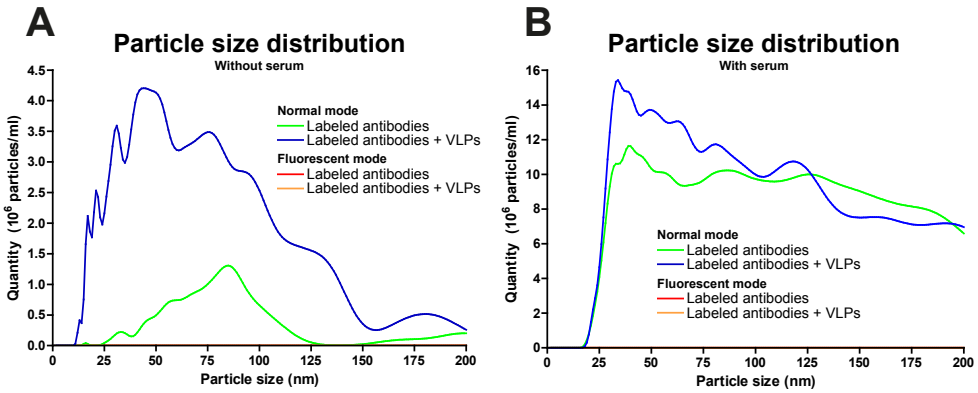

Figure 7. Detection of VLPs using labeled antibodies. TRITC-labeled anti-HaPyV-VP1 antibodies were mixed with unlabeled VLPs and measured using a NanoSight instrument. Both antibodies and VLPs were diluted 1,000 times in PBS before measurement. The size distribution was determined using NTA without (a) or with 10 % v/v serum (b). No VLPs were detected in fluorescence mode.

peated in the presence of 10 % fetal bovine serum (FBS) (see figure 6a). In normal mode, the presence of serum resulted in a very high background level of particles of all sizes, and the addition of VLPs to the serum was not detectable, even at concentrations as high as 2.0 µg/ml. In fluorescence mode, no particles were observed in serum or serum with unlabeled VLPs. However, TRITC-labeled VLPs were readily detectable in serum, yielding a peak at 40–55 nm. The number of particles between 30 and 60 nm in diameter was similar to that without serum (figure 6b).

3.7. Detection of VLPs in serum using labeled antibodies

The fact that labeled VLPs are detectable in serum also opens up options in the field of diagnostics. However, labeling of VP1 itself in a diagnostic setting is not feasible. Therefore, we attempted to use labeled antibodies to detect unmodified VLPs. Anti-HaPyV-VP1 antibodies were labeled with TRITC and mixed with unlabeled VLPs. The antibodies were allowed to bind the VLPs for 60 min, after which the samples were measured using a NanoSight instrument (see figure 7). Although diffuse fluorescence was visible in the samples with labeled antibodies, VLPs could not be detected in fluorescence mode.

4. Discussion

In this chapter we investigated the use of a clonable metallothionein tag as a contrasting agent for the detection of VLPs by transmission electron microscopy. We cloned the tag into insertion sites 1 and 4 of the hamster polyomavirus *VP1* gene [25]. Previous studies showed that the insertion of a large 120 amino acid epitope at these sites did not prevent the formation of VLPs [35]. Site 4 even tolerated the insertion of a complete and functional enhanced green fluorescent protein (EGFP) [33]. The insertion of large peptides into site 1 was shown to cause aggregation of the VP1 proteins, but only at concentrations above 0.5 mg/ml [25]. We found that insertion of the 61 amino acid MT-tag did not reduce the expression of full-length VP1, but did prevent the formation of VLPs.

There are several possible explanations for this. First of all, as shown by the modeling data (figure 2), the close proximity of the attachment sites in VP1 causes the compression of the tag, thereby likely disrupting the tertiary structure of both the tag and VP1. Similar problems were found before when a 38 amino acid WW domain was inserted into site 4 of murine polyomavirus [36]. A possible solution would be the inclusion of a long flexible linker between VP1 and the termini of the MT-tag. Such a strategy was employed to insert the enzyme dihydrofolate reductase into murine polyomavirus VP1, which formed VLPs with enzymatic activity [37]. Next to that, correct disulfide bonding is crucial for the formation of VLPs [38,39] and likely to be involved in the correct folding of VP1 [28]. The MT-tag used in this study contains 20 cysteine residues, and this large amount of thiol groups could result in faulty disulfide bond formation. To encourage proper folding, it might be beneficial to express the MT-VP1 proteins in heavy metal-enriched growth medium. Previous work showed that MT-tagged GroEL formed inclusion bodies upon overexpression under regular growth conditions, but formed soluble proteins upon addition of cadmium chloride to the medium [9].

It is important to consider that the extensive modification of the surface of VLPs might disrupt the native properties of the particles, such as receptor binding and tropism. Insertion of a small RGD-peptide into sites 1 [40] and 4 [41] already completely retargeted VLPs derived from other polyomaviruses. Therefore, it might be better to link the MT-tag to the N-terminus of VP1. The N-terminus is normally responsible for DNA binding, but could also be used to attach proteins [42]. This way the tag would remain buried within the VLP unable to interact with the outside environment. However, it remains questionable whether such MT-VP1 proteins would form VLPs.

Finally, if the sole goal is to track intact VLPs inside cells, it would also be possible to modify VP2 with the MT-tag (see **chapter 2** section 5.2), or even to load VLPs with metal nanoparticles such as quantum dots [43] or magnetic nanoparticles [44]. Although this would solve the problems associated with assembly, the dissociation of such VLPs would release their cargo, limiting their applicability and possibly leading to false (positive) results.
Many viruses, including many polyomaviruses [45–49], are known to agglutinate erythrocytes, and this hemagglutination depends on the source of the blood [48]. We found that HaPyV VLPs do not cause the hemagglutination of mouse RBCs. These results are consistent with literature [50], and allow us to study the integrity of HaPyV VLPs in mouse blood using NTA without the risk of the VLPs attaching to RBCs (see below).
The second strategy we tested for the detection of VLPs in biological environments was nanoparticle tracking analysis. We showed that, by labeling VP1 with the fluorescent rhodamine derivative TRITC, VLPs could specifically be tracked in serum-containing media using NanoSight NTA. The observed size of VLPs in serum was slightly larger than in PBS alone. This might be due to the binding of VLPs to serum components. We observed a rather large (tenfold) difference in titer between NTA and BCA results. This is possibly caused by proteinaceous contaminants in the purified VLP preparation. These contaminants would be detected in the BCA assay, but might be too small or too large to be detected by NTA. Furthermore, the NanoSight NTA cannot detect monomeric or pentameric VP1, which may account for a significant fraction of the VP1 present in the samples. Moreover, losses during labeling could have reduced the concentration of VLPs; the BCA assay was only performed before labeling. Finally, NanoSight NTA was shown to underestimate the titers of adenovirus and latex particles by 15 % [20]. This difference was amplified by the fact that NanoSight NTA was only linear over a very narrow range of dilutions [20], although another study found much smaller deviations from linearity [23].
Not all particles detected in the normal mode in the samples with labeled VLPs were still detected upon switching to the fluorescence mode. Although this might be caused by heterogeneous labeling, this is very unlikely given the high expected amount of labels per VLP. More likely is that NTA is not as sensitive using fluorescence mode, although other factors like photobleaching might also contribute. This difference was less pronounced when larger (>80 nm) particles were measured [23].
Serum completely overshadowed any added VLPs, even at concentrations as high as 2.0 µg/ml (8.0×10^{10} VLPs/ml). Even though the serum had been filtered at 0.1 µm by the supplier, many particles with diameters above 100 nm were found. These particles might have formed by aggregation after filtration.
We also tested if TRITC-labeled antibodies can be used to detect unlabeled VLPs. However, we were not able to detect any VLPs in fluorescence mode. Perhaps the labeling disturbed the binding site of the antibodies, preventing the antibodies from binding VP1. More likely is that too few antibodies bind to each VLP, resulting in an insufficient concentration of dye molecules per VLP. Direct labeling of VLPs results in a much higher degree of labeling, in turn translating to a much brighter signal. A possible solution would be to couple brighter labels to the antibodies. For example, in a previous study antibodies functionalized with quantum dots were used to detect cellular vesicles with high efficiency [23].
For diagnostics such a technique would be very interesting, given the speed of the measurement. However, the concentration of particles required for reliable detection ($>10^6$ per ml) is rather high. Another major drawback of NTA for diagnostics, or for any quantitative application, is the lack of standardization and reproducibility. This is very evident in figure 6a, where the addition of VLPs to serum seemed to cause a 50 % drop in the apparent amount of particles. This variability originates both at the level of measurement (by choosing the

location for the measurement by focusing the microscope on the laser beam) and that of the analysis (by changing the parameters). This method would benefit greatly from a reduction in this variability. A possible alternative would be the use of a newly developed high-resolution, fluorescence-based flow cytometric method [51].

Another application for these fluorescently labeled VLPs would be to study the assembly of VLPs. By combining the fluorescent labeling of VP1 with that of DNA, the interactions between VP1 and DNA, and the assembly of VLPs, could be studied. This could, for example, be done using fluorescence correlation spectroscopy (FCS) [52] or fluorescence single particle tracking (fSPT) [53].

Taken together, we show that there is a limit to the tolerance of the insertion sites of HaPyV VLPs; the insertion of a cysteine-rich tag based on murine metallothionein completely abolished VLP formation. We were able to measure the particle size distribution of wild-type VLPs using NanoSight NTA, and by using fluorescently labeled VLPs, these particles could be detected in a background of serum.

Acknowledgements

The authors would like to thank Ebel Pieters for providing the mouse blood used in the hemagglutination assay and Paulien van Bentum for her helpful support in the preparation of the manuscript.

Molecular graphics and analyses were performed with the UCSF Chimera package. Chimera is developed by the Resource for Biocomputing, Visualization, and Informatics at the University of California, San Francisco, with support from the National Institutes of Health (National Center for Research Resources grant 2P41RR001081, National Institute of General Medical Sciences grant 9P41GM103311).

This work was supported by Technologiestichting STW [budget number 10243].

References

1 Teunissen, E.A., de Raad, M. and Mastrobattista, E. **Production and biomedical applications of virus-like particles derived from polyomaviruses.** J Control Release (2013) 172, 305–321.

2 Mastrobattista, E. *et al.* **Artificial viruses: a nanotechnological approach to gene delivery.** Nat Rev Drug Discov (2006) 5, 115–121.

3 Bae, Y.H. and Park, K. **Targeted drug delivery to tumors: Myths, reality and possibility.** J Control Release (2011) 153, 198–205.

4 Joshi, M.D. *et al.* **Targeting tumor antigens to dendritic cells using particulate carriers.** J Control Release (2012) 161, 25–37.

5 Tsai, B. and Qian, M. **Cellular entry of polyomaviruses.** Curr Top Microbiol Immunol (2010) 343, 177–194.

6 Sosinsky, G.E. *et al.* **Markers for correlated light and electron microscopy.** Methods Cell Biol (2007) 79, 575–591.

7 De Carlo, S. and Harris, J.R. **Negative staining and cryo-negative staining of macromolecules and viruses for TEM.** Micron (2011) 42, 117–131.

8 Mercogliano, C.P. and DeRosier, D.J. **Gold nanocluster formation using metallothionein: mass spectrometry and electron microscopy.** J Mol Biol (2006) 355, 211–223.

9 Nishino, Y., Yasunaga, T. and Miyazawa, A. **A genetically encoded metallothionein tag enabling efficient protein detection by electron microscopy.** J Electron Microsc (Tokyo) (2007) 56, 93–101.

10 Mercogliano, C.P. and DeRosier, D.J. **Concatenated metallothionein as a clonable gold label for electron microscopy.** J Struct Biol (2007) 160, 70–82.

11 Zhou, Q. *et al.* **Structural characterization of the complex of SecB and metallothionein-labeled proOmpA by cryo-electron microscopy.** PLoS One (2012) 7, e47015.

12 Bouchet-Marquis, C. *et al.* **Metallothionein as a clonable high-density marker for cryo-electron microscopy.** J Struct Biol (2012) 177, 119–127.

13 Fukunaga, Y. *et al.* **Enhanced detection efficiency of genetically encoded tag allows the visualization of monomeric proteins by electron microscopy.** J Electron Microsc (Tokyo) (2012) 61, 229–236.

14 Diestra, E. *et al.* **Visualization of proteins in intact cells with a clonable tag for electron microscopy.** J Struct Biol (2009) 165, 157–168.

15 Malloy, A. and Carr, B. **NanoParticle Tracking Analysis – The Halo™ System.** Part. Part. Syst. Charact. (2006) 23, 197–204.

16 Filipe, V., Hawe, A. and Jiskoot, W. **Critical evaluation of Nanoparticle Tracking Analysis (NTA) by NanoSight for the measurement of nanoparticles and protein aggregates.** Pharm Res (2010) 27, 796–810.

17 Du, S. *et al.* **Measuring number-concentrations of nanoparticles and viruses in liquids on-line.** Journal of Chemical Technology & Biotechnology (2010) 85, 1223–1228.

18 Anderson, B. *et al.* **Enumeration of bacteriophage parti-**

cles: Comparative analysis of the traditional plaque assay and real-time QPCR- and nanosight-based assays. Bacteriophage (2011) 1, 86–93.

19 Mironov, G.G. *et al.* **Viral quantitative capillary electrophoresis for counting intact viruses.** Anal Chem (2011) 83, 5431–5435.

20 Kramberger, P. *et al.* **Evaluation of nanoparticle tracking analysis for total virus particle determination.** Virol J (2012) 9, 265.

21 Kapur, N. *et al.* **Hepatitis E virus enters liver cells through receptor-dependent clathrin-mediated endocytosis.** J Viral Hepat (2012) 19, 436–448.

22 Gutierrez-Granados, S. *et al.* **Development and validation of a quantitation assay for fluorescently tagged HIV-1 virus-like particles.** J Virol Methods (2013) 193, 85–95.

23 Dragovic, R.A. *et al.* **Sizing and phenotyping of cellular vesicles using Nanoparticle Tracking Analysis.** Nanomedicine (2011) *7*, 780–788.

24 Teunissen, E.A. *et al.* **Different proteins require different S30 extract protein concentrations for optimal expression.** Manuscript in preparation (2014).

25 Gedvilaite, A. *et al.* **Formation of immunogenic virus-like particles by inserting epitopes into surface-exposed regions of hamster polyomavirus major capsid protein.** Virology (2000) 273, 21–35.

26 Richardson, S.M. *et al.* **GeneDesign: rapid, automated design of multikilobase synthetic genes.** Genome Res (2006) 16, 550–556.

27 Mastrobattista, E. *et al.* **High-throughput screening of enzyme libraries: *in vitro* evolution of a beta-galactosidase by fluorescence-activated sorting of double emulsions.** Chem Biol (2005) 12, 1291–1300.

28 Teunissen, E.A. *et al.* **Assembly of hamster polyomavirus VP1 into virus-like particles takes place in *Escherichia coli* but not after cell-free synthesis.** Manuscript in preparation (2014).

29 Samadi, N. *et al.* **The effect of lauryl capping group on protein release and degradation of poly(d,l-lactic-co-glycolic acid) particles.** J Control Release (2013) 172, 436–443.

30 Schwede, T. *et al.* **SWISS-MODEL: An automated protein homology-modeling server.** Nucleic Acids Res (2003) 31, 3381–3385.

31 Guex, N. and Peitsch, M.C. **SWISS-MODEL and the Swiss-PdbViewer: an environment for comparative protein modeling.** Electrophoresis (1997) 18, 2714–2723.

32 Pettersen, E.F. *et al.* **UCSF Chimera – a visualization system for exploratory research and analysis.** J Comput Chem (2004) 25, 1605–1612.

33 Zvirbliene, A. *et al.* **Generation of monoclonal antibodies of desired specificity using chimeric polyomavirus-derived virus-like particles.** J Immunol Methods (2006) 311, 57–70.

34 Benkert, P., Schwede, T. and Tosatto, S.C. **QMEANclust: estimation of protein model quality by combining a composite scoring function with structural density information.** BMC Struct Biol (2009) 9, 35.

35 Gedvilaite, A. *et al.* **Segments of puumala hantavirus nucleocapsid protein inserted into chimeric polyomavirus-derived virus-like particles induce a strong immune response in mice.** Viral Immunol (2004) 17, 51–68.

36 Schmidt, U., Rudolph, R. and Bohm, G. **Binding of external ligands onto an engineered virus capsid.** Protein Eng (2001) 14, 769–774.

37 Gleiter, S., Stubenrauch, K. and Lilie, H. **Changing the surface of a virus shell fusion of an enzyme to polyoma VP1.** Protein Sci (1999) 8, 2562–2569.

38 Chen, P.L. *et al.* **Disulfide bonds stabilize JC virus capsid-like structure by protecting calcium ions from chelation.** FEBS Lett (2001) 500, 109–113.

39 Ishizu, K.I. *et al.* **Roles of disulfide linkage and calcium ion-mediated interactions in assembly and disassembly of virus-like particles composed of simian virus 40 VP1 capsid protein.** J Virol (2001) 75, 61–72.

40 Langner, J. *et al.* **RGD-mutants of B-lymphotropic polyomavirus capsids specifically bind to alpha(v)beta3 integrin.** Arch Virol (2004) 149, 1877–1896.

41 Takahashi, R.U. *et al.* **Presentation of functional foreign peptides on the surface of SV40 virus-like particles.** J Biotechnol (2008) 135, 385–392.

42 Schmidt, U. *et al.* **Protein and peptide delivery via engineered polyomavirus-like particles.** FASEB J (2001) 15, 1646–1648.

43 Li, F. *et al.* **Imaging viral behavior in Mammalian cells with self-assembled capsid-quantum-dot hybrid particles.** Small (2009) 5, 718–726.

44 Enomoto, T. *et al.* **Viral protein-coating of magnetic nanoparticles using simian virus 40 VP1.** J Biotechnol (2013) 167, 8–15.

45 Li, T.C. *et al.* **Characterization of self-assembled virus-like particles of human polyomavirus BK generated by recombinant baculoviruses.** Virology (2003) 311, 115–124.

46 Vlastos, A. *et al.* **VP1 pseudocapsids, but not a glutathione-S-transferase VP1 fusion protein, prevent polyomavirus infection in a T-cell immune deficient experimental mouse model.** J Med Virol (2003) 70, 293–300.

47 Velupillai, P., Garcea, R.L. and Benjamin, T.L. **Polyoma virus-like particles elicit polarized cytokine responses in APCs from tumor-susceptible and -resistant mice.** J Immunol (2006) 176, 1148–1153.

48 Schowalter, R.M., Pastrana, D.V. and Buck, C.B. **Glycosaminoglycans and sialylated glycans sequentially facilitate Merkel cell polyomavirus infectious entry.** PLoS Pathog (2011) 7, e1002161.

49 Zielonka, A. *et al.* **Serological cross-reactions between four polyomaviruses of birds using virus-like particles expressed in yeast.** J Gen Virol (2012) 93, 2658–2667.

50 Gedvilaite, A. *et al.* **Virus-like particles derived from major capsid protein VP1 of different polyomaviruses differ in their ability to induce maturation in human dendritic cells.** Virology (2006) 354, 252–260.

51 Nolte-'t Hoen, E.N. *et al.* **Quantitative and qualitative flow cytometric analysis of nanosized cell-derived membrane vesicles.** Nanomedicine (2012) 8, 712–720.

52 Remaut, K. *et al.* **Can we better understand the intracellular behavior of DNA nanoparticles by fluorescence correlation spectroscopy?** J Control Release (2007) 121, 49–63.

53 Filipe, V. *et al.* **Fluorescence single particle tracking for the characterization of submicron protein aggregates in biological fluids and complex formulations.** Pharm Res (2011) 28, 1112–1120.

Chapter VIII

Investigation into combined nucleic acid – epitope vaccination with virus-like particles derived from hamster polyomavirus VP1

Erik A. Teunissen[1], Meriem Bourajjaj[1], Emilie M.J. van Brummelen[1], Zahra Karjoo[1], Markus de Raad[1], and Enrico Mastrobattista[1]

[1]Department of Pharmaceutics, Utrecht Institute for Pharmaceutical Sciences, Faculty of Science, Utrecht University, Universiteitsweg 99, 3584 CG Utrecht, The Netherlands

Abstract

Virus-like particles derived from polyomaviruses can be used for both epitope and genetic vaccination. Individually these strategies result in reasonable immune responses, but these immune responses are generally not strong enough to break immune tolerance, which is often needed for effective cancer immunotherapy. In this chapter we investigate the possibility of combining these two strategies into a single particle, based on the hypothesis that such co-delivery will lead to a synergistic effect. Six different epitopes based on CD8+ and CD4+ epitopes from ovalbumin were designed and inserted into site 1 and site 4 of hamster polyomavirus VP1. We show that insertion at both sites is tolerated without interfering with virus-like particle formation. These virus-like particles are smaller (20 nm in diameter) than wild-type virus-like particles, but are capable of inducing a strong immune response in an *in vitro* antigen presentation assay. We also tested different strategies for loading virus-like particles with plasmid DNA. We found that reassembly of virus-like particles from capsomers in the presence of plasmid DNA does not result in significantly better protection against nucleases than observed after mixing the DNA with preformed virus-like particles. Neither strategy resulted in higher transfection efficiency than naked plasmid DNA.

1. Introduction

Virus-like particles (VLPs), supramolecular structures that spontaneously form after overexpression of viral structural proteins, are ideal vectors for epitope presentation. These particles resemble the native viral capsids in their structure and properties, but do not contain any viral genetic material, making them a safer alternative to attenuated and inactivated virus vaccines. Due to their repetitive structure, VLPs can activate the immune system via pattern-recognition receptors on immune cells and cross-link B-cell receptors, leading to a potent immune response [1,2]. VLPs can be derived from many viral proteins and used as a vaccine against the native viral capsid. Examples include the prophylactic HPV vaccines Cervarix® [3] and Gardasil® [4]. Next to that, it is possible to integrate foreign epitopes in the VLPs, allowing the display of these epitopes in a highly immunogenic format.

One of the viral structural proteins that form VLPs is the polyomavirus major capsid protein VP1. Polyomavirus VP1 VLPs are promising vectors for the delivery of therapeutic cargos, such as nucleic acids for gene therapy, or antigens for vaccination [2]. Four distinct sites on polyomavirus VP1 have been tested for antigen display by inserting foreign epitopes. All four sites tolerated the insertion of small epitopes [5], while longer epitopes of up to 120 amino acids were only tolerated in sites 1 and 4 (see figure 1) [6]. Next to humoral immune responses [7], cytotoxic T lymphocyte (CTL) responses can also be induced by foreign epitopes displayed at these sites [8]. Prior contact with the wild-type virus does not prevent an immune response against the displayed epitopes [9], and the presence of antibodies against VP1 does not hamper a specific CTL response induced by the VLPs [10]. However, even though good results have been achieved with epitope-displaying VLPs as prophylaxis in a mouse model [11,12], the current VLPs are not potent enough to work in a therapeutic setting [13,14]. For cancer immunotherapy to become a reality, very strong immunogens are required capable of breaking the tolerance [15].

Polyomavirus VLPs are also very efficient delivery vehicles for genetic vaccines [16]. These VLPs can be loaded with plasmids encoding antigens [16,17] and are rapidly taken up by dendritic cells (DCs) [18], thus showing potential for DNA vaccination. However, the immune responses were not impressive [16,17]. Thus, individually, epitope insertion and genetic vaccination are not strong enough.

Our goal was to test if these two strategies, epitope

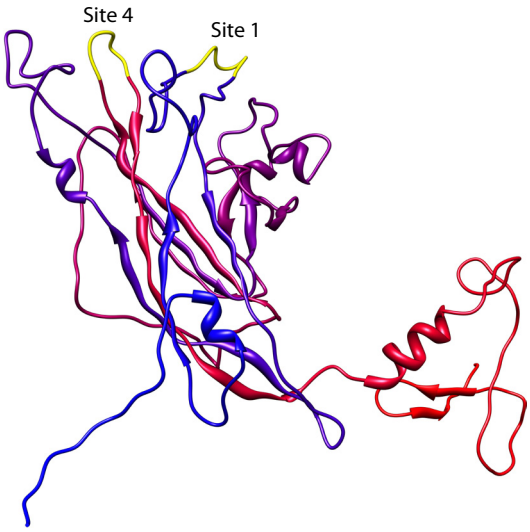

Figure 1. Structure of hamster polyomavirus VP1. Insertion sites 1 and 4, corresponding to the surface-exposed loops BC and HI [2], are indicated. The 3D model of hamster polyomavirus VP1 was predicted using the SWISS-MODEL server at ExPASy [28] based on the structure of murine polyomavirus VP1 (PDB: VPN). The image was created using Chimera [29].

insertion and genetic vaccination, can be combined to form a single, more potent vaccine. Such co-delivery can result in a synergistic effect on the immune response [19] and is exploited in systems such as antigen-expressing immunostimulatory liposomes (AnExILs) [20,21]. Previous studies have also shown that the co-delivery of adjuvants, such as CpG, and epitopes [22,23], or the co-delivery of different toll-like receptor (TLR) ligands [24] to the same dendritic cell is very important for a potent immune response. Such strategies have never before been studied with polyomavirus VLPs.

In this study we used peptides derived from ovalbumin (OVA) as model antigens for tumor vaccination. These peptides were chosen because of the large toolbox available for analysis. For example, transgenic OT-I [25] and OT-II [26] T-cells are available that react specifically with presented CD8+ and CD4+ ovalbumin epitopes, respectively, as well as B3Z hybridoma cells, that react specifically with the major histocompatibility complex (MHC)-bound ovalbumin CD8+ epitope [27]. To achieve this goal of co-delivery, these model epitopes (both CD8+ and CD4+) were integrated into surface-exposed loops 1 and 4 of hamster polyomavirus (HaPyV) VP1. VLPs were generated from these epitope-VP1 proteins and tested for their immunogenicity. Furthermore, we compared different strategies to load the wild-type VLPs with DNA.

2. Materials and Methods

2.1. Chemicals

Ampicillin, bovine serum albumin (BSA), bromophenol blue, calcium chloride, cesium chloride, dithiothreitol (DTT), ethidium bromide, glycerol, heat-inactivated sterile filtered fetal bovine serum (FBS), iodixanol (60 % w/v solution in water), isopropyl β-D-1-thiogalactopyranoside (IPTG), kanamycin, LB agar, LB broth culture medium, 2-mercaptoethanol, Nonidet® P-40 Substitute, polysorbate 20 (TWEEN® 20), SIINFEKL peptide (S7951), sodium acetate, sodium dodecyl sulfate (SDS), and tris(hydroxymethyl)aminomethane (Tris) were purchased from Sigma-Aldrich (St.

Louis, MO, USA). Acetic acid, chlorophenol red-β-D-galactopyranoside (CPRG), ethanol, hydrochloric acid, isopropanol, sodium chloride, and sucrose were purchased from Merck KGaA (Darmstadt, Germany). Agarose MP was purchased from Roche (Basel, Switzerland). Ethylenediaminetetraacetic acid (EDTA) and magnesium chloride were purchased from Acros Organics (Geel, Belgium). Phosphate buffered saline (PBS) was purchased from B. Braun Melsungen AG (Melsungen, Germany). Uranyl acetate was purchased from Electron Microscopy Sciences (Hatfield, PA, USA). iQ™ SYBR®

Table 1. List of oligonucleotides used in this study.

Name	Sequence
eGFP_qPCR_fw	CGACGGCAACTACAAGAC
eGFP_qPCR_rv	TAGTTGTACTCCAGCTTGTGC
VP1_Shuffling_secondary_fw2	CTTTAAGAAGGAGATATACCAT
VP1_Shuffling_secondary_rv	TTTCGGGCTTTGTTAGCA
Site_1_BamHI_fw	CGCGGATCCGAAGTTAAAGCTAACCAGCTG
Site_1_BamHI_rv	CGCGGATCCTTTGATAGACTGAGAGAAACC
Site_4_BamHI_fw	CGCGGATCCTGGCACTGGCGTGGTC
Site_4_BamHI_rv	CGCGGATCCGATGTACCAACCCATAACG
Site_1_L_BamHI_fw	CGCGGATCCGGCGGCGAAGTTAAAGCTAACCAGCTG
Site_1_L_BamHI_rv	CGCGGATCCGCCGCCTTTGATAGACTGAGAGAAACC
Site_4_L_BamHI_fw	CGCGGATCCGGCGGCTGGCACTGGCGTGGTC
Site_4_L_BamHI_rv	CGCGGATCCGCCGCCGATGTACCAACCCATAACG
E1_fw	GATCCGTGAACGGCCTGGAACAGCTGGAAAGCATTATTAACTTTGAAAAACTGACCGAATGGACCAGCAGCAACGTGATGGAAGAACGCAAAATTAAAGTGTATCTGCCGCGCG
E1_rv	GATCCGCGCGGCAGATACACTTTAATTTTGCGTTCTTCCATCACGTTGCTGCTGGTCCATTCGGTCAGTTTTTCAAGTTAATAATGCTTTCCAGCTGTTCCAGGCCGTTCACG
E2_fw	GATCCGTGAACGGCCTGGAACAGCTGGAAAGCATTATTAACTTTGAAAAACTGACCGAATGGACCAGCAGCAACGTGG
E2_rv	GATCCCACGTTGCTGCTGGTCCATTCGGTCAGTTTTTCAAAGTTAATAATGCTTTCCAGCTGTTCCAGGCCGTTCACG
E3_fw	GATCCATTAACTTTGAAAAACTGACCGAATGGACCAGCAGCAACGTGATGGAAGAACGCAAAATTAAAGTGTATCTGCCGCGCATGAAAATGGAAG
E3_rv	GATCCTTCCATTTTCATGCGCGGCAGATACACTTTAATTTTGCGTTCTTCCATCACGTTGCTGCTGGTCCATTCGGTCAGTTTTTCAAAGTTAATG
E4_fw	GATCCATTAGCAGCGCGGAAAGCCTGAAAATTAGCCAGGCGGTGCATGCGGCGCATGCGGAAATTAACGAAGCGGGCCGCGAAGTGGTGGGCAGCGCGGAAGCGG
E4_rv	GATCCCGCTTCCGCGCTGCCCACCACTTCGCGGCCCGCTTCGTTAATTTCCGCATGCGCCGCATGCACCGCCTGGCTAATTTTCAGGCTTTCCGCGCTGCTAATG
E5_fw	CGCGGATCCGTGATTAGCAGCGCGGAAAGCCTGAAAATTAGCCAGGCGGTGCATGCGGCGCATGCGGAAATTAACGAAGCGGGCCGCGAAGTGGTGGGCAGCGCGGAAGCGGTGAACGGC
E5_rv	CGCGGATCCGTTGCTGCTGGTCCATTCGGTCAGTTTTTCAAAGTTAATAATGCTTTCCAGCTGTTCCAGGCCGTTCACCGCTTCCGCGCTGCCCACCACTTCGCGGCCCGCTTCGTTAAT
E6_fw	CGCGGATCCGTGAACGGCCTGGAACAGCTGGAAAGCATTATTAACTTTGAAAAACTGACCGAATGGACCAGCAGCAACGTGATTAGCAGCGCGGAAAGCCTGAAAATTAGCCAGGCGGTG
E6_rv	CGCGGATCCCGCTTCCGCGCTGCCCACCACTTCGCGGCCCGCTTCGTTAATTTCCGCATGCGCCGCATGCACCGCCTGGCTAATTTTCAGGCTTTCCGCGCTGCTAATCACGTTGCTGCT

Green Supermix was purchased from Bio-Rad (Hercules, CA, USA). Dulbecco's Modified Eagle's Medium (DMEM), FBS, and Trypsin-EDTA (L11-004) were purchased from PAA Laboratories (Pasching, Austria). Cell-culture antibiotics, GlutaMAX™ Supplement, glycogen, and Lipofectamine® 2000 were purchased from Life Technologies (Carlsbad, CA, USA). Dulbecco's Phosphate Buffered Saline (DPBS) was purchased from GE Healthcare (Little Chalfont, United Kingdom). GeneRuler 1 kb DNA Ladder, nuclease-free water, PageBlue Protein Staining Solution, PageRuler Prestained Protein Ladder, proteinase K, RNase A, and DNA-modifying enzymes were purchased from Thermo Scientific (Waltham, MA, USA). Iscove's Modified Dulbecco's Media (IMDM) without L-glutamine was purchased from Lonza (Basel, Switzerland).

2.2. Oligonucleotides

All oligonucleotides (see table 1) were purchased from Eurogentec (Seraing, Belgium). The nucleotides were reconstituted in nuclease-free water.

2.3. Plasmids

The plasmid pEGFP-C1 was obtained from Clontech (Mountain View, CA, USA). The cloning and preparation of the plasmid pIVEX-HaPyV-VP1/co, which contains the hamster polyomavirus *VP1* gene codon-optimized for expression in *E. coli* under control of a T7 promoter, was described before [30]. Six different ovalbumin epitopes were inserted into VP1 sites 1 and 4. First, the BamHI site in pIVEX-HaPyV-VP1/co was removed; pIVEX-HaPyV-VP1/co was digested with BamHI, blunted using T4 DNA polymerase, phosphorylated with T4 Polynucleotide Kinase, and re-ligated using T4 DNA Ligase. Next, a BamHI restriction site was inserted into *VP1* in four different ways: either into site 1 or site 4, and either with or without a GG linker sequence (L). Mutagenic PCR was performed with pIVEX-HaPyV-VP1/co as template. The N-terminal part of the *VP1* gene was amplified using VP1_Shuffling_secondary_fw2 as forward primer and Site_1_BamHI_rv, Site_4_BamHI_rv, Site_1_L_BamHI_rv, and Site_4_L_BamHI_rv, as reverse primers for site 1, site 4, site 1 with linker, and site 4 with linker, respectively. The C-terminal part of the *VP1* gene was amplified with VP1_Shuffling_secondary_rv as reverse primer and Site_1_BamHI_fw, Site_4_BamHI_fw, Site_1_L_BamHI_fw, and Site_4_L_BamHI_fw, as forward primers for site 1, site 4, site 1 with linker, and site 4 with linker, respectively. All 8 PCR products were purified and digested with BamHI and NcoI (N-terminal fragments) or BamHI and XhoI (C-terminal fragments). Corresponding fragments were mixed together and ligated into pIVEX-HaPyV-VP1/coΔBamHI digested with NcoI and XhoI, creating pIVEX-HaPyV-VP1/co-S1, -S4, -S1L, and -S4L. Next, the six different epitopes (E1–E6) were inserted into the four vectors using annealed or PCR extended oligonucleotides. Forward and reverse oligonucleotides for E1–4 were mixed together, treated with T4 Polynucleotide Kinase, and ligated into the vectors digested with BamHI. Forward and reverse oligonucleotides for E5 and E6 were mixed together, extended by one round of PCR, digested with BamHI, and ligated into the vectors digested with BamHI. All genes, mutations, and epitope insertions were verified by sequencing (BaseClear; Leiden, The Netherlands). Suitable quantities of circular plasmid DNA were obtained using the NucleoBond® PC 10 000 kit (MACHEREY-NAGEL; Düren, Germany).

2.4. Production of wild-type VP1 VLPs

Wild-type VP1 VLPs were produced and purified as described before [31]. Briefly, *E. coli* BL21(DE3) pREP4 were transformed with pIVEX-HaPyV-VP1/co. Individual colonies were grown in LB medium at 37 °C. VP1 expression was induced at an OD600 of 0.8 by adding IPTG to a final concentration of 1.0 mM. Protein expression was allowed to continue overnight at 37 °C. Afterwards, the bacteria were harvested by centrifugation at 5,000 g at 4 °C for 15 min. The bacteria were washed once in reassem-

bly buffer (10 mM Tris-HCl (pH 7.2), 1.0 M sodium chloride and 1.0 mM calcium chloride in demineralized water), followed by thorough resuspension in 20 volumes of reassembly buffer. The bacteria were lysed by two passes through an EmulsiFlex-C5 high pressure homogenizer (AVESTIN; Ottawa, ON, Canada) at >15,000 psi. VLPs were purified by sequential ultracentrifugation. The lysates were first cleared by centrifugation at 6,000 g at 4 °C for 30 min. VLPs in the supernatant were pelleted through a layer of 60 % w/v sucrose in reassembly buffer for 20 hours at 75,400 g at 4 °C. The pellets were resuspended in 1 ml reassembly buffer per 25 ml lysate. Cesium chloride was added to a final density of 1.30 g/cm^3, and the samples were centrifuged in an SW 41 Ti rotor (Beckman Coulter; Brea, CA, USA) at 40,000 RPM at 4 °C for 70 hours to allow a gradient to form. Afterwards, the tubes were carefully removed and 1 ml fractions were taken by puncturing the bottom of the tubes with a needle and collecting the drops. The fractions were checked for VP1 by reducing SDS-PAGE, and fractions containing VP1 were dialyzed 4 times against 50 volumes of reassembly buffer using Slide-A-Lyzer membrane cassettes (Thermo Scientific) with a MWCO of 20 kDa. After purification, protein concentrations of pure samples were determined using the Pierce™ Micro BCA Protein Assay Kit (Thermo Scientific) according to the manufacturer's protocol.

2.5. Production of epitope-VP1 VLPs

E. coli BL21(DE3)pREP4 were transformed with pIVEX-HaPyV-VP1-epitope constructs. Individual colonies were grown in LB medium at 37 °C. VP1 expression was induced at an OD600 of 0.8 by adding IPTG to a final concentration of 1.0 mM. Protein expression was allowed to continue overnight at 37 °C. Afterwards, the bacteria were harvested by centrifugation at 6,000 g at 20 °C for 15 min. The bacteria were thoroughly resuspended in 5 volumes of reassembly buffer, followed by 4 cycles of sonication (60 sec cycles, 80 % output, 0.5 sec active time interval) with a LABSONIC® P probe sonicator equipped with a 3-mm diameter probe (Sartorius AG; Göttingen, Germany). VLPs were purified by sequential ultracentrifugation. The lysates were first cleared by centrifugation at 6,000 g at 4 °C for 30 min. The supernatants were taken, and the cleared again at 10,000 g at 4 °C for 30 min. VLPs in the supernatant were pelleted through a layer of 30 % w/v sucrose in reassembly buffer for 17 hours at 75,400 g at 10 °C. The pellets were resuspended in 1 ml reassembly buffer per 10 ml lysate. The VLP suspensions were poured into ultracentrifuge tubes and equilibrated to 6.0 ml using reassembly buffer. In each ultracentrifuge tube, 1.4 ml of 27 %, 33 %, and 39 % w/v iodixanol in reassembly buffer was sequentially underlaid. The samples were ultracentrifuged at 40,000 RPM in a SW 41 Ti rotor at 4 °C for 16 hours. Afterwards, the tubes were carefully removed and 0.25 ml fractions were taken by puncturing the bottom of the tubes with a needle and collecting the drops. The fractions were checked for VP1 by reducing SDS-PAGE.

2.6. SDS-PAGE and Western blotting

SDS-PAGE and Western blotting were performed as before [30] with the following modifications. In addition to the samples, 5 µl PageRuler Prestained Protein Ladder was included on each gel. No HaPyV VP1 internal standard was included. For SDS-PAGE, the gels were stained with PageBlue Protein Staining Solution according to the manufacturer's protocol using a microwave oven.

2.7. Transmission electron microscopy

Negative staining was performed as described before [32]. Briefly, samples were diluted 10–100 times in demineralized water, and 25 µl of each diluted sample was pipetted onto parafilm. Glow-discharged formvar/carbon-coated copper grids (Agar Scientific; Stansted, United Kingdom) were placed on top of the droplets for 2 min. After incubation, the grids were taken and excess liquid was

removed by carefully touching filter paper. Next, the grids were placed on top of 20 µl 2 % uranyl acetate droplets for 2 min. After incubation, the grids were taken and excess liquid was again removed. The grids were dried at room temperature for 5 min before measurement. Transmission electron microscopy (TEM) imaging was performed using a Philips Tecnai 10 at 100 kV.

2.8. Cell culture

COS-7 cells were grown in DMEM containing 1 g/L glucose supplemented with 5.0 % v/v FBS and antibiotics (100 IU/ml penicillin, 100 µg/ml streptomycin, and 0.25 µg/ml amphotericin B). D1 cells, GM-CSF-dependent immature dendritic cells derived from spleens of female C57BL/6 (H-2K^b) mice [33], were grown on non-tissue culture treated petri dishes (633180; Greiner Bio-One; Monroe, NC) in D1 medium, which consists of 60 % v/v IMDM without L-glutamine, 30 % v/v R1 supernatant with 10 to 20 ng/ml recombinant mouse GM-CSF [33], and a final concentration (including the contributions from the R1 supernatant) of 35 µM 2-mercaptoethanol, 1.0 % v/v GlutaMAX™, 11.5 % v/v heat-inactivated FBS, and antibiotics (30 IU/ml penicillin, 30 µg/ml streptomycin, and 0.08 µg/ml amphotericin B). R1 supernatant was derived from GM-CSF-producing NIH/3T3 fibroblast cells cultured in DMEM containing 10.0 % heat-inactivated FBS, 1.0 % v/v GlutaMAX™, 50 µM 2-mercaptoethanol, and antibiotics (100 IU/ml penicillin, 100 µg/ml streptomycin, and 0.25 µg/ml amphotericin B). The supernatant was collected from confluent cell cultures and filtered using 0.2 µm syringe filters (Sartorius; Göttingen, Germany) before use. B3Z cells, CD8+ T cell hybridomas specific for the H-2K^b-restricted ovalbumin epitope SIINFEKL, which express β-galactosidase under control of the NFAT-responsive element from the IL-2 promoter upon activation [27], were grown in B3Z medium (IMDM without L-glutamine supplemented with 20 µM 2-mercaptoethanol, 1.0 % v/v GlutaMAX™, and 10 % v/v heat-inactivated FBS). All cells were incubated in a humidified incubator with 5 % CO_2 at 37 °C.

2.9. *In vitro* antigen presentation assay

D1 antigen presenting cells were seeded onto 96-well plates at 5.0×10^4 cells per well in 50 µl D1 medium. Samples were diluted in D1 medium and added to the cells at 50 µl per well. Free SIINFEKL peptide was included as a positive control. After 24 hours, 5.0×10^4 B3Z cells in 100 µl B3Z medium were added to each well. After 24 hours, the β-galactosidase activity was measured using CPRG. The 96-well plates were centrifuged at 250 g for 5 min, washed with DPBS, and centrifuged again at 250 g for 5 min. The supernatant was removed and 100 µl CPRG solution (90 µg/ml CPRG, 9.0 mM magnesium chloride, 0.125 % v/v NP-40, and 100 mM 2-mercaptoethanol in PBS) was added to each well. The plates were incubated at 37 °C for 2 hours, after which the absorbance was measured in a SPECTROstar Nano (BMG Labtech; Ortenberg, Germany) microplate reader at 590 nm with 630 nm as reference wavelength.

2.10. Gel retardation assay

Plasmid DNA was mixed with purified VP1 at different weight ratios in PBS (20 µl total volume). To test for DNA protection, 1.0 µl 1 U/µl DNaseI was added to the indicated samples. The samples were incubated at 37 °C for 10 min. Afterwards, the samples were analyzed by agarose gel electrophoresis.

2.11. Preparation of DNA-loaded wild-type VLPs

To encapsidate plasmid DNA by reassembly, VLPs were first disassembled, mixed with plasmid DNA, and then reassembled. Wild-type VP1 VLPs were disassembled by adding DTT and EDTA at final concentrations of 3.0 or 10 mM and 50 mM, respectively. The samples were incubated on a roller mixer at 4°C overnight. DNA was added at a 1:50 w/w

DNA:VP1 ratio, and the samples were incubated on a roller mixer overnight at 4°C. VLPs were reassembled by dialyzing against reassembly buffer at 4 °C with Slide-A-Lyzer membrane cassettes with a MWCO of 7 kDa. The samples were first dialyzed for 2 hours, and after refreshing the buffer, the samples were dialyzed for another 18 hours at 4 °C. The same protocol was followed for direct interaction, except that no DTT or EDTA was added.

2.12. Analysis of encapsidated DNA

DNA was isolated from samples containing 0.2 µg DNA and/or 10 µg VLPs. Some samples were treated with DNaseI. These samples were incubated with 0.05 U DNaseI in a total volume of 20 µl 1× DNaseI buffer at 37 °C for 30 min. The reactions were stopped by incubating at 65 °C for 10 min. VLPs were degraded by adding a final concentration of 1.0 µg/µl proteinase K, 1.0 % v/v SDS, and 25 mM EDTA (pH 7.5) to the samples, followed by incubating at 55 °C for 24 h. DNA was recovered from the samples by phenol-chloroform extraction. Each sample was equilibrated to 250 µl using demineralized water. Next, 250 µl of a 25:24:1 phenol:chloroform:isoamyl alcohol mixture saturated with 10 mM Tris (pH 8.0) and 1.0 mM EDTA (P3803; Sigma-Aldrich) was added to each sample, mixed by vigorous vortexing for 10 sec, and separated by centrifuging at 20,000 g for 2 min. The upper phase of each sample was carefully collected without disturbing the interface, mixed with 250 µl of the phenol:chloroform:isoamyl alcohol mixture, and separated as above. The upper phase of each sample was again carefully collected without disturbing the interface, and the volumes were adjusted to 250 µl using PBS. Subsequently 1.0 µl 20 mg/ml glycogen, 25 µl 3.0 M sodium acetate (pH 5.3), and 175 µl isopropanol were added to each sample while vortexing after each addition. The mixtures were incubated at −20 °C for 15 min, and centrifuged at 20,000 g at 4 °C for 15 min. The supernatants were removed without disturbing the clearly visible pellets. The pellets were washed twice with 100 µl 70 % v/v ethanol, while centrifuging at 20,000 g for 5 minutes after each washing step. After removing the remaining supernatants the pellets were air-dried overnight at 37 °C. The pellets were finally resuspended in 20 µl nuclease-free water. Extracted DNA was analyzed by agarose gel electrophoresis. Plasmid concentrations in the samples were determined using qPCR. Each reaction (20 µl) contained 0.5 µM eGFP_qPCR_fw, 0.5 µM eGFP_qPCR_rv, 10 µl 2× iQ™ SYBR® Green Supermix, and 1.0 µl sample. PCR was performed using a CFX96™ Real-Time System (Bio-Rad) with the lid temperature set to 105 °C. The PCR was started at 95 °C for 3 min, followed by 40 cycles of 95 °C for 10 sec, 51 °C for 30 sec, 72 °C for 15 sec, and plate reading. The PCR was completed with a melt curve from 65 °C to 95 °C. Next to the samples and controls, a ten-fold dilution series of pEGFP-C1, ranging from 1.0×10^{-7} to 1.0 ng DNA, was also included. The extracted DNA was also subjected to RNase A (0.1 U/µl) and DNaseI (0.01 U/µl) digestion. The reactions were incubated at 37 °C for 30 minutes, terminated at 65 °C for 10 minutes, and analyzed by agarose gel electrophoresis.

2.13. Transfection of COS-7 cells

COS-7 cells were seeded onto 24-well plates at 1.0×10^4 cells per well. After 24 hours, the cells (50 % confluent) were transfected with VLPs reassembled with pEGFP-C1 (0.2, 0.4, and 0.8 µg DNA per well). The same amounts of DNA were also transfected after mixing with intact VLPs (1:50 DNA:VLP weight ratio), as naked DNA, and using Lipofectamine® 2000 according to the manufacturer's protocol. All transfections were performed in duplicate. After 5 hours, the transfection medium was replaced with complete medium. The cells were analyzed by fluorescence microscopy (Eclipse TE2000-U with GFP-B filter; Nikon; Tokyo, Japan) and the transfection rate was determined 48 hours after transfection (90 % confluent).

Table 2. Epitopes based on CD8+ and CD4+ epitopes from ovalbumin. Indicated in bold is the ovalbumin CD8+ epitope, SIINFEKL. The CD4+ epitope naturally flanking SIINFEKL is underlined, and the distant CD4+ is italicized. The locations indicate the amino acid span in ovalbumin.

#	Ovalbumin epitopes	Location	Sequence
E1	**CD8+** and CD4+ with flanking aa	249–284	VNGLEQLE**SIINFEKL**TEWTSSNVMEERKIKVYLPR
E2	**CD8+** with flanking aa	249–*272*	VNGLEQLE**SIINFEKL**TEWTSSNV
E3	CD4+ with flanking aa	259–288	INFEKLTEWTSSNVMEERKIKVYLPRMKME
E4	*CD4+* with flanking aa	315–34*7*	ISSAESLK*ISQAVHAAHAEINEAGR*EVVGSAEA
E5	*CD4+* and **CD8+** with flanking aa	315–34*7* + 249–*272*	ISSAESLK*ISQAVHAAHAEINEAGR*EVVGSAEAVNGLEQLE**SIINFEKL**TEWTSSNV
E6	**CD8+** and *CD4+* with flanking aa	249–*272* + 315–34*7*	VNGLEQLE**SIINFEKL**TEWTSSNVISSAESLK*ISQAVHAAHAEINEAGR*EVVGSAEA

3. Results

3.1. Part I: T-cell epitope display on HaPyV VLPs

3.1.1. Epitope design

Six different epitopes were designed based on CD8+ and CD4+ epitopes from ovalbumin (see table 2). The full ovalbumin sequence was derived from GenBank: AAB59956.1. As CD8+ epitope, the MHC class I H-2K^b-restricted epitope SIINFEKL ($OVA_{257-264}$) was selected [34,35]. SIINFEKL is naturally flanked by the MHC class II I-A^b-restricted CD4+ epitope TEWTSSNVMEERKIKV ($OVA_{265-280}$) [34,35]. However, the transgenic OT-II T-cells recognize the MHC class II I-A^b-restricted CD4+ epitope ISQAVHAAHAEINEAGR ($OVA_{323-339}$), which occurs distant from SIINFEKL [26]. Constructs were designed using both CD4+ epitopes. Two synthetic epitopes were prepared with $OVA_{323-339}$ either in front of or behind SIINFEKL. As far as we could find, this was the first time these synthetic constructs were used. To ensure proper antigen processing, endogenous flanking regions of 8 amino acids long were included. In the synthetic epitopes E5 and E6, the CD4+ and CD8+ epitopes were flanked on both sides. In the case of E1, the previously validated SIINFEKL with extended flanking sequence was used [36], in which the CD4+ epitope is flanked by only 4 additional amino acids. This sequence contains one substitution ($N_{250}S$) in the N-terminal region flanking the CD8+ epitope compared to the GenBank sequence. We chose to adhere to the validated extended sequence, and applied the substitution to the other epitopes. In the case of E3, the N-terminal flanking region was reduced to 6 amino acids to prevent the full CD8+ epitope from being included, which might obscure results.

3.1.2. Insertion of the six epitopes into *VP1*

The wild-type *VP1* sequence from the hamster polyomavirus was modified at sites 1 and 4 to allow the insertion of the epitopes. Constructs were prepared in which a BamHI restriction site replaced all amino acids of the surface-exposed loops (see figure 2). BamHI was chosen as it encodes the flexible glycine-serine (GS). Additional constructs were prepared in which the BamHI site was flanked with a double-glycine linker, resulting in GGGS/GSGG. The six epitopes were inserted into the BamHI restriction sites with or without linker sequence, resulting in a total of 24 epitope-*VP1* constructs. All 24 constructs were successfully cloned as verified by DNA sequencing.

3.1.3. Production of E1-VLPs

The difference between the insertion sites was investigated using the E1 constructs. The four different E1-VP1 proteins were overexpressed in *E. coli*

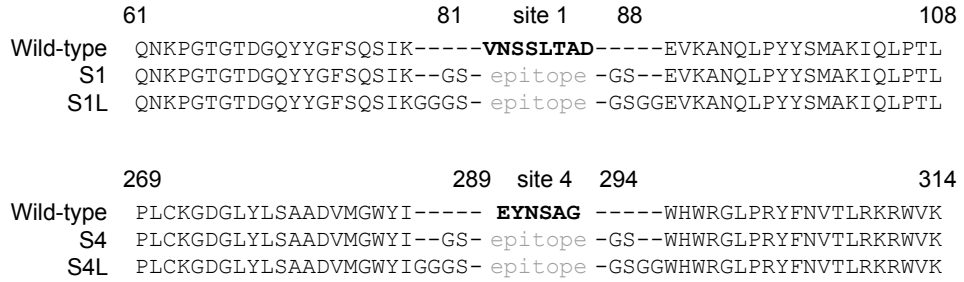

Figure 2. Schematic representation of the insertion sites before and after modification. The original loops are completely replaced by the epitopes, which are flanked by GS (without linker) or GGGS/GSGG (with linker).

BL21(DE3)pREP4. E1-VP1 production was verified by SDS-PAGE (see figure 3a). Insertion at site 1 resulted in a higher yield after purification than at site 4, while the linker had no obvious impact on the yield. The E1-VLPs were purified by density gradient ultracentrifugation and visualized by TEM (see figure 3c–f). Although VP1 was found in iodixanol gradient fractions 6 through 10, which suggests assembly [37,38], the VLPs were smaller than expected, with an average diameter of 20 nm. Wild-type $T=7$ icosahedral VLPs are 45 nm in diameter (see figure 3b). These smaller particles might be $T=1$ icosahedral VLPs, consisting of 12 capsomers instead of the regular 72 [39–41].

3.1.4. *IN VITRO* ANTIGEN PRESENTATION ASSAY

To test if these small E1-VLPs present their CD8+ epitope correctly and are capable of eliciting a CTL response, an antigen presentation assay was performed. Different iodixanol gradient fractions of E1-VLPs were added to D1 antigen presenting dendritic cells. These cells process the VLPs and, if presented correctly by the VLPs, present SIINFEKL on their MHC class I complexes [42]. Next, B3Z CD8+ T-cell hybridomas were added. These cells start to express β-galactosidase once they recognize SIINFEKL bound to MHC class I H-2K^b [27]. This expression is controlled by the transcription factor NFAT, which is activated in T-cells by T-cell receptor engagement [43]. The β-galactosidase expression was then quantified using a CPRG assay as a measure of antigen presentation (see figure 4). Fractions 6 through 10 of S1E1, S1LE1, and S4LE1 resulted in high levels of β-galactosidase expression, indicating excellent SIINFEKL presentation. However, no peak was observed for S4E1, showing that these VLPs failed to induce a CTL response.

3.2. PART II: LOADING OF PLASMID DNA INTO WILD-TYPE HAPYV VLPS

3.2.1. COMPLEXATION OF PLASMID DNA BY WILD-TYPE VLPS

We next explored different strategies to load VLPs with DNA for vaccination. These studies were performed with wild-type VLPs as model delivery vehicles. Because previous studies showed that VLPs loaded by direct interaction are suitable for DNA vaccination, but did not show results in regard to complexation [16,17], we first investigated whether wild-type VP1 VLPs form complexes with plasmid DNA. Plasmid DNA was mixed with purified VLPs and analyzed by gel electrophoresis (figure 5a). The results clearly show that VP1 bound plasmid DNA and formed large complexes that were unable to migrate through the gel. Surprisingly, this DNA is partially protected against nucleases (figure 5b).

3.2.2. LOADING OF PLASMID DNA

To establish how VLPs are best loaded with nucleic

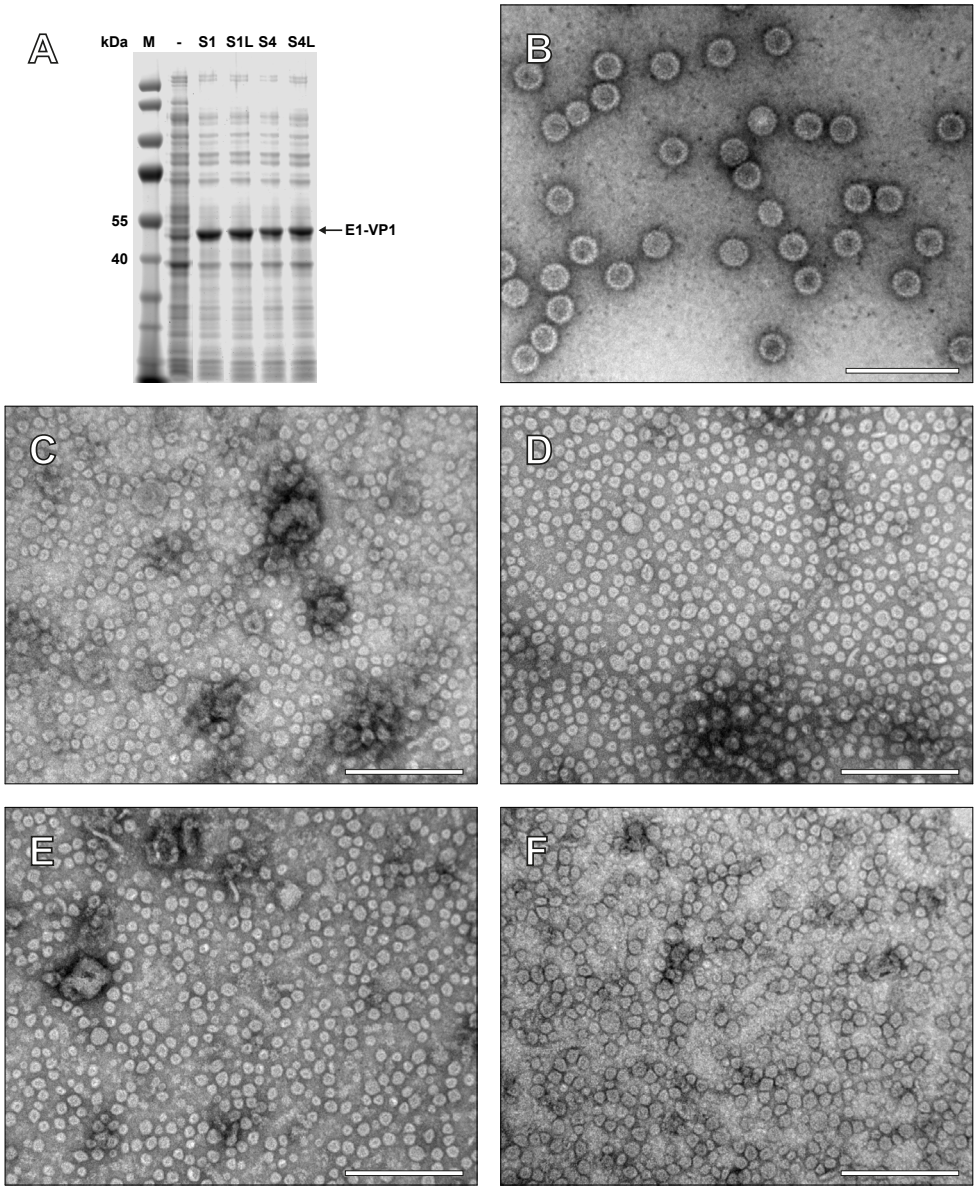

Figure 3. Production and purification of E1-VLPs. The four different E1-VP1 proteins were overexpressed in *E. coli* BL21(DE3) pREP4. (a) SDS-PAGE of bacteria 90 min after induction of expression, showing the expression of the four E1-VP1 proteins. Lane M, PageRuler Prestained Protein Ladder; lane –, induced but untransformed BL21(DE3)pREP4. E1-VLPs were purified after their expression in bacteria. Negative staining TEM was performed to visualize VLPs. (b) Wild-type HaPyV VLPs; (c) S1E1-VLPs; (d) S4E1-VLPs; (e) S1LE1-VLPs; (f) S4LE1-VLPs. The individual E1-VP1 particles measured approximately 20 nm in diameter. Bars = 200 nm.

acids for genetic vaccination, plasmid DNA (pEGFP-C1, size 4.7 kb) was complexed with and encapsidated into wild-type VP1 VLPs. This process was followed by TEM (see figure 6). Wild-type HaPyV

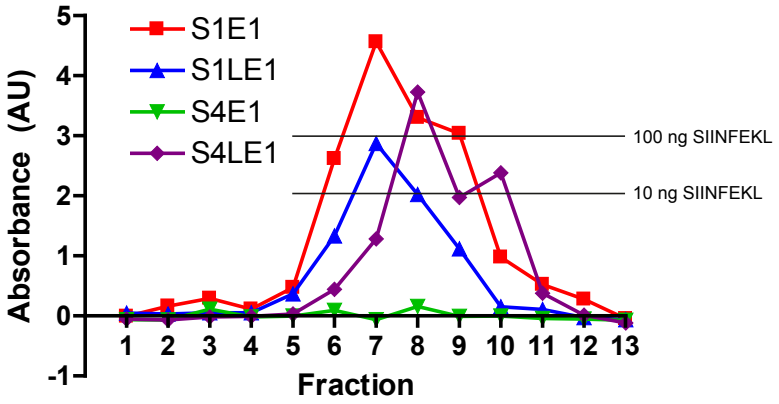

Figure 4. Antigen presentation assay of iodixanol gradient fractions of E1-VLPs. Iodixanol gradient fractions were diluted 100 times, added to D1 dendritic cells and incubated for 24 hours. Next, B3Z CD8+ T-cell hybridomas were added. After 24 hours, antigen presentation was measured by quantifying β-galactosidase expression using CPRG. All E1-VLPs, except S4E1, displayed strong antigen presentation in fractions 6 through 10. No CTL activation was observed with S4E1. The lines indicate the CTL activation induced by 10 and 100 ng SIINFEKL peptide.

VP1 was expressed in *E. coli* BL21(DE3)pREP4. After expression, VLPs were purified, yielding a pure population of VLPs (figure 6a). No big changes were observed when these VLPs were mixed with plasmid DNA, although the VLPs seemed to be more aggregated (figure 6b). To encapsidate plasmid DNA, the VLPs were first disassembled using DTT and EDTA. When DTT was added to a final concentration of 3.0 mM, this led to incomplete disassembly of the VLPs (figure 6c). Some intact and

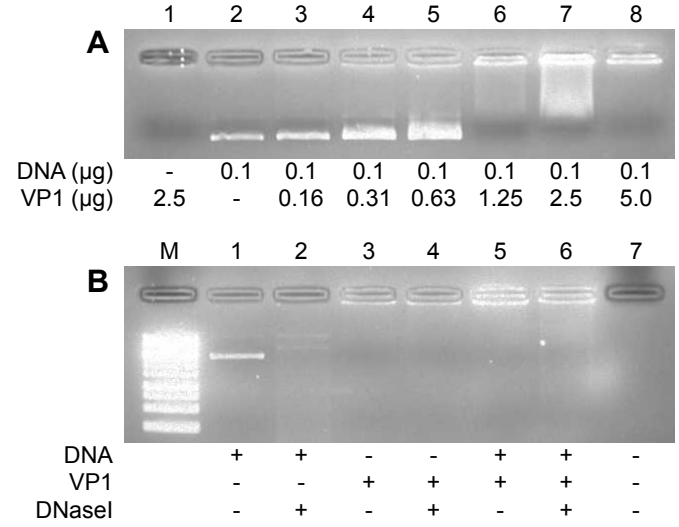

Figure 5. Gel retardation assay using wild-type VP1 VLPs. Plasmid DNA (pIVEX-HaPyV-VP1/co) was mixed with purified VP1 at different ratios and analyzed by agarose gel electrophoresis (a). The DNA was completely complexed by VP1 at a 1:50 weight ratio (lane 8). DNaseI was added to 50 ng plasmid DNA complexed with VP1 at a 1:50 weight ratio. After digestion, the samples were analyzed by agarose gel electrophoresis (b). Partial protection is observed. M, GeneRuler 1 kb DNA Ladder.

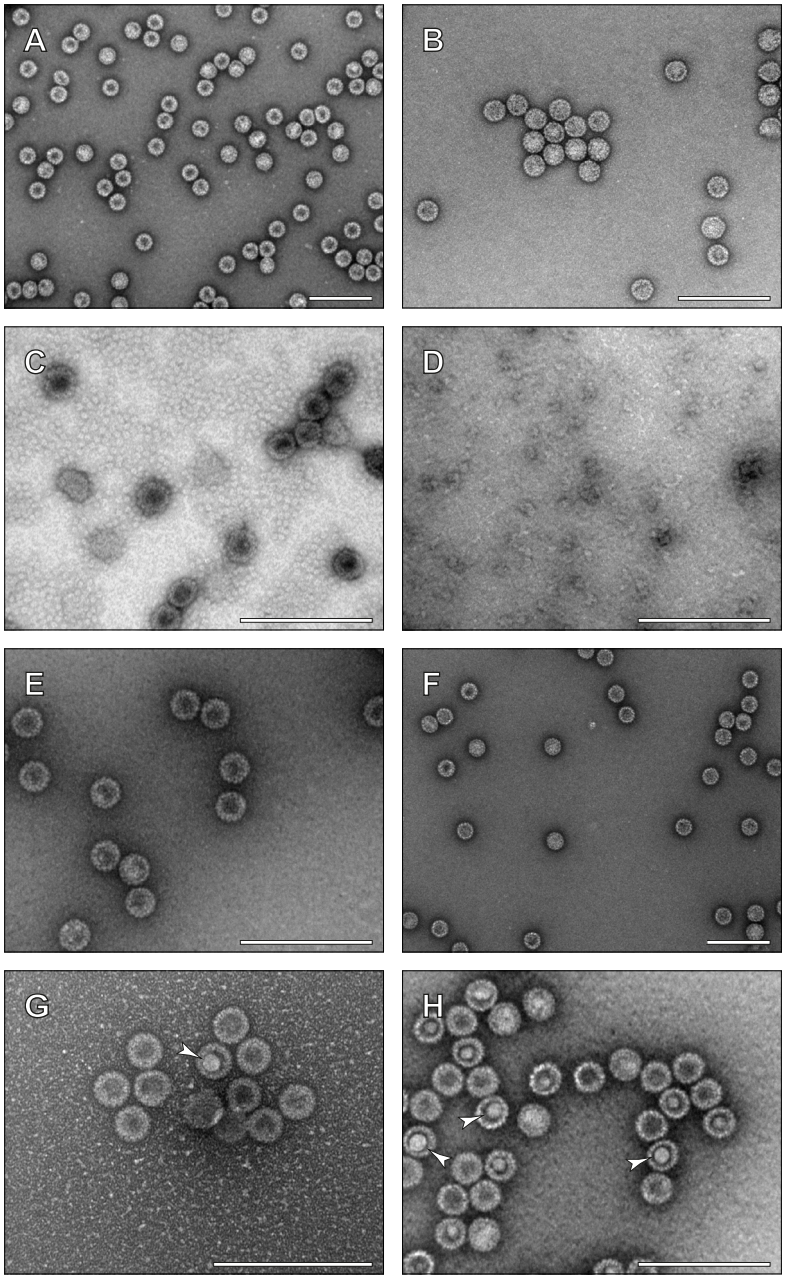

Figure 6. Loading of plasmid DNA into VLPs. Wild-type HaPyV VP1 was expressed in *E. coli* BL21(DE3)pREP4. After expression, the bacteria were lysed and VLPs were purified by sucrose and continuous cesium chloride gradient ultracentrifugation. Negative staining TEM was performed to visualize VLPs. (a) Purified VLPs; (b) purified VLPs mixed with pEGFP-C1 (loading by direct interaction); (c) VLPs partially disassembled after treatment with 3 mM DTT and 50 mM EDTA; (d) VLPs fully disassembled after treatment with 10 mM DTT and 50 mM EDTA; (e) sample (c) after reassembly; (f) sample (d) after reassembly; (g) sample (c) after reassembly with pEGFP-C1; (g) sample (d) after reassembly with pEGFP-C1. The arrowheads indicate some of the typical spheres found inside VLPs after reassembly with pEGFP-C1, possibly indicating encapsidated plasmid DNA. Bars = 200 nm.

some partially disassembled VLPs were visible on a background filled with capsomers. No intact VLPs or capsomers were observed anymore when the DTT concentration was increased to 10 mM (figure 6d). VLPs were reassembled by dialysis against reassembly buffer, a high-salt buffer supplemented with calcium (figures 6e and 6f). When the disassembled VLPs were mixed with plasmid DNA prior to reassembly, at least 10 % of the reassembled VLPs were found to be filled with spherical particles; possibly plasmid DNA (figures 6g and 6h).

3.2.3. Protection of loaded DNA against nucleases

A good indicator of encapsidation is the degree to which the loaded DNA is protected against nucleases. To determine the level of protection, the VLPs were treated with DNaseI to digest unincorporated DNA. Next, the VLPs were degraded and DNA was

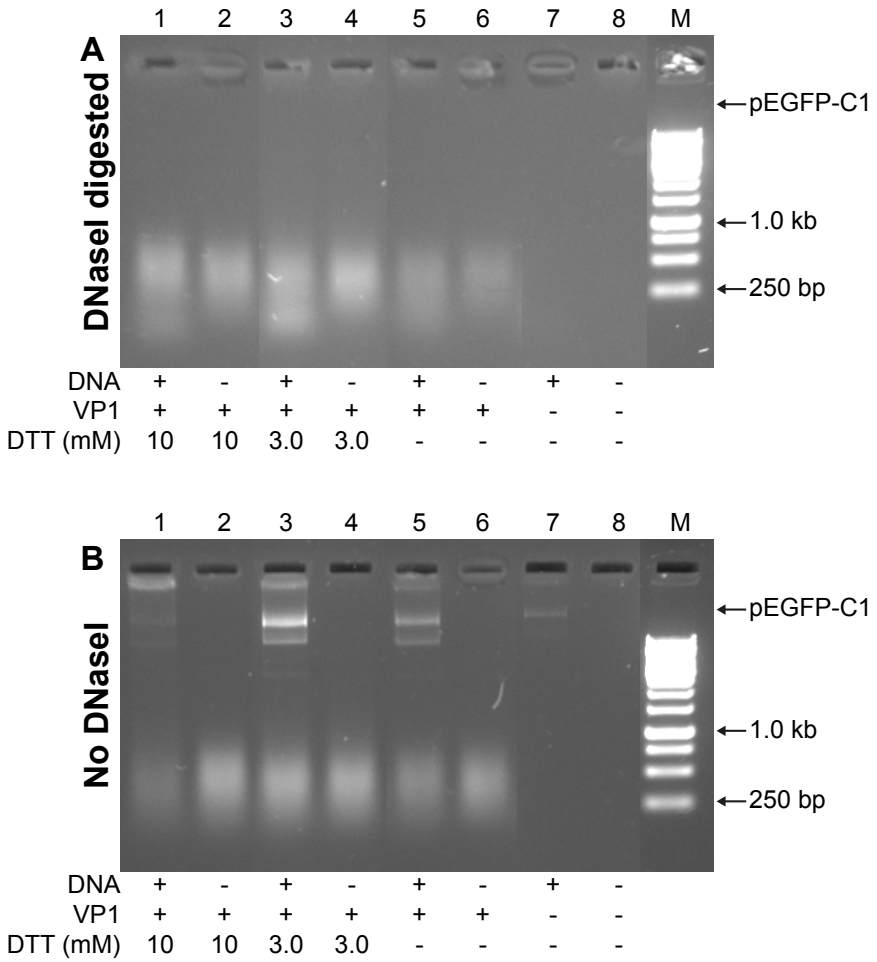

Figure 7. Analysis of encapsidated DNA. DNA was extracted from VLPs with (a) or without (b) prior DNaseI digestion. No intact pEGFP-C1 was observed after DNaseI digestion. No difference was found between reassembly (lanes 1 and 3) and direct interaction (lane 5). A smear of nucleic acids smaller than 1.0 kb in size was found in all samples containing VLPs. These nucleic acids were shielded from the DNaseI action. DTT (mM) refers to the DTT concentration used during reassembly. M, GeneRuler 1 kb DNA Ladder.

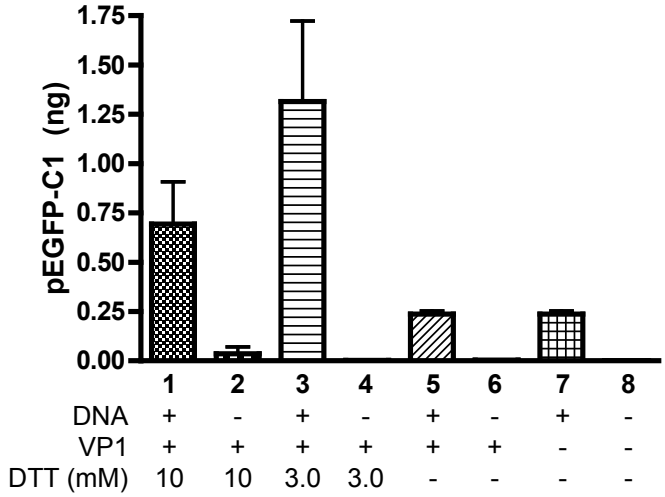

Figure 8. Quantification of encapsidated DNA protected against DNaseI. The amount of pEGFP-C1 DNA was quantified by qPCR. The VLPs were first incubated with DNaseI to remove unincorporated plasmids, followed by the release of the protected DNA by proteinase K treatment. The quantities were derived from a standard curve of pEGFP-C1 assuming an amplification efficiency of 100 % and are given as total amount of pEGFP-C1 after extraction. Each sample contained 0.2 µg pEGFP-C1 and/or 10 µg VLPs before digestion and extraction. The differences between the samples containing DNA were not statistically significant (one-way ANOVA, $p>0.05$). $n = 2$.

extracted from the samples. No intact plasmid DNA was visible by gel electrophoresis after recovery in any of the samples digested with DNaseI, while plasmid DNA was observed in the undigested samples (see figure 7). This shows that very little, if any, plasmid DNA was fully protected against nucleases. A smear of nucleic acids smaller than 1.0 kb in size was found in all samples containing VLPs, even in the ones that had not been reassembled and to which no plasmid DNA had been added, indicating that the VLPs are contaminated with small nucleic acids. The VLPs provide these nucleic acids with full protection against DNaseI digestion, as no decrease in intensity is visible upon pretreatment with DNaseI. The smear consisted of a mixture of DNA and RNA, as neither DNaseI nor RNase A alone could fully digest the nucleic acids (data not shown). After reassembly these nucleic acids were still protected against DNaseI, suggesting that the nucleic acids were either repackaged in the VLPs, or were never released from VP1 during disassembly. When VLPs were analyzed by gel electrophoresis without extraction these nucleic acids barely migrated through the gel; almost no nucleic acids were recovered without proteinase K digestion (data not shown).

This low plasmid DNA protection is striking given the abundance of spheres found inside VLPs after reassembly (figure 6g and 6h). However, ethidium bromide staining has a rather low sensitivity (approximately 2 ng, data not shown). It could be that not enough plasmid DNA was recovered to be detectable by gel electrophoresis. A previous report showed that 10 µg VLPs reassembled with 0.5 µg plasmid DNA can yield as little as 10 ng plasmid DNA after DNaseI digestion and extraction [44]. Therefore, a more sensitive technique, qPCR, was used to quantify the encapsidated pEGFP-C1 after digestion of the freely accessible pEGFP-C1 outside the VLPs (see figure 8). Low levels of pEGFP-C1 were found in the VLPs loaded by reassembly. However, a high background of pEGFP-C1 was also found in the samples with naked pEGPF-C1 and in the samples where pEGFP-C1 had been complexed with VLPs by direct interaction. This indicates that very little DNA was protected against DNaseI, and

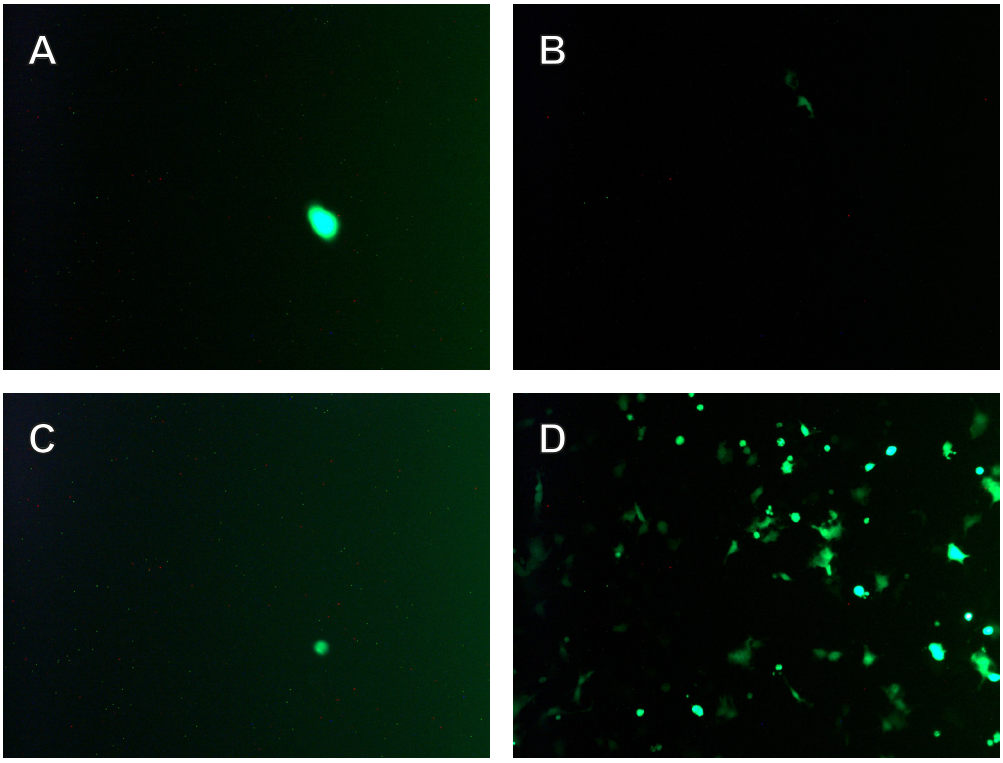

Figure 9. Transfection of COS-7 cells with pEGFP-C1. COS-7 cells were transfected with pEGFP-C1 using different transfection reagents and imaged by fluorescence microscopy two days later. (a) Transfection with VLPs loaded by reassembly; (b) transfection with VLPs loaded by direct interaction; (c) transfection with naked DNA; (d) transfection of DNA using Lipofectamine® 2000.

that DNaseI digestion was not complete in the samples. No significant benefits in terms of protection against nucleases were found for VLPs loaded by reassembly when compared with direct interaction, although all individual values were higher after reassembly.

3.2.4. Transfection of COS-7 cells using wild-type VLPs

Because at least some pEGFP-C1 had been encapsidated by the VLPs, and the recovered amount was comparable to previous results [44], we continued with transfection studies. VLPs loaded with pEGCP-C1 by reassembly and by direct interaction were used to transfect COS-7 cells. These cells were previously shown to be susceptible to transfection with HaPyV VLPs [44]. Naked DNA and Lipofectamine® 2000-mediated transfection were included as controls. The transfection efficiency using VLPs was very low; equal to that using naked DNA (see figure 9). No obvious cytotoxicity was observed for any sample at any of the concentrations tested. Lipofectamine® 2000 yielded good transfection results.

4. Discussion

This study was aimed at investigating the synergistic effect of combined nucleic acid and epitope vaccination with virus-like particles derived from hamster polyomavirus VP1. Towards this end we designed six unique epitope constructs based on

CD8+ and CD4+ epitopes from ovalbumin. These constructs were designed to make optimal use of the extensive toolbox available for analysis. As such, they included the CD8+ epitope $OVA_{257-264}$, which can be recognized by OT-I [25] and B3Z cells [27], and the CD4+ epitope $OVA_{323-339}$, which can be recognized by OT-II cells [26]. We also included the CD4+ epitope $OVA_{265-280}$, which occurs adjacent to the CD8+ epitope. This epitope was shown to be important in generating a strong CTL response [35]. The longest epitopes, E5 and E6, span 57 amino acids. Such a length poses significant restrictions on the choice of insertion site. We inserted these epitopes into sites 1 and 4 of hamster polyomavirus VP1. Previous research showed that these sites were the most likely to tolerate the insertion of large epitopes [6]. The epitopes were inserted into the sites with or without a flexible linker. Similar linker sequences were shown to aid the folding of complex inserts, allowing even the insertion of a complete and functional dihydrofolate reductase into site 4 [45].

Due to time constraints, we limited the production and purification of VLPs to the different E1-VP1 constructs, containing the previously validated CD8+/CD4+ combination OVA249–284 [36]. We found that insertion at site 1 resulted in a higher yield than that at site 4. Although this does not directly influence immunogenicity, it might say something about the folding and solubility of the E1-VP1 proteins. E1-VLPs were found at the same buoyant density as wild-type VLPs (see **chapter 6**), but were smaller in size, with an average diameter of 20 nm, about half that of wild-type VLPs. Most likely these smaller particles are T=1 icosahedral VLPs, consisting of 12 capsomers instead of the regular 72 [39–41]. Similar small-sized particles were observed after the combined insertion of a 60 amino acid N-terminal fragment of urokinase plasminogen activator (uPA) into site 2 and a FLAG epitope into site 4 of murine polyomavirus VP1 [46]. Although we did not investigate the DNA uptake capacity of these smaller VLPs, their reduced size alone makes it impossible to encapsidate the usual 5 kb of DNA. Therefore, it might be important to find conditions that stimulate these proteins to form normal T=7 VLPs if these proteins are to be used for genetic vaccination. Three out of four E1-VLPs caused significant B3Z cell activation after processing by D1 dendritic cells. Apparently the smaller size of the VLPs does not hamper the immune response. We do not know why S4E1-VLPs did not cause B3Z cell activation. Before the CD8+ epitopes can be displayed on MHC class I molecules, the VLPs first have to be taken up by the DCs and processed by proteasomes in the cytosol [47]. One possibility is that the direct insertion of E1 into S4 prevents the binding of the VLPs to DCs, thus also preventing their uptake. The level of uptake of polyomavirus VLPs by DCs was previously shown to correspond to the induced maturation and activity of these cells [48]. It is unlikely that improper folding caused this loss of immunogenicity, as S4E1-VLPs did form and were morphologically indistinguishable from the other E1-VLPs (see figure 3).

We tested both reassembly and direct interaction for loading plasmid DNA into VLPs. Very little plasmid DNA was recovered from reassembled VLPs after DNaseI treatment. This is unfortunate, although these results do agree with previous work, where as little as 10 ng of plasmid DNA was recovered from 10 µg loaded VLPs [44]. This low yield could be caused by losses during DNA extraction. Another possibility, albeit unlikely, is that the VLPs are disrupted during the heat inactivation step before DNaseI is inactivated, exposing the DNA to the nuclease. We found that purified VLPs are associated with small DNA and RNA fragments of less than 1.0 kb in size. This smear of nucleic acids is most likely derived from endogenous bacterial DNA and RNA. VLPs produced in *E. coli* are often contaminated with host DNA and RNA [2,49]. If these nucleic acids fill a significant portion of the VLPs, as is evident from the large fraction of particles with an electron-dense interior when observed by TEM (see figure 5a), and remain associated with VP1 during disassembly (figures 5e and 5f), this

might prevent the uptake of plasmid DNA during reassembly (see **chapter 2** section 4.3). Future loading protocols might therefore benefit from additional purification steps removing contaminating nucleic acids from the VLPs before reassembly [50]. The amount of encapsidated plasmid DNA was quantified by qPCR. This technique might have over-estimated the amount of intact pEGFP-C1 recovered from the VLPs. Even after partial degradation of the plasmid, qPCR might still detect pEGFP-C1, as only a 129 bp fragment of the EGFP gene, and not the entire plasmid, is amplified. Thus, the detected DNA might be present in the smear. Previous studies have shown that loading of DNA does not always lead to the protection of the entire plasmid [51–53].

Protection against nucleases is neither a requirement [54], nor a guarantee for transfection. Nonetheless, both direct interaction and reassembly did not lead to higher transfection efficiencies than naked plasmid DNA. This contrasts with previous results obtained with HaPyV VLPs [44]. Even though the medium was already replaced after 5 hours, the VLPs should have had ample time to enter the cells. Previous studies with another polyomavirus showed that half of the VLPs are already internalized by cells within the first 40 minutes [55]. Moreover, there is some controversy whether optimizing genetic vaccines for high expression of full-length proteins would lead to optimal generation of antigenic epitopes for loading into MHC class I molecules, as defective ribosomal products (DRiPs), which are immediately degraded upon translation, provide a substantial fraction of the MHC class I peptides [56]. The expression of DRiPs varies widely amongst genetic transcripts, and so-called immunoribosomes are thought to play a central role in this process [57].

Encapsidation is not an absolute necessity for genetic vaccination. In fact, previous studies on DNA vaccination with polyomavirus VLPs used direct interaction, and have shown that this works just fine for boosting the immune response [16,17]. We did show that VP1 forms complexes with plasmid DNA. Surprisingly direct interaction did result in at least partial protection against nucleases based on the gel retardation assay. Therefore, despite the fact that our initial attempts to deliver loaded DNA were unsuccessful, it would still be worthwhile to perform antigen presentation studies with complexed DNA.

One of the challenges this system might face would be pre-existing anti-carrier immunity. However, there is some evidence that prior contact with the wild-type virus [9], or previous immunizations with the same VLP [10], do not prevent a successful CTL reponse.

Another possible challenge is the disruption of the natural tropism of the VLPs by the insertion of the epitopes into the capsid, preventing their uptake and processing by antigen presenting cells, and thus an efficient CTL response. The variable loops at sites 1 and 4 are responsible for receptor binding in polyomaviruses [58–61]. Therefore, it is likely that changes to these sites will alter the tropism of the VLPs [62,63]. This could be solved by coupling the epitopes to the C-terminus of VP1 [12,14], which is hidden inside the capsid, or by fusing the antigens to (truncated) VP2/3 [11,64]. Next to that, chimeric VLPs could be prepared where some VP1 proteins or capsomers are modified, while the bulk of the capsid consists of wild-type VP1. Using this strategy, it might also be possible to prepare normal $T=7$ VLPs for the E1-VP1 proteins that now form smaller VLPs (see figure 3).

It is unlikely that inserting more than one copy of the same epitope into the same VP1 protein will enhance the immune response [9]. Although the hamster polyomavirus VP1 protein tolerates the insertion of epitopes at different sites at the same time [65], it is also possible to produce the same effect by preparing VLPs from different VP1 proteins with each a single epitope inserted. It would be very interesting to compare the immune response elicited by such chimeric VLPs composed of E2-VP1 and E4-VP1 (see table 2) with that of VLPs composed solely of a synthetic epitope construct – E5-VP1 or E6-VP1 – which contains both indi-

vidual epitopes linked together.

In conclusion, the strong immune response induced by the E1-VLPs warrants further studies into the use of HaPyV VLPs as a platform for antigen display. It would be interesting to test the other epitope-VP1 VLPs as well using the *in vitro* antigen presentation assay. In particular the S1 and S1L constructs would be of interest as these gave the best results for E1, though this is of course no guarantee. Unfortunately, this assay only provides information on the presentation of the CD8+ epitope $OVA_{257-264}$. To investigate the role of the CD4+ epitopes, other cells, such as OTZ-II and MF2.2D9 T-cell hybridoma cells, could be used. MF2.2D9 cells secrete IL-2 upon recognition of MHC class II I-A^b-bound $OVA_{265-280}$ [66,67]; OTZ-II cells produce β-galactosidase upon recognition of MHC class II I-A^b-bound $OVA_{323-339}$ [68]. If positive results would be obtained, *in vivo* studies would be justified to determine the quality of the presentation of both CD8+ and CD4+ epitopes. These studies could be performed in mice by injecting labeled OT-I and OT-II cells after administering the VLPs, although such an assay would not detect the CD4+ epitope $OVA_{265-280}$. The investigation should specifically focus on the benefit of adding CD4+ epitopes, as the CTL response to inserted CD8+ epitopes alone has already been investigated thoroughly [8,10]. Although the small size of the E1-VLPs and the limited protection wild-type VLPs provide against nucleases might argue against DNA vaccination, it might be worthwhile to test E1-VLPs in combination with CpG or DNA encoding full-length ovalbumin using the antigen presentation assay. If this would lead to a synergistic effect, the same might be tested *in vivo*.

Acknowledgements

The authors would like to thank Maryam Amidi, Ferry Ossendorp, Jan Willem Kleinovink, and Marieke Herbert-Fransen for their help with the design of the study and Paulien van Bentum for her helpful support in the preparation of the manuscript.

Molecular graphics and analyses were performed with the UCSF Chimera package. Chimera is developed by the Resource for Biocomputing, Visualization, and Informatics at the University of California, San Francisco, with support from the National Institutes of Health (National Center for Research Resources grant 2P41RR001081, National Institute of General Medical Sciences grant 9P41GM103311).

This work was supported by Technologiestichting STW [budget number 10243].

References

1 Jennings, G.T. and Bachmann, M.F. **The coming of age of virus-like particle vaccines.** Biol Chem (2008) 389, 521–536.

2 Teunissen, E.A., de Raad, M. and Mastrobattista, E. **Production and biomedical applications of virus-like particles derived from polyomaviruses.** J Control Release (2013) 172, 305–321.

3 Harper, D.M. *et al.* **Sustained efficacy up to 4.5 years of a bivalent L1 virus-like particle vaccine against human papillomavirus types 16 and 18: follow-up from a randomised control trial.** Lancet (2006) 367, 1247–1255.

4 Garland, S.M. *et al.* **Quadrivalent vaccine against human papillomavirus to prevent anogenital diseases.** N Engl J Med (2007) 356, 1928–1943.

5 Gedvilaite, A. *et al.* **Formation of immunogenic virus-like particles by inserting epitopes into surface-exposed regions of hamster polyomavirus major capsid protein.** Virology (2000) 273, 21–35.

6 Gedvilaite, A. *et al.* **Segments of puumala hantavirus nucleocapsid protein inserted into chimeric polyomavirus-derived virus-like particles induce a strong immune response in mice.** Viral Immunol (2004) 17, 51–68.

7 Zvirbliene, A. *et al.* **Generation of monoclonal antibodies of desired specificity using chimeric polyomavirus-derived virus-like particles.** J Immunol Methods (2006) 311, 57–70.

8 Dorn, D.C. *et al.* **Cellular and humoral immunogenicity of hamster polyomavirus-derived virus-like particles harboring a mucin 1 cytotoxic T-cell epitope.** Viral Immunol (2008) 21, 12–27.

9 Chuan, Y.P. *et al.* **Effects of pre-existing anti-carrier immunity and antigenic element multiplicity on efficacy of a modular virus-like particle vaccine.** Biotechnol Bioeng (2013) 110, 2343–2351.

10 Mazeike, E., Gedvilaite, A. and Blohm, U. **Induction of insert-specific immune response in mice by hamster poly-**

omavirus VP1 derived virus-like particles carrying LCMV GP33 CTL epitope. Virus Res (2012) 163, 2–10.

11 Tegerstedt, K. *et al.* **A single vaccination with polyomavirus VP1/VP2Her2 virus-like particles prevents outgrowth of HER-2/neu-expressing tumors.** Cancer Res (2005) 65, 5953–5957.

12 Brinkman, M. *et al.* **Recombinant Murine Polyoma Virus-like-particles Induce Protective Antitumour Immunity.** Letters in Drug Design & Discovery (2004) 1, 137–147(111).

13 Tegerstedt, K. *et al.* **Dendritic cells loaded with polyomavirus VP1/VP2Her2 virus-like particles efficiently prevent outgrowth of a Her2/neu expressing tumor.** Cancer Immunol Immunother (2007) 56, 1335–1344.

14 Brinkman, M. *et al.* **Beneficial therapeutic effects with different particulate structures of murine polyomavirus VP1-coat protein carrying self or non-self CD8 T cell epitopes against murine melanoma.** Cancer Immunol Immunother (2005) 54, 611–622.

15 Topalian, S.L., Weiner, G.J. and Pardoll, D.M. **Cancer immunotherapy comes of age.** J Clin Oncol (2011) 29, 4828–4836.

16 Clark, B. *et al.* **Immunity against both polyomavirus VP1 and a transgene product induced following intranasal delivery of VP1 pseudocapsid-DNA complexes.** J Gen Virol (2001) 82, 2791–2797.

17 Rollman, E. *et al.* **Genetic immunization is augmented by murine polyomavirus VP1 pseudocapsids.** Vaccine (2003) 21, 2263–2267.

18 Samonskyte, L. *et al.* **Immunogenic properties of polyomavirus-derived recombinant virus-like particles: activation of murine spleen cell-derived dendritic cells.** Biologija (2006), 80–84.

19 Laing, P. *et al.* **The 'co-delivery' approach to liposomal vaccines: application to the development of influenza-A and hepatitis-B vaccine candidates.** J Liposome Res (2006) 16, 229–235.

20 Amidi, M. *et al.* **Antigen-expressing immunostimulatory liposomes as a genetically programmable synthetic vaccine.** Syst Synth Biol (2011) 5, 21–31.

21 Amidi, M. *et al.* **Induction of humoral and cellular immune responses by antigen-expressing immunostimulatory liposomes.** J Control Release (2012) 164, 323–330.

22 Nierkens, S. *et al.* ***In vivo*** **colocalization of antigen and CpG [corrected] within dendritic cells is associated with the efficacy of cancer immunotherapy.** Cancer Res (2008) 68, 5390–5396.

23 Molino, N.M. *et al.* **Biomimetic protein nanoparticles facilitate enhanced dendritic cell activation and cross-presentation.** ACS Nano (2013) 7, 9743–9752.

24 Zhu, Q. *et al.* **Toll-like receptor ligands synergize through distinct dendritic cell pathways to induce T cell responses: implications for vaccines.** Proc Natl Acad Sci U S A (2008) 105, 16260–16265.

25 Hogquist, K.A. *et al.* **T cell receptor antagonist peptides induce positive selection.** Cell (1994) 76, 17–27.

26 Barnden, M.J. *et al.* **Defective TCR expression in transgenic mice constructed using cDNA-based alpha- and beta-chain genes under the control of heterologous regulatory elements.** Immunol Cell Biol (1998) 76, 34–40.

27 Karttunen, J., Sanderson, S. and Shastri, N. **Detection of rare antigen-presenting cells by the lacZ T-cell activation assay suggests an expression cloning strategy for T-cell antigens.** Proc Natl Acad Sci U S A (1992) 89, 6020–6024.

28 Schwede, T. *et al.* **SWISS-MODEL: An automated protein homology-modeling server.** Nucleic Acids Res (2003) 31, 3381–3385.

29 Pettersen, E.F. *et al.* **UCSF Chimera – a visualization system for exploratory research and analysis.** J Comput Chem (2004) 25, 1605–1612.

30 Teunissen, E.A. *et al.* **Different proteins require different S30 extract protein concentrations for optimal expression.** Manuscript in preparation (2014).

31 Teunissen, E.A. *et al.* **Assembly of hamster polyomavirus VP1 into virus-like particles takes place in *Escherichia coli* but not after cell-free synthesis.** Manuscript in preparation (2014).

32 Samadi, N. *et al.* **The effect of lauryl capping group on protein release and degradation of poly(d,l-lactic-co-glycolic acid) particles.** J Control Release (2013) 172, 436–443.

33 Winzler, C. *et al.* **Maturation stages of mouse dendritic cells in growth factor-dependent long-term cultures.** J Exp Med (1997) 185, 317–328.

34 Mizukami, S. *et al.* **Both CD4+ and CD8+ T cell epitopes fused to heat shock cognate protein 70 (hsc70) can function to eradicate tumors.** Cancer Sci (2008) 99, 1008–1015.

35 Maecker, H.T. *et al.* **Cytotoxic T cell responses to DNA vaccination: dependence on antigen presentation via class II MHC.** J Immunol (1998) 161, 6532–6536.

36 Holubova, J. *et al.* **Delivery of large heterologous polypeptides across the cytoplasmic membrane of antigen-presenting cells by the Bordetella RTX hemolysin moiety lacking the adenylyl cyclase domain.** Infect Immun (2012) 80, 1181–1192.

37 Tolstov, Y.L. *et al.* **Human Merkel cell polyomavirus infection II. MCV is a common human infection that can be detected by conformational capsid epitope immunoassays.** Int J Cancer (2009) 125, 1250–1256.

38 Teunissen, E.A. *et al.* **Proof of concept for the directed evolution of virus-like particles derived from polyomaviruses.** Manuscript in preparation (2014).

39 Salunke, D.M., Caspar, D.L. and Garcea, R.L. **Polymorphism in the assembly of polyomavirus capsid protein VP1.** Biophys J (1989) 56, 887–900.

40 Kanesashi, S.N. *et al.* **Simian virus 40 VP1 capsid protein forms polymorphic assemblies *in vitro*.** J Gen Virol (2003) 84, 1899–1905.

41 Nilsson, J. *et al.* **Structure and assembly of a *T*=1 virus-like particle in BK polyomavirus.** J Virol (2005) 79, 5337–5345.

42 Rosalia, R.A. *et al.* **Efficient *ex vivo*** **induction of T cells with potent anti-tumor activity by protein antigen encapsulated in nanoparticles.** Cancer Immunol Immunother (2013) 62, 1161–1173.

43 Macian, F. **NFAT proteins: key regulators of T-cell development and function.** Nat Rev Immunol (2005) 5, 472–484.

44 Voronkova, T. *et al.* **Hamster polyomavirus-derived virus-like particles are able to transfer *in vitro*** **encapsidated plasmid DNA to mammalian cells.** Virus Genes (2007) 34, 303–314.

45 Gleiter, S., Stubenrauch, K. and Lilie, H. **Changing the sur-**

face of a virus shell fusion of an enzyme to polyoma VP1. Protein Sci (1999) 8, 2562–2569.

46 Shin, Y.C. and Folk, W.R. **Formation of polyomavirus-like particles with different VP1 molecules that bind the urokinase plasminogen activator receptor.** J Virol (2003) 77, 11491–11498.

47 Kurts, C., Robinson, B.W. and Knolle, P.A. **Cross-priming in health and disease.** Nat Rev Immunol (2010) 10, 403–414.

48 Gedvilaite, A. *et al.* **Virus-like particles derived from major capsid protein VP1 of different polyomaviruses differ in their ability to induce maturation in human dendritic cells.** Virology (2006) 354, 252–260.

49 Ou, W.C. *et al.* **The major capsid protein, VP1, of human JC virus expressed in *Escherichia coli* is able to self-assemble into a capsid-like particle and deliver exogenous DNA into human kidney cells.** J Gen Virol (1999) 80 (Pt 1), 39–46.

50 Pattenden, L.K. *et al.* **Towards the preparative and large-scale precision manufacture of virus-like particles.** Trends Biotechnol (2005) 23, 523–529.

51 Braun, H. *et al.* **Oligonucleotide and plasmid DNA packaging into polyoma VP1 virus-like particles expressed in *Escherichia coli*.** Biotechnol Appl Biochem (1999) 29 (Pt 1), 31–43.

52 Stokrova, J. *et al.* **Interactions of heterologous DNA with polyomavirus major structural protein, VP1.** FEBS Lett (1999) 445, 119–125.

53 Forstova, J. *et al.* **Polyoma virus pseudocapsids as efficient carriers of heterologous DNA into mammalian cells.** Hum Gene Ther (1995) 6, 297–306.

54 Yang, Y.W. and Chen, L.H. **Gene delivery via polyomavirus major capsid protein VP(1), isolated from recombinant *Escherichia coli*.** Biotechnol Appl Biochem (2000) 32 (Pt 1), 73–79.

55 Tegerstedt, K. *et al.* **Murine pneumotropic virus VP1 virus-like particles (VLPs) bind to several cell types independent of sialic acid residues and do not serologically cross react with murine polyomavirus VP1 VLPs.** J Gen Virol (2003) 84, 3443–3452.

56 Neefjes, J. *et al.* **Towards a systems understanding of MHC class I and MHC class II antigen presentation.** Nat Rev Immunol (2011) 11, 823–836.

57 Yewdell, J.W. and Nicchitta, C.V. **The DRiP hypothesis decennial: support, controversy, refinement and extension.** Trends Immunol (2006) 27, 368–373.

58 Stehle, T. *et al.* **Structure of murine polyomavirus complexed with an oligosaccharide receptor fragment.** Nature (1994) 369, 160–163.

59 Stehle, T. and Harrison, S.C. **Crystal structures of murine polyomavirus in complex with straight-chain and branched-chain sialyloligosaccharide receptor fragments.** Structure (1996) 4, 183–194.

60 Neu, U. *et al.* **Structural basis of GM1 ganglioside recognition by simian virus 40.** Proc Natl Acad Sci U S A (2008) 105, 5219–5224.

61 Neu, U. *et al.* **Structure-function analysis of the human JC polyomavirus establishes the LSTc pentasaccharide as a functional receptor motif.** Cell Host Microbe (2010) 8, 309–319.

62 Langner, J. *et al.* **RGD-mutants of B-lymphotropic polyomavirus capsids specifically bind to alpha(v)beta3 integrin.** Arch Virol (2004) 149, 1877–1896.

63 Takahashi, R.U. *et al.* **Presentation of functional foreign peptides on the surface of SV40 virus-like particles.** J Biotechnol (2008) 135, 385–392.

64 Eriksson, M. *et al.* **Murine polyomavirus virus-like particles carrying full-length human PSA protect BALB/c mice from outgrowth of a PSA expressing tumor.** PLoS One (2011) 6, e23828.

65 Aleksaite, E. and Gedvilaite, A. **Generation of chimeric hamster polyomavirus VP1 virus-like particles harboring three tumor-associated antigens.** Biologija (2006), 83–87.

66 Mazzaccaro, R.J. *et al.* **Major histocompatibility class I presentation of soluble antigen facilitated by Mycobacterium tuberculosis infection.** Proc Natl Acad Sci U S A (1996) 93, 11786–11791.

67 Van Meirvenne, S. *et al.* **Efficient genetic modification of murine dendritic cells by electroporation with mRNA.** Cancer Gene Ther (2002) 9, 787–797.

68 Desai, D.D. *et al.* **Fc gamma receptor IIB on dendritic cells enforces peripheral tolerance by inhibiting effector T cell responses.** J Immunol (2007) 178, 6217–6226.

Chapter IX

Summarizing discussion and future perspectives

Summarizing discussion and future perspectives

Part I: Research

The original project plan

Virus-like particles (VLPs) are promising vectors for both gene delivery and vaccination. These particles form a bridge between viral and non-viral gene delivery systems, retaining the elite transduction characteristics of viral vectors, but without the potentially severe adverse effects wrought by viral genetic material. VLPs are formed by the assembly of viral structural proteins without packaging viral genetic material after their recombinant overexpression. For some viruses, such empty capsids are even formed as accidental by-products of infection [1,2]. These particles resemble the structure, immunogenicity, tropism, and transduction efficiency of the virus they are derived from.
The goal of this project was to develop an evolution-based method for the improvement of the characteristics of VLPs for gene delivery. We chose to use the VLPs derived from polyomaviruses – in particular the hamster polyomavirus (HaPyV) – as model vectors for our studies. In **chapter 2** we highlighted the structural characteristics of these VLPs and gave an overview of their current applications in diagnostics, vaccine development and gene delivery. The plan was to create vast libraries of mutant capsid genes, and from these libraries, select clones that possess improved properties for gene delivery. The expression of the libraries would be performed using a cell-free protein synthesis system compartmentalized into small, micrometer-scale emulsion droplets with on average one gene per droplet; a technique called *in vitro* compartmentalization (IVC). Inside these droplets, the genes would be transcribed and translated into capsid proteins, and these proteins would assemble together with their own coding DNA to form what we call *artificial viruses* – VLPs that encapsidate their own synthetic genome. Because the proteins cannot leave the droplets, they would be forced to associate with only their own coding DNA, thus providing the indispensable genotype-phenotype linkage. However, over the course of our research this proved to be impossible.

Cell-free synthesis of VLPs

In **chapter 5** we described our efforts at synthesizing HaPyV VLPs in prokaryotic cell-free expression systems. Despite the many conditions we tested, none of these conditions led to VLP assembly sufficient for *in vitro* compartmentalization. Without assembly, there is no genotype-phenotype linkage, and thus no directed evolution. We also discovered that the formation of VLPs after expression in *E. coli* already takes place inside the cells before lysis. Therefore, the obvious alternative would be to express the libraries inside bacteria, where the expression is, in effect, also compartmentalized. However, in **chapter 8** we showed that, although wild-type HaPyV VLPs did form and did encapsidate nucleic acids after expression inside bacteria, no detectable amounts of plasmid DNA were observed. We were unable to replicate the results of another research group, that showed the packing of plasmid DNA by VLPs derived from JC polyomavirus after their expression in *E. coli* [3,4].
We originally assumed that artificial viruses would form based on several observations. First of all, similar experiments had been performed before with non-viral DNA-binding proteins [5]. Other groups previously demonstrated the formation of VLPs [6,7], including those derived from polyomaviruses [8], after expression of coat proteins in bacteria. For other viruses the same had been demonstrated after cell-free expression [9]. Furthermore, VLPs derived from polyomaviruses were shown to encapsidate nucleic acids after their expression in

bacteria [10]. Nonetheless, we were not able to assemble artificial viruses.

Requirements for artificial virus formation

Based on literature, we identified several factors that might enhance the efficient assembly of polyomavirus VLPs that encapsidate their own coding DNA. These include chaperones (hsp70) [11,12], hyper-acetylated histones [13], transcription factors (Sp1 and AP-2) [14,15], polyomavirus VP2/3 [13,15], SV40 large T antigen [12,16,17], SV40 signal for encapsidation (*ses*) [14,15,18], and SV40 origin of replication (*ori*) [16,17]. According to our current hypothetical model, the SV40 large T antigen causes the amplification of the expression plasmid carrying the SV40 *ori* and SV40 *ses*, resulting in a high copy-number [16,17]. Directly after translation, VP1 binds hsp70 [11], preventing the premature formation of VLPs [12]. The capsid proteins are then transported to the nucleus in the form of capsomers [19]. Hyper-acetylated histones compact the DNA, allowing the entire plasmid to be encapsidated [13]. Transcription factors bind the SV40 *ses* [14] and form a complex that recruits the capsomers, conferring packaging specificity [15]. Next, the SV40 large T antigen induces the assembly of the VLPs [12].
Such a system can be reconstituted effectively in 293TT cells. This mammalian cell line constitutively produces the SV40 large T antigen [16]. Reporter VLPs derived from several polyomaviruses were produced in these cells by co-transfection with plasmids encoding the capsid genes and a reporter plasmid, carrying the SV40 elements and an EGFP gene [17,20]. This resulted in the assembly of VLPs with the reporter plasmid, which could subsequently be used for diagnostic neutralization assays.

Proof of concept for directed evolution

In **chapter 6** we employed the same system to provide a proof of concept for the functional selection of polyomavirus VLPs, using SV40 as model delivery system. For the expression of libraries, we developed an efficient expression vector with functional SV40 elements. To demonstrate genotype-phenotype linkage, we co-transfected 293TT cells with two of these expression vector constructs, one encoding wild-type VP1, the other one a non-functional mutant. After VLP purification, we analyzed the fractions for *VP1* DNA. As the VLPs form, they package available genetic material compartmentalized within the same cell. We observed a 10-fold enrichment of wild-type *VP1* DNA after a single round of selection. This data shows that the VLPs package their own coding DNA, making sure that the genetic origin of improved VLPs can be traced back after selection.
In **chapter 6** we also showed that it is possible to recombine different polyomavirus *VP1* genes using DNA shuffling. This way, beneficial properties of the different polyomaviruses can be combined, and large evolutionary gaps can be bridged. We showed that the binding domains are efficiently exchanged between the different viruses, allowing the creation of VLPs with novel tropism.
We are currently in the process of replicating these results. The next step would be to combine these two experiments, *i.e.* to perform selections with our library. The first selections might be based on VLP formation and DNA packaging. Once successful, more advanced selections, such as retargeting, could be performed. Ultimately, this technique could aid in the development of novel viral vectors suitable for personalized medicine.

Artificial viruses vs. recombinant viral vectors

It must be noted that the modifications described in **chapter 6** have shifted the assembly from a synthetic *in vitro* reaction, to a system mimicking natural polyomavirus infection. In fact, one might argue whether these particles are VLPs at all. Not only do these particles contain DNA encoding VP1, they also contain the viral origin of replication and packaging signal. All things considered, these par-

ticles are nearly identical to recombinant SV40 vectors, a type of viral vector in which the early SV40 genes (T antigens) are replaced by transgenes [21–24]. However, using such vectors does not preclude the possibility of generating VLPs from the VP1 proteins of these viral vectors, and thereby benefitting from the enhanced safety features of VLPs. Therefore, I propose to use viral vectors during directed evolution, to exploit their efficient assembly and to stimulate and maintain genotype-phenotype linkage. The selections can then be performed using these recombinant vectors, and once improved vectors are obtained, VLPs can be generated for production and development.

In theory, these viral vectors might inadvertently lose the ability to form VLPs (*e.g.* the assembly might become dependent on the viral SV40 sequences). However, given the diversity of polyomaviruses known to form VLPs (see **chapter 2**), and the fact that evolution also selects based on DNA packaging, we expect this chance to be negligible. Moreover, if the selections do lead to such unexpected results, this could provide insight into the mechanisms of selective DNA packaging.

Benefits of *in vitro* compartmentalization

No matter how efficient a eukaryotic cell-based expression system might be, it is still confined to the limits of cell culture and transfection. Consequently, this puts a limit on the number of clones from a single library that can be screened [25]. Using different techniques, very large libraries of up to 10^{15} molecules can be created [25–28]. However, transformation of the library into bacteria for propagation and amplification reduces the diversity of the library to around 10^6–10^8 clones [25,27]. Next, transfection further reduces this number, leading to a final amount of 10^5–10^7 clones screened in directed evolution experiments involving viral vectors [29–34]. If bacteria are used to express the library, this number can be somewhat higher, but even after lengthy optimization and by scaling up to several hundreds of transformations no more than about 10^{10} clones can be screened [35,36].

IVC, on the other hand, is not bound to such limitations. Libraries can be emulsified directly after preparation, obviating the need to propagate and amplify the libraries in bacteria. This allows for a much higher number of clones to be screened, up to 10^{15} [27]. Such a high diversity is necessary for the advanced selections that are required for the directed evolution of gene therapy vectors, where a much larger evolutionary distance needs to be crossed [27,28]. Therefore, it might, on the long run, be better to continue the development of an IVC-based method. A good place to start would be to test different eukaryotic extracts for the production of polyomavirus VLPs. These extracts more closely mimic the natural assembly conditions. One of these extracts, based on rabbit reticulocyte lysate, was successfully used for the expression of VLPs derived from the closely-related human papillomavirus [37], although at a low yield. No mention was made of DNA packaging. Another system, based on HeLa cell extract, was used to synthesize infective poliovirus [38]. If the expression is too low for IVC, one might try a mammalian extract with a sufficiently high expression yield, such as the recently described CHO extract [39]. It might, however, also be possible to adhere to prokaryotic cell-free expression systems. Using a large, diverse library of high quality, it might be possible to screen for VP1 proteins that do associate with their coding DNA after prokaryotic cell-free expression. These clones could then be used as the starting point for further rounds of directed evolution. A nuclease treatment could be included to favor those clones that truly encapsidate their genomes. Alternatively, one could choose another virus as the starting point for directed evolution. VLPs are known to form after the cell-free expression of viral proteins, such as bacteriophage Qβ coat protein (CP) [40], human papillomavirus (HPV) type 16 capsid protein L1 [37], bacteriophage MS2 coat protein [9,40], and hepatitis B virus (HBV) core antigen [9,40]. Unfortunately, none of these reports mention anything regarding nucleic acid uptake.

Taken together, the following conditions should be satisfied before IVC can be used for the directed evolution of VLPs. First, enough capsid protein should be expressed within a single droplet to form a VLP. Second, VLPs should be able to form within these droplets after expression. And third, these VLPs should encapsidate their own synthetic genome.

Depending on the intended goal or application, different strategies would be advisable. If one wants to play safe, it might be prudent to cling to the proven strategy involving 293TT cells. Although this puts a significant constraint on the library size, it is likely to provide reasonable results in simple selection experiments such as those involving transfection efficiency or retargeting. If, on the other hand, a more long-term goal, such as the development of viral vectors, is pursued, IVC would be the choice. In this case, it would be wise to first achieve DNA packaging before performing selections based on gene delivery, as a general lack of genotype-phenotype linkage would significantly reduce the quality of the library for these selections. Proving this linkage might be a tough challenge, given the results presented in this thesis. Then again, IVC might be the only realistic option for advanced selections.

Standardization of cell-free expression

The most important component of any cell-free expression system is the cellular extract, which provides the machineries for the translation of proteins. During this project, we prepared numerous batches of *E. coli* S30 extract, the cellular extract used in our cell-free expression system. We noticed that, despite using the same production protocol, cell-free expression suffered from a high batch-to-batch variability of the S30 extracts, with some extracts providing very high activity, while other extracts were almost completely inactive. In **chapter 3** we investigated this variability with the goal of reducing it. We found that the different batches of the S30 extracts differed significantly in their total protein concentration. Moreover, by normalizing this protein concentration after S30 extract production, we could reduce the variability in the activity of the S30 extracts. Importantly, by diluting some of the more concentrated extracts, we could significantly enhance the yield after cell-free expression of our model protein, β-galactosidase.

Although it might seem logical to normalize extracts after their production, to our surprise this is not standard practice. By digging deeper into the literature, we found that very early protocols for cell-free expression do use a standardized amount of extract protein in each reaction [41–46]. However, this changed in 1979, when a protocol was published in which a fixed volume of non-normalized S30 extract, rather than a given amount of S30 extract protein, was used for cell-free expression [47]. We believe this publication to be the source of this change; future protocols copied this publication, and since then S30 standardization based on protein content has died a slow death.

In **chapter 4**, we further investigated the relationship between extract protein concentration and yield of expression. We showed that the relationship is more complex than previously assumed. We expressed several different proteins in our cell-free expression system, and found that the expression of each protein is optimal at a different extract protein concentration. Moreover, this optimal extract protein concentration was shown to change with different reaction conditions such as incubation temperature. We believe that, by optimizing the extract protein concentration for each new protein to be expressed, a lot could be gained in terms of productivity. We extended our results to commercially available systems, showing a similar benefit of optimizing the extract protein concentration.

Standardization of S30 extracts is particularly important for studies in which conclusions are drawn based on expression yields. A lack of standardization can result in false conclusions being drawn. For example, one study, aimed at identifying the limiting components of S30 extract, found none of the components to be limiting [48]. However,

the study was performed by adding the individual components to an extract that already by far exceeded the optimal concentration for expression; at such a concentration none of the extract components were limiting.

Standardization itself is not a requirement *per se*. If the yield of expression is not an issue, as is the case in most studies using cell-free expression as a tool rather than a goal by itself, it is not necessary to optimize the expression unless problems are encountered. Moreover, such optimization is not possible when the cellular extracts are used for high-throughput techniques such as *in vitro* compartmentalization, as each protein would require its own unique extract protein concentration. It does show that the expression with such techniques might be biased based on the extract concentration used. For commercial suppliers of cell-free extracts it would be interesting to normalize their products, although it is likely that this is already standard practice.

The optimal concentration of S30 extract protein in cell-free expression reactions is much lower than the protein concentration inside bacteria, and consequently the synthesis rates and yields of cell-free expression are much lower than those *in vivo* [49]. At this moment it is not known why cell-free expression cannot be achieved at cellular levels. Possible reasons include the degradation of key compounds, such as amino acids, energy sources and mRNA by enzymes not responsible for protein synthesis [50–52], the limited solubility of the produced protein [53], or the denaturation or degradation of the protein synthesis machinery. However, we found no indication that any of these factors are responsible for this discrepancy. It would be very interesting to discover the reasons behind this. Not only might this result in a significantly enhanced expression yield, it would also help us to understand the fundamental differences between biochemical processes *in vitro* and *in vivo* [54,55] and the effects macromolecular crowding has inside cells [56–58], and aid us in the creation of artificial cells [59,60].

In the past, cell-free expression has been used to make many important discoveries, such as the elucidation of the genetic code [61]. Over the years, cell-free expression has undergone a true revolution, giving rise to quite spectacular increases in production yields [62,63]. The technique is indispensable for many high-throughput expression techniques such as IVC. Cell-free expression will likely continue to play an important role in the future. Certainly the purified systems [64], which contain only those components necessary for transcription and translation of genes, are exciting.

Part II: Applications

Analysis of VLPs in serum

In **chapter 7**, we investigated two approaches to study HaPyV VLPs in biological environments. In the first part, we tested a clonable tag based on murine metallothionein, which is capable of binding heavy metal ions and providing additional contrast for transmission electron microscopy. We inserted this tag into surface-exposed loops of VP1. Although full-length VP1 proteins were expressed, we were unable to generate VLPs. In retrospect, it has become clear that, given the bulky dimensions of the tag and the lack of a proper flexible peptide linker, it is questionable whether these constructs will ever be adaptable to forming VLPs. Moreover, the abundance of disulfide bonds in the tag will most likely interfere with the correct folding of VP1. Though unlikely, it might be possible to stimulate assembly by adding heavy metals to the medium to promote the correct folding of the tag [65], and by co-expressing the tagged VP1s with wild-type VP1 to relieve some of the steric hindrance [66]. Yet, even if VLPs would form, it is doubtful whether these particles would provide valuable physiological information, as the tags will probably interfere with properties such as receptor binding and internalization [67,68].

In the second part of **chapter 7** we explored nanoparticle tracking analysis (NTA) for the detection

of VLPs. Using a NanoSight instrument, we were able to measure the particle size distribution of VLPs, and by fluorescently labeling these VLPs, we could detect them in a background of serum, which, under normal conditions, completely obscured detection. However, it is unlikely that nanoparticle tracking analysis with the NanoSight LM10, in its current format, can provide reliable quantitative data on VLPs; it is simply not reproducible enough. Variability originates both at the level of measurement (by choosing the location for the measurement by focusing the microscope on the laser beam) and that of the analysis (by changing the parameters). For future applications, this system would benefit greatly from a reduction in this variability.

VLPs as vaccines

Because of their repetitive structure, VLPs can bind to pattern-recognition receptors on immune cells and cross-link B-cell receptors [69], inducing potent immune responses against the virus they are derived from. The lack of viral genetic material makes them safer as a vaccine than attenuated and inactivated viruses. These benefits have led to the clinical investigation of several VLP-based vaccines [70,71], some of which are already available on the market, such as the prophylactic HPV vaccines Gardasil® [72] and Cervarix® [73].

Although human polyomaviruses can cause severe disease in immunocompromised individuals, it is unlikely that prophylactic vaccination will become cost-effective in the near future, given that the majority of the population is already seropositive for these viruses, and infection is mostly asymptomatic. Prophylactic vaccination against avian polyomaviruses, which cause a much more acute disease [74], is more interesting from an economic perspective, and an inactivated virus vaccine is already available in veterinary medicine for psittacines [75,76].

Besides vaccination against the wild-type virus itself, it is also possible to induce both humoral and cellular immune responses against foreign epitopes inserted into variable loops on the surface of VLPs [77] or fused to VP1 [78] or (truncated) VP2/3 [79]. Furthermore, VLPs can be loaded with plasmids encoding antigens [80,81] and activators of innate immunity, such as CpG [82], further enhancing their immunogenicity. In **chapter 8** we explored the possibility of combining DNA and epitope vaccination, based on the hypothesis that such co-delivery will lead to a synergistic effect [83,84]. We inserted different model epitopes from ovalbumin into surface-exposed loops of VP1. In contrast to the results obtained with the metallothionein tag, expression of these VP1 proteins resulted in VLP formation, although the particles were smaller than wild-type VLPs. Several of the constructs were able to induce potent immune responses *in vitro*, although their smaller size probably limits their DNA uptake capacity. Due to time constraints, we were not able to test these particles in association with DNA. Such a strategy might make it possible to break immune tolerance, a crucial step in the vaccination against autoimmune diseases and cancer, and a step towards the development of therapeutic vaccines. However, we are still very far away from a final product, with several challenges remaining to be solved.

One of the major issues associated with such VLP-based vaccines is pre-existing immunity against the wild-type virus. Although it was recently shown that even after prior immunization with wild-type VLPs, which resulted in high levels of anti-VP1 antibodies, the immune response against displayed epitopes is not completely abolished [85], it is questionable whether this is a general finding, and will not lead to either loss of efficacy or even adverse clinical reactions.

Furthermore, the insertion of epitopes into the surface-exposed loops of VLPs takes a lot of time and effort. Other strategies have been developed to couple foreign antigens to VLPs using universal linkers, thereby speeding up the development process. In the light of rapidly mutating infectious agents and the threat of a pandemic caused by

pathogens such as influenza, rapid vaccine development is required. With these new techniques, polyomavirus VLPs could fulfill the requirements, although the use of such a linker only further increases the complexity of an already complex system. Whole antigens can also be loaded into VLPs to induce strong antigen-specific cytotoxic T cell responses. It remains to be seen which strategy – loading with nucleic acids or loading with whole antigens – results in a better immune response, capable of breaking tolerance.

VLPs FOR GENE THERAPY

It is becoming increasingly clear that the field of gene therapy follows the general shape of the Gartner hype cycle [86]. First, the expectations are inflated out of proportion based on the theoretical potential, followed by an inevitable collapse as the field fails to deliver. Then, after some time, it will slowly start to rise again and produce the first positive, but realistic results. We have just recently entered this phase [87], and it will be many years before we will witness the full potential of gene therapy.

There are many challenges to be overcome to achieve successful gene delivery [88]. Being of viral origin, transfection itself is not the biggest problem for VLPs. Efficient encapsidation protocols have been developed to load VLPs with nucleic acids. Although, as described in **chapter 8**, we found that the two strategies we tested – reassembly of VLPs from capsomers in the presence of plasmid DNA and mixing of preformed VLPs with plasmid DNA – do not provide significant protection against nucleases, and do not result in transfection, more advanced encapsidation protocols, resulting in more efficient loading, have been developed, such as those based on 293TT cells [17,20]. Furthermore, such packaging protocols, incorporating VP2/3, allow the VLPs to reach transfection efficiencies similar to those of wild-type virions. It must be noted that, also here, recent advances have shifted the assembly and transfection from a synthetic *in vitro* reaction, to a system resembling natural polyomavirus assembly and uptake.

Most of the published data on the use of polyomavirus VLPs for gene delivery concerns simple and artificial transfection studies. We reviewed these studies in **chapter 2.** Although good results have been obtained in such studies, they are hardly representative of the real situation. That is, the biggest challenge gene delivery with VLPs faces is targeting; reaching the target cells. This is evident from the fact that, while polyomavirus VLPs have shown good results *in vitro* using single cell lines, up to now, *in vivo* results are still lacking. An efficient anti-tumor response was observed in several studies [3,89]. Yet, these studies were performed using human cancer cells in immunocompromised mice, starting the treatment before the tumor could be detected; a situation which does not mimic reality. After injection, the VLPs have to evade the immune system, extravasate, penetrate through tissue, and bind to the correct cells. Only then are the particles allowed to start their transduction.

Cancer gene therapy has its own unique set of challenges [90]. First of all, cancer is not a single disease, but a collective name of many different, heterogeneous diseases [91]. Moreover, there is a huge variability between patients with the same type of cancer, or even within the same patient, depending on the progression of the disease [91,92], making it impossible for a single vector to specifically reach all cancer cells. Unlike the popular representation of active targeting, this is still a random process based on distribution and binding [93,94]. During this distribution phase, the VLPs again have to avoid the immune system, extravasate, and penetrate through tissue to reach the cancer cells. These challenges are exacerbated by elevated interstitial fluid pressure in the tumor and an abnormal extracellular matrix structure [90]. Then, once the VLPs reach the tumor, they have to bind to the cancer cells and transduce them. This is further frustrated by the high mutation rate of these cells, allowing cells to escape transduction by changing their receptor profile [95,96].

In conclusion, reality is far more complex than usually portrayed. Part of the problem is caused by the human desire to express concepts in anthropomorphic terms such as "active targeting" or "recruitment", which present a false picture of reality. Up to now most studies have incorrectly focused on transfection efficiency, while ignoring the most important challenge – getting there.

Large-scale production of VLPs

Recent advances have enabled the large-scale production and purification of polyomavirus VLPs [97–101]. The mere fact that these VLPs can be produced in prokaryotic hosts at high yields already significantly reduces the production costs. Moreover, the availability of two VLP-based vaccines demonstrates that this can be done in a cost-effective way.

However, production will remain an important issue, certainly with the advent of personalized medicine. The rapid creation of personalized VLPs based on the modification of the surface will be very expensive and unreliable, and will, at least for the near future, remain out of reach. The same holds true for the products of directed evolution. Moreover, next to the many experimental obstacles that still have to be overcome, regulatory issues also prevent the commercial availability of such personalized VLPs, similar to the problems faced by phage therapy [102,103]. These regulatory and patent issues have to be overcome to prevent these particles from becoming merely a curiosity.

Part III: Future

Artificial life

The recent years have seen a blurring of the line between lifeless and living, incited by the construction of synthetic organisms. In 2002, for the first time, a replicating virus (poliovirus) was synthesized without the intervention of living cells [104]. This was done by assembling the complete genome from oligonucleotides, followed by its expression in a HeLa-based cell-free expression system. Similarly, synthetic genomes were also prepared from bacteriophage Phi-X174 [105] and Spanish Flu from 1918 [106], and in 2008 the first complete bacterial genome, from *Mycoplasma genitalium*, was synthesized [107]. The year 2010 saw the birth of the first cell with a synthetic genome [108]. The complete genome of the bacterium *Mycoplasma mycoides* was chemically synthesized, and upon its transplantation into a recipient cell from a different strain, the synthetic DNA took over and formed a new, semi-synthetic organism. This organism was not completely artificial yet, as the genome was transplanted into another, living bacterium. It will probably not be long until the first truly synthetic cell is created. Cell-free expression will continue to play a major role in the progress of this field [109–111], helping us to understand the fundamental basics of life. Such technologies will not only revolutionize the creation of novel microbes for biotechnology; they might, in the distant future, very well be used to bring extinct species back to life. Given the half-life of DNA [112], it will most likely be impossible to do so for dinosaurs, though a mammoth might very well be plausible in the future [113], once and if eukaryotic genomes can be synthesized.

Synthetic perfection

The recent decade has also seen considerable progress in the field of rational protein design. While 15 years ago, the design of functional proteins was still impossible [114–116], now several enzymes have been designed completely *de novo* that catalyze reactions that no known naturally occurring enzymes can catalyze [117–119]. The design of a gene delivery vector, on the other hand, is of a different order of magnitude. For such a vector, there is no transition state that can be stabilized to solve the entire puzzle. While rational design might, for example, suggest adding a different targeting ligand to the particles, this targeting ligand might,

inadvertently, increase the immunogenicity of the particles, thus leading to faster clearance, and, in effect, less binding. As of now, such effects cannot be predicted.

Directed evolution has the potential to solve this problem, as long as the VLPs are selected based on the final goal, and not an intermediate endpoint. However, most selection experiments for the directed evolution of viral vectors are based on *in vitro* transfection efficiency, usually to demonstrate novel tropism [33,120]. These vectors are unlikely to demonstrate the same specificity *in vivo*. Bluntly speaking, one gets what one selects for.

In most of the cases, the first step in directed evolution remains the rational selection of a starting point. This is not strictly necessary, but it facilitates the initial bridging of a large evolutionary gap. However, multiple building blocks may also be chosen, instead of full-length proteins [121]. The complete *de novo* evolution of a gene delivery vehicle is seemingly impossible, as only a miniscule fraction of the total sequence space can be covered by any library [27]. However, the same holds true for any protein in nature, and yet they do exist. This indicates that the total sequence space must contain multiple proteins with similar functionalities, and that libraries of a certain size are expected to contain such a protein. Because natural diversity also originated from only a fraction of the total sequence space, screening such a library is likely to lead to proteins that are completely different from naturally occurring ones, yet have similar properties [28]. This way, novel vectors could be created that are totally different from what currently exists in nature; a feat that could not be accomplished using error-prone PCR or DNA shuffling [122].

Library size and quality will be an important determinant for the success of such an experiment. When using such a library, it might be beneficial to first screen for simple things, such as DNA binding and later transfection efficiency, to increase the likelihood of finding suitable proteins. One must always be aware of genetic drift during these selections, and design the selection experiments accordingly. Once suitable starting points have been found, techniques, similar to DNA shuffling, might be used to combine these novel vectors to create further diversity. For example, the homology-independent recombination technique called incremental truncation for the creation of hybrid enzymes (ITCHY) [123] could then be used to mix different novel genes to form even better vectors.

The future is likely to see a combination of the above-mentioned strategies. Rational design could first be used to create rough estimates of target proteins, which are subsequently refined by directed evolution. Directed evolution could also be incorporated into an iterative process of rational design, leading to an enhanced understanding of the underlying principles [124]. Such semi-rational approaches are likely to give better results than rational design or directed evolution alone [125]. Finally, the recent dramatic decrease in cost of whole genome sequencing will revolutionize health care, allowing patients to have their genomes or malignancies sequenced before treatment, opening opportunities for personalized treatment. We are at the dawn of a new era of personalized, predictive and preventive medicine.

References

1 Mayr, G.A. *et al.* **Immune responses and protection against foot-and-mouth disease virus (FMDV) challenge in swine vaccinated with adenovirus-FMDV constructs.** Vaccine (2001) 19, 2152–2162.

2 Aposhian, H.V., Thayer, R.E. and Qasba, P.K. **Formation of nucleoprotein complexes between polyoma empty capsides and DNA.** J Virol (1975) 15, 645–653.

3 Chen, L.S. *et al.* **Efficient gene transfer using the human JC virus-like particle that inhibits human colon adenocarcinoma growth in a nude mouse model.** Gene Ther (2010) 17, 1033–1041.

4 Fang, C.Y. *et al.* **Analysis of the size of DNA packaged by the human JC virus-like particle.** J Virol Methods (2012) 182, 87–92.

5 Fen, C.X. *et al.* **Directed evolution of p53 variants with altered DNA-binding specificities by *in vitro* compartmen-**

talization. J Mol Biol (2007) 371, 1238–1248.

6 Saini, M. and Vrati, S. **High-level synthesis of Johnson grass mosaic virus coat protein in *Escherichia coli* and its auto-assembly to form virus-like particles.** Protein Expr Purif (2003) 28, 86–92.

7 Aires, K.A. *et al.* **Production of human papillomavirus type 16 L1 virus-like particles by recombinant Lactobacillus casei cells.** Appl Environ Microbiol (2006) 72, 745–752.

8 Goldmann, C. *et al.* **Molecular cloning and expression of major structural protein VP1 of the human polyomavirus JC virus: formation of virus-like particles useful for immunological and therapeutic studies.** J Virol (1999) 73, 4465–4469.

9 Bundy, B.C., Franciszkowicz, M.J. and Swartz, J.R. ***Escherichia coli*-based cell-free synthesis of virus-like particles.** Biotechnol Bioeng (2008) 100, 28–37.

10 Voronkova, T. *et al.* **Hamster polyomavirus-derived virus-like particles are able to transfer *in vitro* encapsidated plasmid DNA to mammalian cells.** Virus Genes (2007) 34, 303–314.

11 Cripe, T.P. *et al.* ***In vivo* and *in vitro* association of hsc70 with polyomavirus capsid proteins.** J Virol (1995) 69, 7807–7813.

12 Chromy, L.R., Pipas, J.M. and Garcea, R.L. **Chaperone-mediated *in vitro* assembly of Polyomavirus capsids.** Proc Natl Acad Sci U S A (2003) 100, 10477–10482.

13 Enomoto, T. *et al.* ***In vitro* reconstitution of SV40 particles that are composed of VP1/2/3 capsid proteins and nucleosomal DNA and direct efficient gene transfer.** Virology (2011) 420, 1–9.

14 Dalyot-Herman, N. *et al.* **The simian virus 40 packaging signal ses is composed of redundant DNA elements which are partly interchangeable.** J Mol Biol (1996) 259, 69–80.

15 Gordon-Shaag, A. *et al.* **Cellular transcription factor Sp1 recruits simian virus 40 capsid proteins to the viral packaging signal, *ses*.** J Virol (2002) 76, 5915–5924.

16 Buck, C.B. *et al.* **Efficient intracellular assembly of papillomaviral vectors.** J Virol (2004) 78, 751–757.

17 Pastrana, D.V. *et al.* **Quantitation of human seroresponsiveness to Merkel cell polyomavirus.** PLoS Pathog (2009) 5, e1000578.

18 Oppenheim, A. *et al.* **A cis-acting DNA signal for encapsidation of simian virus 40.** J Virol (1992) 66, 5320–5328.

19 Ishii, N. *et al.* **Functional complementation of nuclear targeting-defective mutants of simian virus 40 structural proteins.** J Virol (1994) 68, 8209–8216.

20 Tolstov, Y.L. *et al.* **Human Merkel cell polyomavirus infection II. MCV is a common human infection that can be detected by conformational capsid epitope immunoassays.** Int J Cancer (2009) 125, 1250–1256.

21 Strayer, D.S. **SV40 as an effective gene transfer vector *in vivo*.** J Biol Chem (1996) 271, 24741–24746.

22 Strayer, D.S. **Effective gene transfer using viral vectors based on SV40.** Methods Mol Biol (2000) 133, 61–74.

23 Strayer, D.S. *et al.* **Generation of recombinant SV40 vectors for gene transfer.** Methods Mol Biol (2001) 165, 103–117.

24 Vera, M. *et al.* **Factors influencing the production of recombinant SV40 vectors.** Mol Ther (2004) 10, 780–791.

25 Leemhuis, H. *et al.* **New genotype-phenotype linkages for directed evolution of functional proteins.** Curr Opin Struct Biol (2005) 15, 472–478.

26 Cho, G. *et al.* **Constructing high complexity synthetic libraries of long ORFs using *in vitro* selection.** J Mol Biol (2000) 297, 309–319.

27 Griffiths, A.D. and Tawfik, D.S. **Man-made enzymes – from design to *in vitro* compartmentalisation.** Curr Opin Biotechnol (2000) 11, 338–353.

28 Keefe, A.D. and Szostak, J.W. **Functional proteins from a random-sequence library.** Nature (2001) 410, 715–718.

29 Soong, N.W. *et al.* **Molecular breeding of viruses.** Nat Genet (2000) 25, 436–439.

30 Perabo, L. *et al.* **Combinatorial engineering of a gene therapy vector: directed evolution of adeno-associated virus.** J Gene Med (2006) 8, 155–162.

31 Grimm, D. *et al.* ***In vitro* and *in vivo* gene therapy vector evolution via multispecies interbreeding and retargeting of adeno-associated viruses.** J Virol (2008) 82, 5887–5911.

32 Excoffon, K.J. *et al.* **Directed evolution of adeno-associated virus to an infectious respiratory virus.** Proc Natl Acad Sci U S A (2009) 106, 3865–3870.

33 Maguire, C.A. *et al.* **Directed evolution of adeno-associated virus for glioma cell transduction.** J Neurooncol (2010) 96, 337–347.

34 Dalkara, D. *et al.* ***In vivo*-directed evolution of a new adeno-associated virus for therapeutic outer retinal gene delivery from the vitreous.** Sci Transl Med (2013) 5, 189ra176.

35 de Haard, H.J. *et al.* **A large non-immunized human Fab fragment phage library that permits rapid isolation and kinetic analysis of high affinity antibodies.** J Biol Chem (1999) 274, 18218–18230.

36 Vaughan, T.J. *et al.* **Human antibodies with sub-nanomolar affinities isolated from a large non-immunized phage display library.** Nat Biotechnol (1996) 14, 309–314.

37 Iyengar, S. *et al.* **Self-assembly of *in vitro*-translated human papillomavirus type 16 L1 capsid protein into virus-like particles and antigenic reactivity of the protein.** Clin Diagn Lab Immunol (1996) 3, 733–739.

38 Molla, A., Paul, A.V. and Wimmer, E. **Cell-free, *de novo* synthesis of poliovirus.** Science (1991) 254, 1647–1651.

39 Brodel, A.K., Sonnabend, A. and Kubick, S. **Cell-free protein expression based on extracts from CHO cells.** Biotechnol Bioeng (2014) 111, 25–36.

40 Bundy, B.C. and Swartz, J.R. **Efficient disulfide bond formation in virus-like particles.** J Biotechnol (2011) 154, 230–239.

41 Nirenberg, M.W. **Cell-free protein synthesis directed by messenger RNA.** Methods Enzymol (1963) 6, 17–23.

42 Lederman, M. and Zubay, G. **DNA-directed peptide synthesis. 1. A comparison of T2 and Escherichi coli DNA-directed peptide synthesis in two cell-free systems.** Biochim Biophys Acta (1967) 149, 253–258.

43 Lederman, M. and Zubay, G. **DNA directed peptide synthesis. V. The cell-free synthesis of a polypeptide with beta-galactosidase activity.** Biochem Biophys Res Commun (1968) 32, 710–714.

44 Dottin, R.P. and Pearson, M.L. **Regulation by N gene protein**

of phage lambda of anthranilate synthetase synthesis *in vitro*. Proc Natl Acad Sci U S A (1973) 70, 1078–1082.

45 Wetekam, W., Staack, K. and Ehring, R. **DNA-dependent *in vitro* synthesis of enzymes of the galactose operon of *Escherichia coli*.** Mol Gen Genet (1971) 112, 14–27.

46 Zubay, G. ***In vitro* synthesis of protein in microbial systems.** Annu Rev Genet (1973) 7, 267–287.

47 Collins, J. **Cell-free synthesis of proteins coding for mobilisation functions of ColE1 and transposition functions of Tn3.** Gene (1979) 6, 29–42.

48 Freischmidt, A. *et al.* **Limiting factors of the translation machinery.** J Biotechnol (2010) 150, 44–50.

49 Underwood, K.A., Swartz, J.R. and Puglisi, J.D. **Quantitative polysome analysis identifies limitations in bacterial cell-free protein synthesis.** Biotechnol Bioeng (2005) 91, 425–435.

50 Kim, R.G. and Choi, C.Y. **Expression-independent consumption of substrates in cell-free expression system from *Escherichia coli*.** J Biotechnol (2001) 84, 27–32.

51 Michel-Reydellet, N., Calhoun, K. and Swartz, J. **Amino acid stabilization for cell-free protein synthesis by modification of the *Escherichia coli* genome.** Metab Eng (2004) 6, 197–203.

52 Kitaoka, Y., Nishimura, N. and Niwano, M. **Cooperativity of stabilized mRNA and enhanced translation activity in the cell-free system.** J Biotechnol (1996) 48, 1–8.

53 Kommer, A.A. *et al.* **Synthesis of functionally active human proinsulin in a cell-free translation system.** Dokl Biochem Biophys (2005) 401, 154–158.

54 Minton, A.P. **How can biochemical reactions within cells differ from those in test tubes?** J Cell Sci (2006) 119, 2863–2869.

55 Dix, J.A. and Verkman, A.S. **Crowding effects on diffusion in solutions and cells.** Annu Rev Biophys (2008) 37, 247–263.

56 Ellis, R.J. **Macromolecular crowding: obvious but underappreciated.** Trends Biochem Sci (2001) 26, 597–604.

57 Zhou, H.X., Rivas, G. and Minton, A.P. **Macromolecular crowding and confinement: biochemical, biophysical, and potential physiological consequences.** Annu Rev Biophys (2008) 37, 375–397.

58 Tan, C. *et al.* **Molecular crowding shapes gene expression in synthetic cellular nanosystems.** Nat Nanotechnol (2013) 8, 602–608.

59 Noireaux, V. and Libchaber, A. **A vesicle bioreactor as a step toward an artificial cell assembly.** Proc Natl Acad Sci U S A (2004) 101, 17669–17674.

60 Noireaux, V., Maeda, Y.T. and Libchaber, A. **Development of an artificial cell, from self-organization to computation and self-reproduction.** Proc Natl Acad Sci U S A (2011) 108, 3473–3480.

61 Nirenberg, M.W. and Matthaei, J.H. **The dependence of cell-free protein synthesis in *E. coli* upon naturally occurring or synthetic polyribonucleotides.** Proc Natl Acad Sci U S A (1961) 47, 1588–1602.

62 Kim, D.M. *et al.* **A highly efficient cell-free protein synthesis system from *Escherichia coli*.** Eur J Biochem (1996) 239, 881–886.

63 Kigawa, T. *et al.* **Cell-free production and stable-isotope labeling of milligram quantities of proteins.** FEBS Lett (1999) 442, 15–19.

64 Shimizu, Y. *et al.* **Cell-free translation reconstituted with purified components.** Nat Biotechnol (2001) 19, 751–755.

65 Nishino, Y., Yasunaga, T. and Miyazawa, A. **A genetically encoded metallothionein tag enabling efficient protein detection by electron microscopy.** J Electron Microsc (Tokyo) (2007) 56, 93–101.

66 Shin, Y.C. and Folk, W.R. **Formation of polyomavirus-like particles with different VP1 molecules that bind the urokinase plasminogen activator receptor.** J Virol (2003) 77, 11491–11498.

67 Langner, J. *et al.* **RGD-mutants of B-lymphotropic polyomavirus capsids specifically bind to alpha(v)beta3 integrin.** Arch Virol (2004) 149, 1877–1896.

68 Takahashi, R.U. *et al.* **Presentation of functional foreign peptides on the surface of SV40 virus-like particles.** J Biotechnol (2008) 135, 385–392.

69 Jennings, G.T. and Bachmann, M.F. **The coming of age of virus-like particle vaccines.** Biol Chem (2008) 389, 521–536.

70 Roldao, A. *et al.* **Virus-like particles in vaccine development.** Expert Rev Vaccines (2010) 9, 1149–1176.

71 Kushnir, N., Streatfield, S.J. and Yusibov, V. **Virus-like particles as a highly efficient vaccine platform: diversity of targets and production systems and advances in clinical development.** Vaccine (2012) 31, 58–83.

72 Garland, S.M. *et al.* **Quadrivalent vaccine against human papillomavirus to prevent anogenital diseases.** N Engl J Med (2007) 356, 1928–1943.

73 Harper, D.M. *et al.* **Sustained efficacy up to 4.5 years of a bivalent L1 virus-like particle vaccine against human papillomavirus types 16 and 18: follow-up from a randomised control trial.** Lancet (2006) 367, 1247–1255.

74 Johne, R. and Muller, H. **Polyomaviruses of birds: etiologic agents of inflammatory diseases in a tumor virus family.** J Virol (2007) 81, 11554–11559.

75 Ritchie, B.W. *et al.* **An inactivated avian polyomavirus vaccine is safe and immunogenic in various Psittaciformes.** Vaccine (1996) 14, 1103–1107.

76 Ritchie, B.W. *et al.* **Safety, immunogenicity, and efficacy of an inactivated avian polyomavirus vaccine.** Am J Vet Res (1998) 59, 143–148.

77 Dorn, D.C. *et al.* **Cellular and humoral immunogenicity of hamster polyomavirus-derived virus-like particles harboring a mucin 1 cytotoxic T-cell epitope.** Viral Immunol (2008) 21, 12–27.

78 Brinkman, M. *et al.* **Recombinant Murine Polyoma Virus-like-particles Induce Protective Antitumour Immunity.** Letters in Drug Design & Discovery (2004) 1, 137–147(111).

79 Tegerstedt, K. *et al.* **A single vaccination with polyomavirus VP1/VP2Her2 virus-like particles prevents outgrowth of HER-2/neu-expressing tumors.** Cancer Res (2005) 65, 5953–5957.

80 Clark, B. *et al.* **Immunity against both polyomavirus VP1 and a transgene product induced following intranasal delivery of VP1 pseudocapsid-DNA complexes.** J Gen Virol (2001) 82, 2791–2797.

81 Rollman, E. *et al.* **Genetic immunization is augmented by murine polyomavirus VP1 pseudocapsids.** Vaccine

(2003) 21, 2263–2267.

82 Andreasson, K. *et al.* **CD4+ and CD8+ T cells can act separately in tumour rejection after immunization with murine pneumotropic virus chimeric Her2/neu virus-like particles.** PLoS One (2010) 5, e11580.

83 Nierkens, S. *et al.* ***In vivo*** **colocalization of antigen and CpG [corrected] within dendritic cells is associated with the efficacy of cancer immunotherapy.** Cancer Res (2008) 68, 5390–5396.

84 Molino, N.M. *et al.* **Biomimetic protein nanoparticles facilitate enhanced dendritic cell activation and cross-presentation.** ACS Nano (2013) 7, 9743–9752.

85 Chuan, Y.P. *et al.* **Effects of pre-existing anti-carrier immunity and antigenic element multiplicity on efficacy of a modular virus-like particle vaccine.** Biotechnol Bioeng (2013) 110, 2343–2351.

86 van Lente, H., Spitters, C. and Peine, A. **Comparing technological hype cycles: Towards a theory.** Technological Forecasting and Social Change (2013) 80, 1615–1628.

87 Wilson, J.M. **Bulls, bubbles, and biotech.** Hum Gene Ther (2013) 24, 715–716.

88 Mastrobattista, E. *et al.* **Artificial viruses: a nanotechnological approach to gene delivery.** Nat Rev Drug Discov (2006) 5, 115–121.

89 Kimchi-Sarfaty, C. *et al.* **SV40 Pseudovirion gene delivery of a toxin to treat human adenocarcinomas in mice.** Cancer Gene Ther (2006) 13, 648–657.

90 Lammers, T. *et al.* **Drug targeting to tumors: principles, pitfalls and (pre-) clinical progress.** J Control Release (2012) 161, 175–187.

91 Damia, G. and D'Incalci, M. **Contemporary pre-clinical development of anticancer agents – what are the optimal preclinical models?** Eur J Cancer (2009) 45, 2768–2781.

92 Shackleton, M. *et al.* **Heterogeneity in cancer: cancer stem cells versus clonal evolution.** Cell (2009) 138, 822–829.

93 Bae, Y.H. and Park, K. **Targeted drug delivery to tumors: Myths, reality and possibility.** J Control Release (2011) 153, 198–205.

94 Kwon, I.K. *et al.* **Analysis on the current status of targeted drug delivery to tumors.** J Control Release (2012) 164, 108–114.

95 Li, Y. *et al.* **Loss of adenoviral receptor expression in human bladder cancer cells: a potential impact on the efficacy of gene therapy.** Cancer Res (1999) 59, 325–330.

96 Charafe-Jauffret, E. *et al.* **Breast cancer cell lines contain functional cancer stem cells with metastatic capacity and a distinct molecular signature.** Cancer Res (2009) 69, 1302–1313.

97 Chuan, Y.P., Lua, L.H. and Middelberg, A.P. **High-level expression of soluble viral structural protein in *Escherichia coli*.** J Biotechnol (2008) 134, 64–71.

98 Liew, M.W., Rajendran, A. and Middelberg, A.P. **Microbial production of virus-like particle vaccine protein at gram-per-litre levels.** J Biotechnol (2010) 150, 224–231.

99 Middelberg, A.P. *et al.* **A microbial platform for rapid and low-cost virus-like particle and capsomere vaccines.** Vaccine (2011) 29, 7154–7162.

100 Liew, M.W.O., Chuan, Y.P. and Middelberg, A.P.J. **High-yield and scalable cell-free assembly of virus-like particles by dilution.** Biochemical Engineering Journal (2012) 67, 88–96.

101 Liew, M.W.O., Chuan, Y.P. and Middelberg, A.P.J. **Reactive diafiltration for assembly and formulation of virus-like particles.** Biochemical Engineering Journal (2012) 68, 120–128.

102 Fischetti, V.A., Nelson, D. and Schuch, R. **Reinventing phage therapy: are the parts greater than the sum?** Nat Biotechnol (2006) 24, 1508–1511.

103 Thiel, K. **Old dogma, new tricks – 21st Century phage therapy.** Nat Biotechnol (2004) 22, 31–36.

104 Cello, J., Paul, A.V. and Wimmer, E. **Chemical synthesis of poliovirus cDNA: generation of infectious virus in the absence of natural template.** Science (2002) 297, 1016–1018.

105 Smith, H.O. *et al.* **Generating a synthetic genome by whole genome assembly: phiX174 bacteriophage from synthetic oligonucleotides.** Proc Natl Acad Sci U S A (2003) 100, 15440–15445.

106 Tumpey, T.M. *et al.* **Characterization of the reconstructed 1918 Spanish influenza pandemic virus.** Science (2005) 310, 77–80.

107 Gibson, D.G. *et al.* **Complete chemical synthesis, assembly, and cloning of a *Mycoplasma genitalium* genome.** Science (2008) 319, 1215–1220.

108 Gibson, D.G. *et al.* **Creation of a bacterial cell controlled by a chemically synthesized genome.** Science (2010) 329, 52–56.

109 Murtas, G. *et al.* **Protein synthesis in liposomes with a minimal set of enzymes.** Biochem Biophys Res Commun (2007) 363, 12–17.

110 Jewett, M.C. and Forster, A.C. **Update on designing and building minimal cells.** Curr Opin Biotechnol (2010) 21, 697–703.

111 Hodgman, C.E. and Jewett, M.C. **Cell-free synthetic biology: thinking outside the cell.** Metab Eng (2012) 14, 261–269.

112 Allentoft, M.E. *et al.* **The half-life of DNA in bone: measuring decay kinetics in 158 dated fossils.** Proc Biol Sci (2012) 279, 4724–4733.

113 Poinar, H.N. *et al.* **Metagenomics to paleogenomics: large-scale sequencing of mammoth DNA.** Science (2006) 311, 392–394.

114 Corey, M.J. and Corey, E. **On the failure of *de novo*-designed peptides as biocatalysts.** Proc Natl Acad Sci U S A (1996) 93, 11428–11434.

115 Schiweck, W. and Skerra, A. **The rational construction of an antibody against cystatin: lessons from the crystal structure of an artificial Fab fragment.** J Mol Biol (1997) 268, 934–951.

116 Lanio, T., Jeltsch, A. and Pingoud, A. **On the possibilities and limitations of rational protein design to expand the specificity of restriction enzymes: a case study employing EcoRV as the target.** Protein Eng (2000) 13, 275–281.

117 Jiang, L. *et al.* ***De novo*** **computational design of retro-aldol enzymes.** Science (2008) 319, 1387–1391.

118 Rothlisberger, D. *et al.* **Kemp elimination catalysts by computational enzyme design.** Nature (2008) 453, 190–195.

119 Siegel, J.B. *et al.* **Computational design of an enzyme**

catalyst for a stereoselective bimolecular Diels-Alder reaction. Science (2010) 329, 309–313.

120 Asuri, P. *et al.* **Directed evolution of adeno-associated virus for enhanced gene delivery and gene targeting in human pluripotent stem cells.** Mol Ther (2012) 20, 329–338.

121 de Raad, M. **Design and recombinant production of combinatorial peptide libraries for gene delivery.** Ph.D. thesis, Utrecht University, (2013).

122 Bogarad, L.D. and Deem, M.W. **A hierarchical approach to protein molecular evolution.** Proc Natl Acad Sci U S A (1999) 96, 2591–2595.

123 Ostermeier, M., Shim, J.H. and Benkovic, S.J. **A combinatorial approach to hybrid enzymes independent of DNA homology.** Nat Biotechnol (1999) 17, 1205–1209.

124 Privett, H.K. *et al.* **Iterative approach to computational enzyme design.** Proc Natl Acad Sci U S A (2012) 109, 3790–3795.

125 Lutz, S. **Beyond directed evolution – semi-rational protein engineering and design.** Curr Opin Biotechnol (2010) 21, 734–743.

Appendices

Nederlandse samenvatting

Inleiding

Gentherapie

Kanker, genetische aandoeningen, hart- en vaatziekten, infectieziekten, neurologische aandoeningen… Dit zijn slechts voorbeelden van ziekten die, in principe, behandeld of zelfs genezen zouden kunnen worden door middel van gentherapie [1]. Defecte genen zouden kunnen worden gecorrigeerd, missende genen toegevoegd, en ongewilde genen stilgelegd [2]. Door hun enorme grootte, hydrofobe karakter, negatieve lading en vatbaarheid voor nucleasen staan nucleïnezuren echter voor ondoordringbare barrières en worden ze snel afgebroken en geklaard na injectie [3]. Dit gebeurt lang voordat ze hun doel, het binnenste – meestal de kern – van zieke cellen, bereiken. Om deze reden is er veel onderzoek gedaan naar de ontwikkeling van afgiftesystemen voor nucleïnezuren. Deze afgiftesystemen zouden in staat moeten zijn om hun lading, de nucleïnezuren, tegen afbraak te beschermen en af te leveren aan hun doelcellen in het lichaam. Dergelijke dragers worden over het algemeen onderverdeeld in virale of niet-virale vectoren.

Virale vectoren

Virale vectoren zijn van virussen afgeleide dragers voor genetisch materiaal, waarbij het virale genoom is vervangen door de nucleïnezuurlading [4]. Virussen zijn door de natuur geëvolueerd om de perfecte afgiftesystemen voor genetisch materiaal te zijn [5]. Dit stelt de virussen in staat om te reproduceren en ziekte te veroorzaken in geïnfecteerde cellen. Virale vectoren gebruiken deze intrinsieke afgiftekarakteristieken voor de afgifte van therapeutische nucleïnezuren [6]. Deze vectoren kunnen of replicatie-competent [7] of replicatie-deficiënt zijn [8]. Over het algemeen zijn virale vectoren erg efficiënt in het afleveren van hun lading aan cellen, maar deze vectoren zijn wel duur en lastig om te produceren [9], hebben een zeer nauw gedefinieerd tropisme [10], hebben slechts een beperkt laadvermogen [11], en dragen het risico van serieuze bijwerkingen veroorzaakt door hun immunogeniciteit [12] en door insertiemutagenese [13].

Niet-virale vectoren

Niet-virale vectoren omvatten diverse synthetische afgiftesystemen. Ze zijn meestal gebaseerd op complexen met kationische polymeren of lipiden [14], maar kunnen ook bereid worden met andere materialen, zoals peptiden [3], anorganische nanodeeltjes [15] en dendrimeren [16]. Deze vectoren genieten een relatief goedkope en gemakkelijke productie, zijn over het algemeen niet gelimiteerd in hun afgiftecapaciteit, en zijn relatief veilig vergeleken met virale vectoren. Het nadeel is echter dat deze vectoren over het algemeen een zeer lage afgifte-efficiëntie hebben [17,18].

Virusachtige partikels

Een ideaal afgiftesysteem combineert de voordelen van beide systemen, zonder de daarbij behorende nadelen [19]. Door hun positie als tussenvorm van virale en niet-virale vectoren zouden virusachtige partikels (VLPs) deze belofte kunnen vervullen. VLPs zijn supramoleculaire assemblages van virale structuureiwitten. Deze deeltjes vormen spontaan na de recombinante expressie van virale structuureiwitten en bevatten geen virale nucleinezuren. Voor sommige virussen vormen dergelijke lege eiwitmantels zelfs per ongeluk als bijproducten van infectie [20,21]. Deze deeltjes gelijken de natieve virale eiwitmantel in structuur, stabiliteit, tropisme, en transductie efficiëntie, maar bevatten geen viraal genetisch materiaal [22]. Hierdoor

behouden VLPs de efficiënte afgiftekarakteristieken van virale vectoren, terwijl het ontbreken van viraal genetisch materiaal ervoor zorgt dat ze niet langer de gevaren met zich meedragen die kleven aan insertie en reversie.
VLPs zijn reeds gegenereerd van verschillende virussen van vele uiteenlopende virusfamilies [23]. Commercieel worden deze deeltjes vooral gebruikt voor vaccinatie. Verschillende op VLP gebaseerde vaccins worden momenteel klinisch onderzocht [24,25], en sommige zijn reeds op de markt verkrijgbaar, zoals de profylactische humaan papillomavirus (HPV) vaccins Gardasil® [26] en Cervarix® [27]. Deze deeltjes hebben echter ook potentie voor gentherapie.

VLPs afgeleid van polyomavirussen

Met name interessant zijn de VLPs afgeleid van polyomavirussen. Deze VLPs zijn in staat om dubbelstrengs DNA op een sequentie-onafhankelijke manier te encapsideren [28,29], wat het mogelijk maakt om ze te gebruiken voor genafgifte. Deze VLPs zijn relatief gemakkelijk te produceren; ze vereisen geen posttranslationele modificaties en kunnen vormen in prokaryotische expressiesystemen na de expressie van slechts één viraal eiwit, namelijk het voornaamste manteleiwit VP1 [30]. In **hoofdstuk 2** van dit proefschrift worden de productie en biomedische applicaties van deze virusachtige partikels uiteengezet.
Echter, in hun huidige staat zijn deze VLPs niet direct bruikbaar voor gentherapie. Bijvoorbeeld hun gelimiteerde natuurlijke tropisme beperkt de variëteit aan cellen die getransduceerd kunnen worden, en reeds aanwezige immuniteit zal waarschijnlijk de doeltreffendheid verminderen. Daarom zijn wij begonnen met de modificatie van deze VLPs met als doel het verbeteren van hun karakteristieken voor gentherapie.

Gerichte evolutie van virusachtige partikels afgeleid van polyomavirussen

Ondanks de aanzienlijke vooruitgang in het veld van rationeel eiwitontwerp, welke het complete *de novo* ontwerp van enzymen met nieuwe katalytische activiteit mogelijk heeft gemaakt [31–33], is het nog steeds ogenschijnlijk onmogelijk om de gevolgen van mutaties voor gentherapievectoren te voorspellen. Gerichte evolutie, aan de andere kant, stelt ons in staat om eiwitten aan te passen zonder vooraf aanwezige kennis van structuur-functie relaties. Alhoewel deze techniek in het verleden vooral gebruikt is om enzymen aan te passen (voor recente uiteenzettingen zie referenties [34] en [35]), is deze techniek ook geschikt voor de creatie van nieuwe virale vectoren voor gentherapie.
De meeste van dergelijke studies zijn uitgevoerd met adeno-geassocieerd virus (AAV) [36–43], maar ook andere virussen, zoals adenovirussen [44,45] en retrovirussen [46–49], zijn onderhevig geweest aan gerichte evolutie. Verschillende eigenschappen, zoals tropisme [40–42], stabiliteit [47] en immunogeniciteit [36,50], zijn aangepast, waarmee het vermogen van gerichte evolutie is gedemonstreerd.

Het principe van gerichte evolutie

Gerichte evolutie steunt op iteratieve rondes van diversificatie en selectie om eiwitten te verbeteren in een op natuurlijke selectie gelijkend proces. Grote bibliotheken van willekeurige mutanten worden gecreëerd door middel van *high-throughput* combinatorische technieken. Uit deze bibliotheken worden mutanten die gewenste eigenschappen bezitten geselecteerd. Het principe van deze techniek is weergegeven in figuur 1.
Gerichte evolutie begint met de selectie van een startpunt. Dit is normaal gesproken een gen uit de natuur met eigenschappen die dicht bij de gewenste eigenschappen liggen, om te voorkomen dat de evolutionaire kloof te groot is om te overbruggen. Wanneer er meerdere homologen beschikbaar zijn, zoals het geval is voor polyomavirus *VP1*, kunnen deze genen gerecombineerd worden door middel van een techniek genaamd *DNA shuffling* om een bibliotheek the maken van hybride *VP1* genen [51,52]. Diversificatie kan ook bewerkstelligd worden met behulp van andere technieken, zoals *error-*

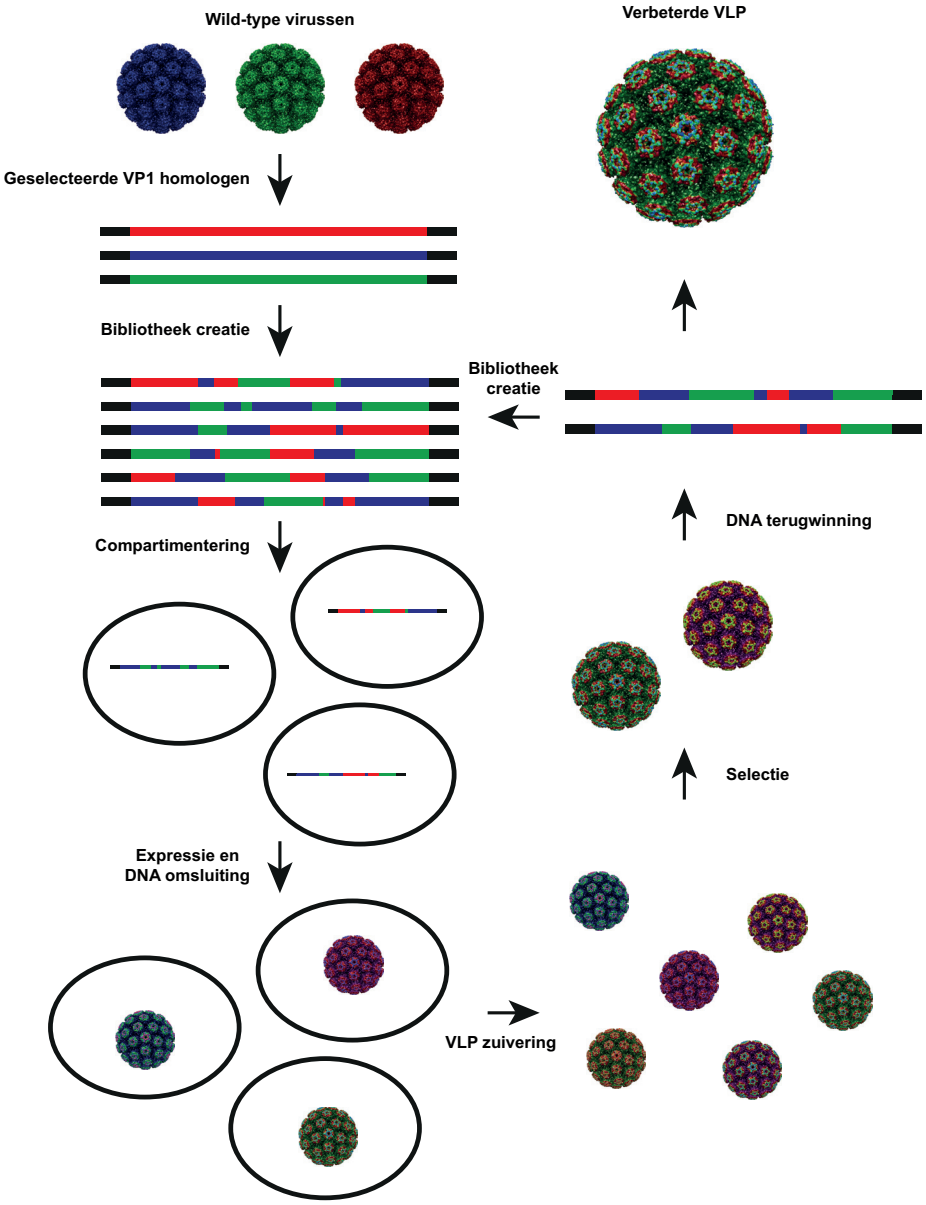

Figuur 1. Principe van gerichte evolutie van virusachtige partikels. Eerst worden de *VP1* genen van enkele wild-type polyomavirussen verkozen als startpunt voor gerichte evolutie. Vervolgens worden deze genen gerecombineerd door middel van de techniek *DNA shuffling* om een diverse bibliotheek van hybride *VP1* genen te maken. Deze hybride genen worden dan gecompartimenteerd in een eiwitexpressiesysteem, waarna de genen tot expressie gebracht worden. Op deze manier blijven de geproduceerde eiwitten in dezelfde ruimte als de coderende genen, en daarmee wordt het genotype aan het fenotype gelinkt. Na expressie vormen de VP1 eiwitten binnen ieder compartiment VLPs, maar daarbij kunnen ze alleen hun eigen coderende DNA omsluiten, aangezien ze de compartimenten niet kunnen verlaten. Zodra de vorming voltooid is, kunnen de VLPs gezuiverd worden en onderworpen worden aan selectiedruk. VLPs met gewenste eigenschappen worden dan geïsoleerd en hun DNA wordt geëxtraheerd. Dit DNA kan gebruikt worden voor additionele rondes van diversificatie en selectie, waarmee de eigenschappen van de VLPs verder verfijnd kunnen worden. Dit proces kan dan herhaald worden totdat de VLPs voldoende verbeterde zijn.

prone PCR [53] of *random oligonucleotide insertion* [54] (voor een overzicht, zie referentie [55]).
Voordat de bibliotheken tot expressie gebracht kunnen worden, dienen de genen te worden gecompartimenteerd. Net zoals bij de cellulaire compartimentering als essentieel onderdeel van het leven op aarde moeten de eiwitten opgesloten blijven binnen dezelfde ruimte als hun coderende genen, om op deze manier een link te vormen tussen het genotype en het fenotype. Deze link waarborgt dat de genetische oorsprong van de geselecteerde eiwitten later ontdekt kan worden, zodat deze genen gebruikt kunnen worden voor verdere rondes van gerichte evolutie of, op het einde, voor de productie. Deze compartimentering kan zowel *in vivo*, door de bibliotheek in prokaryotische of eukaryotische cellen te transfecteren, of compleet *in vitro*, door middel van een techniek genaamd *in vitro compartmentalization* [56,57], bewerkstelligd worden. Vervolgens worden de eiwitten tot expressie gebracht. In het geval van virale structuureiwitten assembleren deze eiwitten tot VLPs, waarbij ze hun eigen coderende DNA omsluiten. Deze deeltjes noemen wij artificiële virussen – VLPs die hun eigen synthetische genoom omsluiten. Deze VLPs kunnen dan worden gezuiverd, waarna mutanten met gewenste eigenschappen kunnen worden geselecteerd onder invloed van selectiedruk. Meerdere iteratieve rondes van diversificatie en selectie worden uitgevoerd om effectieve vectoren voor genafgifte te bemachtigen. Door slimme selectie-experimenten uit te voeren kunnen deze vectoren niet alleen gescreend worden op transfectie-efficiëntie, maar ook op andere eigenschappen, zoals het ontwijken van het immuunsysteem, of weefsel- of orgaanspecificiteit.

Doel van het proefschrift

Dit project was gericht op de ontwikkeling van een op evolutie gebaseerde methode voor de verbetering van VLPs afgeleid van polyomavirussen voor genafgifte. Het originele plan was om daarvoor de techniek *in vitro compartmentalization* (IVC) te gebruiken [56,57]. Deze techniek gebruikt druppeltjes van micrometergrootte van een water-in-olie emulsie als compartimenten voor gerichte evolutie. De druppels bevatten ieder gemiddeld één gen van de bibliotheek, en worden gevormd door de emulsificatie van een celvrij expressiesysteem (CFE systeem), welke alle componenten bevat voor de transcriptie en translatie van genen. Een veelgebruikt CFE systeem is het S30 extract, gebaseerd op het oplosbare deel van het lysaat van de bacterie *Escherichia coli* (*E. coli*) na centrifugatie bij 30,000 g [58–61]. Dit systeem wordt aangevuld met de T7 RNA-polymerase [62]. Op deze manier vormen de druppeltjes artificiële cellen die in staat zijn om eiwitten tot expressie te brengen vanaf genen onder de controle van de T7 promotor. Iedere milliliter aan emulsie bevat ongeveer 10^{10} van deze artificiële cellen, wat ons in staat stelt om zeer grote bibliotheken te gebruiken [63]. Hierdoor kan een zeer groot deel van het evolutionaire landschap gescreend worden. Het merendeel van de gepubliceerde experimenten aangaande de gerichte evolutie van virale vectoren is uitgevoerd met kleinere bibliotheken (tot 10^7 genen) [36,41,46,64]. Derhalve werden slechts individuele stappen van het genafgifteproces veranderd, zonder de consequenties die deze veranderingen zouden kunnen hebben op andere stappen in acht te nemen. Het gebruiken van een grotere bibliotheek zou het mogelijk kunnen maken om meerdere stappen tegelijk te optimaliseren.
Wij kozen voor het gebruik van VLPs afgeleid van het hamsterpolyomavirus (HaPyV) als model vectoren voor het grootste deel van onze studies, omdat voorafgaande studies hebben laten zien dat deze deeltjes gemodificeerd kunnen worden zonder de vorming van VLPs te beïnvloeden [65–68]. Bovendien zijn deze deeltjes niet alleen geschikt als vectoren voor gentherapie, maar ook voor vaccinontwikkeling. HaPyV VLPs zijn goed in staat om vreemde epitopen op hun mantel te tonen om op deze manier sterke immuunreacties te induceren [67,69,70].

Resultaten uit dit proefschrift

In de meeste protocollen voor de bereiding van *E. coli* S30 extract wordt de concentratie van het extract gebaseerd op het natte gewicht van de celpellet. Echter, latere stappen in het productieprotocol introduceren variabiliteit, welke zorgt voor grote verschillen tussen partijen S30 extract. In **hoofdstuk 3** laten we zien dat normalisatie van de totale eiwitconcentratie van het S30 extract na de productie en voor de celvrije expressie de variabiliteit tussen verschillende partijen S30 extracten sterk doet dalen. Dit zorgt er niet alleen maar voor dat verschillende studies, uitgevoerd met verschillende partijen S30 extract, met elkaar vergeleken kunnen worden; ook stelt het ons in staat om verschillende productieprotocollen van S30 extract met elkaar te vergelijken. Ten slotte vonden wij dat het eiwit β-galactosidase het beste tot expressie komt bij een S30 eiwitconcentratie van 3,4–4,8 mg/ml in de celvrije expressiereactie.

In de in **hoofdstuk 4** beschreven experimenten zoomden we in op de relatie tussen de opbrengst van prokaryotische celvrije expressie en de S30 eiwitconcentratie in de reactie. We testten deze relatie voor de expressie van verschillende eiwitten, en vonden dat ieder eiwit zijn eigen unieke S30 eiwitconcentratie heeft waarbij de expressie optimaal is. Bovendien veranderde deze correlatie onder verschillende incubatietemperaturen, terwijl de incubatietijd geen invloed had op deze correlatie. We observeerden een vergelijkbare afhankelijkheid met een commercieel verkrijgbaar prokaryotisch CFE systeem. We hebben ook geprobeerd om stabiliserende hulpstoffen aan de reactie toe te voegen met als doel hogere S30 eiwitconcentraties te kunnen gebruiken in de reactie, maar dit resulteerde niet in betere productie. Wel zagen we voordelige effecten na de toevoeging van DMSO bij suboptimale S30 eiwitconcentraties. Ondanks dat er geen S30 eiwitconcentratie gevonden werd waarbij alle eiwitten optimaal tot expressie kwamen, gaf een concentratie van 5–6 mg/ml voor de meeste eiwitten een redelijke productie. Uit deze studie blijkt dat de S30 eiwitconcentratie een belangrijke variabele is die geoptimaliseerd moet worden voor ieder nieuw tot expressie te brengen eiwit.

Celvrije expressie is een goed alternatief voor de conventionele *in vivo* productie van eiwitten. In **hoofdstuk 5** werd de celvrije expressie en vorming van HaPyV VLPs onderzocht onder verschillende omstandigheden. Bij deze omstandigheden zaten ook condities die in het verleden zijn gebruikt voor de *in vitro* vorming van polyomavirus VP1 VLPs na zuivering van VP1 uit bacteriën, en condities voor de celvrije expressie van andere VLPs die ook afhankelijk zijn van disulfide bruggen. Ondanks dat het manteleiwit VP1 werd geproduceerd met een opbrengst van 100 µg/ml of meer, zorgen geen van de geteste condities voor significante VLP vorming. Dit is een opvallend resultaat, aangezien we vonden dat VP1 wel gemakkelijk VLPs vormt binnen in bacteriën. Zelfs na zuivering waren de manteleiwitten niet in staat om VLPs te vormen onder normaal gesproken gunstige condities. Dit suggereert dat de VP1 eiwitten irreversibel veranderd of verkeerd gesynthetiseerd zijn onder de *in vitro* condities. De verdere toevoeging van chaperonne-eiwitten leidde niet tot een verhoogde assemblage-efficiëntie. Deze resultaten suggereren dat celvrije expressie, naar de huidige inzichten, niet geschikt is voor de productie van polyomavirus VLPs. Bovendien laten deze resultaten duidelijk zien dat er kritieke verschillen zijn tussen bacteriële en celvrije expressie.

Zoals eerder omschreven is gerichte evolutie een goed alternatief voor het rationeel ontwerpen van nieuwe virale vectoren voor gentherapie. In **hoofdstuk 6** leveren we het bewijs dat deze methode gebruikt kan worden voor functionele selecties van polyomavirus VLPs als model genafgiftesysteem. Om de voordelen van verschillende polyomavirussoorten te combineren werden grote bibliotheken van hybride *VP1* genen gemaakt door middel van *DNA shuffling*. Met behulp van deze techniek waren wij in staat om tot 6 verschillende polyomavirus *VP1* genen te recombineren. Om de link tussen het

genotype en fenotype aan te tonen transfecteerden we 293TT cellen met twee typen plasmiden; de één coderend voor het wild-type VP1, en de andere voor een mutant. Na VLP zuivering analyseerden we het *VP1* DNA in de fracties. Tijdens hun vorming omsloten de VLPs het beschikbare genetische materiaal binnen hetzelfde compartiment. We vonden een 10-voudige verrijking van het wild-type DNA na één enkele selectiestap. Deze data laten zien dat VLPs afgeleid van polyomavirussen in staat zijn om hun eigen coderend genetisch materiaal op te nemen na expressie in 293TT cellen, en dus gebruikt kunnen worden voor gerichte evolutie.

Het kleine formaat en het lage intrinsieke contrast van VLPs maakt het moeilijk om hun gedrag in cellen en hun stabiliteit in biologische vloeistoffen te bestuderen met behulp van conventionele methoden. In **hoofdstuk 7** werden twee alternatieve methoden voor het bestuderen van VLPs onderzocht. Allereerst werd een kloneerbare tag van muis metallothioneine gebruikt, welke in staat is om ionen van zware metalen te binden wat het contrast voor transmissie-elektronenmicroscopie (TEM) verhoogt. Deze tag werd in lussen van VP1 aan de buitenkant van de VLP gezet. Ondanks dat de tag de VP1 opbrengst na prokaryotische expressie niet verlaagde, voorkwam deze tag de vorming van VLPs. Ten tweede werd een techniek genaamd *nanoparticle tracking analysis* (NTA) gebruikt voor de detectie van VLPs. Met behulp van een NanoSight instrument waren we in staat om de deeltjesgroottedistributie van VLPs te meten. Gebruikmakend van fluorescent-gelabelde VLPs konden we deze deeltjes in de aanwezigheid van bloedserum meten, wat onder normale omstandigheden de meting compleet overschaduwt.

Naast het gebruik voor gentherapie kunnen VLPs ook gebruikt worden voor vaccinatie. VLPs afgeleid van polyomavirussen kunnen niet alleen als epitoop vaccin, maar ook als genetisch vaccin dienen. Beide strategieën zijn individueel in staat om een redelijke immuunrespons op te wekken, maar deze immuunresponsen zijn over het algemeen niet sterk genoeg om immuuntolerantie te doorbreken, wat vaak nodig is voor effectieve kankerimmunotherapie. In **hoofdstuk 8** worden de mogelijkheden onderzocht om deze twee strategieën te combineren in één enkel deeltje, uitgaande van de hypothese dat gezamenlijke afgifte leidt tot een synergetisch effect. Zes verschillende epitopen gebaseerd op CD8+ en CD4+ epitopen van ovalbumine werden ontworpen en in twee lussen van VP1 aan de buitenkant van de VLPs gezet. De insertie in beide lussen voorkwam niet dat de VLPs vormden. Ondanks dat de gevormde VLPs kleiner (20 nm in diameter) waren dan wild-type VLPs, waren deze deeltjes in staat om een krachtige immuunrespons op te wekken in een *in vitro* antigenpresentatie assay. Ten slotte hebben we verschillende strategieën getest voor het laden van VLPs met plasmide DNA. We vonden dat de re-assemblage van de VLPs in de aanwezigheid van plasmide DNA geen significant betere bescherming biedt tegen nucleasen dan het samenvoegen van DNA met vooraf gevormde VLPs. Geen van beide strategieën resulteerde in een hogere transfectie-efficiëntie dan naakt plasmide DNA.

Referenties

1 Ginn, S.L. *et al.* **Gene therapy clinical trials worldwide to 2012 – an update.** J Gene Med (2013) 15, 65–77.

2 Kay, M.A. **State-of-the-art gene-based therapies: the road ahead.** Nat Rev Genet (2011) 12, 316–328.

3 Mann, A. *et al.* **Peptides in DNA delivery: current insights and future directions.** Drug Discov Today (2008) 13, 152–160.

4 Thomas, C.E., Ehrhardt, A. and Kay, M.A. **Progress and problems with the use of viral vectors for gene therapy.** Nat Rev Genet (2003) 4, 346–358.

5 Kay, M.A., Glorioso, J.C. and Naldini, L. **Viral vectors for gene therapy: the art of turning infectious agents into vehicles of therapeutics.** Nat Med (2001) 7, 33–40.

6 Heilbronn, R. and Weger, S. **Viral vectors for gene transfer: current status of gene therapeutics.** Handb Exp Pharmacol (2010), 143–170.

7 Galanis, E., Vile, R. and Russell, S.J. **Delivery systems intended for *in vivo* gene therapy of cancer: targeting and**

replication competent viral vectors. Crit Rev Oncol Hematol (2001) 38, 177–192.

8 Marconi, P. *et al.* **Replication-defective herpes simplex virus vectors for gene transfer *in vivo*.** Proc Natl Acad Sci U S A (1996) 93, 11319–11320.

9 Merten, O.W., Geny-Fiamma, C. and Douar, A.M. **Current issues in adeno-associated viral vector production.** Gene Ther (2005) 12 Suppl 1, S51–61.

10 Kootstra, N.A. and Verma, I.M. **Gene therapy with viral vectors.** Annu Rev Pharmacol Toxicol (2003) 43, 413–439.

11 Walther, W. and Stein, U. **Viral vectors for gene transfer: a review of their use in the treatment of human diseases.** Drugs (2000) 60, 249–271.

12 Nayak, S. and Herzog, R.W. **Progress and prospects: immune responses to viral vectors.** Gene Ther (2010) 17, 295–304.

13 Baum, C. *et al.* **Chance or necessity? Insertional mutagenesis in gene therapy and its consequences.** Mol Ther (2004) 9, 5–13.

14 Thomas, M. and Klibanov, A.M. **Non-viral gene therapy: polycation-mediated DNA delivery.** Appl Microbiol Biotechnol (2003) 62, 27–34.

15 Ghosh, P. *et al.* **Gold nanoparticles in delivery applications.** Adv Drug Deliv Rev (2008) 60, 1307–1315.

16 Dufes, C., Uchegbu, I.F. and Schatzlein, A.G. **Dendrimers in gene delivery.** Adv Drug Deliv Rev (2005) 57, 2177–2202.

17 Luo, D. and Saltzman, W.M. **Synthetic DNA delivery systems.** Nat Biotechnol (2000) 18, 33–37.

18 Lungwitz, U. *et al.* **Polyethylenimine-based non-viral gene delivery systems.** Eur J Pharm Biopharm (2005) 60, 247–266.

19 Mastrobattista, E. *et al.* **Artificial viruses: a nanotechnological approach to gene delivery.** Nat Rev Drug Discov (2006) 5, 115–121.

20 Mayr, G.A. *et al.* **Immune responses and protection against foot-and-mouth disease virus (FMDV) challenge in swine vaccinated with adenovirus-FMDV constructs.** Vaccine (2001) 19, 2152–2162.

21 Aposhian, H.V., Thayer, R.E. and Qasba, P.K. **Formation of nucleoprotein complexes between polyoma empty capsides and DNA.** J Virol (1975) 15, 645–653.

22 Teunissen, E.A., de Raad, M. and Mastrobattista, E. **Production and biomedical applications of virus-like particles derived from polyomaviruses.** J Control Release (2013) 172, 305–321.

23 Noad, R. and Roy, P. **Virus-like particles as immunogens.** Trends Microbiol (2003) 11, 438–444.

24 Roldao, A. *et al.* **Virus-like particles in vaccine development.** Expert Rev Vaccines (2010) 9, 1149–1176.

25 Kushnir, N., Streatfield, S.J. and Yusibov, V. **Virus-like particles as a highly efficient vaccine platform: diversity of targets and production systems and advances in clinical development.** Vaccine (2012) 31, 58–83.

26 Garland, S.M. *et al.* **Quadrivalent vaccine against human papillomavirus to prevent anogenital diseases.** N Engl J Med (2007) 356, 1928–1943.

27 Harper, D.M. *et al.* **Sustained efficacy up to 4.5 years of a bivalent L1 virus-like particle vaccine against human papillomavirus types 16 and 18: follow-up from a randomised control trial.** Lancet (2006) 367, 1247–1255.

28 Moreland, R.B., Montross, L. and Garcea, R.L. **Characterization of the DNA-binding properties of the polyomavirus capsid protein VP1.** J Virol (1991) 65, 1168–1176.

29 Voronkova, T. *et al.* **Hamster polyomavirus-derived virus-like particles are able to transfer *in vitro* encapsidated plasmid DNA to mammalian cells.** Virus Genes (2007) 34, 303–314.

30 Pattenden, L.K. *et al.* **Towards the preparative and large-scale precision manufacture of virus-like particles.** Trends Biotechnol (2005) 23, 523–529.

31 Jiang, L. *et al.* ***De novo* computational design of retro-aldol enzymes.** Science (2008) 319, 1387–1391.

32 Rothlisberger, D. *et al.* **Kemp elimination catalysts by computational enzyme design.** Nature (2008) 453, 190–195.

33 Siegel, J.B. *et al.* **Computational design of an enzyme catalyst for a stereoselective bimolecular Diels-Alder reaction.** Science (2010) 329, 309–313.

34 Goldsmith, M. and Tawfik, D.S. **Directed enzyme evolution: beyond the low-hanging fruit.** Curr Opin Struct Biol (2012) 22, 406–412.

35 Dalby, P.A. **Strategy and success for the directed evolution of enzymes.** Curr Opin Struct Biol (2011) 21, 473–480.

36 Perabo, L. *et al.* **Combinatorial engineering of a gene therapy vector: directed evolution of adeno-associated virus.** J Gene Med (2006) 8, 155–162.

37 Maheshri, N. *et al.* **Directed evolution of adeno-associated virus yields enhanced gene delivery vectors.** Nat Biotechnol (2006) 24, 198–204.

38 Grimm, D. *et al.* ***In vitro* and *in vivo* gene therapy vector evolution via multispecies interbreeding and retargeting of adeno-associated viruses.** J Virol (2008) 82, 5887–5911.

39 Li, W. *et al.* **Generation of novel AAV variants by directed evolution for improved CFTR delivery to human ciliated airway epithelium.** Mol Ther (2009) 17, 2067–2077.

40 Yang, L. *et al.* **A myocardium tropic adeno-associated virus (AAV) evolved by DNA shuffling and *in vivo* selection.** Proc Natl Acad Sci U S A (2009) 106, 3946–3951.

41 Maguire, C.A. *et al.* **Directed evolution of adeno-associated virus for glioma cell transduction.** J Neurooncol (2010) 96, 337–347.

42 Asuri, P. *et al.* **Directed evolution of adeno-associated virus for enhanced gene delivery and gene targeting in human pluripotent stem cells.** Mol Ther (2012) 20, 329–338.

43 Dalkara, D. *et al.* ***In vivo*-directed evolution of a new adeno-associated virus for therapeutic outer retinal gene delivery from the vitreous.** Sci Transl Med (2013) 5, 189ra176.

44 Kuhn, I. *et al.* **Directed evolution generates a novel oncolytic virus for the treatment of colon cancer.** PLoS One (2008) 3, e2409.

45 Uil, T.G. *et al.* **Directed adenovirus evolution using engineered mutator viral polymerases.** Nucleic Acids Res (2011) 39, e30.

46 Soong, N.W. *et al.* **Molecular breeding of viruses.** Nat Genet (2000) 25, 436–439.

47 Powell, S.K. *et al.* **Breeding of retroviruses by DNA shuf-**

fling for improved stability and processing yields. Nat Biotechnol (2000) 18, 1279–1282.

48 Bupp, K. and Roth, M.J. **Altering retroviral tropism using a random-display envelope library.** Mol Ther (2002) 5, 329–335.

49 Bupp, K. and Roth, M.J. **Targeting a retroviral vector in the absence of a known cell-targeting ligand.** Hum Gene Ther (2003) 14, 1557–1564.

50 Lin, T.Y. *et al.* **A novel approach for the rapid mutagenesis and directed evolution of the structural genes of west nile virus.** J Virol (2012) 86, 3501–3512.

51 Stemmer, W.P. **Rapid evolution of a protein *in vitro* by DNA shuffling.** Nature (1994) 370, 389–391.

52 Crameri, A. *et al.* **DNA shuffling of a family of genes from diverse species accelerates directed evolution.** Nature (1998) 391, 288–291.

53 Cirino, P.C., Mayer, K.M. and Umeno, D. **Generating mutant libraries using error-prone PCR.** In: Directed Evolution Library Creation: Methods and Protocols (eds Frances H. Arnold and George Georgiou) 3–9 (Springer, 2003).

54 Muller, O.J. *et al.* **Random peptide libraries displayed on adeno-associated virus to select for targeted gene therapy vectors.** Nat Biotechnol (2003) 21, 1040–1046.

55 Arnold, F.H. and Georgiou, G. **Directed Evolution Library Creation: Methods and Protocols.** (2003).

56 Tawfik, D.S. and Griffiths, A.D. **Man-made cell-like compartments for molecular evolution.** Nat Biotechnol (1998) 16, 652–656.

57 Miller, O.J. *et al.* **Directed evolution by *in vitro* compartmentalization.** Nat Methods (2006) 3, 561–570.

58 Zubay, G. ***In vitro* synthesis of protein in microbial systems.** Annu Rev Genet (1973) 7, 267–287.

59 Kim, D.M. *et al.* **A highly efficient cell-free protein synthesis system from *Escherichia coli*.** Eur J Biochem (1996) 239, 881–886.

60 Kigawa, T. *et al.* **Preparation of *Escherichia coli* cell extract for highly productive cell-free protein expression.** J Struct Funct Genomics (2004) 5, 63–68.

61 Kim, T.W. *et al.* **Simple procedures for the construction of a robust and cost-effective cell-free protein synthesis system.** J Biotechnol (2006) 126, 554–561.

62 Kigawa, T., Muto, Y. and Yokoyama, S. **Cell-free synthesis and amino acid-selective stable isotope labeling of proteins for NMR analysis.** J Biomol NMR (1995) 6, 129–134.

63 Griffiths, A.D. and Tawfik, D.S. **Man-made enzymes – from design to *in vitro* compartmentalisation.** Curr Opin Biotechnol (2000) 11, 338–353.

64 Excoffon, K.J. *et al.* **Directed evolution of adeno-associated virus to an infectious respiratory virus.** Proc Natl Acad Sci U S A (2009) 106, 3865–3870.

65 Gedvilaite, A. *et al.* **Formation of immunogenic virus-like particles by inserting epitopes into surface-exposed regions of hamster polyomavirus major capsid protein.** Virology (2000) 273, 21–35.

66 Gedvilaite, A. *et al.* **Size and position of truncations in the carboxy-terminal region of major capsid protein VP1 of hamster polyomavirus expressed in yeast determine its assembly capacity.** Arch Virol (2006) 151, 1811–1825.

67 Gedvilaite, A. *et al.* **Segments of puumala hantavirus nucleocapsid protein inserted into chimeric polyomavirus-derived virus-like particles induce a strong immune response in mice.** Viral Immunol (2004) 17, 51–68.

68 Gedvilaite, A. *et al.* **Virus-like particles derived from major capsid protein VP1 of different polyomaviruses differ in their ability to induce maturation in human dendritic cells.** Virology (2006) 354, 252–260.

69 Zvirbliene, A. *et al.* **Generation of monoclonal antibodies of desired specificity using chimeric polyomavirus-derived virus-like particles.** J Immunol Methods (2006) 311, 57–70.

70 Dorn, D.C. *et al.* **Cellular and humoral immunogenicity of hamster polyomavirus-derived virus-like particles harboring a mucin 1 cytotoxic T-cell epitope.** Viral Immunol (2008) 21, 12–27.

Curriculum vitae

Erik Teunissen was born in East Melbourne, Australia, on July 9th 1986. In 2004, he graduated from the Augustinianum secondary school in Eindhoven, after which he started the Bachelor's program Molecular Sciences at Wageningen University. In 2007, he started his Master's program Molecular Life Sciences at the same university. In 2008, he combined this program with the Master's program Drug Innovation at Utrecht University. As part of these programs, he performed a 9-month research project at the Department of Pharmaceutics at the Utrecht University under the supervision of dr. Enrico Mastrobattista, which culminated in his appointment as a graduate student on the same project. Before he started his graduate research, he performed a 6-month internship at the Department of Infectious Diseases, Virology at Heidelberg University under the supervision of dr. Dirk Grimm, where he focused on the modification (increasing the DNA loading capacity) of adeno-associated virus (AAV) for gene therapy. In 2009 he obtained both Master's degrees and started his PhD project at the Department of Pharmaceutics at Utrecht University under the supervision of prof. dr. Daan Crommelin, prof. dr. Peter Rottier, and dr. Enrico Mastrobattista. The project focused on the directed evolution of virus-like particles derived from polyomaviruses; the results of this project are presented in this thesis.

List of publications

Publications from this thesis

E.A. Teunissen, M. de Raad, E. Mastrobattista, Production and biomedical applications of virus-like particles derived from polyomaviruses, J Control Release, 172 (2013) 305–321.

E.A. Teunissen, E. Mastrobattista, P.J. Rottier, D.J. Crommelin, Directed evolution of artificial viruses, in: 16th Annual Meeting of the American Society of Gene & Cell Therapy, Molecular Therapy, Salt Lake City, Utah, 2013, pp. e18–e19.

E.A. Teunissen, Z. Karjoo, E.P. Béguin, E.M.J. van Brummelen, M. de Raad, J.A. Post, E. Mastrobattista, Assembly of hamster polyomavirus VP1 into virus-like particles takes place in *Escherichia coli* but not after cell-free synthesis, Submitted for publication.

E.A. Teunissen, G. Nadibaidze, M. de Raad, E. Mastrobattista, Batch-to-batch variability of *E. coli* S30 extracts can be reduced by normalizing S30 total protein content, Submitted for publication.

E.A. Teunissen, G. Nadibaidze, M. de Raad, E. Mastrobattista, Different proteins require different S30 extract protein concentrations for optimal expression, Submitted for publication.

E.A. Teunissen, J.J. Water, K.M. Kommeren, J.B. van den Dikkenberg, E.M.J. van Brummelen, M. de Raad, E. Mastrobattista, Proof of concept for the directed evolution of virus-like particles derived from polyomaviruses, Manuscript in preparation.

Other publications

M. de Raad, **E.A. Teunissen**, D. Lelieveld, D.A. Egan, E. Mastrobattista, High-content screening of peptide-based non-viral gene delivery systems, J Control Release, 158 (2012) 433–442.

M. de Raad, S.A. Kooijmans, **E.A. Teunissen**, E. Mastrobattista, A Solid-Phase Platform for Combinatorial and Scarless Multipart Gene Assembly, ACS Synth Biol, 2 (2013) 316–326.

E. Ruiz-Hernández, M. Hess, G.J. Melen, B. Theek, M. Talelli, Y. Shi, B. Ozbakir, **E.A. Teunissen**, M. Ramírez, D. Moeckel, F. Kiessling, G. Storm, H.W. Scheeren, W.E. Hennink, A.A. Szalay, J. Stritzker, T. Lammers, PEG-pHPMAm-based polymeric micelles loaded with doxorubicin-prodrugs in combination antitumor therapy with oncolytic vaccinia viruses, Polym Chem, (2014) 1674–1681.

N. Samadi, A. Abbadessa, A. Di Stefano, C.F. van Nostrum, T. Vermonden, S. Rahimian, **E.A. Teunissen**, M.J. van Steenbergen, M. Amidi, W.E. Hennink, The effect of lauryl capping group on protein release and degradation of poly(d,l-lactic-co-glycolic acid) particles, J Control Release, 172 (2013) 436–443.

Y. Shi, M.J. van Steenbergen, **E.A. Teunissen**, L. Novo, S. Gradmann, M. Baldus, C.F. van Nostrum, W.E. Hennink, Pi-pi stacking increases the stability and loading capacity of thermosensitive polymeric micelles for chemotherapeutic drugs, Biomacromolecules, 14 (2013) 1826–1837.

M. de Raad, **E.A. Teunissen**, E. Mastrobattista, Peptide vectors for gene delivery: from single peptides to multifunctional peptide nanocarriers, Submitted for publication.

Selected abstracts

E.A. Teunissen, P.J. Rottier, D.J. Crommelin, E. Mastrobattista, Directed evolution of artificial viruses, 16th Annual Meeting of the American Society of Gene & Cell Therapy, Salt Lake City, Utah, USA, 2013.

E.A. Teunissen, P.J. Rottier, D.J. Crommelin, E. Mastrobattista, Directed evolution of artificial viruses, FIGON Dutch Medicines Days 2013, Ede, The Netherlands, 2013.

M. de Raad, **E.A. Teunissen**, D. Lelieveld, D.A. Egan, E. Mastrobattista, High-content screening of peptide-based non-viral gene delivery systems, Controlled Release Society, Québec City, Canada, 2012.

Dankwoord | *Acknowledgements*

Ik heb heel lang uitgekeken naar het moment dat ik dit zou kunnen zeggen, maar nu is het dan toch eindelijk zover: het is gedaan! Het boekje is af! Veel bloed, zweet en tranen heeft dit werk gekost. Dit was echter nooit gelukt zonder de hulp van de vele mensen die mij tijdens dit traject gesteund hebben, zowel op werk als daarbuiten. Graag sta ik daarom stil om zo veel mogelijk van deze mensen te bedanken.

Beste Daan, geachte promotor, bedankt voor uw betrokkenheid bij dit project. Uw kritische maar vooral realistische blik heeft dit project uiteindelijk naar een succesvol einde geleid. Bedankt voor de kansen die u mij gegeven heeft.
Beste Peter, geachte promotor, bedankt voor al uw input tijdens de werkbesprekingen en het meedenken over het project. Uw kritische kijk op de stukken heeft het werk naar een hoger niveau getild. Bedankt voor alle tijd en moeite, zeker op het einde, toen alles nog zo last-minute geregeld moest worden.
Beste Enrico, geachte copromotor, ik kan mij nog goed herinneren hoe ik ruim 6 jaar geleden aan het begin van mijn Master voor het eerst bij u binnen kwam lopen. Sindsdien bent u betrokken geweest bij ieder aspect van mijn wetenschappelijke leven. Bedankt dat u mij de mogelijkheid heeft geboden om aan dit zeer interessante en uitdagende project te werken. U was altijd bereikbaar, boordevol nieuwe ideeën en immer optimistisch. Het zal niet gemakkelijk zijn geweest voor u om samen te werken met iemand met zo'n andere manier van aanpak. Daarom ben ik u des te meer dankbaar voor al de hulp en al het vertrouwen die u mij geboden heeft.
Beste Markus, oorspronkelijk was het de bedoeling dat onze projecten steeds dichter bij elkaar zouden komen, maar in de praktijk bleek dit eerder andersom. Desondanks heb ik zeer veel gehad aan onze discussies en je input. Je stond altijd open om even mee te kijken als ik er zelf niet uit kwam. Bovendien zorgde je voor veel gezelligheid op het lab. Geniet van je tijd in Berkeley!

Lang niet al de resultaten uit dit proefschrift zijn door mijzelf bij elkaar gepipetteerd; een groot deel heb ik aan mijn trouwe studenten te danken. In chronologische volgorde:
Dear Zahra, thank you for all the help you provided. It was a good time. I still remember all the *broodjes döner* we ate together; I only wish there could have been more. I am looking forward to seeing you again and I still intend to come visit you!
Beste Jorrit, bedankt voor al het harde werk en de gezellige tijd. De helft van hoofdstuk 6 komt van jouw handen! Succes met het afronden van je PhD!
Beste Yolien, Grzegorz, en Vera, het was leuk om ook een keer aan een ander project te werken. Ik heb hier veel van geleerd.
Beste Eelke, je inventiviteit heeft voor een groot deel het succes van hoofdstuk 5 bepaald. Bedankt voor al je inzet en gezelligheid. Succes in de toekomst!
Beste Emilie, bedankt voor je inzet en doorzettingsvermogen. Jouw VLPs komen terug in vrijwel ieder hoofdstuk. Succes met je PhD!
Beste Jeroen, bedankt voor het uitzoekwerk dat je gedaan hebt voor je scriptie, wat mij geholpen heeft bij het schrijven van mijn review. Het was leuk om ook buiten het laboratorium om iemand te begeleiden.
Beste Kasper, je tomeloze inzet is ongeëvenaard. Bedankt voor al het harde werk, maar ook voor de gezelligheid en de vele filosofische discussies. Ik heb er alle vertrouwen in dat jij een goede toekomst tegemoet gaat.

Dan zijn er ook nog de analisten die mij tijdens dit project bij hebben gestaan.
Beste Georgi, bedankt voor alle tijd en moeite die je gestoken hebt in de celvrije expressie. Zonder al je extracten was dit proefschrift niet mogelijk geweest.
Beste Joep, bedankt voor alle hulp die je mij geboden hebt bij het celkweken. Zonder jou was hoofdstuk 6 er nooit geweest. Daarnaast was het altijd heel erg gezellig. Ik kom je vast nog wel eens tegen bij een concert :).
Beste Ebel, Kim, Louis, Mies, Roel M.-B. en Roel v. E., graag zou ik jullie willen bedanken voor jullie bereidheid om mij keer op keer te helpen met mijn project. Al die keren dat ik jullie lastig kwam vallen met mijn lastige maar vaak ook onnozele vragen…

Een groot deel van het werk komt voort uit samenwerkingsverbanden. Graag zou ik daarom de mensen die daarbij betrokken zijn geweest bedanken.
Beste Chris Schneijdenberg, bedankt voor de inleiding in de wondere wereld van de TEM. U stond altijd voor mij klaar, al die keren dat ik wanhopig bij u langskwam nadat ik weer eens alle instellingen compleet door de war gehaald had. Beste Hans Meeldijk, bedankt voor de hulp die u mij geboden heeft alle keren dat ik u lastig kwam vallen.
Beste Jan Andries Post, hartelijk dank voor de samenwerking bij de imaging van de VLPs in bacteriën, wat de mooie plaatjes uit hoofdstuk 5 heeft opgeleverd. Beste Karin Vocking, bedankt voor het praktische deel hiervan; al dat werk met enge stoffen waar ik zelf nooit mee om zou durven gaan!
Beste Maryam, Meriem, Marieke Herbert-Fransen, Jan Willem Kleinovink en Ferry Ossendorp, bedankt voor jullie hulp bij het vaccinatie-onderdeel. Helaas is het er niet van gekomen om de deeltjes ook *in vivo* te testen, ondanks de veelbelovende resultaten. Hopelijk gaat dit in de toekomst nog gebeuren.
Helaas hebben de volgende onderdelen dit proefschrift niet gehaald. Dat wil echter niet zeggen dat ze niet interessant of veelbelovend waren.
Beste Kevin Braeckmans en Katrien Remaut, bedankt voor jullie hulp met de FCS.
Beste Jan Willem de Vries en Andreas Herrmann, bedankt voor jullie samenwerking met de DNA micellen.
Beste Matthijn de Boer en Berend Jan Bosch, bedankt voor de hulp bij het project en de materialen die ik van jullie heb mogen ontvangen.

Dan zijn er nog de vele mensen van wie ik de kans heb gekregen om hun deeltjes met de TEM te mogen bekijken. Het was zeer leuk om op deze manier mee te werken aan andere projecten. I would particularly like to thank Eduardo, Neda S. and Yang, whose collaborations resulted in co-authorships.
Het grootste deel van dit werk is uitgevoerd in de laboratoria van Biofarmacie, eerst in 't Went, later in 't DdW. Graag zou ik alle leden van deze grote en levendige onderzoeksgroep bedanken voor de gezelligheid. Tijdens mijn tijd bij Biofarmacie heb ik veel mensen zien komen en gaan. Het zijn er te veel om allemaal te noemen, al is het maar om het risico te vermijden dat ik mensen zou vergeten.
Beste Wim, graag zou ik u willen bedanken voor het bieden van de mogelijkheid om dit werk in uw toonaangevende onderzoeksgroep uit te voeren. Ik vond het zeer leuk om met u te dineren in Salt Lake City.
Beste Herre, bedankt voor al het officiële regelwerk. Het was geen eenvoudige klus met al die artificiële virussen, maar toch heeft u voor elkaar gekregen dat al het onderzoek ongehinderd kon verlopen.

Tijdens mijn promotietraject heb ik ook de kans gekregen mee te helpen met het onderwijs. Ik vond het leuk om ook dit eens te proeven. Graag wil ik de mensen bedanken die dit mogelijk gemaakt hebben, in het bijzonder Paul Henricks. Daarnaast wil ik alle studenten bedanken voor het braaf aanhoren van mijn

eindeloze verhalen over oninteressante dingen zoals kwantummechanica :).
In particular I would like to thank all the ever-so-enthusiastic students who spent their time at our department. Dear Sander, Iris, Zoltán, Jitze, and Rebecca, thank you for your *gezelligheid* at the lab, at the lunch breaks, and at the borrels.

Ook buiten het werk om zijn er nog veel mensen die mij bij hebben gestaan en geholpen hebben bij het bereiken van dit resultaat, al was het maar door voor afleiding te zorgen, en daarmee te voorkomen dat ik helemaal gek werd. Voor mijn vrienden, waar ik de afgelopen jaren zo weinig tijd voor had, bedankt voor het lange wachten; hopelijk is dat nu eindelijk voorbij!
Beste Balder, je hebt me inmiddels weer ingehaald :). Het wordt echt tijd dat we weer eens een keer afspreken!
Beste Jaarclubgenoten, Caroline, Eline, Jacob, Jouke, Leendert Jan en Mikel, bedankt voor jullie vriendschap, gezelligheid en de memorabele vakanties. Wanneer gaan we weer eens gezellig Brouwmeester drinken? RAM!
Beste Andy, Bas, Guido, Ivo, Linda, Nico, Remko en Richard, bedankt voor het begrip voor het vaak te laat komen. Het was fijn om de wekelijkse afleiding te hebben, mijn hoofd te kunnen legen en al het falen op het lab te kunnen vergeten. Dat er nog vele mooie avonturen mogen volgen!
Beste Cynthia, bedankt voor het zeggen van de dingen die ik wel dacht maar niet durfde te zeggen. Je hebt me laten zien hoe het is om weer levend te zijn. Zonder jouw steun was dit boekje er zeker niet geweest. Dat er nog vele epische avonden mogen volgen!
Beste Rob Goldbach, dankzij u ben ik het pad ingeslagen wat geleid heeft tot waar ik nu sta. Als geen ander wist u mensen te motiveren voor de levenswetenschappen. Helaas heb ik nooit de mogelijkheid gekregen om u hiervoor te bedanken. Ik ben erg trots u gekend te hebben en zal alle fijne gesprekken nooit vergeten.

Lieve familie, hier is dan eindelijk het product van het werk waar ik al die tijd mee bezig ben geweest. Ik ben benieuwd wie het verst komt met het doorlezen :).
Lieve ouders, het zal niet altijd even gemakkelijk voor jullie geweest zijn om zo'n lastige zoon als ik te hebben. Bedankt voor alle steun die ik over de jaren van jullie gekregen heb. Zonder jullie had ik het nooit gered. Lieve Michiel, klein broertje, ik ben nu dan toch eindelijk klaar met studeren! Nu jij nog! Maar ik geloof er nog steeds heilig in: jij zult later mijn baas zijn :).
Dan blijft er nog maar één persoon over. Mijn liefste Paulien, bedankt voor al je begrip, steun en hulp; al die uren en nachten die je hebt besteed om dit hele werk door te nemen en mij te helpen wanneer ik weer eens ergens op vastliep. Je behoort tot een select groepje van mensen die dit proefschrift van top tot teen hebben doorgelezen. Ook voor jou geldt dat het niet gemakkelijk zal zijn om met zo iemand als ik op te trekken, maar toch houd je het al ruim 9 jaar met me vol! Voor dit alles ben ik je oneindig dankbaar. Nog even volhouden, en dan ben jij ook klaar. Er zullen nog mooiere tijden volgen. I love you! sp^3!

$\infty+1$